Spatio-temporal evolution of glacial lakes in the Hindu Kush Himalaya

Cumulative dissertation

With the aim of achieving a doctoral degree

at the Faculty of Mathematics, Informatics, and Natural Sciences

Department of Earth Sciences

at University of Hamburg

submitted by Atul Kumar

2025 in Hamburg

Department of Earth Sciences

Date of Oral Defense	04.04.2025
Reviewers:	Prof. Dr. Udo Schickhoff
	Dr. Suraj Mal
Members of Examination Commission:	Prof. Dr. Jürgen Böhner
	Prof. Dr. Gerhard Schmiedl
	Prof. Dr. Olena Dubovyk
Chair of the Subject Doctoral Committee	
Earth System Sciences:	Prof. Dr. Hermann Held
Dean of Faculty MIN:	Prof. Dr.-Ing. Norbert Ritter

Acknowledgements

It is with profound gratitude and genuine humility that I reflect on the journey leading to the completion of this doctoral thesis on “Spatio-temporal Evolution of Glacial Lakes in the Hindu Kush Himalayas.” This path has been both intellectually challenging and personally transformative, and I have been fortunate to receive generous support, guidance, and encouragement from many extraordinary individuals.

First and foremost, I owe my deepest thanks to my supervisors, Prof. Dr. Udo Schickhoff and Dr. Suraj Mal, for their motivation, unwavering support, and dedicated mentorship. I extend my sincere gratitude to Prof. Dr. Schickhoff for graciously agreeing to supervise this doctoral thesis, welcoming me into his working group, and supporting my application for DAAD funding. His continued encouragement, academic guidance, and willingness to expose me to new opportunities have fueled both my professional and personal growth. I am deeply grateful for the chance to undertake this research, which has only heightened my passion for glacial lakes and the Hindu Kush Himalaya.

Furthermore, I would like to thank Dr. Suraj Mal, who introduced me to Prof. Dr. Schickhoff and recognized my potential to complete this project. Dr. Mal played an instrumental role in shaping the research proposal and provided essential guidance in carrying out the project. I am especially appreciative of his support during field visits to the northwestern parts of the Hindu Kush Himalaya and for imparting valuable lessons—not only about glacial lakes but also about life. Words cannot adequately express my gratitude for the mentorship, guidance, support, and academic freedom provided by both of my supervisors, all of which have profoundly influenced and nurtured my future career interests.

I would also like to thank the editors and reviewers of my published and submitted manuscripts. Their constructive feedback greatly contributed to improving the overall quality of my work.

My heartfelt appreciation goes to Prof. A. P. Dimri and Prof. Jeelani, who offered vital support during my first field visit to the Hindu Kush Himalaya. A special thanks as well to our porter and guide, Tanzin (from Gya village), whose assistance in collecting bathymetric data was invaluable.

I am grateful for the financial assistance provided by the German Academic Exchange Service (DAAD), which enabled me to pursue my doctoral studies smoothly. I would also like to thank the Department of Geography at the University of Zurich for endorsing my application to the Geochronology Summer School (2021).

I extend my sincere appreciation to my fellow colleagues, researchers, and friends—(Aashay, Ama, Anshu, Jitin, Maria, Niels, Prasanth, Gagan, Suraj Bhanu, Ujjwal, and Vishnu)—for their unwavering camaraderie and intellectual inspiration. Your willingness to share ideas, provide feedback, or simply share a good laugh made the long days (and nights) of research far more rewarding.

I am also thankful to Ravi, Vivek, Vinod, Bilal, and Yasir for their unconditional support during the 2021 and 2023 field visits.

On a personal level, I owe a debt of gratitude to my family, whose steadfast support and belief in me served as the emotional foundation upon which this research was built. Their constant reminders to maintain perspective and balance throughout this demanding process have been invaluable.

Finally, I wish to acknowledge the breathtaking Hindu Kush Himalayan landscapes themselves. Witnessing the evolution of glacial lakes firsthand reminded me of both the power and vulnerability of nature—a profound inspiration that fueled my resolve to persevere.

This thesis consists of four publications, which are provided in the Appendix.

To increase the readability of the thesis, all figures and tables have been renumbered in a consecutive manner.

One section containing all supplementary material is given at the end of the thesis.

Abstract

The glacial lakes are an important part of the cryosphere, originating from the deposition of glacial meltwater in the depressions created mainly by the glacial movements. Under the ongoing trend of rising annual mean temperatures, glacial lakes around the world are observing an increase in both number and area. An increase in the annual mean temperature is responsible for the rapid melting of glaciers. However, at the regional scale, the evolution of glacial lakes is a complex process due to the interplay between factors like the differential rate of glacial melting, change in annual mean temperature, change in annual mean precipitation, local topography, etc.

Hindu Kush Himalaya (HKH), being no exception, has experienced rapid growth in both the number and area of glacial lakes in the recent past. This rapid expansion of glacial lakes has some serious consequences, such as an increase in the risk of Glacial Lake Outburst Floods (GLOFs) in the region. In fact, the population of HKH has the highest exposure to the risk of GLOFs in the world. Furthermore, due to harsh topography and a large number of glacial lakes, it is very difficult to monitor each and every one based on in-situ information. The recent development of remote sensing techniques and computer-aided mapping has helped researchers immensely monitor the evolution of glacial lakes in the HKH. Therefore, this doctoral thesis systematically investigates the spatio-temporal evolution of glacial lakes at the sub-basin level in the HKH, factors affecting the growth of glacial lakes, and associated risks with the continuous expansion of glacial lakes.

Firstly, glacial lake inventories were developed for four decades (1990, 2000, 2010, and 2020) using Landsat satellite imagery (TM/OLI) and the Shuttle Radar Topography Mission's (SRTM) Digital Elevation Model (DEM) at the subbasin level for the Indus, Ganga, and Brahmaputra (IGB) river basins. We then employed spatial analysis tools to comprehend the distribution, growth, and factors influencing the growth of glacial lakes in the IGB river basins. We found that the distribution of glacial lakes is uneven in the IGB river basins. The Brahmaputra River basin had the highest concentration of glacial lakes in the HKH, followed by the Indus basin and Ganga basin (Article I). However, the Ganga basin shows the highest growth rate in both the number and area of glacial lakes, followed by the Indus and Brahmaputra river basins (Articles I and IV). The main cause of the expansion is believed to be the rapid melting of glaciers. The mean distance between glaciers and glacial lakes also saw a reduction between 1990 and 2020 (Article I). The Ganga and Indus river basins have significantly lower mean distances as compared to the Brahmaputra river basin, which helps explain the above-average expansion of glacial lakes in the Ganga and Indus river basins as compared to the Brahmaputra river basin (Article I). Furthermore, end-moraine dammed lakes, especially those within 10 km of the nearby glaciers, are the most dominant type of glacial lakes, and supraglacial lakes show the highest increase in growth among different types of glacial lakes. This again highlights the contribution of the rapid melting of glaciers and the aggravating risk of future GLOF events in the region.

Secondly, new empirical equations were developed to estimate the mean depth and volume of glacial lakes using primary field-based and secondary literature-based bathymetry data to further enhance the understanding of glacial lake evolution and facilitate the modelling of GLOF scenarios and risk assessments (Article II). We developed the empirical equations using the area-scaling method. It was observed that regional lake characteristics play a crucial role in the development of empirical equations. Factors like lake shape, dam material, glacier movement, sedimentation rate, and lake bottom topography play a crucial role in determining the depth and volume of glacial lakes.

The findings of present research highlight the rapid expansion of glacial lakes, with subregional heterogeneities in glacial lake characteristics and changes in them. The study recommends continuous monitoring of glacial lakes with high-resolution satellite data and, wherever possible, by field-based observations, to better understand the evolution of glacial lakes, factors affecting the evolution, identification of potential hazardous glacial lakes, employment of early warning systems at potentially hazardous glacial lakes, and development of GLOF mitigation strategies.

Zusammenfassung

Die Gletscherseen sind ein wichtiger Teil der Kryosphäre und entstehen durch die Ablagerung von Schmelzwasser in den hauptsächlich durch die Gletscherbewegungen geschaffenen Vertiefungen. Im Zuge des anhaltenden Trends steigender Jahresmitteltemperaturen, nehmen die Gletscherseen weltweit sowohl in ihrer Anzahl als auch in ihrer Fläche zu. Der Anstieg der Jahresmitteltemperatur ist für das schnelle Abschmelzen der Gletscher verantwortlich. Auf regionaler Ebene ist die Entwicklung von Gletscherseen jedoch ein komplexer Prozess, der durch das Zusammenspiel von Faktoren wie der unterschiedlichen Geschwindigkeit der Gletscherschmelze, der Änderung der Jahresmitteltemperatur, der Änderung des Jahresmittelwertes des Niederschlags, der lokalen Topografie und Ähnlichem bedingt ist.

Der Hindukusch-Himalaya (HKH) bildet da keine Ausnahme und hat in der jüngsten Vergangenheit ein rasches Wachstum sowohl in der Anzahl als auch der Fläche der Gletscherseen erfahren. Diese rasche Ausdehnung der Gletscherseen hat einige schwerwiegende Folgen, wie z. B. eine Zunahme des Risikos von Gletscherseeausbrüchen (GLOFs) in der Region. Tatsächlich ist die Bevölkerung von HKH dem Risiko von GLOFs weltweit am stärksten ausgesetzt. Außerdem ist es aufgrund der rauen Topographie und der großen Anzahl von Gletscherseen sehr schwierig, jeden einzelnen See anhand von Informationen vor Ort zu überwachen. Die jüngste Entwicklung von Fernerkundungstechniken und computergestützter Kartierung hat den Forschern bei der Überwachung der Entwicklung von Gletscherseen im HKH sehr geholfen.

In dieser Dissertation werden daher systematisch die räumlich-zeitliche Entwicklung der Gletscherseen auf der Ebene der Teileinzugsgebiete im HKH, die Faktoren, die das Wachstum der Gletscherseen beeinflussen, und die mit der kontinuierlichen Ausdehnung der Gletscherseen verbundenen Risiken untersucht.

Zunächst wurden mit Hilfe von Landsat-Satellitenbildern (TM/OLI) und dem Digitalen Höhenmodell (DEM) der Shuttle Radar Topography Mission (SRTM) für vier Jahrzehnte (1990, 2000, 2010 und 2020) Bestandsaufnahmen der Gletscherseen in den Einzugsgebieten von Indus, Ganges und Brahmaputra (IGB) erstellt. Anschließend setzten wir räumliche Analysewerkzeuge ein, um die Verteilung, das Wachstum und die Faktoren, die das Wachstum von Gletscherseen in den IGB-Flusseinzugsgebieten beeinflussen, zu verstehen. Wir stellten fest, dass die Verteilung der Gletscherseen in den IGB-Flusseinzugsgebieten ungleichmäßig ist. Das Brahmaputra-Einzugsgebiet wies die höchste Konzentration von Gletscherseen im HKH auf, gefolgt vom Indus-Einzugsgebiet und dem Ganges-Einzugsgebiet (Artikel I). Das Ganges -Einzugsgebiet weist jedoch die höchste Zuwachsrate sowohl bei der Anzahl als auch bei der Fläche der Gletscherseen auf, gefolgt von den Flusseinzugsgebieten des Indus und des Brahmaputra (Artikel I und IV). Als Hauptursache für die Ausdehnung wird das schnelle Abschmelzen der Gletscher vermutet. Auch der mittlere Abstand zwischen Gletschern und

Gletscherseen hat sich zwischen 1990 und 2020 verringert (Artikel I). Die Einzugsgebiete des Ganges und Indus weisen im Vergleich zum Einzugsgebiet des Brahmaputra deutlich geringere mittlere Abstände auf, was die überdurchschnittliche Ausdehnung der Gletscherseen in den Einzugsgebieten von Ganges und Indus im Vergleich zum Einzugsgebiet des Brahmaputra erklärt (Artikel I). Darüber hinaus sind Endmoränenstauseen, vor allem die, die sich in einem Umkreis von 10 km von den nahen gelegenen Gletschern befinden, der vorherrschende Typ von Gletscherseen. Außerdem weisen supraglaziale Seen unter den verschiedenen Typen von Gletscherseen den höchsten Zuwachs auf. Dies verdeutlicht erneut den Beitrag des raschen Abschmelzens der Gletscher und das zunehmende Risiko künftiger GLOF-Ereignisse in dieser Region.

Zweitens haben wir neue empirische Gleichungen zur Schätzung der mittleren Tiefe und des Volumens von Gletscherseen unter Verwendung primärer feldbasierter und sekundärer literaturbasierter bathymetrischer Daten entwickelt, um das Verständnis der Entwicklung von Gletscherseen weiter zu verbessern und die Modellierung von GLOF-Szenarien und Risikobewertungen zu erleichtern (Artikel II). Die empirischen Gleichungen wurden mit Hilfe der Area-Scaling-Methode entwickelt. Es wurde festgestellt, dass die regionalen Seecharakteristika eine entscheidende Rolle bei der Entwicklung der empirischen Gleichungen spielen. Faktoren wie die Seeform, das Dammmaterial, die Gletscherbewegung, die Sedimentationsrate und die Topographie des Seebodens spielen eine entscheidende Rolle bei der Bestimmung der Tiefe und des Volumens von Gletscherseen.

Die Ergebnisse dieser Forschung zeigen die rasche Ausdehnung der Gletscherseen mit subregionalen Heterogenitäten in den Eigenschaften der Gletscherseen und deren Veränderungen. Die Studie empfiehlt die kontinuierliche Überwachung von Gletscherseen mit hochauflösenden Satellitendaten und, wo möglich, auch Beobachtungen vor Ort, um die Entwicklung von Gletscherseen und die Faktoren, die diese Entwicklung beeinflussen, besser zu verstehen, potenziell gefährliche Gletscherseen zu identifizieren, Frühwarnsysteme an potenziell gefährlichen Gletscherseen einzusetzen und Strategien zur Eindämmung von GLOF zu entwickeln.

Contents

List of Figures

List of Tables

List of Supplementary Material

List of Abbreviations

APHRODITE: Asian Precipitation Highly Resolved Observation Data Integration Towards Evaluation

ASTER: Advanced Spaceborne Thermal Emission and Reflection Radiometer

B(c): Cirque lake

B(o): other bedrock-dammed lake

CBERS: China-Brazil Earth Resources Satellite

CHELSA: Climatologies at high resolution for the earth's land surface areas

CSV: Comma-separated values

DEM: Digital Elevation Models

E: Relative error

GIS: Geographic Information System

GLOF: Glacial Lake Outburst Floods

GT/yr: Gega Tons per year

HKH: Hindu Kush Himalaya

HMA: High Mountain Asia

ICT: Information and Technology

IGB: Indus, Ganga, and Brahmaputra

ISM: Indian Summer Monsoon

IRS: Indian Remote Sensing

LISS: Linear Imaging Self-Scanning Sensor

MD: Mean Depth

M(e): End moraine-dammed lake

M(l): lateral moraine-dammed lake

M(m): medial moraine-dammed lake

MMU: Minimum Mapping Unit

MSS: Multispectral Scanner

NDWI: Normalized Difference Water Index

NIR: Near InfraRed

OLI: Operational Land Imager

RMSE: Residual Mean Square Error

SDB: Satellite Derived Bathymetry

SPOT: Satellite pour I'Observation de la Terre

SRTM: Shuttle Radar Topography Mission

TM: Thematic Mapper

V: Volume

1. Introduction

1.1 Definition, significance and types of glacial lakes

1.1.1 Definition

Glacial lakes are inland water bodies developed on or near glaciers mainly because of the accumulation of glacial meltwater in depressions created by glacial erosion, moraine deposition, or tectonic activities **(Yao et al., 2018; Wang et al., 2020).** Glacial lakes are regarded as a crucial part of the cryosphere **(Bolch et al., 2019; Shugar et al., 2020)**. The location, extent, and stability of these lakes are influenced by several factors, such as the extent of glacial retreat, outflow, local topography, and climate conditions **(Bolch et al., 2019; Shugar et al., 2020; Zhang et al., 2023)**.

1.1.2 Significance of glacial lakes

Glacial lakes are crucial for the cryospheric environment, playing a dual role, especially in high-altitude mountains, offering both opportunities and challenges. Their significance spans environmental, hydrological, and socio-economic dimensions:

- *Indicators of Climate Change*

Glacial lakes are important markers of climate change. New glacial lakes are forming and existing ones are getting bigger because glaciers are melting faster, which is directly linked to the rise in the mean annual temperature **(Bolch et al., 2019).** Continuous monitoring of glacial lakes can provide highly accurate information not only about glacier melting but also about climate change **(Adrian et al., 2009)**. Limnological studies based on varve analysis and dating techniques can help provide high resolution insights about the changing climate, especially in the high mountain systems across the world, where climatic conditions vary within a distance of a few kilometres **(Larsen et al., 2011; Breckenridge et al., 2021)**.

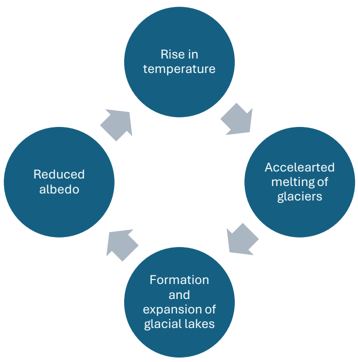

Fig. 1: *Feedback loop showing cycle of glacial lake expansion in the glaciated region (source: created by author).*

- ***Contributions to Hydrological Systems***

Several of these glacial lakes are sources of some of the largest river systems in the world. For example, Brahmaputra, Indus, Sutluj, Ravi, and many others originate from glacial lakes **(Maharjan et al., 2018)**. Glacial lakes help regulate the annual flow of these rivers. Especially during the dry seasons, when glacial melt is the primary source of water for such rivers **(Molden et al., 2016)**. Furthermore, the lakes help in recharging the local aquifers in the upstream regions **(Reeve et al., 2001; Lemieux et al., 2008)**.

- ***Supporters of High-Altitude Ecosystems***

Glacial lakes play a critical role in supporting unique and fragile ecosystems in high-altitude regions **(Moser et al., 2019; Vanderwall et al., 2024)**. These ecosystems are characterised by harsh environmental conditions, including low temperatures, reduced oxygen levels, and limited nutrient availability **(Bolch et al., 2019; Krishnan et al., 2019)**. Despite these challenges, glacial lakes sustain diverse biological communities, including aquatic and terrestrial species adapted to such extremes **(Moser et al., 2019)**. Their role as ecological hubs is particularly significant in the context of climate change, as these lakes are both vulnerable to and influenced by environmental shifts. For example, glacial lakes provide habitat for cold-adapted aquatic species, including microorganisms, invertebrates, and fish that thrive in oligotrophic (nutrient-poor) water **(Barta et al., 2018).** Furthermore, these lakes provide refuge to several migratory wildlife, including snow leopards and several types of birds **(Jamwal et al., 2020; Farrington & Li, 2024)**.

- ***Socio-Economic Significance of Glacial Lakes***

Socio-economically, these lakes are immensely important, as ~15 million people are exposed to them directly by living in their vicinities **(Taylor et al., 2023).** These lakes not only provide freshwater resources for drinking, agriculture, and industrial use, but also promote tourism and help in generating hydropower and transportation **(Yao et al., 2018)**. Furthermore, these lakes are of immense cultural importance as well. In several religions (e.g., Hinduism and Buddhism), many of these glacial lakes are regarded as sacred, and people make holy pilgrimages to these lakes.

- ***Cause of Outburst Floods in the Downstream Regions***

Glacial lakes, while being essential for hydrological, ecological and socio-economic systems, they also pose significant risk of causing sudden outburst floods and causing immense damages. These **Glacial Lake Outburst Floods (GLOFs)** mainly occur due to dam-failure or overtopping mechanisms **(Taylor et al., 2023; Zhang et al., 2023)**. The outburst can release massive volumes of water downstream, causing catastrophic floods that threaten lives, infrastructure, and surrounding ecosystems.

Table 1: *Examples of famous GLOF events from different regions of the world.*

Name/Year	**Causing Mechanism**	**Dam Type**	**Region**	**Volume of the Lake (m^3)**	**Damage Caused**	**Reference**
Dig Tsho / 1985	Ice-avalanche	End-moraine dammed	Nepal Himalayas	$5.1 * 10^6$	Destruction of hydroelectric power plant, 14 bridges, ~30 houses, many hectares of arable land, degradation of water quality, and heavily damaged trail network	Vuichard and Zimmermann (1987)
Lake Palcacocha / 1941	Avalanche	End-moraine dammed	Peruvian Andes	$9 – 11 *10^6$	~1800 people died, destroyed agricultural land, degradation of water quality, and vital infrastructure	Somos-Valenzuela et al. (2016)
Kyagar Lake / 2013	Piping (sub-glacial drainage)	Ice-dammed	Karakoram, China-Pakistan Economic Corridor	$22*10^6$	Localized flooding	Haemmig et al. (2014)
Franz Josef Glacier Lake / 2003	Over-topping	Ice-dammed	South Westland, New Zealand	<Nil>	Localized flooding	Goodsell et al. (2005)
Tulsequah Lake / 2001	Sub-glacial drainage	Ice-dammed	Alaska, United States	$19.74*10^6$	Affected navigation and commercial fishing	Neal, E. G. (2007)
South Lhyonk Lake/2023	Collapse of lateral moraine	End moraine-dammed lake	Eastern Himalayas, India	$96.65*10^6$	~178 people died, destruction of three downstream hydropower plants, damage to arable land, degradation of water quality, and loss of basic road infrastructure.	Zhang et al. (2025)

1.1.3 Types of Glacial Lakes

Several studies have attempted to classify glacial lakes **(Ives et al., 2010; ICIMOD, 2011; Zhang et al., 2015; Yao et al., 2018)**. However, there is no universally accepted classification scheme for the glacial lakes **(Mal et al., 2020)**. Previous studies have classified glacial lakes mainly based on their formation process, dam material, location, and distance from the glacier. It is very important to have classification schemes for glacial lakes because they help us figure out what processes cause each type of glacial lake to form and which glacial lakes might be dangerous. Based on the formation processes, glacial lakes can be classified into two major categories: (i) depositional and (ii) erosional glacial lakes **(Table 2 & Fig. 2**). Based on the dam material, glacial lakes can be classified into three major categories: (i) moraine-dammed lakes, (ii) bedrock-dammed lakes, and (iii) ice-dammed lakes **(Table 2 & Fig. 2)**. Based on the location, glacial lakes can be classified into four major categories: (i) supraglacial, (ii) subglacial, (iii) englacial, and (iv) proglacial lakes; and at last, based on the distance from the glacier, glacial lakes can be classified into two major categories: (i) connected glacial lakes and (ii) not-connected glacial lakes **(Table 2 & Fig. 2)**.

Table 2: *Types of glacial lakes based on different criteria.*

Criteria	**Type**	**Definition**
Process	Depositional	Glacial lakes formed by accumulation of glacial meltwater in the depression surrounded by rock material deposited by glaciers.
	Erosional	Glacial lakes formed by accumulation of glacial meltwater in the depression carved by glaciers.
	Others	Glacial lakes formed by blocking of glacial meltwater by other geomorphological processes such as landslides, tectonic activities, rockfall, etc.
Dam material	1. Moraine dammed	Glacial lakes formed by accumulation of glacial meltwater dammed by the moraine material deposited by the glaciers
	1.i End moraine-dammed lakes M(e)	Glacial lakes formed by accumulation of glacial meltwater behind the terminal moraine deposited by a glacier.
	1.ii Lateral moraine-dammed lakes M(l)	Glacial lakes formed when glacial meltwater is trapped between the side of a glacier and lateral moraine.
	1.iii Medial moraine-dammed lakes M(m)	Glacial lakes formed when meltwater is impounded behind two lateral moraines created where two glaciers merges.
	2. Bedrock-dammed lakes	Glacial lake formed when glacial meltwater is accumulated in depressions carved into bedrocks by glacial erosion.
	2.i Cirque lakes B(c)	Glacial lakes formed by glacial erosion that form in bowl-shaped depressions know as cirques. Cirques are created by the erosional activity of a glacier near its source area.
	2.ii Other bedrock-dammed lakes B(o)	Glacial lakes formed in depressions or valleys where bedrock acts as a natural dam, but not necessarily in a cirque setting.
	3. Ice-dammed lakes	Glacial lakes formed when meltwater is impounded by a glacier or an ice sheet. The glacial ice act as natural dam.
	3.i Ice valley-dammed lakes I(v)	Glacial lakes formed when a glacier blocks a valley, creating a barrier that impounds meltwater upstream. These lakes can also form when advancing glaciers block the flow of rivers or streams within valleys.
	3.ii Supraglacial lakes	Supraglacial lakes are a sub-type of ice-dammed lakes, which forms by the accumulation of glacial meltwater on the surface of glaciers.

Location	Englacial lakes	Glacial lakes formed within the glaciers itself, trapped in cavities, fractures, or within the ice layers.
	Subglacial lakes	Subglacial lakes form beneath a glacier or ice-sheet, when glacial meltwater trapped between the ice and the underlying bedrock. They are sustained by pressure-induced melting at the glacier base, geothermal heat, or frictional heat generated by the glacier's melting
	Supraglacial lakes	Supraglacial lakes are a sub-type of ice-dammed lakes, which forms by the accumulation of glacial meltwater on the surface of glaciers.
	Proglacial	Glacial lakes formed in front of the glaciers, typically in the space left behind as the glacier retreat is known as Proglacial lakes.
Distance from glacier	Connected glacial lakes	Glacial lakes which forms in the depressions created by glacial action, and continuous to receive water from parent glaciers.
	Not-connected glacial lakes	Glacial lakes which forms in the depressions created by glacial action, and have received glacial meltwater in the past, however, in present there is not connect with the parent glaciers.

* different colors represents different criteria

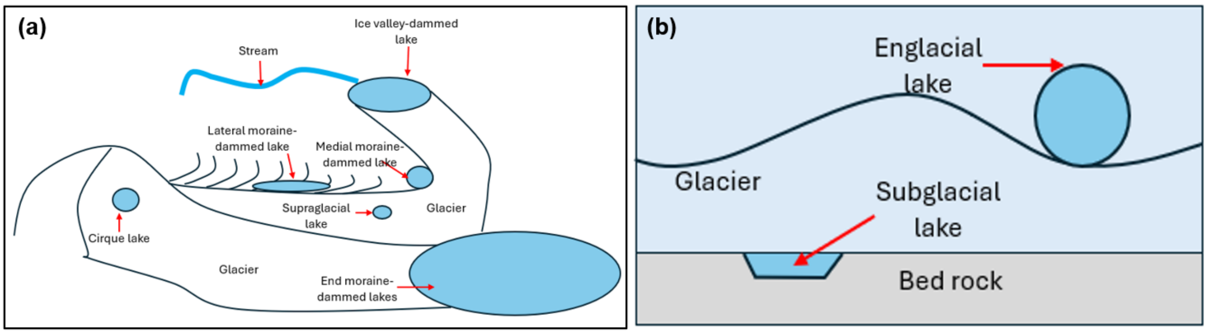

Fig. 2: Illustration of different types of glacial lakes based on different formation criteria (source: created by author).

1.2 Glacial lake expansion, causes and implications

1.2.1 Glacial lake expansion

It has been observed by several researchers that glacial lakes are expanding rapidly at the global scale **(Shugar et al., 2020; Taylor et al., 2023; Zhang et al., 2024)**. However, the rate of expansion is uneven at the regional level **(Shugar et al., 2020; Zhang et al., 2024)**. Furthermore, it is important to highlight that continuous monitoring of glacial lakes at the global scale is a difficult task, even after the advent of remote sensing, Geographic Information System (GIS), and big data technologies. Therefore, only a few researchers have attempted to analyse the continuous evolution of glacial lakes at the global scale. **Shugar et al. (2020)** made one of such attempts. In their study, they monitor the evolution of glacial lakes (area: >0.05 km^2) at the global scale between 1990 and 2018. In that study they found that the number of glacial lakes increased from 9,414 (1990) to 14,394 (2018), which is an increase of 53%. Similarly, they observed an increase of ~51% in the total area of glacial lakes between 1990 ($5.93*10^3$ km^2) and 2018 ($8.95*10^3$ km^2). And an increase of ~48 % percentage in the volume of glacial lakes between 1990 (105 km^3) and 2020 (156 km^3). Similarly, Zhang et al. (2024) attempted to understand the evolution of glacial lakes at the global scale between 1990 and 2020. They found that the number, area, and volume of glacial lakes increased by 54%, 11%, and 9%, respectively **(Zhang et al., 2024)**. Interestingly, both studies took the base year as 1990, mainly because of the wide availability of stable satellite images at the global scale. And observed a relatively similar % of change in number; however, when it comes to the area and volume of glacial lakes, there are discrepancies in the results of both studies (Shugar et al., 2020; Zhang et al., 2024). One possible reason for the discrepancies in the results can be the use of different methods to develop the global glacial lake inventories. For example, **Shugar et al. (2020)** employed a Minimum Mapping Unit (MMU) of 0.05 km^2, whereas **Zhang et al. (2024)** employed a MMU of 0.002 km^2. Furthermore, the study confirms regional heterogeneity and lays emphasis on the detailed regional studies for better monitoring of glacial lake expansion, identifying potentially hazardous glacial lakes, deploying early warning systems on potentially hazardous glacial lakes, and developing better GLOF mitigation policies.

At the regional scale, several studies has been conducted in the past to monitor the evolution of glacial lakes **(Huggel et al., 2002; Ives et al., 2010; Zhang et al., 2015; Viani et al., 2016; Maharjan et al., 2018; Wilson et al., 2018; Shugar et al., 2020; Ma et al., 2021; Wood et al., 2021; Zhang et al., 2024)**. These studies show that glacial lakes change over time in different ways depending on the geography, climate, melting glaciers, and geological setting. Understanding these regional heterogeneities is of immense importance as it helps in developing region-specific policies for GLOF risk reduction. Broadly, at the regional level, glacial lakes can be divided into two: ice-sheet glacial lakes (mainly in polar regions) and mountain glacial lakes (mainly in HKH, Andes, Alps, etc.) **(Shugar et al., 2020; Zhang et al., 2024)**. The glacial lakes associated with continental ice sheets are primarily ice-dammed lakes, particularly supraglacial lakes, while the glacial lakes associated with mountain glaciers are primarily moraine-dammed lakes, particularly end moraine-dammed lakes **(Zhang et al., 2024).** Among the major regions (>200 glacial lakes), at the global level, the high-latitude regions with continental ice sheets observed the highest growth in number and area of glacial lakes **(Shugar et al., 2020; Zhang et al., 2024) (Table 3)**. For example, the growth rate in the number of glacial lakes in Iceland is the highest (241.83%), followed by Antarctica (221.38%). Whereas among the mountain glaciers, Scandinavian glacial lakes observed an increase of 103.4% in the number **(Table 3)**.

However, in terms of the concentration of glacial lakes, High Mountain Asia (HMA) has the highest concentration of glacial lakes in the world **(Maharjan et al., 2018; Bolch et al., 2019; Wang et al., 2020)**. There were ~30000 glacial lakes in the HMA **(Wang et al., 2020)**. However, due to differences in the methodologies employed to map these glacial lakes in HMA, different studies gave different expansion rates. For example, according to **Wang et al. (2020)**, glacial lakes in the HMA grew at a rate (n = 10.71% and a = 15.14%) between 1990 and 2018, whereas **Zhang et al. (2015)** found that the glacial lake in the HMA grew at a rate of (n = 23.88% and a = 23.19%) between 1990 and 2015.

Furthermore, **Li et al. (2022)** found that glacial lakes in the Hindu Kush Himalaya (HKH) expanded (n = 65.77% and a = 35.31%) between 1990 and 2020**.** Differences in factors like selecting a minimum mapping unit, threshold distance from glaciers, elevation threshold, slope threshold, quality of imagery, and manual expertise lead to these variations in the growth rate of glacial lakes among different studies.

Table 3: *Regional distribution and growth of glacial lakes at the global scale.*

Region	**Glacier Type**	**Year**	**Number**	**Area (km^2)**	**Growth in Number (%)**	**Growth In Area (%)**	**Reference**
Alaska	Mountain	1990	4347	2533.49	96.27	27.27	Zhang et al. (2024)
		2020	8532	3224.57			
Andes	Mountain	1990	4376	2324.07	75.59	15.42	Zhang et al. (2024)
		2020	7684	2682.53			
Antarctica	Continental	1990	173	90	221.38	26.23	Zhang et al. (2024)
		2020	556	113.61			
Arctic	Continental	1990	5560	2684.69	50.73	10.42	Zhang et al. (2024)
		2020	8381	2964.63			
Caucasus	Mountain	1990	76	0.98	131.57	338.77	Zhang et al. (2024)
		2020	176	4.3			
Swiss Alps	Mountain	2016	987	6.22			Mölg et al. (2021)
Greenland	Continental	1990	9063	4590.84	43.8	3.21	Zhang et al. (2024)
		2020	13033	4738.47			
High Mountain Asia	Mountain	1990	27205	1806.47	10.71	15.14	Wang et al. (2020)
		2018	30121	2080.12			
Iceland	Mountain	1990	251	111	241.83	133.7	Zhang et al. (2024)
		2020	858	261.05			
Southern Alps	Mountain	1990	54	351.61	137.03	6.96	Zhang et al. (2024)
		2020	128	376.09			
Scandinavia	Mountain	1990	1615	969.57	103.4	9.48	Zhang et al. (2024)
		2020	3285	1061.56			
Western Canada and USA	Mountain	1990	6300	1479.64	42.47	6.55	Zhang et al. (2024)
		2020	8976	1576.65			
Hindukush – Karakoram - Himalayas	Mountain	1990	5835	664.84	65.77	35.31	Li et al. (2022)
		2020	9673	899.66			

* where red color shows the highest growth rate

1.2.2 Causes of glacial lake expansion

The ongoing glacial lake expansion across the cryospheric environment of the world is mainly attributed to the continuous melting of glaciers caused by the steady rise in the global mean annual temperature **(Zemp et al., 2019; Zhang et al., 2024)**. However, it is a complex and heterogeneous process. The glacial lakes are not expanding at the same rate around the world **(Nie et al., 2017; Wilson et al., 2018; Bolch et al., 2019; Shugar et al., 2020; Wang et al., 2020; Zhang et al., 2024)**. This is mainly due to differences in the rising mean annual temperature at the regional level, differences in the glacial responses to rising mean annual temperature, and local geomorphological setting **(Bolch et al., 2019; Zemp et al., 2019; Zhang et al., 2019)**. Since the mid-19th century, global mean annual temperatures have increased by 1.1°C **(Allen et al., 2018)**, and since the late 20th century, the rate of increase has steadily increased to 0.2°C/10yr **(Allen et al., 2018)**. However, the rate of increase varies regionally **(Table 4)**. Interestingly, all of the major glaciated regions of the world are observing above-average warming **(Table 4)**.

Table 4: *Regional variations in the increasing mean annual temperature.*

Region	**Time Period**	**Temperature increase (°C)**	**Reference**
Alaska	Since 1950s	~1.7	Chapin et al. (2014)
Alps	Since 1980s	~1.5	Gobiet et al. (2014)
Andes	Since 1900s	~0.8	Marengo et al. 2011
Antarctica	Since 1950s	~3	Turner et al. 2005
Greenland	Since 1950s	~1.2	Vandecrux et al. 2024
HKH	Since 1900s	~1.1	Krishnan et al. (2019)

Within HKH itself, the rate of increase is not uniform **(Krishnan et al., 2019) (Fig. 3a)**. The eastern and western margins of the HKH have observed the highest increase in the annual mean temperature between 1990 and 2020 **(Fig. 3a)**. In terms of the aspect, the south-facing sub-basins in the HKH observed relatively higher warming as compared to the north-facing sub-basins **(Fig. 3b)**.

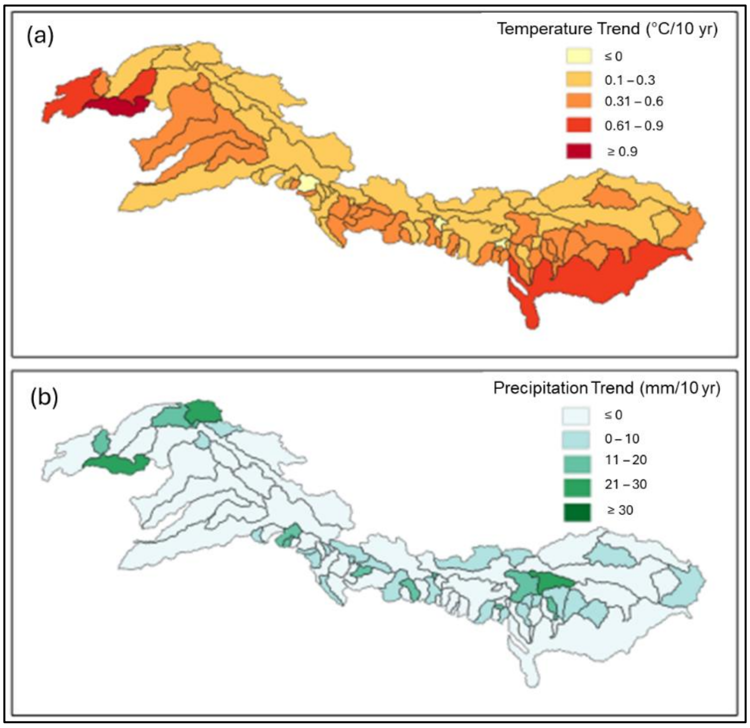

Fig. 3: *Spatial trend of (a) temperature (°C/10 yr) and (b) precipitation (mm/10 yr) between 1990 and 2020 based on the CHELSA data (source: created by author).*

This continuous rise in the mean annual temperature has caused rapid melting of glaciers all over the globe. According to **Zhang et al. (2024)**, the total estimated ice lost from glaciers is 7129.7 Gt between 1990 and 2020. However, there are regional variations in the melting rate of glaciers **(Hugonnet et al., 2021) (Table 5)**. Glaciers in Alaska observed the highest change in mass between 2000 and 2019 (-66.7 GT/yr) **(Hugonnet et al., 2021)**. Furthermore, it was found that glaciers terminating in the maritime are losing mass faster than glaciers with land terminus **(Table 5)**. Glaciers are mainly losing ice mass mainly by two processes: (1) headward retreating and (2) glacial thinning. Where glacial retreat is the main cause of the emergence of new proglacial lakes (especially end moraine-dammed lakes) and the expansion of existing ones by providing more space for water accumulation. Whereas glacial thinning, because of surface melting, can lead to the development of englacial and supraglacial lakes **(Sundal et al., 2009; Sakai, 2012)**.

Table 5: *Glacial mass change between 2000 and 2019 at region level based on* ***Hugonnet et al. (2021).***

Region	*Mass Change rate (GT/yr)*
Alaska	-66.7
Antarctica	-20.9
Arctic Canada North	-30.6
Arctic Canda South	-26.5

Greenland Periphery North	-11.9
Greenland Periphery East	-10.6
Greenland Periphery West	-13
Iceland	-9.4
Central Asia	-9.6
Russian Arctic West	-8.4
Southern Andes South	-18.7
South Asia East	-4.6
South Asia West	-6.9
Svalbard and Jan Mayen	-10.5

*source: Hugonnet et al. (2021)

Additionally, it is important to highlight that in some cases precipitation (both liquid and solid) can lead to the expansion of existing glacial lakes, especially in the case of non-connected glacial lakes **(Sun et al., 2018; Zhang et al., 2021)**. In the HKH, there is no uniform trend of precipitation at the basin level, mainly because of the large spatial extent and complex topography. However, sub-basins in the western margins of the HKH experienced a significant increase (> 30 mm/10 yr) in the precipitation **(Fig. 3b)**. Whereas sub-basins in the central Himalaya observed a considerable increase (10–30 mm/10 yr), and eastern Himalayas observed negligible or negative change in the precipitation between 1990 and 2020 **(Kumar et al., 2024) (Fig. 3b)**. And in specific instances, the rising temperature, especially in the case of non-connected glacial lakes in the regions with very low precipitation and high summer temperature (Central Asia, South Asia West, and Andes), can cause negative growth in the glacial lakes, mainly due to the potential evapotranspiration **(Song et al., 2016; Xiao et al., 2018)**.

1.2.3 Implications of glacial lake expansion

Cryospheric environments all across the globe are experiencing the expanding of glacial lakes both in terms of number and area **(Shugar et al., 2020; Zhang et al., 2024)**. This continuous expansion of glacial lakes has wide-ranging implications for both natural and humanly modified environments across the world. And some of these implications, such as impending sea level rise and Glacial Lake Outburst Floods (GLOFs), are not limited to the cryospheric environment. These implications are multidimensional, encompassing both positive and negative outcomes, which vary depending on the regional setting and specific lake characteristics.

Positive implications of glacial lakes

- ***Enhanced water resources:*** Glacial lakes can act as the freshwater reservoirs. They not only provide fresh water for domestic purposes, but also water for agricultural and industrial activities not only in surrounding areas but also for downstream communities **(Taylor et al., 2023)**. These lakes are of special significance, especially in the dry-cold regions (e.g. the

Karakoram range, Tibetan plateau, and Andes), which are reasonably populated by humans and lacks other sources of fresh water **(Nie et al., 2021)**.

- ***Hydropower potential:*** These glacial lakes are natural reservoirs of water and are generally located in regions with a downstream gradient. These characteristics allow humans to convert glacial lakes into hydroelectric dams by constructing artificial dams on these lakes. There are several examples around the world where humans are using glacial lakes as the resource for generating renewable electricity, for example, hydroelectricity project at Tsho Rolpa glacial lake in Nepal.
- ***Tourism and recreation***: Many of these glacial lakes have majestic and pristine attributes associated with them and are part of an awestruck landscape (e.g., Lake Louise in Canada). These characteristics make them one of the favourite tourist destinations in the world. This helps local communities in generating more income and developing their surroundings.
- ***Delays sea level rise:*** Glacial lakes also help in temporarily delaying the rate of sea level rise by temporarily storing the glacial meltwater **(Zhang et al., 2024)**.

Negative implications of glacial lakes:

- ***Increase in the risk of GLOFs:*** According to **Taylor et al. (2023)**, ~15 million people globally live in the vicinity of areas susceptible to flooding from glacial lakes. The continuous expansion of glacial lakes, especially ones with unstable moraine and ice-dammed, poses a serious threat of GLOFs in the downstream region (**Taylor et al., 2023; Zhang et al., 2024)**. GLOF events like *South Loknak lake (2023)* have caused immense loss of human life and surrounding environment in the recent past. Furthermore, according to **Taylor et al. (2023)**, the population of High Mountain Asia (HMA) is most exposed to the threat of future GLOF events. **Lützow et al.** (**2023)** reported 512 GLOF events in the HMA, which is the second highest after NW North America; however, the HMA observed the highest human fatality (n = 3093) among different regions of the world. And it is estimated to increase due to the continuous increase in population and expansion of glacial lakes in the HMA region if correct GLOF mitigation policies are not developed and employed.
- ***Accelerate glacial melting:*** The emergence and expansion of glacial lakes connected with glaciers can start a feedback mechanism, which can lead to the acceleration of glacial melting **(Zhang et al., 2024)**. For example, when glacial lakes emerge next to or on the glaciers, they tend to absorb infrared solar radiation due to their lower albedo as compared to the surroundings, which results in warming of the surroundings.

1.3 Mean depth and Volume estimation of glacial lakes

The mean depth and volume of glacial lakes are two very important categories, which needed to be measured regularly, especially in the current time, when glacial lakes are expanding at a rapid rate and can influence the lives of people living in the surrounding areas. Information about the mean depth and volume of glacial lakes is of immense importance for purposes such as estimating the total water resources, building water use policies for agriculture, domestic and industrial use, identifying potentially hazardous glacial lakes, simulating previous GLOF events, modelling future GLOF events, calculating run-off distance, and calculating run-off speed **(Huggel et al., 2002; Sakai, 2012; Qi et al., 2022)**. However, measuring the depth and volume of each and every glacial lake, especially in the inaccessible mountain environment, is not an easy task due to constraints such as high cost, time consumption, and inaccessible terrain. Therefore, researchers opted for the estimation of the mean depth and volume of glacial lakes using different methods like empirical equations, Satellite Derived Bathymetry (SDB), and computer-based models **(Evans, 1986; Huggel et al., 2002; Shugar et al., 2020; Qi et al., 2022; Zhang et al., 2024)**. SDB is a relatively new method to develop a depth profile of glacial lakes. Several studies have employed this method on glacial lakes as well **(Legleiter et al., 2014; Datta & Wouters, 2021)**. SDB can be further divided into two categories: (i) optical-based and (ii) altimetry-based approaches. The optical approach is the traditional approach, which uses the spectral signature of water bodies to estimate the depth of water bodies. The main principle at work in the optical approach is estimating depth based on the light attenuated in water. This technique requires preconditions such as water bodies with low or no turbidity for better penetration of light to greater depths. Whereas altimetry-based methods, which employ ICESat and ICESat-2, use water surface elevation and estimate the water depth by integrating water surface elevation with shoreline mapping. However, altimetry-based methods have several limitations as well. Some of these limitations are limited data availability and low spatial resolution, which makes them unsuitable for small or irregularly shaped glacial lakes, especially in mountainous regions like HKH.

Computer-aided models can also estimate the mean depth and volume of glacial lakes by employing different datasets, such as Digital Elevation Models (DEMs), slope, glacier thickness, glacier retreat rate, rock structure, etc. **(Zhang et al., 2023)**. While these models can be highly accurate, they also fail to estimate the mean depth and volume of glacial lakes at a large scale, such as HKH, mainly because the majority of these models work on a single lake and associated characteristics; these models can't incorporate the complex nature of glacial lake characteristics at a large scale.

Whereas empirical equations, mainly based on the area-scaling method, have been widely used for large-scale assessments **(Huggel et al., 2002; Cook and Quincey, 2015; Shugar et al., 2020; Zhang et al., 2024)**. Most of these empirical equations are based on the positive relationship between area, depth, and volume **(Cook and Quincey, 2015; Qi et al., 2022; Zhang et al., 2024)**. However, area, depth, and volume have a non-linear relationship with each other and should be employed after careful evaluation **(Cook and Quincey, 2015; Muñoz et al., 2020)**. Furthermore, the relationship is a dynamic one, prone to change under the ongoing climate change **(Zhang et al., 2024)**. Therefore, HKH, being the highest mountain system in the world, requires specific empirical equations for estimating the mean depth and volume of glacial lakes. Several researchers in the past have attempted to develop these equations for HKH **(Sakai, 2012; Wang et al., 2012; Fujita et al., 2013; Patel et al., 2017; Sharma et al., 2018; Qi et al., 2022)**. However, all of these equations were built on focusing on a particular part of HKH, primarily the central Himalaya. This led to misleading results. Therefore, there is an urgent need for the development of new empirical equations, which are based on samples from the whole HKH region, so that glacial lake depth and volume can be estimated with greater accuracy.

2 Framework and Objectives

2.1 Conceptual background and institutional framework

The research for this thesis was conducted within the "Spatio-temporal Development of Glacial Lakes and Associated Flood Risks in Indus, Ganga, and Brahmaputra (IGB) Integrated River Basin" project, which was funded by the German Academic Exchange Service (DAAD) (Doctoral Programmes in Germany, 2020/21 (57507871)). The research endeavour was overseen by Prof. Dr. Udo Schickhoff (University of Hamburg, first supervisor) and Dr. Suraj Mal (Jawaharlal Nehru University, second supervisor). The objective of the interdisciplinary project was to: analyse the changes in glacial lake characteristics between 1990 and 2020 (at the decadal level), develop new empirical equations to estimate the mean depth and volume of glacial lakes in the HKH region, and develop an updated glacial lake inventory for the HKH region at the sub-basin level for three major rivers (Indus, Ganga, and Brahmaputra).

In order to accomplish these objectives, the current study examines the spatial and temporal evolution of glacial lakes in the HKH region at the sub-basin level, utilising both primary and secondary data sources.

2.2 Objectives

The following objectives were pursued in this thesis to address the existing research gaps associated with the expansion of glacial lakes and associated risks:

1) Analyse the spatio-temporal evolution of glacial lakes in Indus, Ganga and Brahmaputra (IGB) basin:

- To develop an updated glacial lake inventory for the IGB basins at the sub-basin level (*Article I*);
- To examine the growth of glacial lakes between 1990 and 2020 at the sub-basin level (*Article I*);

2) Identify the factors for evolution of glacial lakes in the IGB basins

- To understand the evolving relationship between glaciers and glacial lakes due to global warming (*Article I & III*);

- To understand the relationship between climate change and evolution of glacial lakes (*Article I & III*)

3) Develop Empirical equations for mean depth and volume estimation

- To create new empirical equations for estimating mean depth and volume of glacial lakes based on combination of in-situ and literature based bathymetric surveys (Article II)
- To examine the role of lake characteristics influencing the relationship between lake area, depth and volume (*Article II*)

4) Estimate the mean depth and volume of glacial lakes

- To estimate the mean depth and volume of individual glacial lakes at the sub-basin level in the HKH (*Article II & IV*)

3) Material and Methods

3.1 Study area

Spatial extend

The HKH is one of the youngest mountain systems in the world, extending from 16°N to 39°18'N and 60°51'E to 105°1'E, latitude and longitude, respectively. HKH is a trans-political boundary mountain system, which is spread over 8 countries (Afghanistan, Bangladesh, Bhutan, China, India, Myanmar, Nepal, and Pakistan) and a total area of ~4.2 million km^2. The north-to-south extent of the region is ~2,500 km, and east-to-west extent is about ~4,200 km. Among the HKH, Himalayan range between the Nanga Parbat (Indus basin, west) and Namche Barwa (Brahmaputra basin, east) is the longest range, with an approximate length of ~2,500 km.

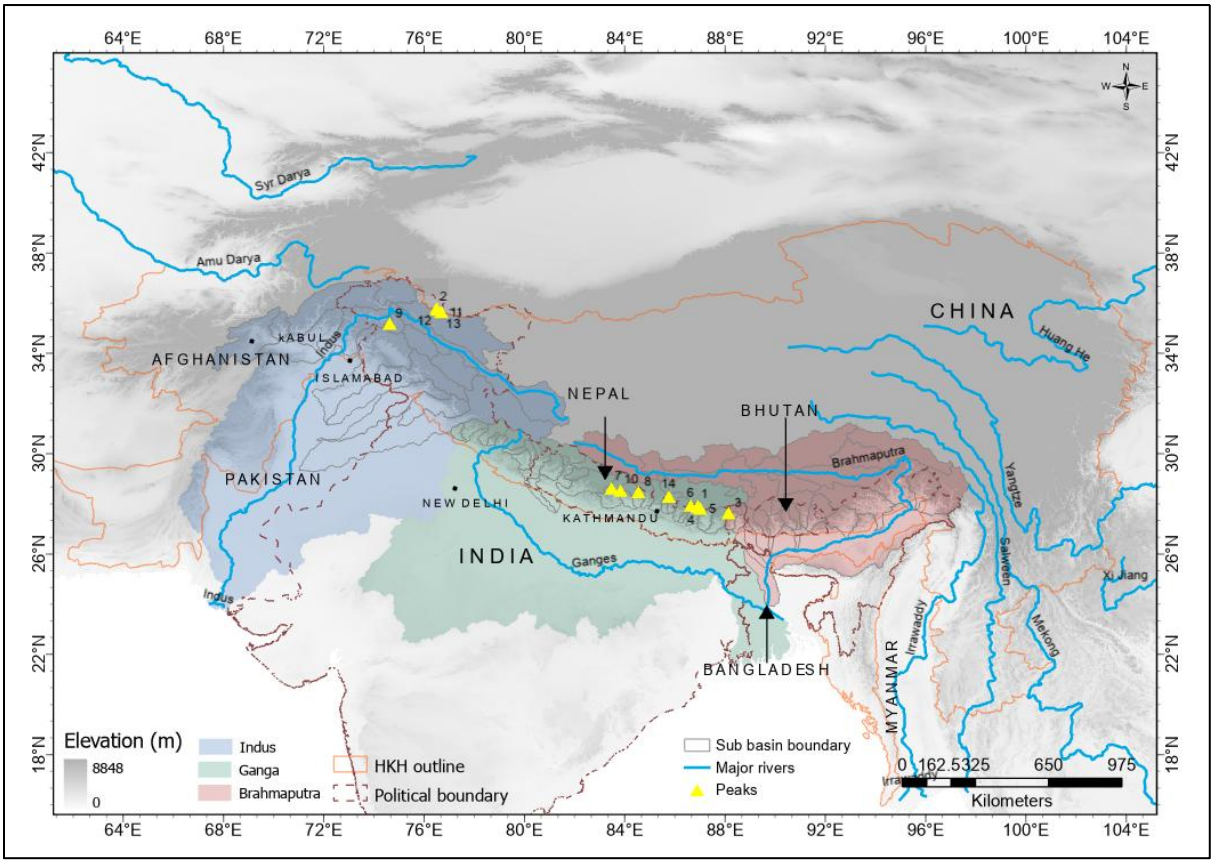

Fig. 4: Map of HKH showing major rivers originating in the region, along with catchment area of Indus, Ganga and Brahmaputra. The yellow triangles shows all eight thousander peaks of the world. The numbers of the peaks show their rank in terms of highest peaks in the world (S1 Table 1) (source: created by author).

Physiography

The HKH mountain system represents a complex physiography, which emerged due to the subsidence of the Indian plate under the Eurasian plate **(Bose, 1972)**. However, different ranges of HKH evolved or originated at different points in time (~115 Ma to ~50 Ma) **(Owen et al., 2024);** the HKH is primarily composed of sedimentary rocks but also consists of igneous and metamorphic rocks in small proportions **(Gansser, 1964)**. It is the highest mountain system of the world, which agglomerates all the 7000+ m asl peaks of the world, including 14 peaks over 8,000 m asl in the world **(Sharma et al., 2019)**. The average elevation of HKH is 3,265 m asl, whereas the highest elevation is 8,848 m (Mt. Everest) and the lowest elevation is ~0 near the southern margins of the region. Based on the elevation and geographical setting, HKH is divided into several ranges. The Himalaya is the longest range among them. Furthermore, the Himalaya is divided into the following ranges: (i) Shiwaliks, (ii) the lower Himalaya, (iii) the greater Himalaya, and (iv) Trans-Himalaya **(Negi et al., 1998)**.

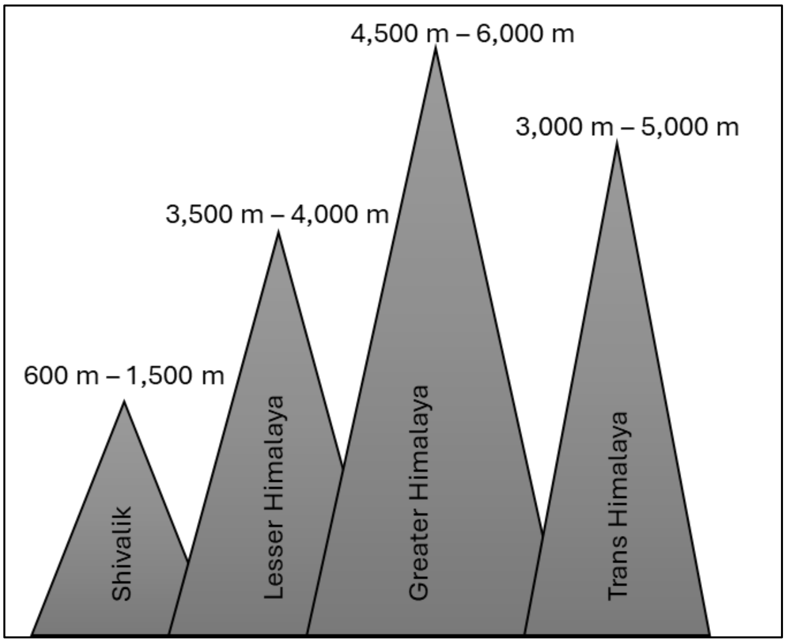

Fig. 5: *Diagram showing mean elevation range in different mountain ranges of Himalaya (source: created by author).*

Climate

The climate of HKH is primarily dominated by the Indian Summer Monsoon (ISM); however, because of the large geographical extent and orographic effect, there are huge variations in different climate variables within the HKH **(You et al., 2017; Krishnan et al., 2019)**. Within the few hundred kilometres within the HKH, one can experience extreme cold and dry climatic conditions and hot and humid conditions in the northwestern and southwestern sections of the HKH, respectively. Because of a lack of monitoring stations and undulating topography, it is very difficult to continuously monitor the climatic conditions of the region with high accuracy. In general, there is a south-to-north gradient in the annual average temperatures **(Singh et al., 2011; Krishnan et al., 2019)**, whereas longitudinally, there is no significant gradient in the annual average temperatures. During the summer months, the southern margins of the study domain can experience a temperature of as high as ~40°C, whereas higher elevations (>5000 m asl) can still observe a sub-zero temperature in the summer months, within a distance of a few hundred kilometres (e.g., between Haridwar and Leh). In winters, the temperature in the high elevations (>8000 m asl) can dip down ~-40°C **(Singh et al., 2011; Krishnan et al., 2019)**. This shows an extremely high annual range of temperature (~80°C).

In terms of the precipitation, the region shows huge variation. In general, there is an east-to-west gradient. The southeastern margins of the HKH receive >3,000 mm of precipitation per year, whereas in certain areas of the northwestern margin, the precipitation is <200 mm per year **(Singh et al., 2011; Krishnan et al., 2019; Mishra et al., 2023)**. The majority of the precipitation is received during the summer months (**Krishnan et al., 2019; Mishra et al., 2023)** and is brought by ISM **(Krishnan et al.,**

2019; Mishra et al., 2023). Furthermore, the majority of the summer precipitation is in liquid form **(Krishnan et al., 2019)**. The northwestern HKH also received winter precipitation brought mainly by western disturbances **(Dimri et al., 2015; Dimri et al., 2021)**, and the majority of precipitation in the winter months is in solid form **(Dimri et al., 2015; Krishnan et al., 2019)**. The southern slopes of the HKH receive higher precipitation as compared to the northern slopes because of the orographic nature of the HKH **(Mishra et al., 2023)**.

Cryosphere

The HKH is also known as the "**third pole" (Zhang et al., 2015; Sharma et al., 2019)** because the region has the highest concentration of glaciers outside the polar regions **(Zhang et al., 2015)**. However, the glaciers in the HKH are not classified as ice sheets but as mountain glaciers, mainly because of their relatively smaller size (confined to valleys where the rate of snowfall accumulation is higher than the melting rate of the glaciers) **(Bolch et al., 2019)**. The snow cover area during winter varies between 951,000 km² and 1,390,000 km², and in summers it ranges between 388,000 and 481,000 km² (https://icmod.org/who-we-are/the-hindu-kush-himalaya). The cryosphere also includes permafrost and glacial lakes. Total glacier area can extend up to 87,340 km² **(**https://www.icimod.org/who-we-are/the-hindu-kush-himalaya/**).** The cryosphere of HKH is the source of several major rivers of Asia, including the Indus, Ganga, and Brahmaputra.

Due to ongoing climate warming, the glaciers of HKH are retreating at a rapid rate **(Bolch et al., 2012; Bolch et al., 2019)**. The rate of glacier mass loss increased by 65% between the time period of 2000-2009 (-0.17 meters water equivalent per year) to -0.28 meters water equivalent per year (2010-2019) **(ICIMOD, 2023)**. However, the rate of retreating is not uniform along the HKH (**Bolch et al., 2019; Kulkarni et al., 2021)**. The eastern Himalayas observed the highest negative mass balance among the HKH **(ICIMOD, 2023)**. The Karakoram range in the northwestern part of HKH used to indicate stable or slight gains in the glacier mass between 2000 and 2009 **(Gardelle et al., 2012; 2013)**; however, between 2010 and 2019, this region also experienced wastage of between -0.09±0.04 meters (water equivalent per year) **(Xu et al., 2023)**.

Glacial lakes and Glacial Lake Outburst Floods

Glacial lakes

Glacial lakes are an important component of the cryosphere of HKH **(Bolch et al., 2019)**. It is now well established that rapid melting of glaciers due to the ongoing increase in the mean annual temperatures in the HKH is causing the expansion of existing glacial lakes and the formation of new glacial lakes **(Hock et al., 2019; Schickhoff et al., 2022)**. Therefore, it is of immense importance to continuously monitor the evolution of these glacial lakes. The advent of remote sensing and GIS had helped the researchers immensely in mapping and monitoring the glacial lakes **(Zhang et al., 2015; Wang et al., 2020; Li et al., 2022)**.

There are several studies that attempted to map and monitor the changes in the glacial lakes in the HKH or parts of it **(Mool et al., 2001a & b; Campbell & Pradesh, 2005; Ives et al., 2010; Nie et al., 2013; Worni et al., 2013; Zhang et al., 2015; Nie et al., 2017; Bhambri et al., 2018; Maharjan et al., 2018; Bolch et al., 2019; Mal et al., 2020; Shugar et al., 2020; Wang et al., 2020; Chen et al., 2021; Rao et al., 2021; Zheng et al., 2021; Li et al., 2022)**. However, different studies produced different results. This is mainly due to the employment of different data sources and methodologies **(Table 6)**.

Table 6: *Selected previous glacial lake inventories developed since 2000.*

Authors	Study area	Data source	Method	Criteria	Number	Area (km^2)	Inventory year
Mool et al (2001a)	Nepal	Topographic maps, Landsat (MSS/TM), IRS-1D, and SPOT	Manual	Elevation: ≥ 3,500 m asl	2,323	75.64	2000
Mool et al (2001b)	Bhutan	Topographic maps, Landsat (MSS/TM), IRS-1D, and SPOT	Manual	Elevation: ≥ 3,500 m asl	2,674	106.8	2000
Campbell & Pradesh (2005)	China, India & Pakistan	Topographic maps, Landsat TM and ETM+, IRS 1C LISS III, CBERS, and ASTER	Semi-automated	Elevation: ≥ 3,500 m asl	3,866	613.95	-
Ives et al (2010)	Selected parts of HKH*	Topographic maps, Landsat TM and ETM+, IRS 1C LISS III, CBERS, and ASTER	Semi-automated	Elevation: ≥ 3,500 m asl	8,790	801.83	1999-2004
Xin et al (2012)	Chinese Himalaya	Topographic maps, Landsat (TM) and ASTER DEM	Manual mapping	NA	1,680	215.27	2000
Nie et al (2013)	Central Himalaya	Landsat (TM/ETM+)	Semi-automated	MMU** ≥ 0.0081 km^2	1,314	197.22	2010
Worni et al (2013)	Indian Himalya	LANDSAT ETM+	Automated mapping	MMU ≥ 0.01 km^2	251	-	2000
Zhang et al (2015)	HMA	LANDSAT (TM/ETM+) and SRTM DEM	Manual mapping	MMU ≥ 0.003 km^2; Within 10 km from glacier	5,701	682.4	2010
Nie et al (2017)	Himalaya	Landsat (TM/ETM+/OLI)	Automatic object-oriented mapping and manual correction	MMU ≥ 0.0081 km^2	4,950	455.3	2015
Bhambri et al (2018)	Himachal Pradesh, India	Landsat OLI, Resourcesat-1&2, and SRTM DEM	Automated mapping	MMU ≥ 0.0005 km^2	958	9.6	2011-2013

Maharjan et al (2018)	HKH	Landsat TM/ETM+, and SRTM DEM	Automated mapping with manual inspection	MMU ≥ 0.003 km^2	2,5614	1444	2005
Mal et al (2020)	Eastern Himalaya	Landsat OLI	Manual mapping	MMU ≥ 0.001 km^2	1,532	93.7	2016-2018
Shugar et al (2020)	HMA	Landsat TM/OLI, ASTER GDEM2, and SRTM DEM	Automated mapping	MMU ≥ 0.05 km^2; Slope < 10°	2,037	444	2010-14
Wang et al (2020)	HMA	Landsat (TM/ETM+/OLI)	Manual	MMU	3,0121	2080.12	2018
Chen et al (2021)	HMA	Landsat OLI	Automated	MMU ≥ 0.0081 km^2; Slope < 10°; Hillshade factor < 0.25; and distance from glacier	1,5348	1519.58	2017
Rao et al (2021)	Ganga basin	Resourcesat - 2	Manual	MMU ≥ 0.0025 km^2	4,707	206.65	2016-18
Zheng et al (2021a)	HMA	Landsat (TM/ETM+/OLI), and SRTM DEM	Semi - automated	MMU ≥ 0.0036 km^2; and within 10 km from glacier	2,6633	1968.8	2015
Li et al (2022)	HKH	Landsat (TM/ETM/OLI) and SRTM DEM	Semi - automated	MMU ≥ 0.0036 km^2; and within 10 km from glacier	1,1809	1073.77	2020

* Includes parts of Bhutan, China, India, Nepal and Pakistan;

** MMU = Minimum mapping unit

GLOFs

GLOFs are sudden releases of large volumes of water from glacial lakes due to either dam breaches or overtopping mechanisms, which are caused by several trigger events (**Table 7)** and have the potential to cause devastation in downstream regions **(Zheng et al., 2021; Taylor et al., 2023)**. HKH being heavily populated, as ~240 million people live in the region **(Taylor et al., 2023)**, is one of the most populated mountain systems in the world **(ICIMOD, 2023; Taylor et al., 2023; Zhang et al., 2024)**. The continuous expansion of glacial lakes, coupled with the huge population of HKH, has increased the potency of GLOFs in the region **(Bolch et al., 2019; ICIMOD et al., 2023; Taylor et al., 2023; Zhang et al., 2024)**.

GLOFs are not a new phenomenon in the HKH region **(Lützow et al., 2023)**. However, due to the lack of monitoring tools and rugged terrain, it was difficult to record them in the past **(Nie et al., 2018; Lützow et al., 2023)**. Since the early 1990s, with the availability of remotely sensed data for the region, along with the Information and Technology (ICT) revolution, several researchers and organisations have made serious attempts to understand the processes of GLOFs **(Nie et al., 2018)**. However, because the majority of these events in the HKH region take place in inhospitable conditions, it is extremely difficult to understand them completely. Therefore, continuous attempts should be made to extend our understanding of GLOF processes.

***Table** 7: GLOF mechanisms and their potential trigger events.*

Mechanisms	Trigger events	Impact
Dam breach	Ice core melting in the moraine dam	Degradation of moraine dam; Encourages pipping in the moraine dam; and Reduced dam height.
	Displacement of ice-dam due to the movement of damming glacier	Deforming of ice dam
	Pipping through the moraine dam	Degradation of moraine dam; and Reduction in the strength of glaciers.
	Seismic activity	Destabilizing the moraine or ice dams; Triggering mass movement of surrounding material which falls in the glacial lake causing displacement waves.
Overtopping	Ice and rock avalanches	Causing overtopping waves; Increases hydrological stress on the dam
	Excessive precipitation	Sudden increase in water level; Increases hydraulic stress; and Causes moraine degradation through additional erosion
	Sudden release of excessive water from upstream smaller glacial lakes	Sudden increase in water level; Overtopping waves; and Increase in the hydraulic pressure.

Furthermore, several researchers have attempted to map the historical GLOF events in the HKH or parts of it based on the existing knowledge **(Veh et al., 2018; Nie et al., 2018; Veh et al., 2019; ICIMOD, 2022; Lützow et al., 2023; Shrestha et al., 2023)**. However, different studies provided different numbers of reported GLOF events; this is mainly due to the application of different methodologies and the availability of different data sources **(Table 8)**.

***Table 8:** Selected GLOF inventories developed by researchers and organizations since 2000.*

Inventory name/source	**Study area**	**Number of GLOFs recorded**	**Time period**
Nie et al. (2018)	Himalaya	62	1930 – 2018
Veh et al. (2018)	Himalaya	32	1988 - 2016

Veh et al. (2019)	Himalaya	40	1935 – 2017
ICIMOD (2022)	HKH	736	1533 – till present
Lützow et al. (2023)	HMA	569	1900 – 2022
Shrestha et al. (2023)	HMA	697	1833 - 2022

Major rivers and their tributaries

Rivers are carriers of freshwater from upstream towards downstream, which enables civilisations to evolve and supports local flora and fauna. The HKH is the source of headwater for 10 major transboundary rivers (Amo Darya, Brahmaputra, Ganga, Indus, Irrawaddy, Mekong, Salween, Tarim, Yangtze, and Yellow) **(Fig. 4) (Table 9)**, which provides freshwater for supporting the lives of ~240 million people in the HKH and ~1.65 billion people in the downstream regions **(ICIMOD, 2023)**. Among these, the Ganga basin is the most populous river basin in the world **(ICIMOD, 2023) (Table 9)**.

Table 9: *Major rivers of the HKH.*

Name of the rivers	**Countries**	**Length (km)**	**Basin area (km^2)**	**Population (in million)**
Amo Darya	Afghanistan, Kazakhstan, Kyrgyzstan, Tajikistan, Turkmenistan, and Uzbekistan	~2,540	590,939	~80
Brahmaputra	Bhutan, Bangladesh, China, and India	~2,900	~651,334	~130
Ganga	Bangladesh, India, and Nepal	~2,525	~1,320,000	~650
Indus	Afghanistan, China, India, and Pakistan	~3,180	~1,165,000	~268
Irrawaddy	Myanmar	~2,170	~404,100	~51
Mekong	China, Cambodia, Lao PDR, Myanmar, Thailand and Vietnam	~4,800	~795,000	~70
Salween	China, Myanmar, and Thailand	~3,289	~324,000	~10
Tarim	China	~1,321	~435,500	~25.85
Yangtze	China	~6,300	~1,800,000	~400
Yellow	China	~5,464	~752,000	~120

3.2 Data collection

Glacial lake mapping

To map the glacial lakes and monitor the growth of glacial lakes, we employed 483 satellite images obtained from the Landsat satellite mission (TM/OLI) between 1990 and 2020 (**https://earthexplorer.usgs.gov/**) **(Table 10)**. In the past, researchers and organisations have used several other data sources for the development of glacial lakes, like IRS, SPOT, topographic maps, Sentinel, aerial photographs, and others. Some of these data sources, like Sentinel and IRS, have higher spatial resolution than Landsat satellite images; however, the Landsat satellite mission, being the oldest running Earth observation, provides an immense advantage for temporal analysis and a better understanding of the evolution of glacial lakes.

Table 10: *Details of satellite images used in the study.*

Year	**Satellites**	**Sensors**	**Spatial Resolution**	**Satellite images (n) used for individual lake inventory**
1990 (±3)	Landsat 5	Thematic Mapper (TM)	30 m	148
2000 (±3)	Landsat 5	Thematic Mapper (TM)	30 m	138
2010 (±3)	Landsat 5/8	Thematic Mapper (TM)	30 m	88
2020 (±3)	Landsat 8	Operational Land Imager (OLI)	30 m	109

Furthermore, in addition to the Landsat satellite images, DEM using SRTM (Ver. 4) (**https://earthexplorer.usgs.gov/**) for reducing misclassification of glacial lakes due to shadows and surrounding land use. In addition, SRTM DEM (Ver. 4) also helped us in gathering valuable information about lake characteristics such as lake elevation and lake aspect.

Glacier

Glacial lakes are a byproduct of glacial movement and melting. Therefore, it is of immense importance to understand the ongoing relationship between glaciers and glacial lakes. To address this, we used the RGI glacier inventory (Ver. 7) **(RGI 7.0 Consortium, 2023)**. We used the glacier inventory to calculate the distance between glaciers and glacial lakes.

Climate

Asian Precipitation Highly Resolved Observation Data Integration Towards Evaluation (APHRODITE) (https://www.chikyu.ac.jp) mean annual temperature and precipitation data (1981-2015) was employed to understand the relationship between changing climate and glacial lake evolution in the Dibang Valley district, Arunachal Pradesh, India. APHRODITE is a gridded dataset, which is specifically designed for Asia. The spatial resolution of APHRODITE is 0.25° (~25 km). Furthermore, to assess the impact of changing climate on glacial lakes in Indus, Ganga, and Brahmaputra (IGB), we employed Climatologies at High Resolution for the Earth's Landsat Surface Areas (CHELSA) (https://chelsa-climate.org/) mean annual temperature and mean annual precipitation data (1990–2020). The CHELSA dataset was chosen instead of APHRODITE as CHELSA provides higher spatial resolution (~1 km) and incorporates orographic effects while modelling the climatic parameters.

Glacial lake bathymetry

In the present study, we attempted to collect bathymetric surveys of 8 glacial lakes in the western Himalaya (Indus) with the aim of developing new empirical equations representing the whole HKH. However, due to the bad weather conditions and COVID-19, only four were completed **(Fig. 6)**. The four lakes that were completed were (a) Gangabal Lake (2021), (b) Kela Tsho (2022), (c) Lato Lake (2023), and (d) Gya Lake (2023) **(Fig. 6)**. Primary bathymetric data was collected in the month of September, as it marks the end of the ablation season, which is characterised by the minimum snow extent, cloud cover, calm weather, and full extent of glacial lakes. The primary criteria for selecting these glacial lakes were (a) the glacial origin and (b) the distance from the parent glaciers (< 10 km). A remote-controlled vehicle with Garmin's echoMAP 52dv and GT20-TM transducer In addition, a carefully curated dataset of 21 glacial lakes was collected from the previous studies for the Ganga and Brahmaputra basins **(S2 Table 2)**. Therefore, a dataset of 25 glacial lakes (4 based on primary bathymetric data and 21 based on literature-based bathymetric data) was used to develop the empirical equations to estimate the mean depth and volume of glacial lakes **(S2 Table 2)**.

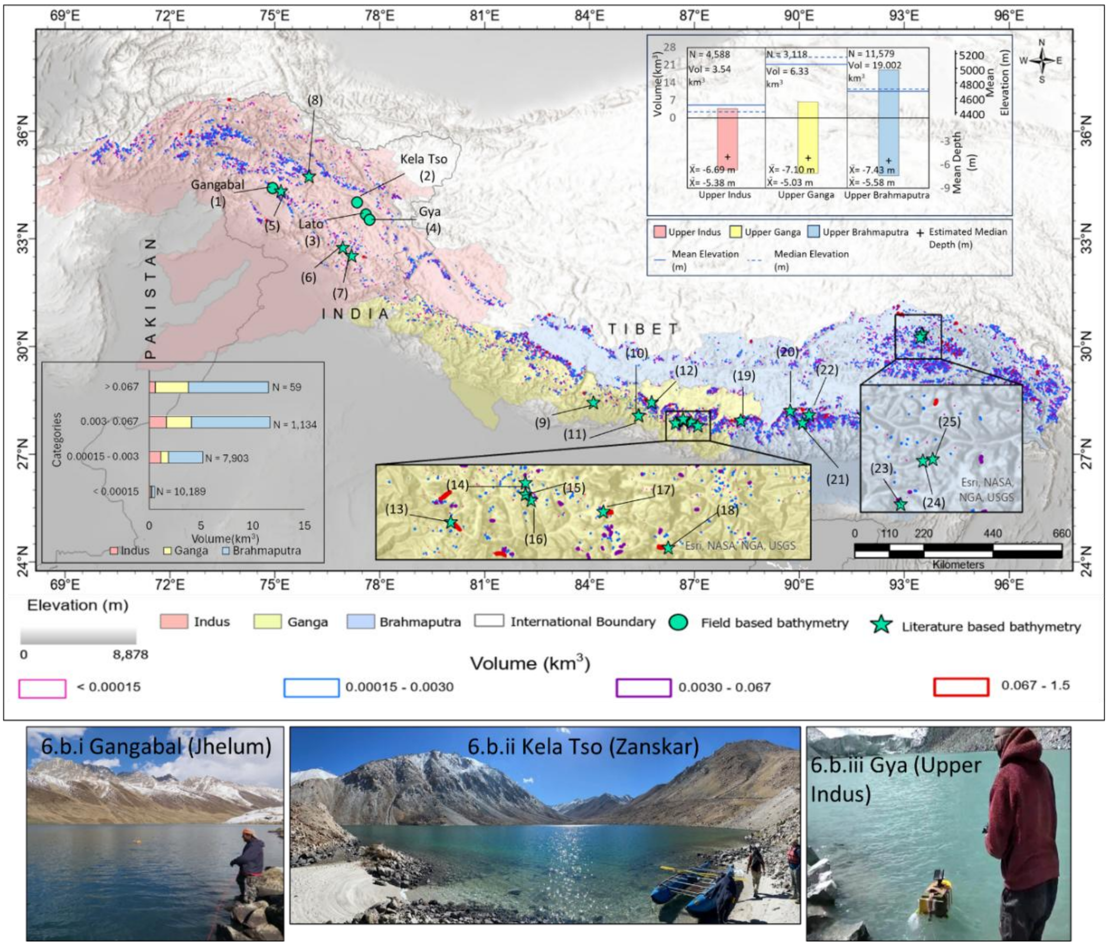

Fig. 6: *Spatial distribution of glacial lakes in the IGB basins. The different colors of glacial lakes on the map shows the volume of glacial lakes (km^3). The inset figure shows the total volume (km^3) (primary axis), average estimated mean depth (m) (secondary axis), and mean depth (m). The + symbol shows*

the estimated median depth at major basin level. Solid circles and star symbols for glacial lakes on the map show field-based and literature-based bathymetry, respectively (S2 Table 2). ***Fig. 6b*** *shows the bathymetric surveys of glacial lakes, surveyed between September 2021 and September 2023, where (a) Gangabal Lake was surveyed using remote-controlled vehicles and ropes. Ropes were used to complete the inaccessible sections for remote-controlled vehicles and safety against the strong waves and winds around the lake; (b) a survey of Kela Tso Lake was completed in September2022 using a Catamaran raft; and (c) a survey of Gya Lake using the remote-controlled vehicle in September 2023 (source: updated from Article II).*

3.3 Data analysis

3.3.1 Glacial lake mapping (Article I)

Glacial lake mapping can be classified into three categories: (i) manual mapping **(Zhang et al., 2015; Mal et al., 2020; Wang et al., 2020; Rao et al., 2021)**, (ii) automated mapping (**Shugar et al., 2020; Chen et al., 2021)**, and (iii) semi-automated **(Ives et al., 2010; Nie et al., 2017; Maharjan et al., 2018; Li et al., 2022) (Table 6)**. Manual mapping of glacial lakes is based on the visual interpretation of satellite images/aerial photographs by a human. Based on the skill of the individual, manual mapping can be highly accurate in identifying and mapping glacial lakes. However, it is labour, time, and cost intensive. On the other hand, automated mapping, still in developing stages for mapping of glacial lakes, is a labor-, time-, and cost-effective way but can lead to moderate levels of accuracy in the presence of shadows, cloud cover, snowfall, and mixed land use. Whereas semi-automated mapping of glacial lakes, which combines benefits of both manual mapping (ensuring high accuracy) and automated mapping (saving time and resources), is regarded as the best way to identify and map glacial lakes **(Raj et al., 2013; Li et al., 2022; Zhang et al., 2023)**. Therefore, in the present study, we developed a semi-automated mapping framework to map glacial lakes **(Fig. 7)**.

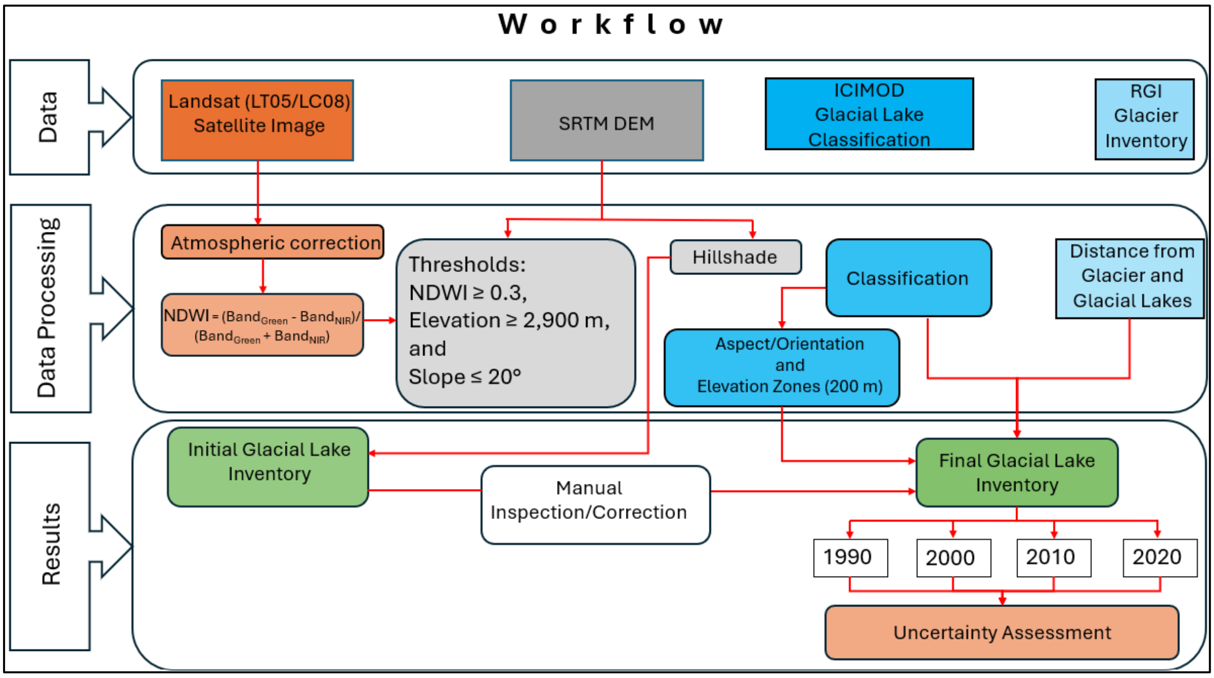

Fig. 7: *Methodological framework of glacial lake mapping used to prepare glacial lake inventories for IGB basins, HKH (source: Article I).*

Once all the Landsat satellite images were collected, atmospheric correction was performed on all (n = 483) satellite images. Atmospheric corrections reduce the impact of atmospheric gases and aerosols and help in deriving correct surface reflectance values, which are necessary for high-accuracy temporal analysis. Once the atmospheric correction was completed, the next step was to generate water masks for 1990, 2000, 2010, and 2020 using the Normalised Difference Water Index (NDWI) **(Eqn. 1)**. NDWI is a band ratioing method based on green and Near InfraRed (NIR) bands of satellite images, and the values range between -1 and 1 **(Gao, 1996)**.

$$NDWI = \frac{Brand_{Green} + Brand_{NIR}}{Brand_{Green} + Brand_{NIR}} \qquad (1)$$

Once the NDWI (≥ 0.3) was calculated for the IGB basins using Landsat images, the optimal NDWI threshold was employed to generate the water mask for IGB. Once the water mask was generated, the next step was to employ the elevation threshold (elevation ≥ 2,900 m asl). The elevation threshold was employed for the purpose of differentiating between glacial lakes and non-glacial lakes in the study domain. In the past, different studies have used different elevation thresholds to differentiate glacial lakes from non-glacial lakes **(Mool et al., 2001a & b; Campbell et al., 2005; Ives et al., 2010)** based on the study area and purpose of the study. In the present study, we used the elevation threshold of ≥ 2,900 m asl because the snouts of several glaciers were found at ~2,900 m asl in the HKH region, especially in the northwestern HKH. Furthermore, in addition, a slope threshold of ≤20° is used because glacial lakes require a stable slope for the storage of melted water collected from parent glacier(s). After employing the above-mentioned thresholds, the next was to select the MMU. Selecting the correct MMU is a critical step in identifying and mapping glacial lakes with high accuracy. According to previous studies, in the case of Landsat images, at least 4 pixels (0.0036 km²) are required for correct detection of the smallest water body **(Mal et al., 2020; Li et al., 2022)**. Therefore, all glacial lakes ≥ 0.0036 km², which fulfil the above-mentioned threshold, are mapped. Once the initial glacial lake inventories for 1990, 2000, 2010, and 2020 were developed after applying the above-mentioned thresholds, the next step was to visually inspect each and every glacial lake using Google Earth Pro for correcting misidentification of glacial lakes that were induced because of automated mapping. Once each and every lake was inspected and the misidentified lakes/pixels were corrected, the final glacial lake inventories of 1990, 2000, 2010, and 2020 were finalised.

3.3.2 Uncertainty assessment of glacial lake mapping (Article I)

Glacial lakes mapped using satellite imagery, irrespective of the method employed, are prone to uncertainties up to ± 1 pixel, depending on the spatial resolution and quality of the satellite image **(Salerno et al., 2012; Chen et al., 2021)**. It is well established that automated mapping of glacial lakes can induce an error of up to 1 pixel while demarcating the glacial lake. Whereas in manual and semi-automated mapping, which includes the correction of lake boundaries, the mapping error can be reduced to half a pixel **(Rinzin et al., 2021)**. This can result in error in calculating glacial lake area and other characteristics such as estimating mean depth and volume. Therefore, accounting for the error is of immense importance.

The present study used the uncertainty estimation method developed by **Hanshaw and Bookhagen (2014)**, which is based on the pixelated polygons and performs better on glacial lake polygons based on automated and semi-automated methods, as compared to the manually extracted glacial lake polygons **(Lesi et al., 2022)**. The method proposed by Hanshaw and Bookhagen (2014) performed better with automated and semi-automated methods because the lake boundaries follow the edge of the pixels, while the same may or may not be true about the manually mapped glacial lakes **(Wang et al., 2020)**. Hanshaw and Bookhagen's (2014) equations are as follows:

$$Error\ (1\sigma) = \left(\frac{P}{G}\right) * 0.6872 * \frac{G^2}{2} \qquad (2)$$

Where, G is the cell size of the remote sensing imagery (30 m for Landsat images), P is the perimeter of an individual glacial lake (m), and 0.6872 is the revised co-efficient based on the assumption that area measurement uncertainty follows a Gaussian distribution.

In addition, to the absolute uncertainties have been converted to the relative uncertainties using the following formula:

$$E = \left(Error\frac{(1\sigma)}{A}\right) * 100\% \quad (3)$$

Where, E is the relative error of glacial lakes and A is the total area of glacial lake.

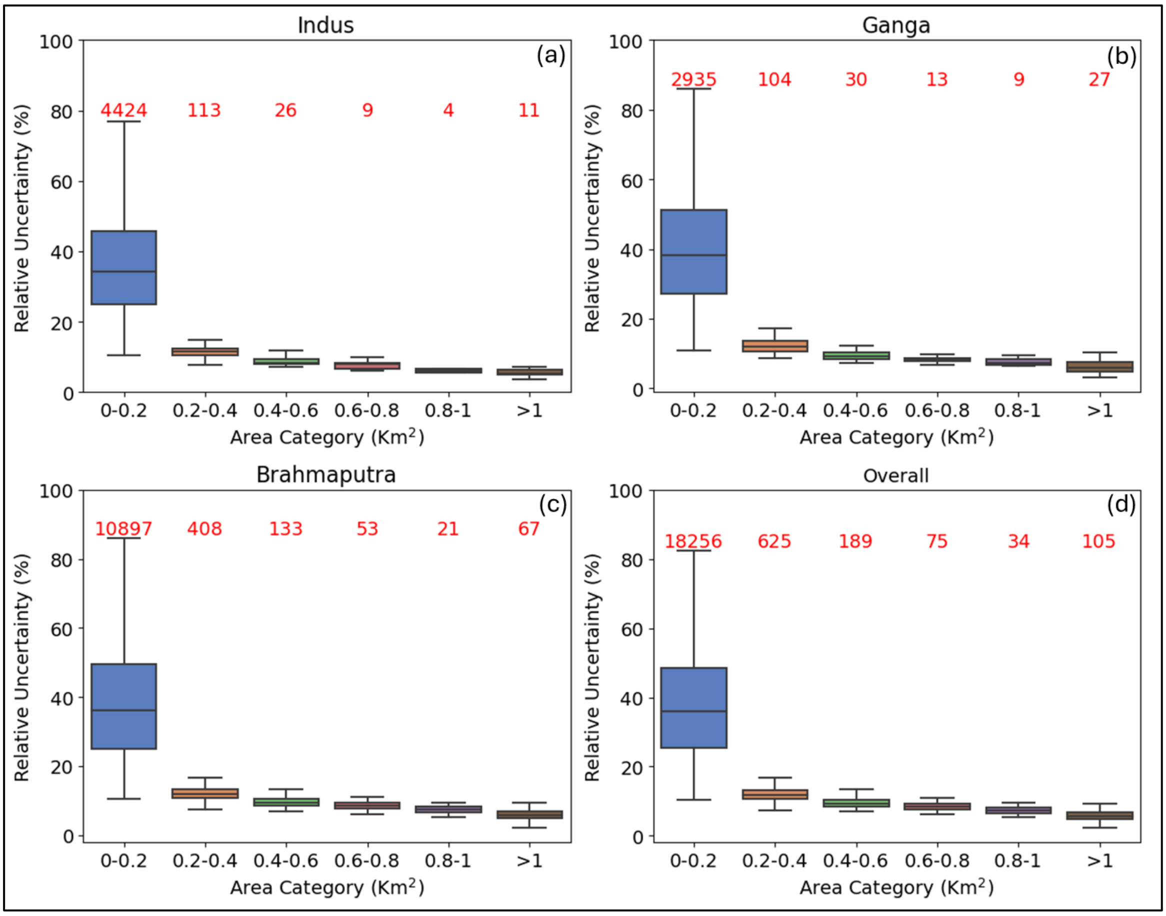

__Fig. 8:__ Box plot representing the relationship between relative uncertainty (%) and area of glacial lakes, where a, b, c, and d show the relationship in the Indus basin, Ganga basin, Brahmaputra basin, and over the entire study domain, respectively (source: Article I).

3.3.3 Processing of field-based bathymetry data (Article II)

The in-situ bathymetry data was processed using Garmin's Homeport software and ArcGIS Pro (Ver. 3.2). Only four glacial lakes with complete bathymetric transects were selected for the processing of the field-based bathymetric data **(Fig. 9)**. The first step was to import the depth waypoints to Garmin's Homeport software from Garmin's echoMAP 52dv sonar. The second step was to export depth waypoints for a lake to a CSV file and clean the lake's depth data for any anomalies. The bathymetry data points were then interpolated using the spline technique, with lake outlines as a barrier, which produced a raster surface of lake depth. This mean depth raster surface was multiplied by lake area to estimate the volume of the glacial lakes.

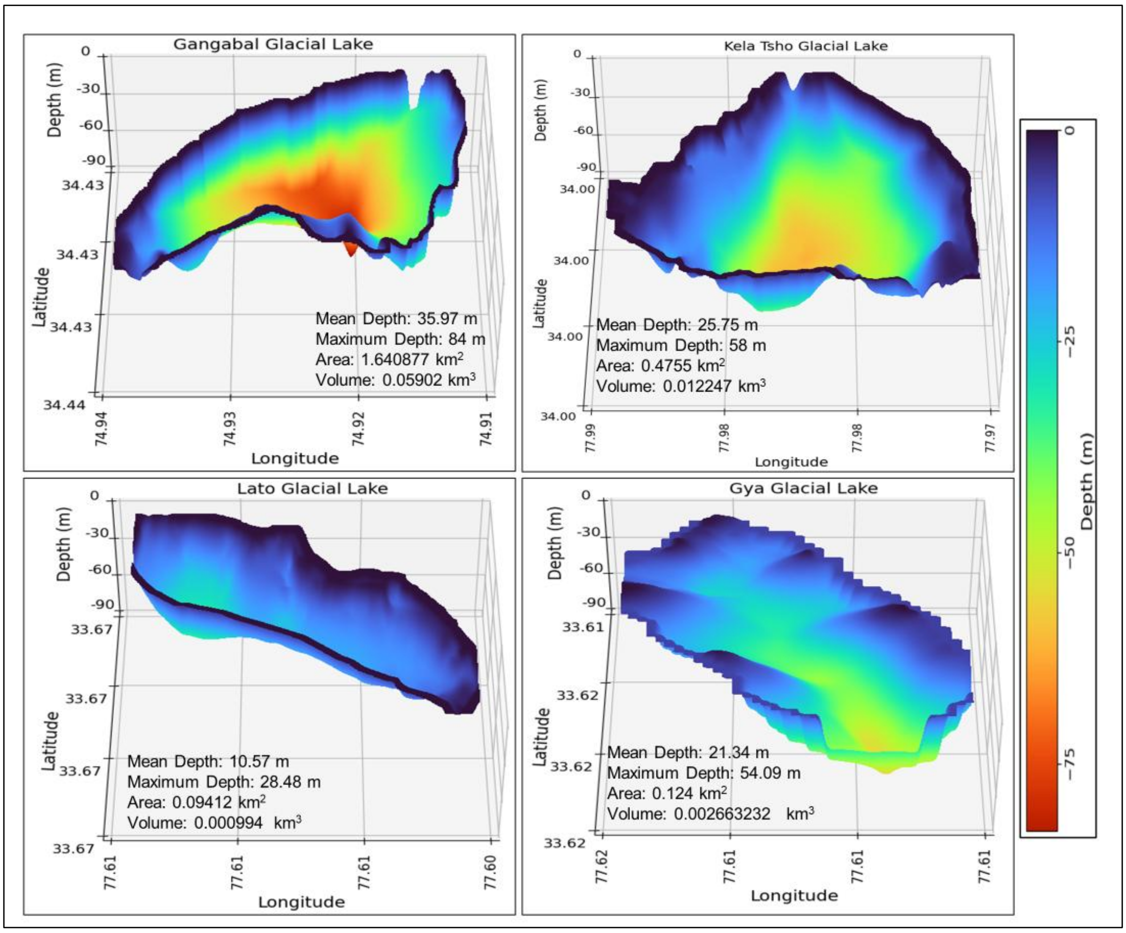

Fig. 9: *Bathymetric maps of surveyed glacial lakes in the Indus basin between September 2021 and September 2023 (source: Article II).*

3.3.4 Empirical equations for estimation of mean depth and volume based on primary and literature based bathymetry (n = 25) (Article II)

Based on the glacial lake inventory developed for 2020 in the present study, there are 19,284 glacial lakes in the upper IGB river basins of HKH. Information on lake characteristics like mean depth and volume of glacial lakes is of immense importance for better water management policies, estimating potential flood volumes, run-off distance, and modelling GLOF scenarios **(Huggel et al., 2002; Fujita et al., 2013; Qi et al., 2022)**. In the present study, we developed 8 empirical equations using power regression between lake depth/volume and lake area for the Indus, Ganga, Brahmaputra, and entire HKH for a better understanding of regional characteristics of the relationship between lake depth/volume and lake area **(Fig. 10)**. Equations (a to d) and (e to h) were developed to estimate the mean depth (m) and volume (m^3) of glacial lakes as a function of lake area, respectively.

The equations were based on following key assumptions:

i) There is a consistent and predictable relationship between surface area, depth and volume of glacial lakes;

ii) Geometric similarities exist between different sizes of glacial lakes; and

iii) Scaling laws accurately describe how men depth and volume change with surface area.

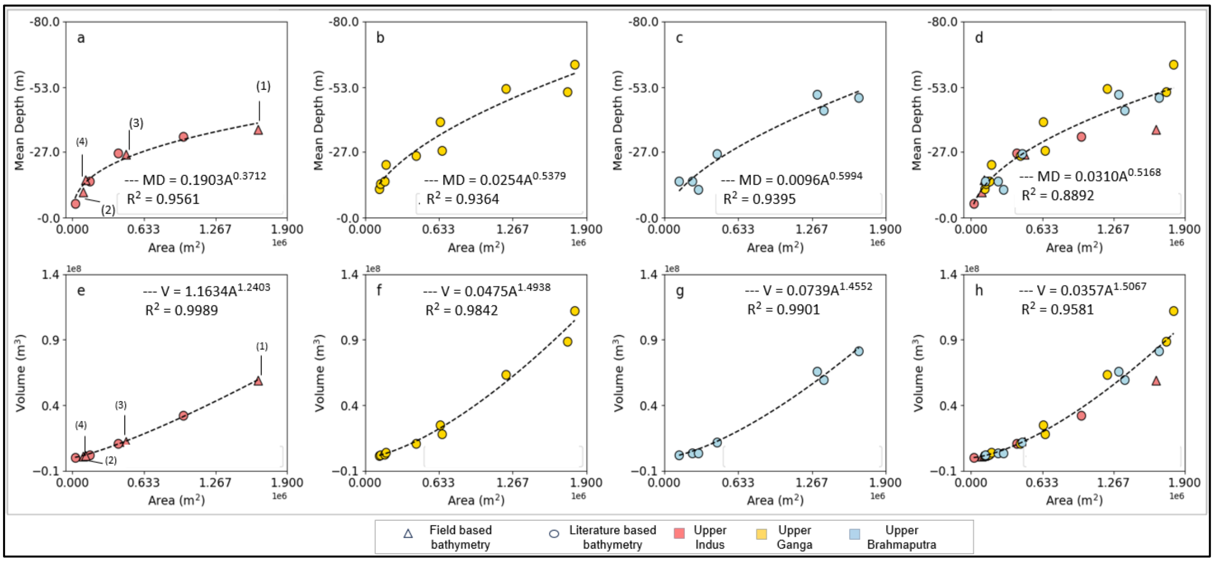

Fig. 10: *Empirical equations for estimating the mean depth and volume of glacial lakes, where sample lakes (a) to (d) were used to develop the equation to estimate the mean depth using glacial lakes (a) in the upper Indus, (b) in upper Ganga, (c) in upper Brahmaputra, and (d) in upper IGB. Similarly, equations (e) to (h) were developed to estimate the volume (m³) using glacial lakes (e) in upper Indus, (f) in upper Ganga, (g) in upper Brahmaputra, and (h) in upper IGB. Field and literature-based bathymetry, as mentioned in S2 Table 2* ***(source: Article II)***

3.3.5 Uncertainty assessment of estimated mean depth and volume (Article II)

The uncertainty assessment of estimated mean depth and volume of glacial lakes is of immense importance, as it provides valuable insights into the reliability of the volume and depth measurements. To improve the precision of our estimated mean depth and volume across the 19,284 glacial lakes, we employed a Bayesian updating approach that integrates both observed data and model estimates **(Gantayat et al., 2024)**. For each metric, we first calculated the RMSE between observed and model-estimated values. The RMSE, representing the typical model error, served as the standard deviation for the prior distribution. The Bayesian update formula we used to obtain the posterior mean ($\boldsymbol{\mu}_{\text{post}}$) and posterior standard deviation (σ_{post}) combines the prior information with observed data as follows:

$$\mu_{post} = \frac{\left(\frac{\mu_{prior}}{\sigma^2_{prior}}\right)+\left(\frac{\mu_{obs}}{\sigma^2_{obs}}\right)}{\left(\frac{1}{\sigma^2_{prior}}\right)+\left(\frac{1}{\sigma^2_{obs}}\right)} \quad (4)$$

$$\sigma_{post} = \sqrt{\frac{1}{\left(\frac{1}{\sigma^2_{prior}}\right)+\left(\frac{1}{\sigma^2_{obs}}\right)}} \quad (5)$$

Where $\boldsymbol{\mu}_{prior}$ and σ_{prior} represent the prior mean and standard deviation from the model estimates, while $\boldsymbol{\mu}_{obs}$ and σ_{obs} are the mean and standard deviation of the observed data **(Gelman et al., 2013)**. For total estimated volume, we scaled the posterior mean to align with the known total estimated volume of 28.8 km^3, yielding a refined 95% confidence interval that captures the full dataset's uncertainty. The uncertainty of the estimated volume using the Bayesian approach was between 28.79 km^3 and 28.99 km^3.

Similarly, for estimated mean depth, we adjusted the posterior mean to reflect the estimated mean depth of 7.20 m across all lakes. This scaling produces a final estimate of mean depth with a 95% confidence interval that represents the range within which the true mean likely falls. The uncertainty of the estimated mean depth using the Bayesian approach was between 4.70 m and 9.70 m. The Bayesian updating approach uses both observed data and model estimates to find the best balance between empirical accuracy and practical constraints. This lets us get strong uncertainty intervals for both the estimated mean depth and volume. The method is particularly valuable for large-scale assessments in remote, data-limited regions where field measurements are challenging, thereby providing a statistically grounded basis for future glacial lake risk assessment **(Carlin and Louis, 2009)**.

4. *Overview of original publications*

4.1 Article I

Kumar, A., Mal, S., Schickhoff, U., & Dimri, A. P. (2025). Basin-scale spatio-temporal development of glacial lakes in the Hindukush-Karakoram-Himalayas. *Global and Planetary Change*, *245*, 104656. doi: https://doi.org/10.1016/j.gloplacha.2024.104656

Abstract

Glacial lakes are expanding exponentially in the cryospheric environment of the Hindukush-Karakoram-Himalayas (HKH). Rapid glacier melting due to an above mean global annual temperature increase in HKH is attributed as the main reason for the expansion of the glacial lakes. The rapid expansion of glacial lakes increases the risk of future Glacial Lake Outburst Floods (GLOFs) events in the HKH.

In the present study, glacial lake inventories for the Indus, Ganga and Brahmaputra (IGB) river basins in the HKH were generated for 1990, 2000, 2010 and 2020 using Landsat (TM & OLI) at the sub-basin level to understand the spatio-temporal and regional patterns of glacial lakes dynamics, elevational evolution, and changes in the typology. We mapped 17,641 glacial lakes (area: 1082.57 ± 192.601 km^2) in 1990, 18,206 (area: 1120.95 ± 198.49 km^2) in 2000, 18,399 (area: 1147.12 ± 201.26 km^2) in 2010, and 19,284 (area: 1191.81 ± 209.21 km^2) in 2020. Between 1990 and 2020, IGB basins showed an increase of 9.31 % in total number and 10.09 % in total area of glacial lakes. In 2020, the Brahmaputra basin had the maximum total area (area: 763.59 ± 132.14 km^2), followed by Indus basin (area: 217.47 ± 43.39 km^2) and the Ganga basin (area: 210.74 ± 33.66 km^2). However, between 1990 and 2020, glacial lakes in the Ganga basin (n: 22.08 %) had the highest growth rate, followed by the Indus basin (n: 14.73 %) and the Brahmaputra basin (n: 4.41 %). In 2020, 76.11 % of glacial lakes were end-moraine-dammed M(e) lakes, followed by other bedrock-dammed B(o) lakes (16.45 %), supraglacial lakes (2.79 %), lateral moraine-dammed M(l) lakes (2 %), cirque B(c) lakes (1.06 %), other moraine-dammed M(o) lakes (0.38 %), and other glacial (O) lakes (1.18 %). Given the rapid growth of glacial lakes in the region along with their likely flood volumes and damage potential in case of their failures, the present study will be of importance for disaster management authorities, an important input for detection of potentially hazardous glacial lakes and for development of mitigation strategies to minimize the impact of potential future GLOF events.

Authors contribution

Atul Kumar: Writing – review & editing, Writing – original draft, Visualization, Validation, Methodology, Funding acquisition, Formal analysis, Data curation, & Conceptualization.

Suraj Mal: Writing – review & editing, Visualization, Validation, Supervision, Resources, Project administration, Methodology, & Conceptualization.

Udo Schickhoff: Writing – review & editing, Supervision, Resources, Project administration, Methodology, Investigation, Funding acquisition, & Conceptualization.

A.P. Dimri: Writing – review & editing, & Methodology.

4.2 Article II

Kumar, A., Mal, S., Schickhoff, U., Allen, S., & Dimri, A. P. (**Accepted)**. Assessing the role of regional characteristics in estimating the volume of glacial lakes in the upper Indus-Ganga-Brahmaputra basins, Hindu Kush Himalaya (Manuscript No: HYDROL60046R1).

Abstract

Glacial lakes have exponentially increased in the recent decades across the world's mountains, particularly in the Hindu Kush Himalaya (HKH), caused by rapid rates of climate change. Consequently, their water volume and hence the hazard potential has also increased in recent decades. Robust water volumes of hazardous glacial lakes located in remote locations are rarely available, limiting the accuracy of current glacial lake outburst flood (GLOF) models that heavily rely on empirical water volume estimation equations. Currently used equations are based on data collected in the European Alps and have limited applicability in the HKH region. Thus, accurately predicting GLOF extents and likely damages in the downstream regions remains a critical challenge in the HKH region. In this study, we developed eight empirical equations to estimate mean depth (4) and volume (4) of glacial lakes in the upper Indus-Ganga-Brahmaputra (IGB) river basins. The study is based on a field-based bathymetric dataset of 25 glacial lakes from different parts of the upper IGB river basins. Separate equations were formulated for the major basins to understand the influence of regional lake characteristics on depth and volume estimations of glacial lakes. Our analysis revealed a non-linear negative relationship between the circularity ratio of glacial lakes and their mean depth, indicating that elongated lakes tend to be deeper than the circular ones. The average circularity ratio of glacial lakes in the upper IGB basins was 0.51 (as of 2020).

We estimated the mean depth and total volume for a dataset comprising 19,284 glacial lakes in the upper IGB basins. The estimated mean depth and total estimated volume of these lakes in 2020 was 7.20 m and 28.88 km^3, respectively. The empirical equations generated in the study based on the field-based bathymetry will be helpful in assessing the GLOF threats from continuously expanding glacial lakes in the upper IGB basins.

Atul Kumar – Writing – original draft, Writing – review and editing, conceptualization, data acquisition, Visualization, funding acquisition, Validation, Methodology, & Formal analysis.

Suraj Mal – Writing – review & editing, Visualization, Validation, Supervision, Resources, Project administration, Methodology, & Conceptualization.

Udo Schickhoff – review & editing, Supervision, Resources, Project administration, Methodology, Investigation, Funding acquisition, & Conceptualization.

Simon Allen – Writing – review and editing, & Methodology.

A.P. Dimri – Writing – review and editing, & Methodology.

2/26/25, 3:44 AM View Letter

Date: 20 Feb 2025
To: "Atul Kumar" atul.sbsc@gmail.com
From: "Journal of Hydrology" noreply_EMsupport@elsevier.com
Subject: HYDROL60046R2: Editor's decision: accepted

Dear Mr. Kumar,

I am pleased to inform you that the manuscript
"Assessing the role of regional characteristics in estimating the volume of glacial lakes in the upper Indus-Ganga-Brahmaputra basins, Hindu Kush Himalaya" (Mr. Atul Kumar) has now been accepted for publication.

Your accepted manuscript will now be transferred to our production department and work will begin on creation of the proof. If we need any additional information to create the proof, we will let you know. If not, you will be contacted again in the next few days with a request to approve the proof and to complete a number of online forms that are required for publication.

Thank you for considering our journal for the publication of your research.

We encourage authors of original research papers to share the research objects – including raw data, methods, protocols, software, hardware and other outputs – associated with their paper. More information on how our open access Research Elements journals can help you do this is available at https://www.elsevier.com/authors/tools-and-resources/research-elements-journals?dgcid=ec_em_research_elements_email.

We appreciate and value your contribution to Journal of Hydrology. We regularly invite authors of recently published manuscript to participate in the peer review process. If you were not already part of the journal's reviewer pool, you have now been added to it. We look forward to your continued participation in our journal, and we hope you will consider us again for future submissions.

With kind regards,

Nandita Basu
Editor
Journal of Hydrology

At Elsevier, we want to help all our authors to stay safe when publishing. Please be aware of fraudulent messages requesting money in return for the publication of your paper. If you are publishing open access with Elsevier, bear in mind that we will never request payment before the paper has been accepted. We have prepared some guidelines (https://www.elsevier.com/connect/authors-update/seven-top-tips-on-stopping-apc-scams) that you may find helpful, including a short video on Identifying fake acceptance letters (https://www.youtube.com/watch?v=o5l8thD9XtE). Please remember that you can contact Elsevier s Researcher Support team (https://service.elsevier.com/app/home/supporthub/publishing/) at any time if you have questions about your manuscript, and you can log into Editorial Manager to check the status of your manuscript (https://service.elsevier.com/app/answers/detail/a_id/29155/c/10530/supporthub/publishing/kw/status/).

#AU_HYDROL#

To ensure this email reaches the intended recipient, please do not delete the above code

---

4.3 Article III

Kumar, A., Mal, S., Schickhoff, U., & Sreekesh, S. (2024). Glacial Lake Dynamics in Dibang Valley District, Arunachal Pradesh, Eastern Himalaya. *Journal Of The Geological Society Of India*, *100*(11), 1521-1530.4.4. doi: https://doi.org/10.17491/jgsi/2024/174012

Abstract

Glacial lakes (GLs) are integral components of the cryospheric environment. Due to the persistent melting of glaciers and steady rise in the annual mean temperatures, GLs are expanding across the Himalayan mountains. Since the 1980s, the eastern Himalaya has observed a steady increase (0.031°C/year) in annual mean temperature, causing rapid glacial melting, formation of new GLs and expansion of existing ones. Therefore, to assess the role of the increasing annual mean temperature on the expansion of GLs in the eastern Himalaya., we generated GL inventories for 1987, 2005 and 2018 for Dibang Valley district, Arunachal Pradesh, in the eastern Himalaya. We used Landsat multi-temporal satellite images along with the ASTER Digital Elevation Model V2 (DEM). Using the Segment Mean Shift (SMS) method, the GL inventories were generated. Our results shows that there were 509 GLs in 2018, whereas 484 in 2005, and 469 in 1987. GLs observed a growth rate of 8.52% in number and 11.13% in area between 1987 and 2018. Most of the GLs in the study area were of Moraine-dammed lakes (MDL) (~56%), whereas Ice-dammed lakes (IDL) showed the highest expansion rate between 1987 to 2018. GL hotspots show a concentration of GLs in the eastern and southern sections of Dibang Valley but new GLs are forming in the north-western and eastern sections of the study area. An increase in annual mean temperature enhanced the glacial melt water, leading to the growth of GLs connected with the glaciers.

Authors contribution

Atul Kumar: Conceptualization, Data collection, Methodology, Data analysis, Writing – original draft, & funding acquisition.

Suraj Mal: Conceptualization, Methodology, Data analysis, Writing - original draft, Writing – review & editing.

Udo Schickhoff: Data analysis, Writing – review & editing, & funding acquisition.

S. Sreekesh: Conceptualization, Methodology, Data analysis, & Writing – review & editing.

4.4 Article IV

Kumar, A., Mal, S., & Schickhoff, U. (**Accepted**). Spatio-temporal evolution of glacial lakes in the Upper Ganga Basin, Central Himalayas. Himalaya: Mountains of Destiny, Springer book series.

Abstract

Glacial lakes in the central Himalayas are expanding at an unprecedented rate due to the rapid melting and thinning of glaciers. Continuous growth of glacial lakes increases the availability of freshwater for the downstream communities, and escalates the risk of future Glacial Lake Outburst Floods (GLOFs) in the upper Ganga basin. In the present study, glacial lake inventories for the years 1990, 2000, 2010 and 2020 were prepared at the sub-basin level to understand the evolution of glacial lakes in the upper Ganga basin at the micro-regional scale. We found that, between 1990 and 2020, the total number of glacial lakes increases by 564 (22.08%) and the total area increased by 40.71 km^2 (23.93%). We found that glacial lakes were present in the 28 sub-basins of the upper Ganga basin. Among different types of glacial lakes, end moraine-dammed (M(e)) (n: 2,413 & a: 178.89 km^2) had the highest proportion both in terms of number and area of different types of glacial lakes.

We, furthermore, estimated the volume and mean depth of glacial lakes using Huggel et al. (2002) empirical equations. The total estimated volume of glacial lakes was 5.548 km^3 (2020) and the average estimated mean depth was 8.26 m (2020). Between 1990 and 2020, the estimated volume of glacial lakes increased by 1.46 km^3 and the average estimated mean depth decreased by -0.20 m.

Authors contribution

Atul Kumar – Writing – original draft, Writing – review & editing, data collection, , Methodology, Data analysis, & funding acquisition.

Suraj Mal – Writing – review & editing, Methodology, & Data analysis.

Udo Schickhoff – Writing – review & editing, Methodology, & funding acquisition.

Acceptance letter

Department of Geography

Delhi School of Economics

University of Delhi

Delhi -110 007

Prof. Suresh C. Rai

M. Sc., Ph.D.

Date: 20/01/2025

TO WGHOM IT MAY CONCERN

This is to certify that your paper entitled "***Spatio-temporal evolution of glacial lakes in the Upper Ganga Basin, Central Himalayas***" has been accepted for publication in the book entitled **"Himalaya: Mountains of Destiny"** to be published by Springer Nature.

(Prof. Suresh Chand Rai)

5. Synthesis

The presented PhD thesis consists of four articles attempting to understand the evolution of glacial lakes and their associated risks in the IGB river basins of the HKH. Article I aims to understand the evolution of glacial lakes at the sub-basin level of IGB in the HKH, whereas Article II attempted to develop new empirical equations for the estimation of mean depth and volume of glacial lakes in the HKH. Article III is based on a smaller study area (Dibang Valley, Arunachal Pradesh, India, eastern Himalaya) that focuses on the relationship between glacial lake evolution and climate change, and Article IV (focused on the Ganga basin) attempted to understand the changes in lake characteristics (area, elevation, mean depth, and volume) of glacial lakes in the Ganga basin of HKH at the sub-basin level. In the following sub-sections, the key findings of the above-mentioned articles were briefly summarised and discussed based on the objectives of the thesis.

5.1 Glacial lake dynamics

We generated glacial lake inventories for the IGB river basins of HKH at the sub-basin level for the years 1990, 2000, 2010, and 2020. The total number of glacial lakes increased between 1990 and 2020 from 17,641 (1082.57±192.60 km²) to 19,284 (1,191.81±209.21 km²), respectively **(Table 11)**. Between 1990 and 2020, the total number and total area of glacial lakes increased by 9.31% and 10.11%, respectively **(Fig. 11)**. Other studies also confirm the expansion of glacial lakes in the HKH **(Zhang et al., 2015; Nie et al., 2017; Wang et al., 2020; Li et al., 2022)**. However, the rate of expansion varies among various studies; this is primarily because of the employment of different data sources and methodologies to prepare the glacial lake inventories. In 2020, at the major basin level, Brahmaputra had the highest number (11,579) and area (763.59±132.14 km²) of glacial lakes, followed by Indus with the second highest number (4,587) and area (217.47±43.39 km²), and Ganga had the lowest number (3,118) and area (210.74±33.66 km²) **(Table 11)**. However, between 1990 and 2020, Ganga had the highest expansion rate of both number (22.08%) and area (23.85%), followed by the Indus, where the number and area of glacial lakes expanded by 14.73% and 9.37%, respectively **(Fig. 11)**. And Brahmaputra had the lowest expansion rate, where the number and area of glacial lakes expanded by 4.42% and 7.01%, respectively **(Fig. 11)**. Previous studies also confirm that the Ganga basin experienced the highest growth rate **(Gardelle et al., 2011; Zhang et al., 2015; Nie et al., 2017)**. This uneven expansion of glacial lakes across IGB is the result of several local factors, such as the rate of increase in the annual mean temperature, available precipitation, form of precipitation, distance from the glacier, melting rate of glaciers, and local topography.

Table 11: *Decadal distribution of glacial lakes in IGB basin of HKH.*

	1990		2000		2010		2020	
	N	A (km^2)	N	A (km^2)	N	A (km^2)	N	A (km^2)
Indus	3,998	198.84±39.09	4,228	205.47±40.72	4,285	207.99±41.22	4,587	217.47±43.39

Ganga	2,554	170.15±27.81	2,783	191.03±30.55	2,834	201.44±31.40	3,118	210.74±33.66
Brahmaputra	11,089	713.56±125.68	11,195	724.44±127.21	11,280	737.67±128.64	11,579	763.59±132.14
Total	17,641	1,082.56±192.60	18,206	1,120.94±198.49	18,399	1,147.12±201.26	19,284	1,191.81±209.21

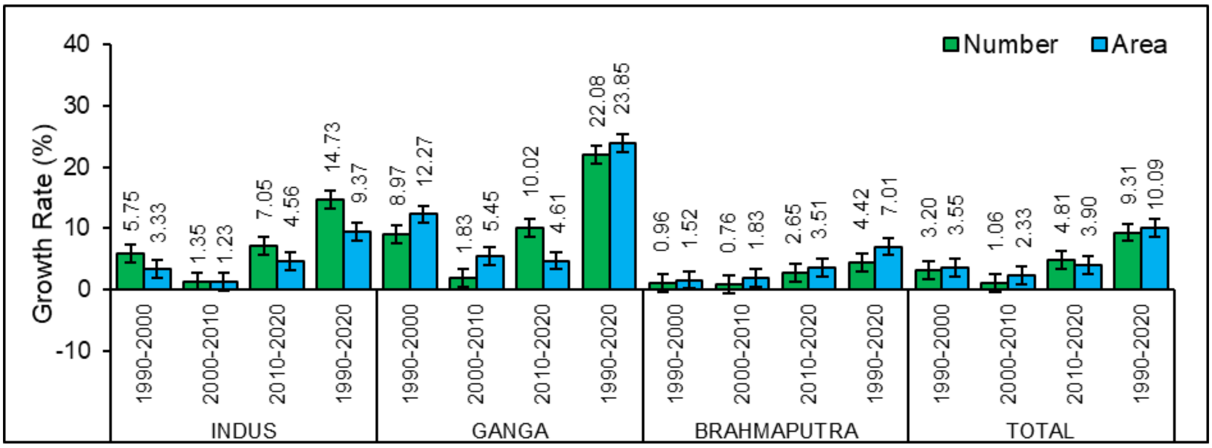

Fig. 11: *Decadal growth rate of glacial lakes in tems of number and area between 1990 and 2020, where green color show growth (%) of number and blue color show the growth (%) of area at the major basin level (source: created by author).*

Previous studies highlighted that the mean elevation of glacial lakes in different sections is increasing **(Nie et al., 2017; Wang et al., 2020; Li et al., 2022)**. In our study, we found that the mean elevation of glacial lakes increased from ~4,737 m asl (1990) to 4,754 m asl (2020), which is an increase of ~17 m. For the year 2020, glacial lakes in Ganga (5,052 m asl) had the highest mean elevation, followed by Brahmaputra (4,755.07 m asl) and Indus (4,549.77 m asl). The primary reason for the rise in the mean elevation of glacial lakes is attributed to accelerated and elevation-dependent warming-led rapid melting of glaciers in the recent past **(Pepin et al., 2015; Bolch et al., 2019; Bhattacharya et al., 2021)**.

In terms of different types of glacial lakes, M(e) lakes were most dominant across the HKH between 1990 and 2020 **(Fig. 12)**. In 1990 there were 13,510 M(e) lakes, which increased to 13,941 (2000), 14,066 (2010), and 14,677 (2020). Whereas supraglacial lakes show the highest percentage increase in number among different types of glacial lakes. Supraglacial lakes more than double between 1990 (218) and 2020 (539) **(Fig. 12)**. This rapid expansion of supraglacial lakes between 1990 and 2020 played a crucial role in the declining mean distance between glaciers and glacial lakes.

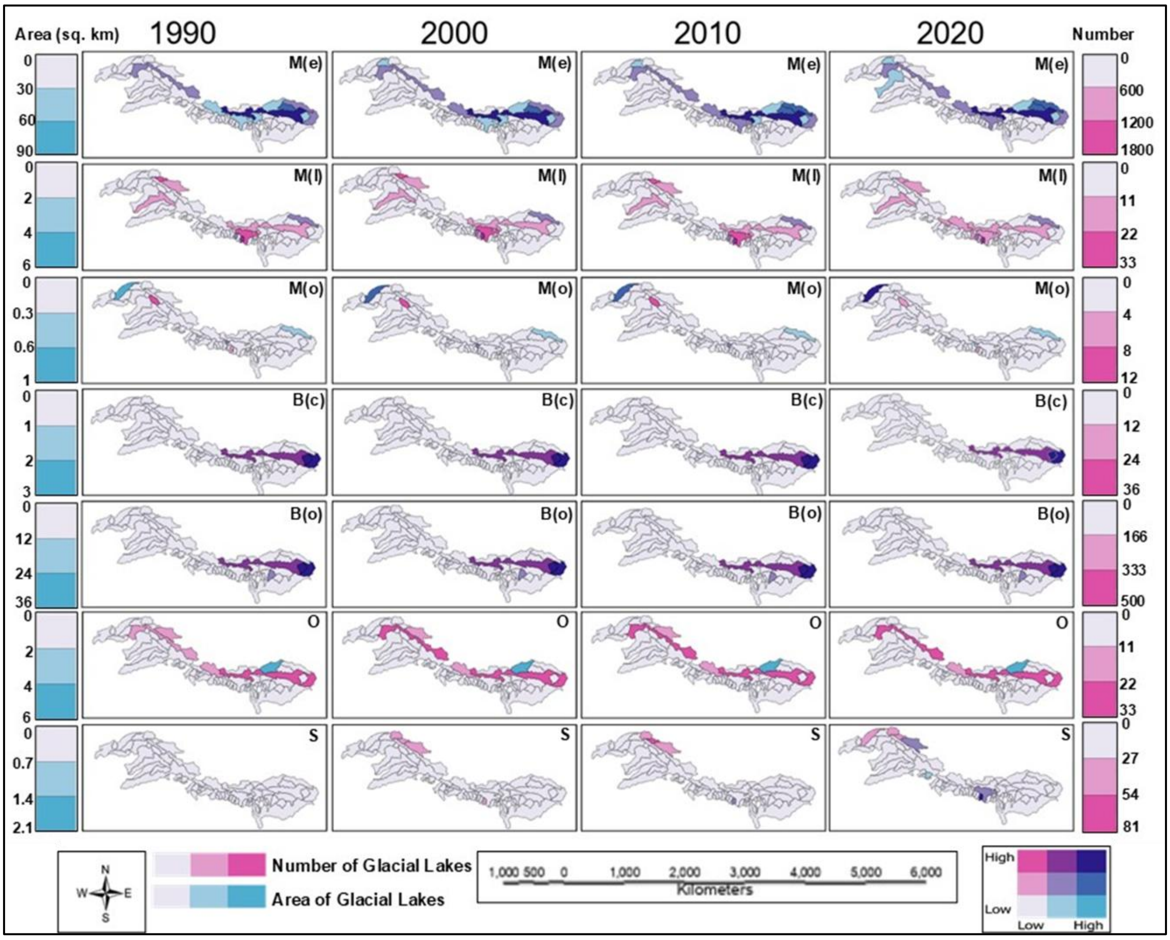

Fig. 12*: Type-wise change in bivariate distribution of glacial lakes n the study domain, where shades of blue/pink colors represent the area (km^2) and number of glacial lakes, respectively, at the sub-basin level between 1990 and 2020 (source: Article I).*

What were the challenges in developing glacial lake inventories and continuous monitoring of glacial lakes in HKH?

The recent advancements in remote sensing and computer-aided mapping made it possible to continuously monitor glacial lakes in the recent past. Before the early 2000s, the majority of glacial lake studies were focused on primary surveys and used to be costly and time-consuming. Furthermore, the studies used to focus on smaller study areas, restricting our understanding of glacial lake evolution in the HKH. The technological advances in remote sensing and computer-aided mapping allowed researchers to continuously monitor the glacial lakes and trace their evolution effectively, especially for larger study areas like HKH. However, there are still several challenges while mapping and continuously monitoring glacial lake evolution in HKH using remote sensing as well. These challenges include *limited availability of satellite images with high spatial resolution, lake characteristics (turbidity, debris cover, snow cover), shadow effect, and surrounding land cover*. Furthermore, different methodologies applied by different studies also pose problems while comparing studies and understanding the evolution of glacial lakes **(Table 6)**.

5.2 Estimating mean depth and volume of glacial lakes in HKH

Mean depth and volume for 19,284 (a = 1,191.81 ± 209.21 km²) developed in the article were estimated. There are several empirical equations that already exist and are employed to estimate the mean depth and volume of glacial lakes in HKH **(Huggel et al., 2002; Sakai et al., 2012; Fujita Muñoz et al., 2020; Shugar et al., 2020; Qi et al., 2022; Zhang et al., 2023)**. But most of the equations that have been made so far that use lake bathymetric data from HKH are based on the central Himalaya. This makes the equations biassed and doesn't take into account how glacial lakes are formed in different areas. This affects how the average depth and volume of glacial lakes are estimated. Therefore, in Article II, eight new empirical equations were developed, four each for mean depth and volume of glacial lakes **(Fig. 10)**. To understand the regional influence on the estimation of the mean depth and volume of glacial lakes. Finally, equations **(6 & 7)** were developed based on 25 glacial lakes from IGB river basins of HKH. In total, 8 glacial lakes were selected from the upper Indus basin (4 of which were based on a primary bathymetry survey), 10 were selected from the upper Ganga basin, and 7 were selected from the upper Brahmaputra basin. Furthermore, while developing the empirical equation for estimating the mean depth and volume of glacial lakes, we found that, although the relationship between area, mean depth, and volume is strongly positive, the relationship is of a non-linear nature. This can be because of several factors, such as the shape of the individual lake, bank slopes, depositional rate, etc. To further understand non-linearity between area, mean depth, and volume, we also calculated the circularity ratio of glacial lakes. circularity ratio **(Table 12)**. And found that the circularity ratio is negatively related to the area, mean depth, and volume of glacial lakes **(Table 12)**.

Table 12: *Correlation matrix (r-values) between glacial lake characteristics for the selected glacial lakes (n = 25) in the upper IGB using Pearson correlation coefficient.*

	Area (km^2)	**Mean Depth (m)**	**Volume (km^3)**	**Circularity ratio**	**Elevation (m asl)**
Area (km^2)	1	0.92	0.97	-0.66	-0.04
Mean Depth (m)		1	0.94	-0.66	0.08
Volume (km^3)			1	-0.66	0.007
Circularity ratio				1	-0.27
Elevation (m asl)				-0.27	1

$$MD = 0.0310*A^{5168} \quad (6)$$

$$V = 0.0357*A^{1.5067} \quad (7),$$

Where, MD is mean depth of glacial lake, A is the area of glacial lake, and V is the volume of glacial lake.

Estimating the mean depth and volume of glacial lakes is of immense importance for gathering valuable data regarding lake topography, calculating total freshwater reserves, identifying potentially hazardous glacial lakes, and modelling GLOF scenarios. The average estimated mean depth of glacial lakes in the IGB river basins was 7.20 m, whereas the total estimated volume of glacial lakes was 28.8 km^3. The uncertainty of the estimated mean depth using the Bayesian approach was between 4.70 m and 9.70 m. And the uncertainty of the estimated volume using the Bayesian approach was between 28.79 km^3 and 28.99 km^3. At the major basin level, glacial lakes of the upper Brahmaputra basin have the highest average mean depth (7.43 m) and total estimated volume (19.002 km^3), followed by glacial lakes in the upper Ganga basin (depth = 7.10 m and volume = 6.33 km^3) and glacial lakes in the upper Indus basin (depth = 6.69 m and total volume = 3.55 km^3). It is essential to highlight that the upper Ganga basin (n = 3,118; a = 210.74 ± 33.66 km^2) had a higher estimated volume per glacial lake (0.002 km^3) than the upper Brahmaputra (n = 11,579; a = 763.59 ± 132.14 km^2, volume/lake: 0.0016 km^3) and the upper Indus basin (n = 4,587; a = 217.47 ± 43.39 km^2, volume/lake: 0.0008 km^3) (**Fig. 6**).

Factors affecting the estimation of mean depth and volume of glacial lakes

Collecting information about the depth and volume of glacial lakes is of immense importance for a broader understanding of glacial lake expansion, its causes, and its impacts. However, collecting the primary data on depth and volume for each and every glacial lake in the HKH is near impossible with present technology because of the rugged terrain, immense cost, and labour involvements. Therefore, estimating the mean depth and volume of glacial lakes becomes even more important, although it is a complex process. Several factors, such as the availability of in-situ data, lake geometry (area, width, shape), dam material, melting rate of glaciers, distance from the glacier, sub-glacial topography and rock structure, precipitation pattern, and sedimentation rate, affect the estimation of the depth and volume of glacial lakes **(Cook & Quincey, 2015; Muñoz et al., 2020; Qi et al., 2022**). The area-scaling method is the most commonly used method to estimate the mean depth and volume of glacial lakes **(Huggel et al., 2002; Sakai et al., 2012; Fujita et al., 2013; Muñoz et al., 2020; Qi et al., 2022)**. However, till now, there is no universal equation that can estimate the mean depth and volume of glacial lakes accurately. This is primarily because of regional variations in the lake characteristics **(Cook and Quincey, 2015; Zhang et al., 2023)**. Few studies attempted to understand the role of local lake characteristics in influencing the relationship between area and mean depth/volume of glacial lakes (**Huggel et al., 2002; Cook and Quincey, 2015; Muñoz et al., 2020; Qi et al., 2022; Zhang et al., 2023**). **Cook and Quincey (2015)** suggested that the shape of the glacial lake influences the relationship between area and mean depth/volume. However, they did not quantify it. In our study, we have used the circularity ratio to quantify the shape of glacial lakes. Our study shows that there is a negative correlation between circularity ratio and mean depth/volume of glacial lakes. Furthermore, we found the low circularity ratio of glacial lakes is the key reason for the non-linearity between the area and mean depth/volume of glacial lakes.

Also to enhance the understanding of the role of regional lake characteristics in estimating mean depth and volume, Article II also evaluated the relationship between dam type and other lake characteristics (area, mean depth, volume, and circularity ratio) **(Fig. 13)**. B(o) lakes tend to have a broader range of characteristics, with notable variability in area and estimated volume, potentially indicating greater morphometric diversity **(Fig. 13)**. The supraglacial lakes had the lowest average estimated mean depth (4.13 m), whereas B(o) lakes had the highest average estimated mean depth (7.44 m), highlighting the different geomorphic settings where such lakes form and differences in dam geometries. Therefore, it is of immense importance to acknowledge the differences in the dam type before developing future empirical equations.

Furthermore, as discussed above, glaciers of HKH are melting rapidly under the influence of ongoing climate change **(Krishnan et al., 2019)**, which not only leads to the formation of new glacial lakes and the expansion of existing ones but also leads to modification in local lake characteristics such as lake shape and lake bottom topography **(Bolch et al., 2019; Qi et al., 2022; Zhang et al., 2023)**. These changes in lake characteristics prompt the enquiries regarding the relevance of existing empirical equations based on the area-scaling method. The majority of the empirical equations are based on the assumption that geometric similarities exist between different sizes of glacial lakes and that these relationships are static **(Huggel et al., 2002; Cook and Quincey, 2015)**. However, under the influence of rapid melting of glaciers, this assumption may not apply, especially for glacial lakes that are directly connected with glaciers. Therefore, it is of immense importance to evaluate the role of ongoing climate change and glacier melting in developing new empirical equations for the future.

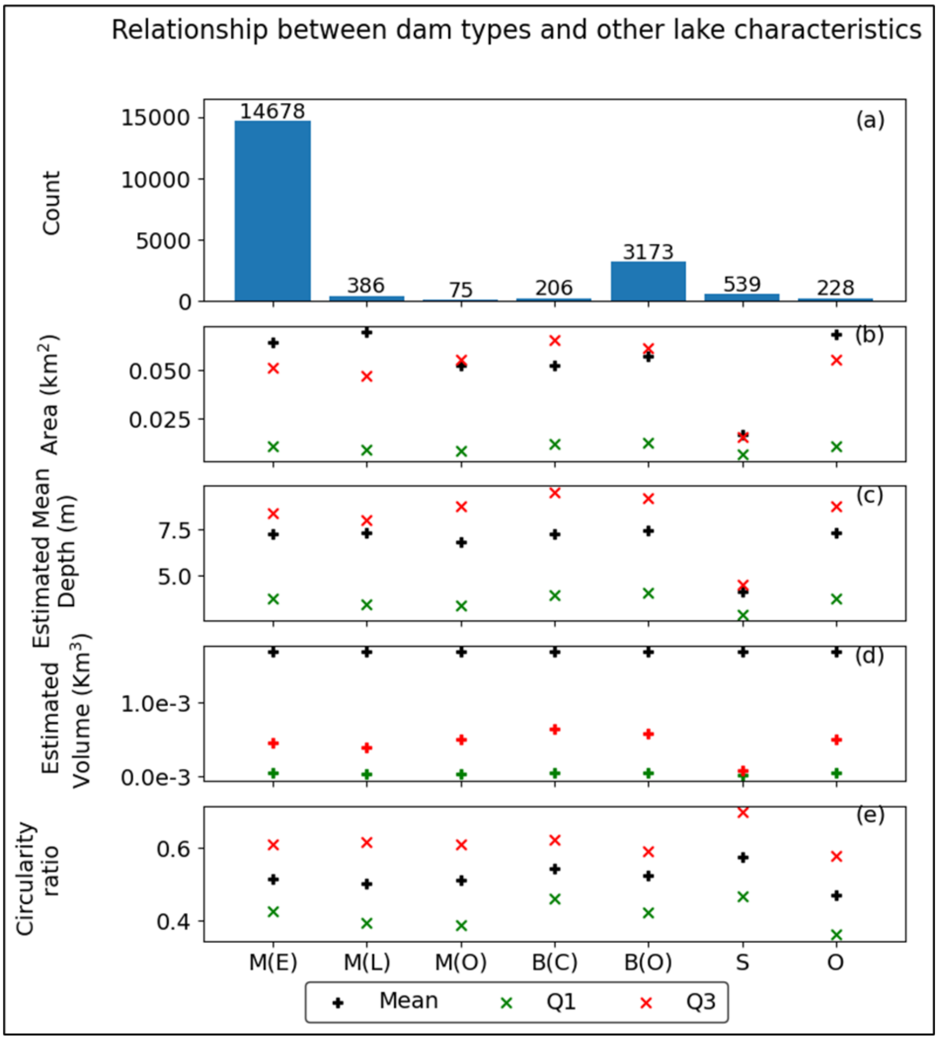

***Fig. 13**: Relationship between dam type and different glacial lake characteristics, where (a) shows the relationship between different dam types and count, (b) dam type and area (km^2), (c) dam type and estimated mean depth (m), (d) dam type and estimated volume (km^3), and (e) dam type and circularity ratio. Where (+) shows the mean, (x) in green color shows the first quartile, and (x) in red color shows the third quartile.*

6. Conclusion

The aim of the doctoral thesis was to understand the spatio-temporal evolution of glacial lakes in upper IGB river basins of the HKH region, providing valuable insights about the evolution of glacial lakes, mean depth and volume estimation, and associated hazards at the sub-basin level.

The findings reveal that glacial lakes in IGB river basins expanded rapidly (n = **9.31% and a = 10.09%)** between 1990 and 2020. The rapid melting of glaciers due to the ongoing above-average increase in mean annual temperature is regarded as the main driver for this expansion. The mean distance between glaciers and glacial lakes decreased from **5.29 km (1990) to 4.87 km (2020)**. However, the growth of glacial lakes is heterogeneous in the HKH. Among the major basins, the Ganga basin showed the highest growth both in terms of number **(22.08%) and area (23.85%)** between 1990 and 2020. Whereas the Brahmaputra basin has the highest number of glacial lakes (**11,579)** among the three major basins. M(e) lakes are the most dominant type of glacial lakes in the HKH, and supraglacial lakes increased more than doubled between 1990 and 2020. Both of these types of glacial lakes have unstable dam characteristics, which can lead to GLOF events and cause huge damage to downstream communities. Furthermore, the new glacial lakes are developing at higher elevations, as compared to previously, mainly due to the elevation-dependent warming in the HKH. These new lakes are difficult to reach and conduct field-based studies, mainly due to the rugged terrain and extremely high cost of operations.

Another vital contribution of this thesis is the development of new empirical equations to estimate the glacial lake mean depth and volume. The study presents the first empirical equations, which are based on the glacial lakes from all three major basins of IGB, which helps in providing practical tools to analyse the hydrological characteristics and future hazard assessment of glacial lakes. These equations are thoroughly validated against field measurements and offer a scalable and effective solution for understanding the glacial lake evolution in the rugged and harsh conditions where conducting field-based studies is not suitable.

The study also highlights the diversity in the evolution of glacial lakes across the HKH region. Rapid melting of glaciers, especially those thinning due to elevation-dependent warming, is driving the formation of new glacial lakes at higher altitudes, increasing the risk of GLOFs. These floods, primarily triggered by mainly natural events like avalanches, dam breaching, earthquakes, or extreme rainfall, can cause serious damage to downstream natural and human environments. Therefore, the present study recommends continuous monitoring of glacial lakes, understanding of heightened risks of GLOFs, and integrating GLOF mitigation strategies into regional planning.

Both the number of people living and GLOF is increasing in the HKH region; therefore, there is an urgent need for systematic monitoring, intergovernmental cooperation, hazard assessment, the establishment of early warning systems, and community-based disaster preparedness.

7. Bibliography

Adrian, R., O'Reilly, C. M., Zagarese, H., Baines, S. B., Hessen, D. O., Keller, W., ... & Winder, M. (2009). Lakes as sentinels of climate change. *Limnology and oceanography*, *54*(6part2), 2283-2297. https://doi.org/10.4319/lo.2009.54.6_part_2.2283

Allen, M.R., O.P. Dube, W. Solecki, F. Aragón-Durand, W. Cramer, S. Humphreys, M. Kainuma, J. Kala, N. Mahowald, Y. Mulugetta, R. Perez, M. Wairiu, and K. Zickfeld, 2018: Framing and Context. In: *Global Warming of 1.5°C. An IPCC Special Report on the impacts of global warming of 1.5°C above pre-industrial levels and related global greenhouse gas emission pathways, in the context of strengthening the global response to the threat of climate change, sustainable development, and efforts to eradicate poverty* [Masson-Delmotte, V., P. Zhai, H.-O. Pörtner, D. Roberts, J. Skea, P.R. Shukla, A. Pirani, W. Moufouma-Okia, C. Péan, R. Pidcock, S. Connors, J.B.R. Matthews, Y. Chen, X. Zhou, M.I. Gomis, E. Lonnoy, T. Maycock, M. Tignor, and T. Waterfield (eds.)]. Cambridge University Press, Cambridge, UK and New York, NY, USA, pp. 49-92, doi:10.1017/9781009157940.003.

Barta, B., Mouillet, C., Espinosa, R., Andino, P., Jacobsen, D., & Christoffersen, K. S. (2018). Glacial-fed and páramo lake ecosystems in the tropical high Andes. *Hydrobiologia*, *813*, 19-32. https://doi.org/10.1007/s10750-017-3428-4

Bhattacharya, A., Bolch, T., Mukherjee, K., King, O., Menounos, B., Kapitsa, V., ... & Yao, T. (2021). High Mountain Asian glacier response to climate revealed by multi-temporal satellite observations since the 1960s. *Nature communications*, *12*(1), 4133. https://doi.org/10.1038/s41467-021-24180-y

Bhambri, R., Misra, A., Kumar, A., Gupta, A. K., Verma, A., & Tiwari, S. K. (2018). Glacier lake inventory of Himachal Pradesh. *Himalayan Geol*, *39*(1), 1-32.

Bolch, T., Kulkarni, A., Kääb, A., Huggel, C., Paul, F., Cogley, J. G., ... & Stoffel, M. (2012). The state and fate of Himalayan glaciers. *Science*, *336*(6079), 310-314.

Bolch, T., Shea, J. M., Liu, S., Azam, F. M., Gao, Y., Gruber, S., ... & Zhang, Y. (2019). Status and change of the cryosphere in the extended Hindu Kush Himalaya region. *The Hindu Kush Himalaya assessment: Mountains, climate change, sustainability and people*, 209-255. https://doi.org/10.1007/978-3-319-92288-1_7

Bose, S. C. (1972). Geography of the Himalaya, National Book Trust, New Delhi, 1-210.

Breckenridge, A., Lowell, T. V., Peteet, D., Wattrus, N., Moretto, M., Norris, N., & Dennison, A. (2021). A new glacial varve chronology along the southern Laurentide Ice Sheet that spans the Younger Dryas–Holocene boundary. *Geology*, *49*(3), 283-288. https://doi.org/10.1130/G47995.1

Campbell, J. G., & Pradesh, H. (2005). Inventory of glaciers, glacial lakes and the identification of potential glacial lake outburst floods (GLOFs) affected by global warming in the mountains of India, Pakistan and China/Tibet Autonomous Region. *International Centre for Integrated Mountain Development, GP O. Box*, *3226*.

Carlin, B. P., & Louis, T. A. (2008). *Bayesian methods for data analysis*. CRC press: Boca Raton, Florida, USA.

Chapin, F. S., III, S. F. Trainor, P. Cochran, H. Huntington, C. Markon, M. McCammon, A. D. McGuire, and M. Serreze, 2014: Ch. 22: Alaska. Climate Change Impacts in the United States: The Third National Climate Assessment, J. M. Melillo, Terese (T.C.) Richmond, and G. W. Yohe, Eds., U.S. Global Change Research Program, 514-536. doi: https://10.7930/J00Z7150

Chen, F., Zhang, M., Guo, H., Allen, S., Kargel, J. S., Haritashya, U. K., & Watson, C. S. (2021). Annual 30 m dataset for glacial lakes in High Mountain Asia from 2008 to 2017. *Earth System Science Data*, *13*(2), 741-766. https://doi.org/10.5194/essd-13-741-2021

Cook, S. J., & Quincey, D. J. (2015). Estimating the volume of Alpine glacial lakes. *Earth Surface Dynamics*, *3*(4), 559-575. https://doi.org/10.5194/esurf-3-559-2015

Datta, R. T., & Wouters, B. (2021). Supraglacial lake bathymetry automatically derived from ICESat-2 constraining lake depth estimates from multi-source satellite imagery. *The Cryosphere*, *15*(11), 5115-5132. https://doi.org/10.5194/tc-15-5115-2021

Dimri, A. P., Niyogi, D., Barros, A. P., Ridley, J., Mohanty, U. C., Yasunari, T., & Sikka, D. R. (2015). Western disturbances: a review. Reviews of Geophysics, 53(2), 225-246. https://doi.org/10.1002/2014RG000460

Dimri, A. P., Allen, S., Huggel, C., Mal, S., Ballesteros-Canovas, J. A., Rohrer, M., ... & Pandey, A. (2021). Climate change, cryosphere and impacts in the Indian Himalayan Region. *Current Science*, *120*(5), 774-790. https://www.jstor.org/stable/27310281

Evans, S. G. (1986, April). Landslide damming in the Cordillera of Western Canada. In *Landslide dams: Processes, risk, and mitigation* (pp. 111-130). ASCE.

Farrington, J. D., & Li, J. (2024). Climate change impacts on snow leopard range. In *Snow leopards* (pp. 81-93). Academic Press. https://doi.org/10.1016/B978-0-323-85775-8.00037-6

Fujita, K., Sakai, A., Takenaka, S., Nuimura, T., Surazakov, A. B., Sawagaki, T., & Yamanokuchi, T. (2013). Potential flood volume of Himalayan glacial lakes. *Natural Hazards and Earth System Sciences*, *13*(7), 1827-1839. https://doi.org/10.5194/nhess-13-1827-2013

Gantayat, P., Sattar, A., Haritashya, U. K., Watson, C. S., & Kargel, J. S. (2024). Bayesian Approach to Estimate Proglacial Lake Volume (BE-GLAV). *Earth and Space Science*, *11*(6), e2024EA003542. https://doi.org/10.1029/2024EA003542

Gardelle, J., Berthier, E., & Arnaud, Y. (2012). Slight mass gain of Karakoram glaciers in the early twenty-first century. *Nature Geoscience*, 5(5), 322–325. https://doi.org/10.1038/ngeo1450

Gardelle, J., Berthier, E., Arnaud, Y., & Kääb, A. (2013). Region-wide glacier mass balances over the Pamir-Karakoram-Himalaya during 1999–2011. *The Cryosphere*, *7*(4), 1263-1286. https://doi.org/10.5194/tc-7-1263-2013

Gansser, A. (1964). *Geology of the Himalayas.* Wiley-Interscience, London, United Kingdom.

Gao, B. C. (1996). NDWI—A normalized difference water index for remote sensing of vegetation liquid water from space. *Remote sensing of environment*, *58*(3), 257-266. https://doi.org/10.1016/S0034-4257(96)00067-3

Gelman, A., & Shalizi, C. R. (2013). Philosophy and the practice of Bayesian statistics. *British Journal of Mathematical and Statistical Psychology*, *66*(1), 8-38. https://doi.org/10.1111/j.2044-8317.2011.02037.x

Gobiet, A., Kotlarski, S., Beniston, M., Heinrich, G., Rajczak, J., & Stoffel, M. (2014). 21st century climate change in the European Alps—A review. *Science of the total environment*, *493*, 1138-1151. https://doi.org/10.1016/j.scitotenv.2013.07.050

Goodsell, B., Anderson, B., Lawson, W. J., & Owens, I. F. (2005). Outburst flooding at Franz Josef Glacier, South Westland, New Zealand. *New Zealand Journal of Geology and Geophysics*, *48*(1), 95-104. https://doi.org/10.1080/00288306.2005.9515101

Haemmig, C., Huss, M., Keusen, H., Hess, J., Wegmüller, U., Ao, Z., & Kulubayi, W. (2014). Hazard assessment of glacial lake outburst floods from Kyagar glacier, Karakoram mountains, China. *Annals of Glaciology*, *55*(66), 34-44. https://doi.org/10.3189/2014AoG66A001

Hanshaw, M. N., & Bookhagen, B. (2014). Glacial areas, lake areas, and snow lines from 1975 to 2012: status of the Cordillera Vilcanota, including the Quelccaya Ice Cap, northern central Andes, Peru. *The Cryosphere*, *8*(2), 359-376. https://doi.org/10.5194/tc-8-359-2014

Hock, R., G. Rasul, C. Adler, B. Cáceres, S. Gruber, Y. Hirabayashi, M. Jackson, A. Kääb, S. Kang, S. Kutuzov, Al. Milner, U. Molau, S. Morin, B. Orlove, and H. Steltzer, (2019). High Mountain Areas. In: IPCC Special Report on the Ocean and Cryosphere in a Changing Climate [H.-O. Pörtner, D.C. Roberts, V. Masson-Delmotte, P. Zhai, M. Tignor, E. Poloczanska, K. Mintenbeck, A. Alegría, M. Nicolai, A. Okem, J. Petzold, B. Rama, N.M. Weyer (eds.)]. Cambridge University Press, Cambridge, UK and New York, NY, USA, pp. 131–202. https://doi.org/10.1017/9781009157964.004

Huggel, C., Kääb, A., Haeberli, W., Teysseire, P., & Paul, F. (2002). Remote sensing based assessment of hazards from glacier lake outbursts: a case study in the Swiss Alps. *Canadian Geotechnical Journal*, *39*(2), 316-330.

Hugonnet, R., McNabb, R., Berthier, E., Menounos, B., Nuth, C., Girod, L., ... & Kääb, A. (2021). Accelerated global glacier mass loss in the early twenty-first century. *Nature*, *592*(7856), 726-731. https://doi.org/10.1038/s41586-021-03436-z

ICIMOD. (2011). Glacial Lakes and Glacial Lake Outburst Floods in Nepal. ICIMOD, Kathmandu.

Ives, J. D., Shrestha, R. B.., Mool, P. K., (2010). Formation of Glacial Lakes I the Hindu-Kush-Himalayas and GLOF Risk Assessment. ICIMOD, Kathmandu.

ICIMOD. (2022). GLOF database of High Mountain Asia [Data set]. ICIMOD. https://doi.org/10.26066/RDS.1973283

ICIMOD. (2023). *Water, ice, society, and ecosystems in the Hindu Kush Himalaya: An outlook.* (P. Wester, S. Chaudhary, N. Chettri, M. Jackson, A. Maharjan, S. Nepal, & J. F. Steiner [Eds.]). ICIMOD. https://doi.org/10.53055/ICIMOD.1028

Jamwal, P. S., Shrotriya, S., & Takpa, J. (2020). The pattern of waterbird diversity of the trans-Himalayan wetlands in Changthang Wildlife Sanctuary, Ladakh, India. *Journal of Threatened Taxa*, *12*(1), 15129-15139. https://doi.org/10.11609/jott.5122.12.1.15129-15139

Krishnan, R., Shrestha, A. B., Ren, G., Rajbhandari, R., Saeed, S., Sanjay, J., ... & Ren, Y. (2019). Unravelling climate change in the Hindu Kush Himalaya: rapid warming in the mountains and increasing extremes. *The Hindu Kush Himalaya assessment: Mountains, climate change, sustainability and people*, 57-97. https://doi.org/10.1007/978-3-319-92288-1_3

Kulkarni, A. V., Shirsat, T. S., Kulkarni, A., Negi, H. S., Bahuguna, I. M., & Thamban, M. (2021). State of Himalayan cryosphere and implications for water security. *Water Security*, *14*, 100101. https://doi.org/10.1016/j.wasec.2021.100101

Lemieux, J. M., Sudicky, E. A., Peltier, W. R., & Tarasov, L. (2008). Dynamics of groundwater recharge and seepage over the Canadian landscape during the Wisconsinian glaciation. *Journal of Geophysical Research: Earth Surface*, *113*(F1). https://doi.org/10.1029/2007JF000838

Larsen, D. J., Miller, G. H., Geirsdóttir, Á., & Thordarson, T. (2011). A 3000-year varved record of glacier activity and climate change from the proglacial lake Hvítárvatn, Iceland. *Quaternary Science Reviews*, *30*(19-20), 2715-2731. https://doi.org/10.1016/j.quascirev.2011.05.026

Legleiter, C. J., Tedesco, M., Smith, L. C., Behar, A. E., & Overstreet, B. T. (2014). Mapping the bathymetry of supraglacial lakes and streams on the Greenland ice sheet using field measurements and high-resolution satellite images. *The Cryosphere*, *8*(1), 215-228. https://doi.org/10.5194/tc-8-215-2014

Li, W., Wang, W., Gao, X., Wang, X., & Wang, R. (2022). Inventory and Spatiotemporal Patterns of Glacial Lakes in the HKH-TMHA Region from 1990 to 2020. *Remote Sensing*, *14*(6), 1351. https://doi.org/10.3390/rs14061351

Lesi, M., Nie, Y., Shugar, D. H., Wang, J., Deng, Q., & Chen, H. (2022). Landsat and Sentinel-derived glacial lake dataset in the China-Pakistan Economic Corridor from 1990 to 2020. *Earth System Science Data Discussions*, *2022*, 1-33. https://doi.org/10.5194/essd-14-5489-2022

Lützow, N., Veh, G., & Korup, O. (2023). A global database of historic glacier lake outburst floods. *Earth System Science Data Discussions*, *2023*, 1-27. https://doi.org/10.5194/essd-15-2983-2023

Ma, J., Song, C., & Wang, Y. (2021). Spatially and Temporally Resolved Monitoring of Glacial Lake Changes in Alps During the Recent Two Decades. *Frontiers in Earth Science*, *9*, 723386. https://doi.org/10.3389/feart.2021.723386

Marengo, J. A., Pabón, J. D., Díaz, A., Rosas, G., Ávalos, G., Montealegre, E., ... & Rojas, M. (2011). Climate change: evidence and future scenarios for the Andean region. *Climate change and biodiversity in the tropical Andes*, 110-127.

Maharjan, S. B., Mool, P. K., Lizong, W., Xiao, G., Shrestha, F., Shrestha, R. B., ... & Baral, P. (2018). The Status of Glacial Lakes in the Hindu Kush Himalaya-ICIMOD Research Report 2018/1. International Centre for Integrated Mountain Development (ICIMOD).

Mal, S., Kumar, A., Bhambri, R., Schickhoff, U., & Singh, R. B. (2020). Inventory and spatial distribution of glacial lakes in Arunachal Pradesh, Eastern Himalaya, India. *Journal of the Geological Society of India*, *96*, 609-615. https://doi.org/10.1007/s12594-020-1610-1

Mishra, B., Panthi, S., Ghimire, B. R., Poudel, S., Maharjan, B., & Mishra, Y. (2023). Gridded precipitation products on the Hindu Kush-Himalaya: Performance and accuracy of seven precipitation products. *PLoS Water*, *2*(8), e0000145. https://doi.org/10.1371/journal.pwat.0000145

Molden, D. J., Shrestha, A. B., Nepal, S., & Immerzeel, W. W. (2016). Downstream implications of climate change in the Himalayas. *Water security, climate change and sustainable development*, 65-82. https://doi.org/10.1007/978-981-287-976-9_5

Mool, P. K., Bajracharya, S. R., & Joshi, S. P. (2001a). *Inventory of glaciers, glacial lakes and glacial lake outburst floods. Monitoring and early warning systems in the Hindu Kush-Himalayan Region: Nepal*.

Mool, P. K., Wangda, D., Bajracharya, S. R., Kunzang, K., Raj Gurung, D., & Joshi, S. P. (2001b). Inventory of Glaciers, Glacial Lakes and Glacial Lake Outburst Floods Monitoring and Early Warning Systems in the Hindu Kush-Himalayan Region: Bhutan.

Mölg, N., Huggel, C., Herold, T., Storck, F., Allen, S., Haeberli, W., ... & Odermatt, D. (2021). Inventory and evolution of glacial lakes since the Little Ice Age: Lessons from the case of Switzerland. *Earth Surface Processes and Landforms*, *46*(13), 2551-2564. https://doi.org/10.1002/esp.5193

Moser, K. A., Baron, J. S., Brahney, J., Oleksy, I. A., Saros, J. E., Hundey, E. J., ... & Smol, J. P. (2019). Mountain lakes: Eyes on global environmental change. *Global and Planetary Change*, *178*, 77-95. https://doi.org/10.1016/j.gloplacha.2019.04.001

Muñoz, R., Huggel, C., Frey, H., Cochachin, A., & Haeberli, W. (2020). Glacial lake depth and volume estimation based on a large bathymetric dataset from the Cordillera Blanca, Peru. *Earth surface processes and landforms*, *45*(7), 1510-1527. https://doi.org/10.1002/esp.4826

Neal, E. G. (2007). *Hydrology and Glacier-Lake-Outburst Floods (1987-2004) and Water Quality (1998-2003) of the Taku River near Juneau, Alaska* (No. 2007-5027). https://doi.org/10.3133/sir20075027

Negi, S. S. (1998). *Discovering the Himalaya* (Vol. 1). Indus Publishing Company, New Delhi.

Nie, Y., Liu, Q., & Liu, S. (2013). Glacial lake expansion in the Central Himalayas by Landsat images, 1990–2010. *PloS one*, *8*(12), e83973. https://doi.org/10.1371/journal.pone.0083973

Nie, Y., Sheng, Y., Liu, Q., Liu, L., Liu, S., Zhang, Y., & Song, C. (2017). A regional-scale assessment of Himalayan glacial lake changes using satellite observations from 1990 to 2015. *Remote Sensing of Environment*, *189*, 1-13. https://doi.org/10.1016/j.rse.2016.11.008

Nie, Y., Liu, Q., Wang, J., Zhang, Y., Sheng, Y., & Liu, S. (2018). An inventory of historical glacial lake outburst floods in the Himalayas based on remote sensing observations and geomorphological analysis. *Geomorphology*, *308*, 91-106. https://doi.org/10.1016/j.geomorph.2018.02.002

Nie, Y., Pritchard, H. D., Liu, Q., Hennig, T., Wang, W., Wang, X., ... & Chen, X. (2021). Glacial change and hydrological implications in the Himalaya and Karakoram. *Nature reviews earth & environment*, *2*(2), 91-106. https://doi.org/10.1038/s43017-020-00124-w

Owen, L. , Allan, . Nigel John Roger and Maraini, . Fosco (2024, November 13). *Hindu Kush*. *Encyclopedia Britannica*. https://www.britannica.com/place/Hindu-Kush

Patel, L. K., Sharma, P., Laluraj, C. M., Thamban, M., Singh, A., & Ravindra, R. (2017). A geospatial analysis of Samudra Tapu and Gepang Gath glacial lakes in the Chandra Basin, Western Himalaya. *Natural Hazards*, *86*, 1275-1290. https://doi.org/10.1007/s11069-017-2743-4

Pepin, N., Bradley, R., Diaz, H., Baraer, M., Caceres, E.B., Forsythe, N., Yang, D.Q. (2015). Elevation-dependent warming in mountain regions of the world. Nature Climate Change, 5, 424-430. https://doi.org/10.1038/nclimate2563.

Qi, M., Liu, S., Wu, K., Zhu, Y., Xie, F., Jin, H., ... & Yao, X. (2022). Improving the accuracy of glacial lake volume estimation: A case study in the Poiqu basin, central Himalayas. *Journal of Hydrology*, *610*, 127973. https://doi.org/10.1016/j.jhydrol.2022.127973

Raj, B. K. G., Kumar, V. K., & Remya, S. N. (2013). Remote sensing-based inventory of glacial lakes in Sikkim Himalaya: semi-automated approach using satellite data. *Geomatics, Natural Hazards and Risk, 4(3), 241-253. https://doi.org/10.1080/19475705.2012.707153*

Rao, B. S., Gupta, A., Sweta, Maheshwari, R., Raju, P. V., Rao, V. V. (2021). Glacial Lake Atlas of Ganga River Basin. National Remote Sensing Centre, ISRO, Hyderabad, India, pp. 1-194.

Reeve, A. S., Warzocha, J., Glaser, P. H., & Siegel, D. I. (2001). Regional ground-water flow modeling of the Glacial Lake Agassiz Peatlands, Minnesota. Journal of Hydrology, 243(1-2), 91-100. https://doi.org/10.1016/S0022-1694(00)00402-9

RGI 7.0 Consortium (2023). Randolph Glacier Inventory - A Dataset of Global Glacier Outlines, Version 7.0. Boulder, Colorado USA. NSIDC: National Snow and Ice Data Center. doi:10.5067/f6jmovy5navz. Online access: https://doi.org/10.5067/f6jmovy5navz

Rinzin, S., Zhang, G., Wangchuk, S. (2021). Glacial lake area change and potential outburst flood hazard assessment in the Bhutan Himalaya. *Frontier in Earth Science*. *9, 775195.* https://doi.org/10.3389/feart.2021.775195

Sakai, A. (2012). Glacial lakes in the Himalayas: a review on formation and expansion processes. *Global Environmental Research*, *16*(2011), 23-30.

Salerno, F., Thakuri, S., D'Agata, C., Manfredi, E.C.., Viviano, G., Tartari, G. (2012). Glacial lake distribution in the Mount Everest region: Uncertainty of measurement and conditions of formation. *Global and Planetary Change, 92, 30-39.* https://doi.org/10.1016/j.glopacha.2012.04.001.

Schickhoff, U., Bobrowski, M., Mal, S., Schwab, N., & Singh, R.B. (2022). The world's mountains in the Anthropocene. In: Schickhoff, U., Singh, R.B., & Mal, S, (eds,): Mountain landscapes in transition: effects of land use and climate change. Springer, Cham, pp 1-144.

Sharma, R. K., Pradhan, P., Sharma, N. P., & Shrestha, D. G. (2018). Remote sensing and in situ-based assessment of rapidly growing South Lhonak glacial lake in eastern Himalaya, India. *Natural Hazards*, *93*, 393-409. https://doi.org/10.1007/s11069-018-3305-0

Sharma, E., Molden, D., Rahman, A., Khatiwada, Y. R., Zhang, L., Singh, S. P., ... & Wester, P. (2019). Introduction to the hindu kush himalaya assessment. *The Hindu Kush Himalaya Assessment: mountains, climate change, sustainability and people*, 1-16.

Shrestha, F., Steiner, J. F., Shrestha, R., Dhungel, Y., Joshi, S. P., Inglis, S., ... & Zhang, T. (2023). A comprehensive and version-controlled database of glacial lake outburst floods in High Mountain Asia. *Earth System Science Data*, *15*(9), 3941-3961. https://doi.org/10.5194/essd-15-3941-2023

Shugar, D. H., Burr, A., Haritashya, U. K., Kargel, J. S., Watson, C. S., Kennedy, M. C., ... & Strattman, K. (2020). Rapid worldwide growth of glacial lakes since 1990. Nature climate change, 10(10), 939-945. https://doi.org/10.1038/s41558-020-0855-4

Singh, SP; Bassignana-Khadka, I; Karky, BS; Sharma, E (2011) *Climate change in the Hindu Kush-Himalayas: The state of current knowledge*. Kathmandu: ICIMOD

Somos-Valenzuela, M. A., Chisolm, R. E., Rivas, D. S., Portocarrero, C., & McKinney, D. C. (2016). Modeling a glacial lake outburst flood process chain: the case of Lake Palcacocha and Huaraz, Peru. *Hydrology and Earth System Sciences*, *20*(6), 2519-2543. https://doi.org/10.5194/hess-20-2519-2016.

Song, C., Sheng, Y., Ke, L., Nie, Y., & Wang, J. (2016). Glacial lake evolution in the southeastern Tibetan Plateau and the cause of rapid expansion of proglacial lakes linked to glacial-hydrogeomorphic processes. *Journal of hydrology*, *540*, 504-514. https://doi.org/10.1016/j.jhydrol.2016.06.054

Sun, J., Zhou, T., Liu, M., Chen, Y., Shang, H., Zhu, L., ... & Sha, Y. (2018). Linkages of the dynamics of glaciers and lakes with the climate elements over the Tibetan Plateau. *Earth-Science Reviews*, *185*, 308-324. https://doi.org/10.1016/j.earscirev.2018.06.012

Sundal, A. V., Shepherd, A., Nienow, P., Hanna, E., Palmer, S., & Huybrechts, P. (2009). Evolution of supra-glacial lakes across the Greenland Ice Sheet. *Remote Sensing of Environment*, *113*(10), 2164-2171. https://doi.org/10.1016/j.rse.2009.05.018

Taylor, C., Robinson, T. R., Dunning, S., Rachel Carr, J., & Westoby, M. (2023). Glacial lake outburst floods threaten millions globally. *Nature Communications*, *14*(1), 487. https://doi.org/10.1038/s41467-023-36033-x

Turner, J., Colwell, S. R., Marshall, G. J., Lachlan-Cope, T. A., Carleton, A. M., Jones, P. D., ... & Iagovkina, S. (2005). Antarctic climate change during the last 50 years. *International journal of Climatology*, *25*(3), 279-294. doi: https://10.1002/joc.1130

Vanderwall, J. W., Muhlfeld, C. C., Tappenbeck, T. H., Giersch, J., Ren, Z., & Elser, J. J. (2024). Mountain glaciers influence biogeochemical and ecological characteristics of high-elevation lakes across the northern Rocky Mountains, USA. *Limnology and Oceanography*, *69*(1), 37-52. https://doi.org/10.1002/lno.12434

Vandecrux, B., Fausto, R. S., Box, J. E., Covi, F., Hock, R., Rennermalm, Å. K., ... & Ahlstrøm, A. P. (2024). Recent warming trends of the Greenland ice sheet documented by historical firn and ice temperature observations and machine learning. *The Cryosphere*, *18*(2), 609-631. https://doi.org/10.5194/tc-18-609-2024

Veh, G., Korup, O., Roessner, S., & Walz, A. (2018). Detecting Himalayan glacial lake outburst floods from Landsat time series. *Remote Sensing of Environment*, *207*, 84-97. https://doi.org/10.1016/j.rse.2017.12.025

Veh, G., Korup, O., von Specht, S., Roessner, S., & Walz, A. (2019). Unchanged frequency of moraine-dammed glacial lake outburst floods in the Himalaya. *Nature Climate Change*, *9*(5), 379-383. https://doi.org/10.1038/s41558-019-0437-5

Viani, C., Giardino, M., HuGGel, C., Perotti, L., & Mortara, G. (2016). An overview of glacier lakes in the Western Italian Alps from 1927 to 2014 based on multiple data sources (historical maps, orthophotos and reports of the glaciological surveys). *Geografia Fisica e Dinamica Quaternaria*, *39*(2), 203-214. https://doi.org/10.5167/uzh-136706

Vuichard, D., & Zimmermann, M. (1987). The 1985 catastrophic drainage of a moraine-dammed lake, Khumbu Himal, Nepal: cause and consequences. *Mountain Research and Development*, 91-110. https://doi.org/10.2307/3673305

Wang, X., Liu, S., Ding, Y., Guo, W., Jiang, Z., Lin, J., & Han, Y. (2012). An approach for estimating the breach probabilities of moraine-dammed lakes in the Chinese Himalayas using remote-sensing data. *Natural Hazards and Earth System Sciences*, *12*(10), 3109-3122. https://doi.org/10.5194/nhess-12-3109-2012

Wang, X., Guo, X., Yang, C., Liu, Q., Wei, J., Zhang, Y., ... & Tang, Z. (2020). Glacial lake inventory of high-mountain Asia in 1990 and 2018 derived from Landsat images. *Earth System Science Data*, *12*(3), 2169-2182. https://doi.org/10.5194/essd-12-2169-2020

Wilson, R., Glasser, N. F., Reynolds, J. M., Harrison, S., Anacona, P. I., Schaefer, M., & Shannon, S. (2018). Glacial lakes of the Central and Patagonian Andes. *Global and Planetary Change*, *162*, 275-291. https://doi.org/10.1016/j.gloplacha.2018.01.004

Wood, J. L., Harrison, S., Wilson, R., Emmer, A., Yarleque, C., Glasser, N. F., ... & Villafane, H. (2021). Contemporary glacial lakes in the Peruvian Andes. *Global and Planetary Change*, *204*, https://doi.org/10.1016/j.gloplacha.2021.103574

Worni, R., Huggel, C., & Stoffel, M. (2013). Glacial lakes in the Indian Himalayas—From an area-wide glacial lake inventory to on-site and modeling based risk assessment of critical glacial lakes. *Science of the Total Environment*, *468*, S71-S84. https://doi.org/10.1016/j.scitotenv.2012.11.043

Xiao, K., Griffis, T. J., Baker, J. M., Bolstad, P. V., Erickson, M. D., Lee, X., ... & Nieber, J. L. (2018). Evaporation from a temperate closed-basin lake and its impact on present, past, and future water level. *Journal of Hydrology*, *561*, 59-75. https://doi.org/10.1016/j.jhydrol.2018.03.059

Xin, W., Shiyin, L., Wanqin, G., Xiaojun, Y., Zongli, J., & Yongshun, H. (2012). Using remote sensing data to quantify changes in glacial lakes in the Chinese Himalaya. *Mountain Research and Development*, *32*(2), 203-212. https://doi.org/10.1659/MRD-JOURNAL-D-11-00044.1

Xu, X., Wang, W., Huang, D., Hu, X., & Fu, W. (2023). Assessment of interannual and seasonal glacier mass changes in the Karakoram during 2018–2022 using ICESat-2 data. *Journal of Hydrology*, *626*, 130223. https://doi.org/10.1016/j.jhydrol.2023.130223

Yao, X., Liu, S., Han, L., Sun, M., & Zhao, L. (2018). Definition and classification system of glacial lake for inventory and hazards study. *Journal of Geographical Sciences*, *28*, 193-205. https://doi.org/10.1007/s11442-018-1467-z

You, Q. L., Ren, G. Y., Zhang, Y. Q., Ren, Y. Y., Sun, X. B., Zhan, Y. J., ... & Krishnan, R. (2017). An overview of studies of observed climate change in the Hindu Kush Himalayan (HKH) region. *Advances in Climate Change Research*, *8*(3), 141-147. https://doi.org/10.1016/j.accre.2017.04.001

Zemp, M., Huss, M., Thibert, E., Eckert, N., McNabb, R., Huber, J., ... & Cogley, J. G. (2019). Global glacier mass changes and their contributions to sea-level rise from 1961 to 2016. *Nature*, *568*(7752), 382-386. https://doi.org/10.1038/s41586-019-1071-0

Zhang, G., Yao, T., Xie, H., Wang, W., & Yang, W. (2015). An inventory of glacial lakes in the Third Pole region and their changes in response to global warming. *Global and Planetary Change*, *131*, 148-157. https://doi.org/10.1016/j.gloplacha.2015.05.013

Zhang, G., Bolch, T., Allen, S., Linsbauer, A., Chen, W., & Wang, W. (2019). Glacial lake evolution and glacier–lake interactions in the Poiqu River basin, central Himalaya, 1964–2017. *Journal of Glaciology*, *65*(251), 347-365. doi:10.1017/jog.2019.13

Zhang, M., Chen, F., Zhao, H., Wang, J., & Wang, N. (2021). Recent changes of glacial lakes in the high mountain asia and its potential controlling factors analysis. *Remote Sensing*, *13*(18), 3757. https://doi.org/10.3390/rs13183757

Zhang, T., Wang, W., An, B., & Wei, L. (2023). Enhanced glacial lake activity threatens numerous communities and infrastructure in the Third Pole. *Nature Communications*, *14*(1), 8250. https://doi.org/10.1038/s41467-023-44123-z

Zhang, T., Wang, W., & An, B. (2023). A conceptual model for glacial lake bathymetric distribution. *The Cryosphere Discussions*, *2023*, 1-35. https://doi.org/10.5194/tc-17-5137-2023

Zhang, T., Wang, W., & An, B. (2024). Heterogeneous changes in global glacial lakes under coupled climate warming and glacier thinning. *Communications Earth & Environment*, *5*(1), 374. https://doi.org/10.1038/s43247-024-01544-y

Zhang, T., Wang, W., & An, B. (2025). A massive lateral moraine collapse triggered the 2023 South Lhonak Lake outburst flood, Sikkim Himalayas. *Landslides*, *22*(2), 299-311. https://doi.org/10.1007/s10346-024-02358-x

Zheng, G., Allen, S. K., Bao, A., Ballesteros-Cánovas, J. A., Huss, M., Zhang, G., ... & Stoffel, M. (2021). Increasing risk of glacial lake outburst floods from future Third Pole deglaciation. *Nature Climate Change*, *11*(5), 411-417. https://doi.org/10.1038/s41558-021-01028-3

8. List of publications

Original publications in the framework of the PhD thesis

Kumar, A., Mal, S., Schickhoff, U., & Dimri, A. P. (2025). Basin-scale spatio-temporal development of glacial lakes in the Hindukush-Karakoram-Himalayas. *Global and Planetary Change*, *245*, 104656. doi: https://doi.org/10.1016/j.gloplacha.2024.104656

Kumar, A., Mal, S., Schickhoff, U., Allen, S., & Dimri, A. P. (**accepted**). Assessing the role of regional characteristics in estimating the volume of glacial lakes in the upper Indus-Ganga-Brahmaputra basins, Hindu Kush Himalaya (Manuscript No: HYDROL60046R1)

Kumar, A., Mal, S., Schickhoff, U., & Sreekesh, S. (2024). Glacial Lake Dynamics in Dibang Valley District, Arunachal Pradesh, Eastern Himalaya. *Journal Of The Geological Society Of India*, *100*(11), 1521-1530.4.4. doi: https://doi.org/10.17491/jgsi/2024/174012

Kumar, A., Mal, S., & Schickhoff, U. (**accepted**). Spatio-temporal evolution of glacial lakes in the Upper Ganga Basin, Central Himalayas. Himalaya: Mountains of Destiny.

List of oral presentations

IGU, 2022: Kumar, A.; Mal, S., Schickhoff, U (2022). Spatio-temporal Distribution of Glacial Lakes in Indus-Ganga-Brahmaputra River Basin: First Results. IGU Paris.

EGU, 2024: Kumar, A., Mal, S., & Schickhoff, U. (2024). Spatio-temporal evolution of glacial lakes in the Upper Ganga basin, Central Himalayas (No. EGU24-3373). Copernicus Meetings.

High Mountain Conference, 2024: Kumar, A., Schickhoff, U., Mal, S. (2024). Estimating mean depth and volume of glacial lakes in the upper Indus, Ganga and Brahmaputra basin, Hindu-Kush-Himalayas. Bad Hindelang.

Appendix

Original publication

Article I

Kumar, A., Mal, S., Schickhoff, U., & Dimri, A. P. (2025). Basin-scale spatio-temporal development of glacial lakes in the Hindukush-Karakoram-Himalayas. *Global and Planetary Change*, *245*, 104656. doi: https://doi.org/10.1016/j.gloplacha.2024.104656

Global and Planetary Change 245 (2025) 104656

Contents lists available at ScienceDirect

Global and Planetary Change

journal homepage: www.elsevier.com/locate/gloplacha

Research Article

Basin-scale spatio-temporal development of glacial lakes in the Hindukush-Karakoram-Himalayas

Atul Kumar [a,*], Suraj Mal [b], Udo Schickhoff [a], A.P. Dimri [c]

[a] CEN Center for Earth System Research and Sustainability, Institute of Geography, University of Hamburg, Hamburg 20146, Germany
[b] Centre for the Study of Regional Development, Jawaharlal Nehru University, New Delhi 110067, India
[c] School of Environmental Sciences, Jawaharlal Nehru University, New Delhi 110067, India

ARTICLE INFO

Editor: Dr. Jed O Kaplan

Keywords:
Climate change
Glacial lakes
Glacial Lake Outburst Floods
Hindukush-Karakoram-Himalayas
Remote Sensing

ABSTRACT

Glacial lakes are expanding exponentially in the cryospheric environment of the Hindukush-Karakoram-Himalayas (HKH). Rapid glacier melting due to an above mean global annual temperature increase in HKH is attributed as the main reason for the expansion of the glacial lakes. The rapid expansion of glacial lakes increases the risk of future Glacial Lake Outburst Floods (GLOFs) events in the HKH.

In the present study, glacial lake inventories for the Indus, Ganga and Brahmaputra (IGB) river basins in the HKH were generated for 1990, 2000, 2010 and 2020 using Landsat (TM & OLI) at the sub-basin level to understand the spatio-temporal and regional patterns of glacial lakes dynamics, elevational evolution, and changes in the typology. We mapped 17,641 glacial lakes (area: 1082.57 ± 192.601 km^2) in 1990, 18,206 (area: 1120.95 ± 198.49 km^2) in 2000, 18,399 (area: 1147.12 ± 201.26 km^2) in 2010, and 19,284 (area: 1191.81 ± 209.21 km^2) in 2020. Between 1990 and 2020, IGB basins showed an increase of 9.31 % in total number and 10.09 % in total area of glacial lakes. In 2020, the Brahmaputra basin had the maximum total area (area: 763.59 ± 132.14 km^2), followed by Indus basin (area: 217.47 ± 43.39 km^2) and the Ganga basin (area: 210.74 ± 33.66 km^2). However, between 1990 and 2020, glacial lakes in the Ganga basin (n: 22.08 %) had the highest growth rate, followed by the Indus basin (n: 14.73 %) and the Brahmaputra basin (n: 4.41 %). In 2020, 76.11 % of glacial lakes were end-moraine-dammed M(e) lakes, followed by other bedrock-dammed B(o) lakes (16.45 %), supra-glacial lakes (2.79 %), lateral moraine-dammed M(l) lakes (2 %), cirque B(c) lakes (1.06 %), other moraine-dammed M(o) lakes (0.38 %), and other glacial (O) lakes (1.18 %). Given the rapid growth of glacial lakes in the region along with their likely flood volumes and damage potential in case of their failures, the present study will be of importance for disaster management authorities, an important input for detection of potentially hazardous glacial lakes and for development of mitigation strategies to minimize the impact of potential future GLOF events.

1. Introduction

Glacial lakes are water bodies that develop in depressions through accumulation of glacial and snow meltwater due to glacial processes (Yao et al., 2018; Wang et al., 2020). Distributed mainly above 3500 m asl (Ives et al., 2010; Nie et al., 2017; Maharjan et al., 2018), glacial lakes are a vital component of alpine systems in the Hindukush-Karakoram-Himalayas (HKH) mountains and play a crucial role in regional hydrology (Emmer, 2018; Immerzeel et al., 2020). In many cases, high-altitude lakes contribute to the discharge of great rivers like the Indus and the Brahmaputra (Maharjan et al., 2018; Immerzeel et al., 2020), which support life, agriculture, economy and ecosystem services in the source and downstream regions.

Ives et al. (2010) provided the first comprehensive glacial lake inventory for the HKH region and mapped 8790 glacial lakes, covering an area of 801.83 km^2. Several studies have been conducted since then to map and monitor changes of glacial lakes in the HKH region (Zhang et al., 2015; Nie et al., 2017; Maharjan et al., 2018; Shugar et al., 2020; Li et al., 2022). However, there are discrepancies in their results, in terms of the number, area, and growth rate of glacial lakes across the

Abbreviations: GLOF, Glacial Lake Outburst Flood; HKH, Hindukush-Karakoram-Himalayas; HMA, High Mountain Asia; IGB, Indus, Ganga and Brahmaputra; NDWI, Normalized Difference Water Index; ISM, Indian Summer Monsoon.

* Corresponding author.
E-mail address: atul.sbsc@gmail.com (A. Kumar).

https://doi.org/10.1016/j.gloplacha.2024.104656
Received 11 February 2024; Received in revised form 20 November 2024; Accepted 21 November 2024
Available online 28 November 2024

different studies, owing to variations in data and methods adopted (Mal et al., 2020; Mal et al., 2021; Ahmed et al., 2021).

Previous studies confirm the exponential growth of glacial lakes in the HKH mountains, which is mainly attributed to enhanced glacial melting in the recent past (Zhang et al., 2015; Schickhoff et al., 2016; Nie et al., 2017; Bolch et al., 2019; Yang et al., 2019; Li et al., 2022), caused by accelerated warming trends (Schickhoff and Mal, 2020; Schickhoff et al., 2022). Nie et al. (2013) estimated an increase of 10.32 % in the number of glacial lakes, and 17.2 % increase in their area between 1990 and 2010 in the central Himalayan region. Zhang et al. (2015) observed a growth of 23.88 % and 23.19 % in total number and area of glacial lakes, respectively, in the HKH region between 1990 and 2010, while Nie et al. (2017) observed a significantly lower rise of 8.81 % and 14.1 % in the total number and area of glacial lakes, respectively, in the Himalayan region between 1990 and 2015. Wang et al. (2020) detected an increase of 10.71 % and 15.14 % in the total number and area of glacial lakes, respectively, over High Mountain Asia during 1990 and 2018. Overall, it is observed that glacial lakes on the southern slopes of the central Himalayan region are expanding at the highest rate, followed by eastern and western HKH region (Gardelle et al., 2011; Nie et al., 2017; Bolch et al., 2019). The differences in the growth rates of glacial lakes as observed in different studies, can be attributed to 1) the spatial resolutions and time of satellite data acquisitions, 2) % of cloud and snow cover, 3) shadow from the mountain ridges on the satellite images, 4) minimum mapping and elevation thresholds of glacial lakes, 5) distance from the glaciers, and 6) expertise in identification of glacial lakes affecting the overall accuracy of mapping, hence these studies are not directly comparable (Ahmed et al., 2021; Dimri et al., 2021).

Proglacial lakes connected with parent glaciers have seen the highest growth rate (area) in the study region (Nie et al., 2017; King et al., 2018; Krause et al., 2019; Ahmed et al., 2021). In recent decades, significant glacial lake activity (emergence/disappearance) has been observed at higher elevations (more than 5500 m asl) in the HKH region, due to significant elevation dependent warming in the region (Gardelle et al., 2011; Nie et al., 2017; Li et al., 2022). Consequently, the number of potentially hazardous glacial lakes capable of causing outburst flood events and significant damage to physical and human environment, critical infrastructure and economy, are also increasing across the HKH region (Ahmed et al., 2021; Mal et al., 2021; Emmer et al., 2022; Hu et al., 2022; Taylor et al., 2023).

Recent studies consider the HKH region as the most susceptible mountain range to hazardous Glacial Lake Outburst Flood (GLOF) events, given the large human population and infrastructure being highly vulnerable (Taylor et al., 2023). Continuous expansion of glacial lakes and their hazardous potential coupled with the rising population and growing infrastructure in the inner-high alpine valleys put pressure on the HKH region (Mal et al., 2021; Taylor et al., 2023). High Mountain Asia (HMA) including HKH has the highest exposure to future GLOF events as ~1 million people are living within 10 km of glacial lakes Zheng et al., 2021a; Taylor et al., 2023). Several studies attempted to conduct and update the GLOFs inventory (n: 34–154) across the HKH region (Zheng et al., 2021b; Shrestha et al., 2023; Zhang et al., 2023a, 2023b). Lützow et al. (2023) mapped 512 GLOF events in the extended HMA. In addition, several of the past GLOF events in the HKH remain unreported due to lack of monitoring and inaccessible terrain (Veh et al., 2019). An increase in the GLOF events has been observed in the last decades in the study domain (Harrison et al., 2018). Some of the recent GLOF events in the HKH region, including Chorabari floods (2013), Gongbatongshaco (2016), and South Lhonak (2023), have caused severe damage to human population and infrastructure (Shugar et al., 2021; Ahmed et al., 2023; Zhang et al., 2023a, 2023b). Therefore, continuous mapping and monitoring of glacial lakes in the HKH region is of immense importance, given their ongoing and future growth in the 21st century and increase in their hazard potential (Zheng et al., 2021a).

To the best of our knowledge, studies on the spatio-temporal development of glacial lakes in the HKH region, considering east-west gradient at the basin and sub-basin levels are still lacking. Also, change in different types of glacial lakes across the study region and for different elevation zones have not yet been analyzed in detail. Therefore, the present study with focus on the spatial gradients aims 1) to investigate the development of glacial lakes at the sub-basin level, 2) to analyze the changes in distance between glaciers and glacial lakes, 3) to examine the changes in different glacial lake types, and 4) to analyze the orientation and elevation zone-wise changes in the glacial lakes in the HKH region from 1990 to 2020 at decadal scale.

2. Study area

Geographically, the Indus, Ganga, and Brahmaputra (IGB) river basins are located in the HKH region, with an area of ~1.2 million km^2, and extend from 21° to 37° N latitudes and from 66° to 97° E longitudes, respectively (Supplementary Fig. 1). The IGB rivers originating from the glaciers and lakes of the Greater Himalayas and are fed in their upper catchments by meltwater from snow and glaciers. Having the largest concentration of glaciers (~40,800 km^2) outside the polar region, the study domain is popularly known as the "water tower of Asia" and the "third pole" (Bolch et al., 2012; Zheng et al., 2021b).

The study domain exhibits complex physiographic, climatic, hydrological, ecological, and socio-economic characteristics owing to the large geographical extent and elevation range. The mean elevation generally increases from south (sea level) to north (8848 m asl: Mount Everest) and from east to west. The climate of the study domain varies from dry-cold in the north-western parts to the humid sub-tropical in the eastern Himalayas (Pant and Kolli, 1997). Most of the precipitation (~80 %) is caused by the Indian Summer Monsoon (ISM) system from June to September, while winters receive ~10 % of the annual precipitation from Western Disturbances from December to February (Dimri et al., 2016; Maharana et al., 2021). The temperature in the study domain can vary between −40 °C in the winters to 40 °C in the summers (Krishnan et al., 2019). Ongoing climate change in the study domain and related cryospheric changes have led to the emergence of new glacial lakes, to the growth of existing ones (Nie et al., 2017; Zheng et al., 2021a), and to GLOF events (Bolch et al., 2019; Krause et al., 2019; Veh et al., 2022), making the study domain one of the most vulnerable regions of the GLOF disaster globally (Zheng et al., 2021a; Taylor et al., 2023).

3. Data and methodology

3.1. Data

Landsat missions, with a moderate spatial resolution (30 m) and a 16-days repeat cycle, provide the longest and most consistent satellite data for the mapping and monitoring of glacial lakes in the HKH region and other mountain ranges of the world (Shugar et al., 2020; Chen et al., 2021). A total of 483 Landsat (TM/OLI) (https://earthexplorer.usgs.gov/) images were used to generate glacial lake inventories of 1990, 2000, 2010 and 2020 for the study domain. The selection of suitable satellite images for the particular years was a complex process due to conditions of 1) cloud cover, 2) snow cover, and 3) shadows from the ridge, which remain a challenge for the mapping of glacial lakes (Bhambri et al., 2018; Mal et al., 2020). Therefore, images from adjacent years (± 3) were obtained to complete glacial lake inventories for various years (Table 1). The satellite images were carefully selected from the ablation period with minimum snow and cloud cover and minimum shadow effects from the mountain ridges for a relatively accurate mapping of glacial lake extents (Bhambri et al., 2015; Maharjan et al., 2018).

In addition, the Shuttle Radar Topography Mission (SRTM) V4 (30 m) Digital Elevation Model (DEM) was obtained from the United States Geological Survey (USGS, https://earthexplorer.usgs.gov/). Hillshades, slope and aspect maps were generated from SRTM DEM to aid the

Table 1
Details of the satellite images used in the study.

Years	Satellites	Sensors	Spatial Resolution	Satellite images (n) used for individual lake inventory
1990 (± 3)	Landsat 5	Thematic Mapper (TM)	30 m	148
2000 (± 3)	Landsat 5	Thematic Mapper (TM)	30 m	138
2010 (± 3)	Landsat 5/8	Thematic Mapper (TM)	30 m	88
2020 (± 3)	Landsat 8	Operational Land Imager (OLI)	30 m	109

mapping of glacial lakes. We also used Randolph Glacier Inventory (RGI Ver. 7.0) (https://www.glims.org/RGI/) to calculate the distance between glacial lakes and glaciers. Furthermore, to understand the distribution of glacial lakes at the sub-basin level, we used sub-basin boundaries developed by Regional Database System (RDS), International Centre for Integrated Mountain Development (ICIMOD) (ICIMOD, 2021).

3.2. Methodology

3.2.1. Glacial lake mapping

Glacial lake mapping techniques are mainly categorized into three groups, 1) manual (Ashraf et al., 2017; Wang et al., 2020; Rao et al., 2021), 2) automated (Worni et al., 2013; Shugar et al., 2020;), and 3) semi-automated (Mal et al., 2020; Zheng et al., 2021a; Li et al., 2022). Manual glacial lake mapping is based on the experience and expertise of the interpreter and is labour and time inefficient (Bhambri et al., 2018). Automated glacial lake mapping, on the other hand, is the quickest way to map glacial lakes. However, it generates erroneous results due to misidentification of pixels as glacial lakes in the presence of shadow, and snow, especially in high mountainous region (Mal et al., 2020; Li et al., 2022). The semi-automated glacial lake mapping methods integrate automated detection of glacial lakes, followed by manual corrections, which is usually relatively accurate and is preferred for large-scale assessments, e.g., in the HKH region (Nie et al., 2017; Li et al., 2022). Therefore, in the present study, we adopted a semi-automated method for generating inventories of glacial lakes in the study domain. The first step for glacial lake mapping was to extract the water mask from the Landsat satellite images based on the Normalized Difference Water Index (NDWI), with values ranging between ±1, using Green and Near InfraRed (NIR) bands (Gao, 1996).

$$NDWI = \frac{(Band_{GREEN} - Band_{NIR})}{(Band_{GREEN} + Band_{NIR})} \quad (1)$$

An optimal threshold of NDWI (>0.3) to extract the glacial lakes was carefully chosen based on the visual interpretation of lake and non-lake pixels, which has been generally used by previous studies (Ji et al., 2009; Shugar et al., 2020; Zhang et al., 2022). We, then, applied the elevation threshold of ≥2900 m asl on the NDWI image (Fig. 1). The elevation threshold of 3500 m asl in the glacial lake classification is suggested in many studies (Mool et al., 2001a&Mool et al., 2001b; Campbell and Pradesh, 2005; Ives et al., 2010). However, it was observed during the generation of the glacial lake inventory that some such lakes were found as low as 2900 m, as also confirmed in some previous studies (Nie et al., 2017; Maharjan et al., 2018). Furthermore, the slope threshold is selected at ≤20°, because glacial lakes require stable slope for accumulating water into the depressions (Zhang et al., 2015).

The last step in generating the glacial lake inventories was to select a minimum mapping unit of glacial lakes. In the case of Landsat images, at least four pixels (or 0.0036 km^2) are required for the efficient identification of glacial lakes (Mal et al., 2020; Li et al., 2022), hence, the same area threshold was chosen in the present study. However, some studies have also applied a relatively larger threshold of nine pixels (0.0081 km^2) (Nie et al., 2017; Wang et al., 2020), which significantly reduces the number of glacial lakes, as smaller lakes (less than 0.0081 km^2) are omitted from the mapping process. Each glacial lake was then inspected in Google Earth Pro for the manual correction of lake outlines. The glacial lake inventories for various years were then finalized, which were further characterized by their area, elevation, orientation, and type and distance from nearby glacier (up to 10 km) for the purpose of comparing with other studies.

3.2.2. Uncertainty analysis

Glacial lake outline extraction based on the satellite datasets using automated, semi-automated and manual method involves mapping uncertainties up to one pixel, depending on the resolution and overall

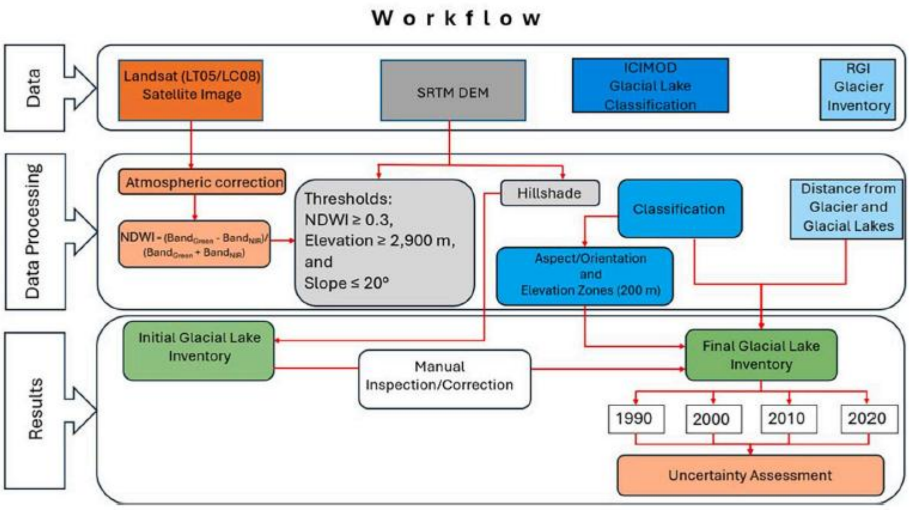

Fig. 1. Methodological framework used in the study.

quality of the satellite image (Salerno et al., 2012; Zhang et al., 2015; Nie et al., 2017; Wang et al., 2020; Chen et al., 2021). In the automated mapping, the satellite pixel can either be mapped as glacial lake or not, therefore resulting in the uncertainty of maximum of one pixel. On the contrary, in case of semi-automated, which involves manual correction of lake boundary obtained from automated mapping process, roughly half of a satellite data pixel can be mapped as glacial lake, as the surrounding pixels can represent a mix of lake and other features (Rinzin et al., 2021).

In the present study, we used a lake uncertainty estimation method as proposed by Hanshaw and Bookhagen (2014), which is based on the pixelated polygons and performs better on automated and semi-automated method based glacial lake inventories, as compared to the manually extracted glacial lakes (Lesi et al., 2022). The main reason for the better performance of this method is, that the automated and semi-automated extracted glacial lake boundaries follow the pixels, while the same may not be true with manually extracted glacial lake (Wang et al., 2020). Using the Hanshaw and Bookhagen (2014) equation, absolute uncertainty of glacial lake outlines for all inventories generated in the present study are estimated as below:

$$Error(1\sigma) = \frac{P}{G} {*}0.6872{*}G^2 \Big/ 2 \qquad (2)$$

Where, G is the cell size of the remote sensing imagery (30 m for Landsat images), P is the perimeter of an individual glacial lake (m), and 0.6872 is the revised co-efficient based on the assumption that area measurements uncertainty follows a Gaussian distribution.

In addition, the absolute uncertainties have been converted to the relative uncertainties using the following formula:

$$E = \frac{\mathrm{Error}(1\sigma)}{A} \times 100\% \qquad (3)$$

Where, E is the relative error of glacial lakes and A is the total area of glacial lake.

Furthermore, the same is applied to calculate the uncertainty of change in area for newly emerged and expanded glacial lakes between 1990 and 2020, as estimated using the erase tool in ArcGIS Pro.

3.2.3. Glacial lake classification

There is no universally agreed-upon classification scheme of glacial lakes in different mountain systems. Nevertheless, several scholar and organizations devised different schemes for glacial lake classification (Ives et al., 2010; ICIMOD, 2011; Nie et al., 2013; Zhang et al., 2015; Yao et al., 2018). For instance, Nie et al. (2017) classified glacial lakes into two major categories viz., glacier-fed and non-glacier-fed. Yao et al. (2018) classified glacial lakes based on their formation processes, dam-material, and location, into 6 major categories (glacial erosion lakes, moraine-dammed lakes, ice-blocked lakes, supraglacial lakes, subglacial lakes, and other glacial lakes).

Here, the ICIMOD (2011) glacial lake classification scheme for the HKH region as modified by Maharjan et al., 2018 (Supplementary table 2) is used in the present study with slight modifications. They classified glacial lakes into four major categories based on the dam type and formation processes, viz. 1) moraine-dammed lakes (M), 2) bedrock-dammed lakes (B), 3) ice-dammed lakes (I), and 4) other glacial lakes (O) that are formed by accumulation of glacial meltwater, but not essentially dammed by material generated by glacial processes (Maharjan et al., 2018). Moraine-dammed lakes were further divided into three categories: end moraine-dammed lakes (M(e)), lateral moraine-dammed lakes (M(l)), and other moraine-dammed lakes (M(o)), bedrock-dammed lakes were divided into two categories: cirque lakes (B(c)) and other bedrock-dammed lakes (B(o)), and ice-dammed lakes are divided into two sub-categories: Supraglacial (S) and dammed by tributary glaciers (I(v)), thus there are eight sub-categories of glacial lakes (Maharjan et al., 2018). Each glacial lake was manually inspected in ArcGIS Pro (Ver 2.9) and Google Earth Pro for classification purposes and assigned relevant classes. However, I(v) lake category was omitted from the lake classification due short-lived nature and difficulties in their identification, thus considering only seven sub-categories in the present study.

3.2.4. Glacier and glacial lake relationship

To better understand the relationship between glaciers and glacial lakes for 1990, 2000, 2010 and 2020, the RGI (Ver. 7.0) was obtained from the National Snow and Ice Data Centre (NSIDC) (RGI Consortium, 2017). Near distance tool in ArcGIS Pro (Ver 3.2) was applied to calculate the distance of all glacial lakes to the glaciers within the threshold of 10 km for the ease of comparison with previous studies (Zhang et al., 2015; Wang et al., 2020; Li et al., 2022).

4. Results

4.1. Spatio-temporal distribution and dynamics of glacial lakes

There is an east-west of gradient of glacial lakes distribution (2020) at the sub-basin level in the study domain (Fig. 2). The concentration of glacial lakes decreases from the Brahmaputra basin (n: 11,579, area: 763.6 ± 132.14 km^2) in the eastern Himalayas to the Ganga basin (n: 3118, area: 210.45 ± 33.66 km^2) in the central Himalayas. Proceeding further to the west, a slight increase is observed towards the Indus basin (n: 4587, area: 217.48 ± 43.39 km^2) in the western Himalayas (Fig. 2 and Supplementary Table 3).

The total number of glacial lakes in the study domain was 17,641 (area: 1082.56 ± 192.60 km^2) in 1990, which increased to 18,206 (area: 1120.94 ± 198.49 km^2) in 2000, 18,399 (area: 1147.12 ± 201.26 km^2) in 2010, and 19,284 (area: 1191.81 ± 209.21 km^2) in 2020. Overall, the number and area of glacial lakes increased by 9.31 % and 10.1 %, respectively from 1990 to 2020. At the major river basin scale, the Brahmaputra basin had the highest number of glacial lakes with 11,089 (1990), 11,195 (2000), 11,280 (2010), and 11,579 (2020), followed by the Indus basin with 3998 (1990), 4228 (2000), 4285 (2010), and 4587 (2020), and the Ganga basin with 2554 (1990), 2783 (2000), 2834 (2010), and 3118 (2020) (Fig. 2 and Supplementary Table 3). All three river basins experienced accelerated growth of glacial lakes during the study period, with the recent decade (2010–2020) observing highest growth (n: 4.81 %, area: 3.89 %) (Supplementary Table 4). The Ganga basin had the highest glacial lakes growth rate (n: 22.08 %, and area: 23.85 % from 1990 to 2020, followed by the upper Indus (n: 14.73 % and area: 9.37 %) and the Brahmaputra (n: 4.41 % and area: 7.01 %) (Fig. 2, Supplementary Fig. 2, and Supplementary Table 4). At the decadal scale, growth rate of glacial lakes was relatively low in the Indus and Ganga basin for the decade between 2000 and 2010 as compared to the previous decade between 1990 and 2000. However, it significantly increased in the later decade between 2010 and 2020. Some of the examples of accelerated growth rate of glacial lakes is depicted in Fig. 2b.

Between 1990 and 2020, the mean area of glacial lakes increased from 0.61 km^2 (1990) to 0.62 km^2 (2020). At the major basin level, the Brahmaputra (0.002 km^2) and Ganga (0.001 km^2) showed a positive change in the mean area of glacial lakes, whereas a decline is observed in the Indus basin (−0.002 km^2) during the same time (Supplementary Table 5).

The sub-basins of Ganga River on the southern slopes of central Himalayas, and three sub-basins of Indus basin (e.g., Shyok: n-133) show significantly higher growth in numbers of glacial lakes, while the Brahmaputra basin observed lowest growth specially in the northern basins, except Yigong Zangbo river basin (13.27 ± 0.32 km^2) (Fig. 3, Supplementary Table 1). Furthermore, of 73 sub-basins, 60 showed overall positive change in number of glacial lakes, while 9 sub-basins showed no change, and 4 showed negative changes, located in the eastern Himalayan basins (Supplementary Table 1). Overall, 64 sub-basins showed a positive change in the area of glacial lakes, while 9 showed negative change in the area of glacial lakes between 1990 and

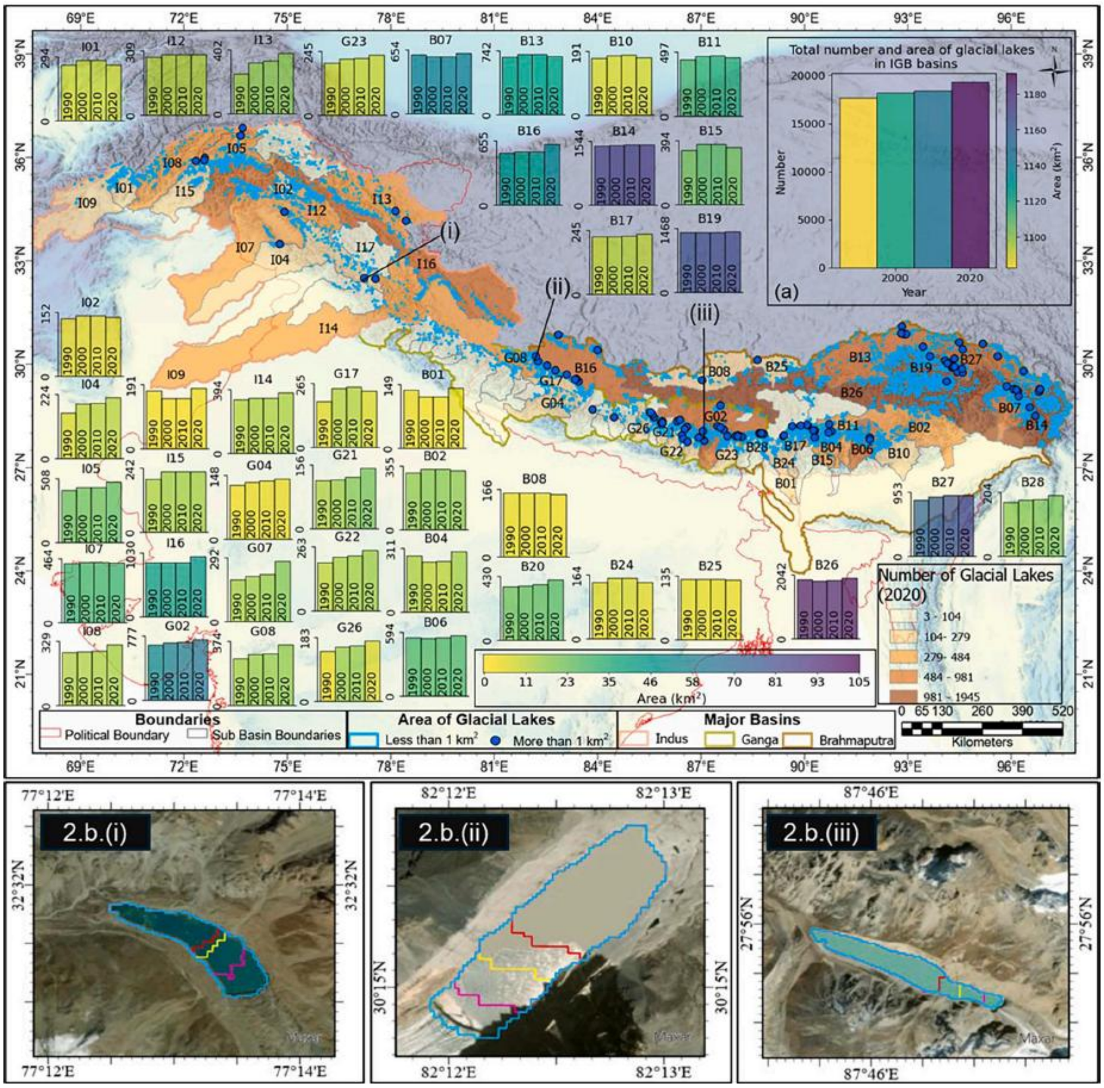

Fig. 2. Distribution of glacial lakes (n) at the sub-basin level in the study area (2020) is shown in the main map. Large dark blue and small light blue circles represent larger (area ≥ 1 km^2) and smaller (area < 1 km^2) glacial lakes. Bar diagrams represent the decadal distribution of glacial lakes for different sub-basins (n: >100) between 1990 and 2020. X/Y axis indicate years and numbers of glacial lakes, respectively, while the area is indicated by different colors (see horizontal colour palette). For codes of all sub-basins, please see Supplementary Table 1 and Fig. 1. The sub-basin boundaries are acquired from RDS, ICIMOD (ICIMOD, 2021). Fig. 2b depicts decadal change of number and area of glacial lakes in the entire study region. Fig. 2b shows examples of glacial lake expansion, which are marked (i-iii) in the main map. (For interpretation of the references to colour in this figure legend, the reader is referred to the web version of this article.)

2020, which are largely located in the eastern Himalayas (Fig. 3 and Supplementary Table 1), exhibiting an east-west gradient.

In 1990, there were only 79 larger glacial lakes (area: ≥ 1 km^2) with a total area of 158.74 ± 8.16 km^2 in the study domain. The number increased to 105 (area: 211.13 ± 10.96 km^2) by 2020. The Ganga basin had the highest increase in the number of larger glacial lakes from 12 (1990) to 27 (2020), followed by Brahmaputra basin from 59 (1990) to 67 (2020), while in the Indus basin such lakes increased from 8 (1990) to 11 (2020).

4.2. *Relationship between glacier and glacial lakes*

The distance between glaciers and glacial lakes is an important indicator to understand the evolution of glacial lakes caused by ongoing climate change-led glacier recession. At the sub-basin level, an east-west gradient of mean distance between glacial lakes and glaciers is observed in the study region in 2020. Southern and eastern sub-basins of Brahmaputra basin exhibit maximum distance between glacial lakes and glaciers (>12 km), while all the sub-basins of the Indus, except Ravi (7.23 km), and the Ganga, except Koshi1 (9.19 km), have a distance of less than 6 km (Fig. 4). The average distance between glaciers and glacial lakes was 5.29 km in 1990, which decreased to 5.13 km (2000), 5.08 km (2010), and further to 4.87 km (2020), with an overall distance change of −0.42 km between 1990 and 2020 (Supplementary Fig. 3). Among the major basins, Brahmaputra (7.14 km) had the highest average distance between glaciers and glacial lakes, followed by Ganga

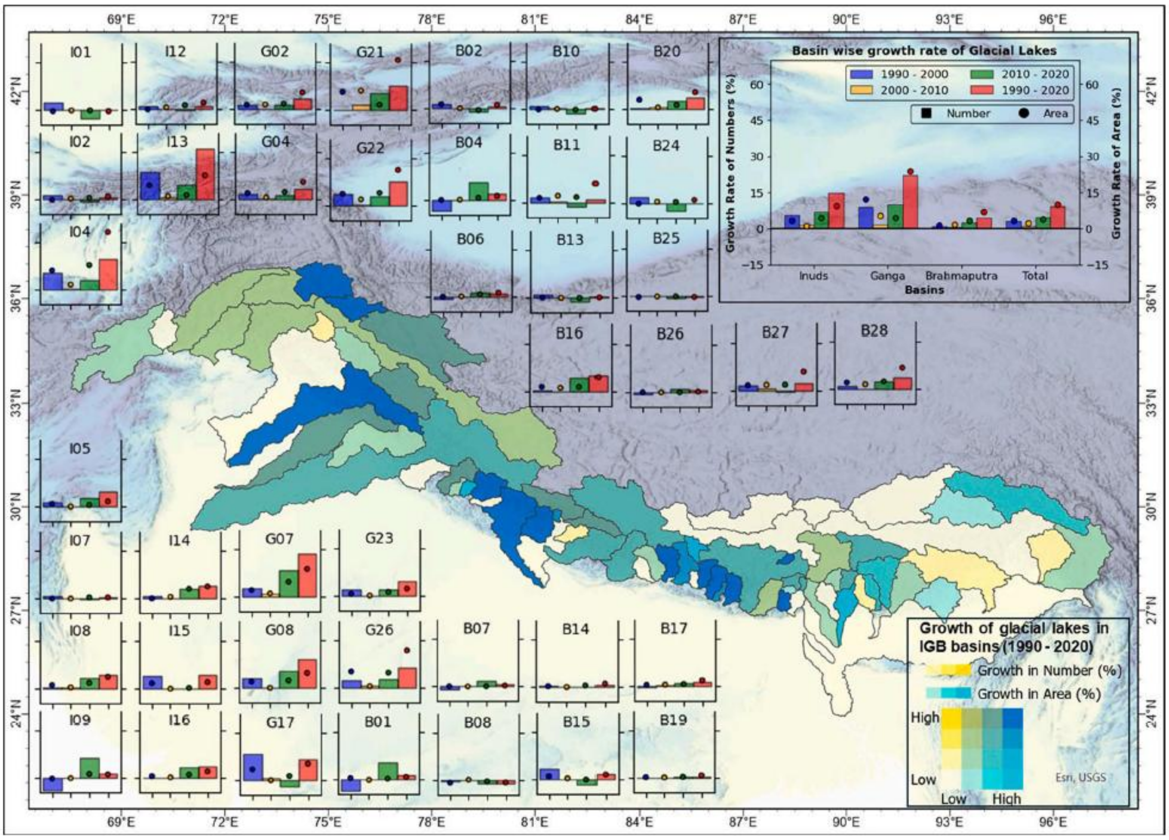

Fig. 3. The bivariate spatial distribution of growth (%) of glacial lakes at the sub–basin level (n: > 100) between 1990 and 2020. Bar plots show growth (%) in number (bars) and area (point) for different decades at the sub–basin level. Sub-plot (top-right) shows decadal growth (%) of glacial lakes at basin scale.

(2.18 km), and Indus (2.16 km) (Fig. 4) in 1990. The average distance between glaciers and glacial lakes declined maximum in Ganga (−0.4 km) basin, followed by Brahmaputra (−0.27 km), and Indus (−0.2 km) basin, whereas overall mean distance change is observed as −0.42 km during the study period (Fig. 4).

4.3. Elevational changes in glacial lakes

Glacial lakes were divided into 18 elevation zones (200 m interval) to understand their altitudinal distributions and dynamics. In the study domain, the glacial lakes are distributed between 2900 m asl and 6216 m asl, with a mean elevation ~4754 m asl in 2020. The mean elevation of glacial lakes in Ganga basin is highest (5052.3 m asl), followed by Brahmaputra basin (4755.07 m asl) and the Indus basin (4549.77 m asl). In most of the sub-basins of Ganga and Brahmaputra basins, glacial lakes have mean elevation ranging from 4500 m asl to ~6000 m asl, while in Indus basin nearly half of the sub-basins are located between 4000 and 4500 m asl (Fig. 5). The elevation zone of 4400 to 4600 m asl has the maximum number of glacial lakes. This elevation zone also had the maximum proportion of lake area between 1990 and 2010, whereas for 2020 the maximum proportion of lake area was in the elevation zone 5000 to 5200 m asl (Fig. 5a).

The mean elevation of glacial lakes has marginally increased from ~4737 m asl in 1990, to 4754 m asl in 2020. In 1990, at the major basin level, the glacial lakes in the Ganga basin had the highest mean elevation of 5044.8 m asl, followed by those in the Brahmaputra (4740.5 m asl), and Indus basin (4531.1 m asl). An increase up to 20 m was observed in all the basins by 2020, with the Indus showing maximum change (18.68 m), followed by Brahmaputra (14.58 m) and Ganga (7.48 m) (Supplementary Fig. 4).

Maximum growth of the number and area of glacial lakes had been observed in the elevation zone of 5000 to 5400 m asl between 1990 and 2020. Significant growth of glacial lakes has also taken place in the elevation zone 5400 to 5800 m asl, while lake activity has been observed above 6000 m asl in 2020 (Fig. 5a and Supplementary Fig. 4).

4.4. Dynamics of glacial lakes on different slope aspects

The slope aspect of glacial lakes plays a crucial role in glacial lake dynamics, as the northern/southern slopes receive lower/higher insolation and have observed varying warming trends. In 1990, of all the 17,641 glacial lakes, 3017 were located on the southern slopes, followed by southeastern (n: 2562), southwestern (n: 2439), northern (n: 2073), eastern (n: 1928), western (n: 1881), northwestern (n: 1872) and northeastern slopes (n: 1869). The number of glacial lakes has significantly grown (5.61–14.95 %) in all cardinal directions from 1990 to 2020 (Fig. 6 and Supplementary Fig. 5).

In 1990, glacial lakes located on northern slopes had the highest aggregate area of 175.70 ± 31.25 km^2, followed by southern slopes (area: 171.32 ± 30.47 km^2), northeastern (147.11 ± 26.17 km^2), southeastern (139.85 ± 24.87 km^2), northwestern (area: 130.35 ± 23.18 km^2), southwestern (area: 125.30 ± 22.29 km^2), western (area: 98.29 ± 17.48 km^2) and eastern slopes (area: 94.32 ± 16.77 km^2). The reason for higher accumulated area of lakes on the northern slopes is the

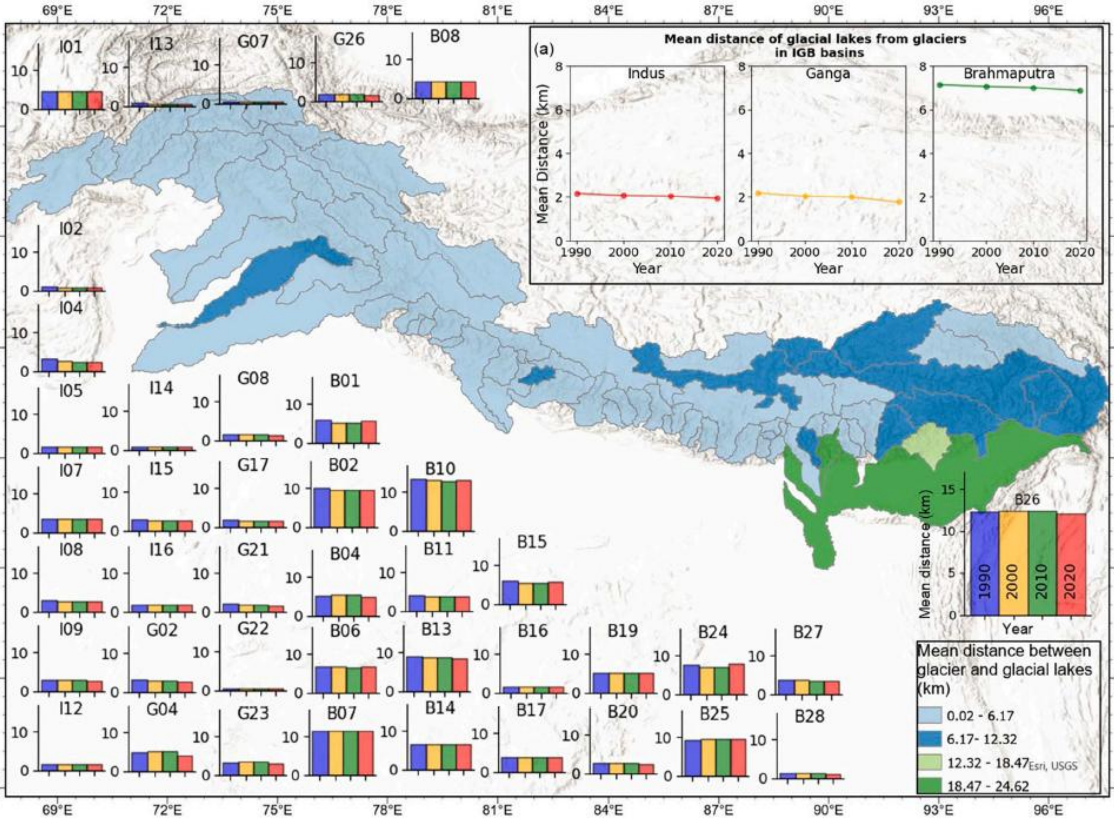

Fig. 4. Mean distance of glacial lakes and glaciers at the sub-basin level is shown in the main map (2020). Sub-plots (bars and line) show the decadal changes in the mean distance of glacial lakes from glaciers at sub-basin and at major basin level (4a) between 1990 and 2020, respectively.

significant presence of larger ($\geq$1 km^2) glacial lakes. However, between 1990 and 2020, glacial lakes orienting towards southeast showed the maximum increase in the area (18.88 $\pm$ 3.35 km^2), followed by north-eastern (area: 16.17 $\pm$ 2.87 km^2), eastern (area: 15.04 $\pm$ 2.67 km^2), northwestern (area: 14.18 $\pm$ 2.52 km^2), southwestern (area: 13.44 $\pm$ 2.39 km^2), southern (area: 10.37 $\pm$ 1.84 km^2), and western aspects (area: 10 $\pm$ 1.77 km^2) (Fig. 6).

4.5. Changes in the typology of glacial lakes

Changes across the categories of glacial lakes have also been observed between 1990 and 2020. Overall, M(e) lakes dominate the number and area of glacial lakes in all the inventories accounting for more than 70 % of all lakes. In the Indus basin, M(e) lakes account for more than 85 % of all lakes in all the inventories, while in the Ganga basin this category accounts for more than 80 % (except in 2020 with 78 %) and in the Brahmaputra basin for more than 71 %. B(o) is the second dominant lake type in the study region, with 4–5 % in the Indus, 8 % in the Ganga basin, and ~ 25 % in the Brahmaputra basin (Supplementary Table 9). All other types of lakes account for very low percentage share in all the inventories across the basins.

All types of glacial lakes showed an increase between 1990 and 2020 (Fig. 7). There were 13,510 (area: 846.49 $\pm$ 147.73 km^2) M(e) lakes in 1990, which increased to 13,941 (area: 881.29 $\pm$ 152.37 km^2) in 2000, 14,066 (area: 905.67 $\pm$ 154.62 km^2) in 2010, and 14,677 (945.27 $\pm$ 161.17 km^2) in 2020, with an overall increase of ~9 % (area: ~12 %) (Supplementary Table 8 and 9). However, the proportion of M(e) lakes in the total number (area) of glacial lakes has declined from 88.1 % (89.4 %) to 85.7 % (86.2 %) in the Indus basin, and from 81.5 % to 77.9 % in the Ganga basin, while it remained nearly unchanged in the Brahmaputra basin. On the contrary, M(e) glacial lake area (%) increased from 73.7 % to 75.9 % in the Brahmaputra basin during the study period. There is a sharp increase in all other types of lakes, however, most noticeable changes are observed in supraglacial lakes, which nearly doubled in Indus and Brahmaputra basin, while they increased by about 4 times in the Ganga basin between 1990 and 2020.

4.6. Newly emerged and disappeared glacial lakes

Glacial lake activities are essentially revealed by newly emerged and disappeared lakes, indicating their dynamic nature caused by accelerated climate change conditions in the study domain. Overall, 1956 (area: 48.56 $\pm$ 8.59 km^2) new glacial lakes were formed, and 307 (area: 4.42 $\pm$ 0.78 km^2) disappeared in the study domain between 1990 and 2020 (Fig. 7 and 8).

In the recent decade of 2010–2020, the highest number of glacial lakes (n: 1144) emerged in the study domain, followed by the decade of 1990–2000 (n: 854) and the decade of 2000–2010 (n: 251). In terms of their area, the decades of 1990–2000 and 2010–2020 had the maximum area (> ~18 km^2 in each decade) of newly emerged glacial lakes, while the area of such lakes was very low (area: 5.13 $\pm$ 0.90 km^2) in the decade 2000–2010 (Fig. 8a and b). On the contrary, the decade of 1990–2000 showed the maximum disappearance of glacial lakes (n: 290, area: 4.64 $\pm$ 0.82 km^2), followed by 2010–2020 (n: 259, area: 4.42

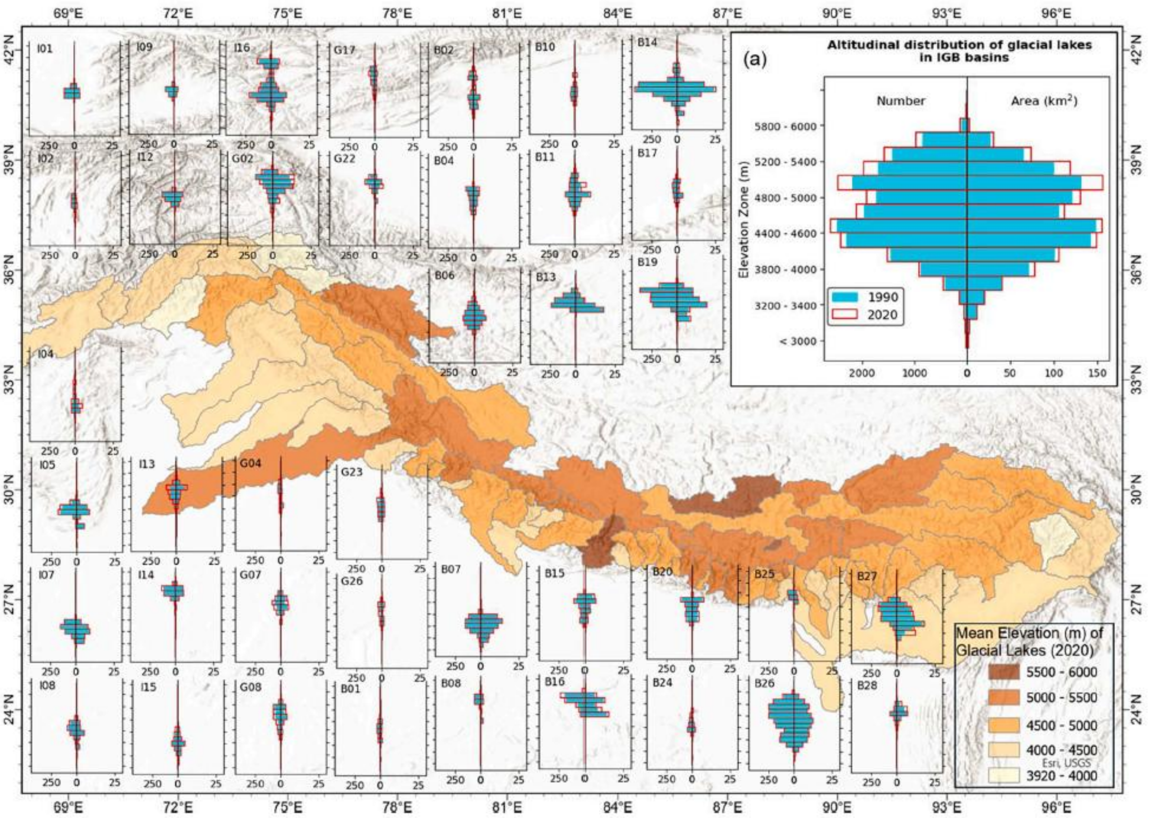

Fig. 5. Altitudinal distribution of glacial lakes at sub-basin level in the study domain between 1990 and 2020. The main map shows the mean elevation of glacial lakes (m asl) in 2020 at the sub-basin level. The sub-plots show the number of glacial lakes (on the left) and the area of glacial lakes (on the right) in the sub-basins (n: >100). The red/blue colors show the number/area for the year 1990/2020/ Fig. 5a shows altitudinal distribution of glacial lakes for the entire study area between 1990 and 2020. (For interpretation of the references to colour in this figure legend, the reader is referred to the web version of this article.)

$\pm$ 078 km^2), while the lowest number of glacial lakes disappeared between 2000 and 2010 (n: 58, area: 0. 69 $\pm$ 0.12 km^2) (Fig. 8a and b).

Out of 1956 newly emerged glacial lakes between 1990 and 2020, 777 were found in the Indus basin, 651 in the Ganga basin, and 528 in the Brahmaputra basin. However, the Brahmaputra basin observed the highest area (18.24 $\pm$ 3.22 km^2) of newly emerged glacial lakes, followed by the Ganga basin (area: 17.10 $\pm$ 3.02 km^2) and the Indus basin (area: 13.21 $\pm$ 2.33 km^2). Out of 307 disappeared glacial lakes, 180 (area: 2.41 $\pm$ 0.42 km^2) were in the sub-basins of the Indus basin, followed by the Ganga basin with 72 (area: 1.02 $\pm$ 0.18 km^2), and the Brahmaputra basin with 55 (area: 0.98 $\pm$ 0.17 km^2) glacial lakes between 1990 and 2020 (Fig. 8a and b).

Of 1956 glacial lakes, which emerged between 1990 and 2020, 1336 (area: 38.74 $\pm$ 6.85 km^2) were M(e) lakes, followed by 485 (area: 6.91 $\pm$ 1.22 km^2) of supraglacial type, 60 (area: 1.22 $\pm$ 0.21 km^2) of M(l) lakes, 51 (area: 1.30 $\pm$ 0.23 km^2) B(o) lakes, 15 (area: 0.17 $\pm$ 0.03 km^2) of other lake types, 7 (area: 0.08 $\pm$ 0.01 km^2) of M(o) lakes, and 2 (are: 0.11 $\pm$ 0.01 km^2) of B(c) lakes (Fig. 8a and Fig. 9d). The emergence of dominant M(e) lake type is observed across the study region, while the supraglacial lakes largely emerged in the northwestern parts of the study region and southern slopes of the central Himalayan region. In terms of 307 disappeared glacial lakes between 1990 and 2020, 166 (area: 2.82 $\pm$ 0.49 km^2) M(e) lakes, 112 (area: 1.15 $\pm$ 0.20 km^2) supraglacial lakes, 24 (area: 0.41 $\pm$ 0.07 km^2) M(l) lakes, 3 (area: 0.019 $\pm$ 0.003 km^2) other glacial lakes, and 2 (area: 0.013 $\pm$ 0.002 km^2) M(o) lakes disappeared during this time period, while no B(c) and B(o) lakes were lost. Mainly M (e) lakes are observed to have disappeared across the study region, while supraglacial lakes follow the same pattern as the emerged lakes of this type. The mean elevations of emerged and disappeared glacial lakes between 1990 and 2020 were 4889 m (area: 0.0248 km^2) and 4734 m (area: 0.0144 km^2), respectively, suggesting that the majority of newly formed glacial lakes formed above the overall mean elevation of glacial lakes in 1990 (4737.66 m asl), and indicating an accelerated climate change in the study region. Furthermore, there are several glacial lakes, which disappeared and then re-emerged in the later years (Fig. 8c). The majority of the re-emerged glacial lakes were of the supraglacial type, highlighting their dynamic nature.

The study also observed an altitudinal dependence of glacial lake changes. The decade of 1990–2000 showed high activity of emerged and disappeared lakes (Fig. 9a). Significant disappearance of glacial lakes is observed at higher elevations (above 4200 m asl), while their number significantly increased above 5000 m asl, especially in the Indus and Brahmaputra basins from 1990 to 2000. Low glacial lake activity is observed in the later decade (2000–2010), which significantly increased between 2010 and 2020, especially above 5000 m asl (Fig. 9b and c). A large number of lakes disappeared between 3600 and 4400 m asl in the Indus basin, while in the Ganga basin, lakes largely disappeared above 4600 m asl. Glacial lakes emerged in all elevation zones in the Indus basin, while in the Ganga and Brahmaputra basins the emergence was largely confined to elevations above 5000 m asl. Overall,

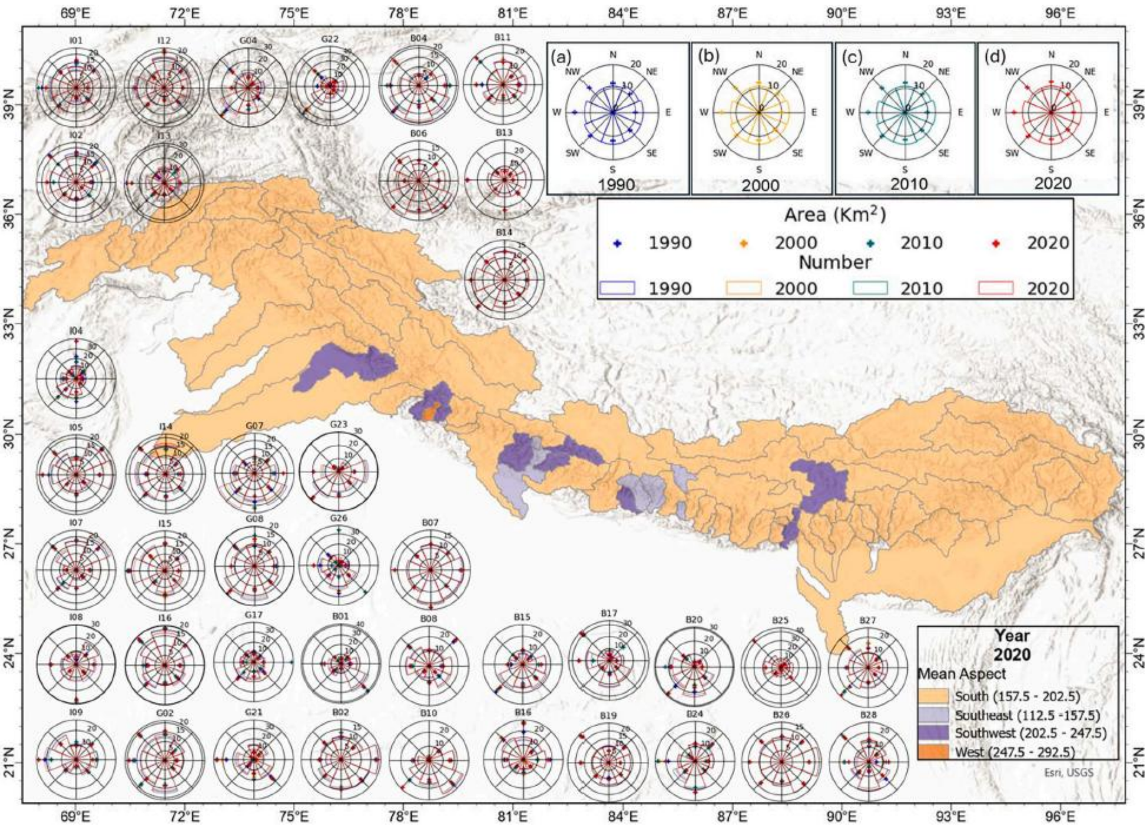

Fig. 6. The choropleth map in the background is showing the mean aspect of glacial lakes at sub-basin level. The polar sub-plots (n: >100) show aspect-wise distribution of number and area of glacial lakes between 1990 and 2020. The bars show distribution of numbers and plus mark (+) distribution of area based on the aspect. The inset a-d show aspect-wise distribution of glacial lakes for 1990, 2000, 2010 and 2020 for the study domain.

the emergence of new lakes, belonging to M(o) and S type, is significantly high in the higher elevation zones (above 5400 m asl) in the recent decade (Fig. 9).

5. Discussion

5.1. Production of glacial lake inventories and their comparison with previous studies

Several attempts have been made to map glacial lakes in the HKH region at the regional and sub-regional scales in the last decades (Ives et al., 2010; Nie et al., 2017; Maharjan et al., 2018; Zheng et al., 2021a; Chen et al., 2021; Li et al., 2022). However, these inventories are not directly comparable, mainly because of (i) use of different definitions of glacial lakes in different studies, (ii) different satellite datasets with different spatial resolutions, (iii) cloud and snow cover, (iv) mountain's shadow conditions in the remotely sensed images; and (v) application of different methodologies to detect glacial lakes in terms of minimum mapping, elevation thresholds, and (vi) area coverage (Table 2).

In the present study, we considered each water body as glacial lake, which received glacial and snow melt water and formed due to ongoing and past glacial processes (Ives et al., 2010; Bhambri et al., 2015, 2018; Maharjan et al., 2018). Many studies, for instance, (Nie et al., 2017) classified glacial lakes broadly into two major categories viz., glacier-fed and non-glacier-fed, while Yao et al. (2018) classified glacial lakes into 6 major categories. Such a difference in the definition and classification of glacial lakes essentially leads to varying results. In addition, a large number of studies using Landsat satellite data, are still not comparable mainly due to methodological and area coverage issues (Table 2).

Many of the previous studies used a minimum elevation threshold of 3500 m asl to map glacial lakes in the different parts of the IGB basin (Mool et al., 2001a; Mool et al., 2001b; Campbell and Pradesh, 2005; Bajracharya and Mool, 2009; Khadka et al., 2018). However, in the present study, glacial lakes were observed as low at 2900 m asl in the western portion of the study domain, yielding slightly higher number of glacial lakes, when compared with other studies.

Applying different minimum area thresholds yield different results (number and area) for glacial lakes. For instance, many studies using semi-automated methods on Landsat satellite data (30 m pixel size) applied 0.0036/0.0081 km^2 (4/6-pixels) as a minimum mappable lake area (Nie et al., 2013, 2017; Zhang et al., 2015; Wang et al., 2020; Li et al., 2022), while other applied different area thresholds (for instance 0.001, 0.025 km^2) (Gupta et al., 2022; Zhang et al., 2023a, 2023b). Some of the studies have attempted to map glacial lakes applying manual methods, with smallest mappable lakes having been used in the inventory (Ives et al., 2010; Ashraf et al., 2017; Rao et al., 2021), hence results obtained from different studies are not directly comparable (Table 2).

The utilization of different thresholds of glacial lakes distance from glaciers is another challenge in directly comparing glacial lake inventories (Table 2). We therefore attempted to compare our results with those studies used similar data (Landsat satellite images, 30 m pixel),

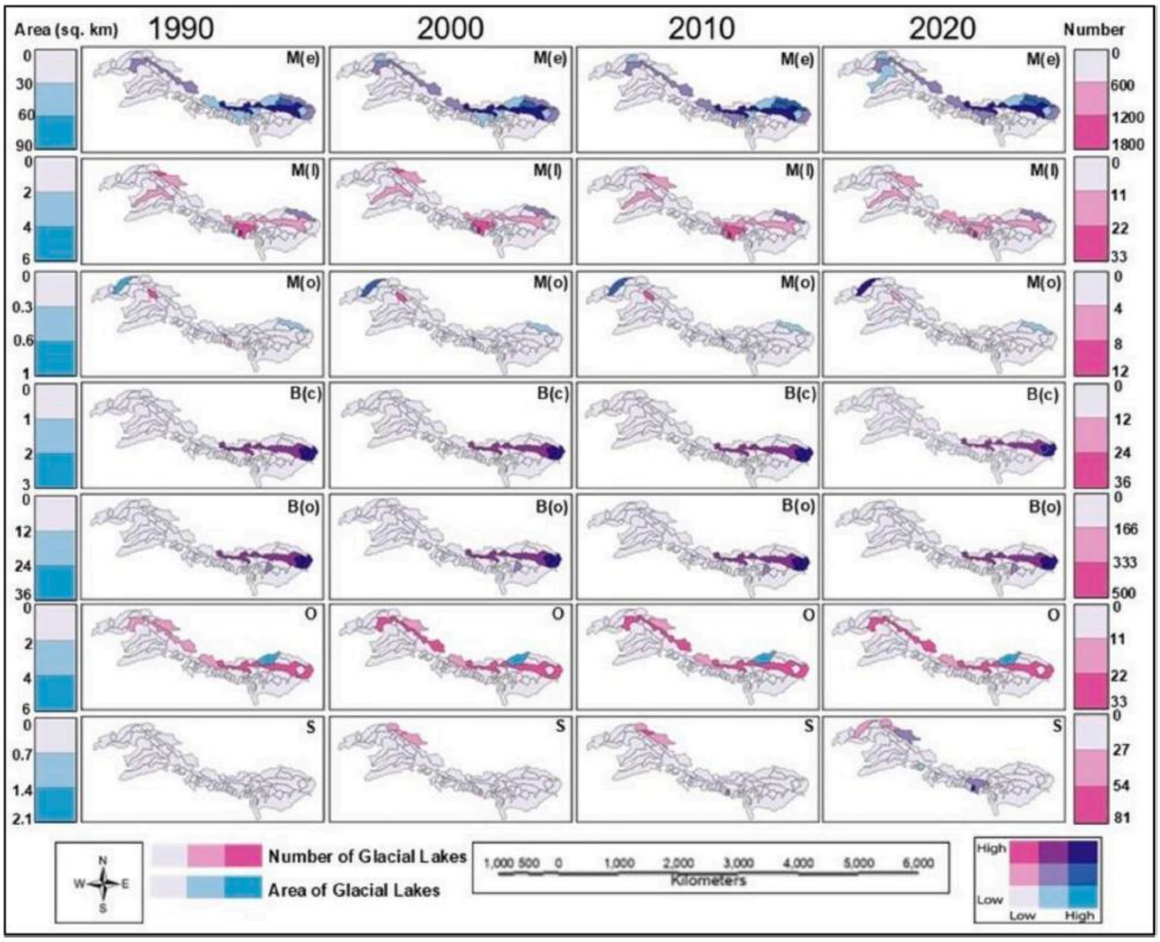

Fig. 7. Type-wise change in bivariate distribution of glacial lakes in the study domain, where shades of blue/pink colors represent the area (km^2) and number of glacial lakes, respectively, at the sub-basin level between 1990 and 2020. (For interpretation of the references to colour in this figure legend, the reader is referred to the web version of this article.)

mapping area threshold (4-pixels, i.e., 0.0036 km^2), area coverage and distance of 10 km between glaciers and glacial lakes (Zhang et al., 2021; Li et al., 2022). Also, we down-scaled our inventories to the thresholds (0.0081 km^2 and 10 km distance between lakes and glaciers) applied by other studies over the same study domain for the sake of comparison (Li et al., 2022; Zhang et al., 2023a, 2023b) (Table 2).

A total of 19,284 ($\geq$0.0036 km^2) glacial lakes covering an area of 1191.81 $\pm$ 209.21 km^2 were mapped in the present study for the year of 2020. The number/area of glacial lakes as observed in the present study significantly reduces to 16,269/1041.21 km^2, when downscaling it to Li et al. (2022) (n:9662, area: 896.5 km^2) criteria, i.e., $\geq$0.0036 km^2 and within 10 km from glaciers for the study region. Li et al. (2022) assessed a significantly lower number/area compared to our results (Table 2). This might relate to the definition of a glacial lake by Li et al. (2022), considering only the moraine-dammed lakes and the lakes that receive water from modern glacial melt, as well as to under-reporting due to snow cover conditions and shadow effects. On the contrary, we mapped all the lakes that are formed through past and ongoing glacial processes and that receive water from glacial/snow melt following the modified glacial lake classification scheme tailored to the HKH region (Bhambri et al., 2015; Bhambri et al., 2018; Maharjan et al., 2018; Mal et al., 2020). Our results are quite close to the results obtained by Wang et al. (2020), with a difference of only 353 (area: ~8 km^2) lakes (Table 2). This slight difference might be related to the difference in the images used in both studies, in particular in terms of mapping supraglacial lakes, being highly dynamic at monthly/annual scales.

5.2. Glacial lakes dynamics

In the present study, the number and area of glacial lakes increased by 1643 (9.31 %) and 109.38 $\pm$ 19.36 km^2 (10.10 %), respectively, between 1990 and 2020. Most previous studies confirmed glacial lake expansion since the 1990s in the HKH region (Zhang et al., 2015; Nie et al., 2017; Shugar et al., 2020; Ahmed et al., 2021). We found glacial lakes having evolved at different rates in different sub-basins of the IGB basins between 1990 and 2020. The Ganga basin observed the highest growth rate, corroborating the results of previous studies in the region (Gardelle et al., 2011; Zhang et al., 2015; Nie et al., 2017). Furthermore, we found that the number of supraglacial lakes varies significantly among different studies, which might be the result of the selection of diverse satellite datasets with variations in spatial resolution, of differences in the timings/months of satellite data, and of the ephemeral

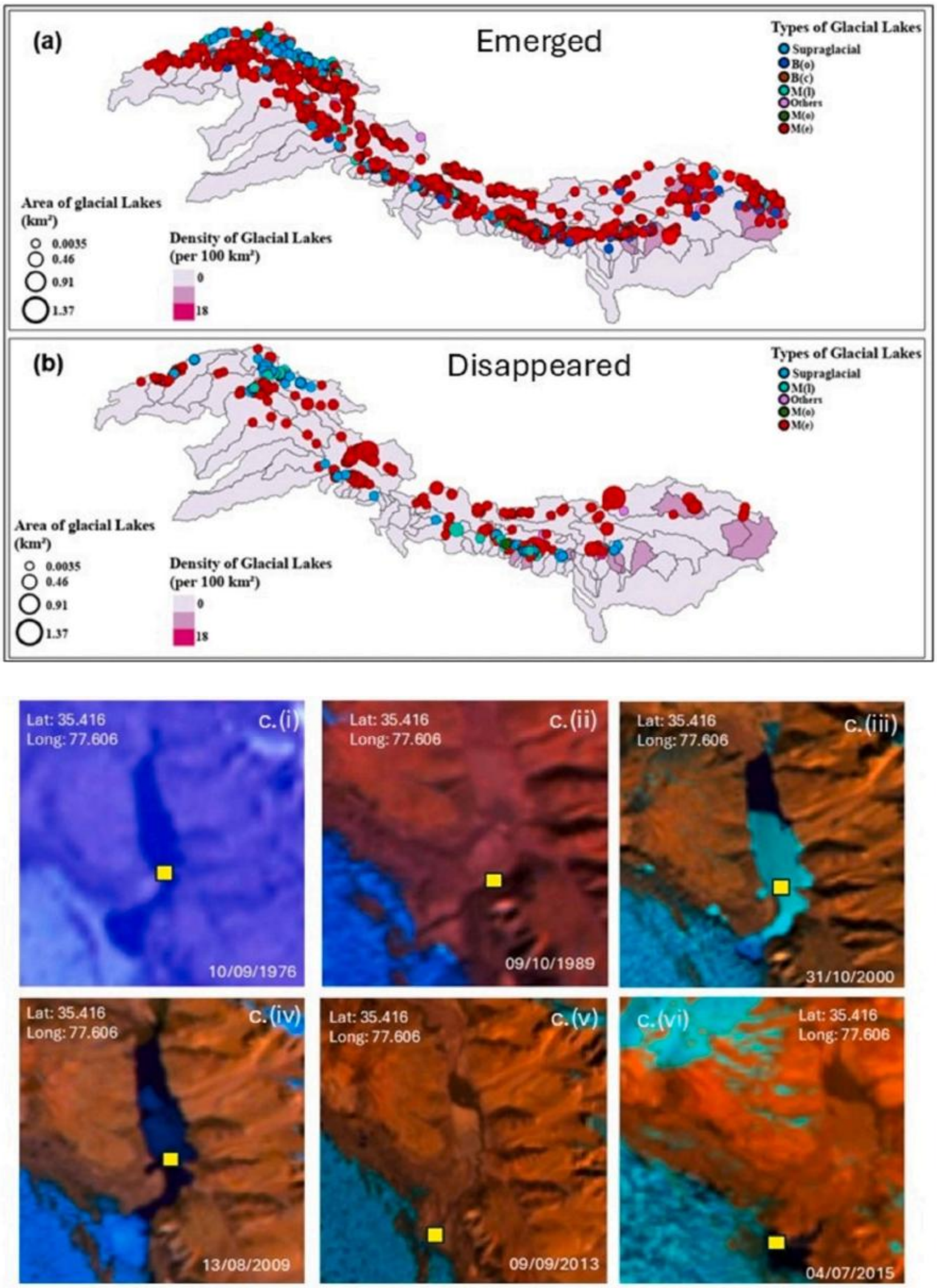

Fig. 8. Spatial variation of newly emerged and disappeared glacial lakes at the sub-basin level in the study domain, where (a) shows the number and area of newly emerged glacial lakes along with their types, and (b) shows the same but for disappeared glacial lakes. Background maps show the density of glacial lakes (per 100 km^2) (2020) at the sub-basin level. (c) shows an example of a highly dynamic (disappeared and then re-emerged) lake in the study region with yellow maker. (For interpretation of the references to colour in this figure legend, the reader is referred to the web version of this article.)

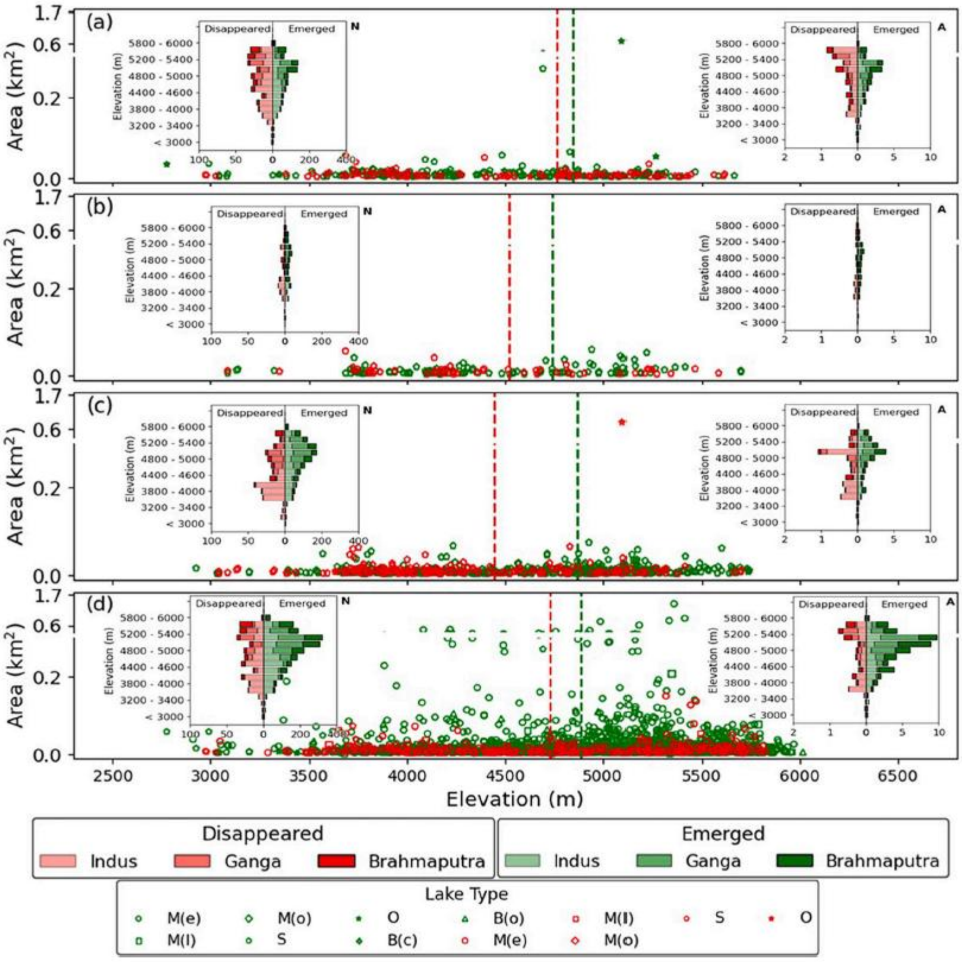

Fig. 9. Distribution of newly emerged and disappeared glacial lakes in the study domain, where x and y axes represent area (km^2) and elevations (m) of glacial lakes, respectively, at 500 m elevation zones. Green/red colors represent the emerged/disappeared glacial lakes, (a) between 1990 and 2000; (b) between 2000 and 2010; (c) between 2010 and 2020; and (d) between 1990 and 2020. The vertical lines show the mean elevation of disappeared (red) and emerged glacial lakes (green) for the respective decades. (For interpretation of the references to colour in this figure legend, the reader is referred to the web version of this article.)

nature of supraglacial lakes (Mohanty and Maiti, 2021). The increase of mean and upper elevations of glacial lakes in the IGB basins, as observed by the present study, is well supported by previous studies (Nie et al., 2017; Wang et al., 2020; Li et al., 2022). This increase is caused by accelerated and elevation dependent warming-led rapid melting of glaciers in recent decades (Bolch et al., 2019; Krishnan et al., 2019; Pepin et al., 2015; Hock et al., 2019; Bhattacharya et al., 2021). Melting processes have reduced the overall distance between glaciers and glacial lakes (Supplementary Fig. 3a and b). Furthermore, there are several studies,which attempted to map glacial lakes within a buffer distance (10 km; 20 km; and 30 km), however, only a few studies calculated distance between glaciers and glacial lakes (e.g., Maharjan et al., 2018). In the present study, we calculated the distance between glaciers and glacial lakes for all the mapped lakes using RGI (Ver. 7.0). We found that the mean distance between glaciers and glacial lakes have decreased between 1990 and 2020, with the Ganga basin having the lowest mean distance, to be attributed to the rapid expansion of glacial lakes in the Central Himalayan region (Nie et al., 2013; Nie et al., 2017; Wang et al., 2020; Li et al., 2022). Most of the new lakes that evolved in the study region during the last decade are of M(e) and (S) categories, developing either next to the glacier margin or on the glaciers respectively, and leading to the decline in the distance between glaciers and these lakes. However, in case of the glacial lakes disconnected from the glaciers, the distance has increased (Zhang et al., 2015; Nie et al., 2017). Our results align well with the previous studies and found rapid glacial lakes expansion on the southern slopes (Nie et al., 2017; Li et al., 2022). However, several sub-basins in the Ganga and Brahmaputra basins show rapid expansion of glacial lakes on the northern slopes as well (Fig. 6), caused by subregionally enhanced climate warming. Even the three largest mapped glacial lakes in the present inventory (Chumba Yumco, Shie Co and Jiongpu Co) are on north-facing slopes.

Above-average warming rates in the Himalayan region (Bhutiyani et al., 2010; Krishnan et al., 2019; Schickhoff et al., 2022) are associated with accelerated glacier recession (Bolch et al., 2019; Hock et al., 2019), eventually leading to the formation of new glacial lakes, especially supraglacial lakes, and expansion of the existing ones, especially proglacial lakes (Yang et al., 2019; Shugar et al., 2020; Rounce et al., 2023). Glacial lakes connected with parent glaciers can further enhance

Table 2
Comparison of different glacial lake inventories with downscaling of selected studies highlighted in grey colour.

Authors	Study Area	Data	Methods	Criteria	Number	Area	Year	Change in Number/Area (km^2)
Ashraf et al. (2017)	Northwestern Himalaya	Topographic maps, Landsat (ETM/OLI) and SRTM DEM	Manual mapping	NA	2420 3044	NA NA	2001 2013	624 (2001 − 2013)
Gupta et al. (2022)	Indus River Basin	Resourcesat-2 (LISS-IV) and SRTM DEM	Band ratioing	$\geq$ 0.01 km^2	5335	173.95	2015–2017	
Nie et al. (2013)	Ganga River Basin	Landsat (TM/ETM) and SRTM DEM	Object-oriented image classification	$\geq$0.0081 km^2	1191 1290 1303 1314	168.4 185.28 190.84 197.22	1990($\pm$2) 2000($\pm$1) 2005($\pm$2) 2010($\pm$1)	99/16.88 (1990–2000) 13/5.56 (2000–2005) 123/6.38 (2005–2010)
Rao et al. (2021)	Ganga River Basin	Resourcesat-2 (LISS-IV) and SRTM DEM	Manual mapping	$\geq$0.025 km^2	4707	206.85	2016–2018	
Xin et al. (2012)	Chinese Himalaya	Topographic maps, Landsat (TM) and ASTER DEM	Manual mapping	NA	1750 1680	166.48 215.27	1970s 2000s	−70/48.79 (1970s–2000s)
Worni et al. (2013)	Indian Himalaya	Landsat (ETM+)	Automated Mapping	$\geq$0.01 km^2	251	NA	2000–2002	NA
Nie et al. (2017)	Himalayas	Landsat (TM/ETM/OLI)	Automatic object-oriented mapping and manual correction	$\geq$0.0081 km^2	4549 4671 4691 4723 4950	398.9 421.2 431.4 442.3 455.3	1990($\pm$2) 2000($\pm$1) 2005($\pm$2) 2010($\pm$1) 2015($\pm$1)	122/22.3 (1990–2000) 20/10.2 (2000–2005) 32/10.9 (2005–2010) 223/13 (2010–2015)
Zhang et al. (2015)	HMA	Landsat (TM/ETM+) and SRTM DEM	Manual mapping	$\geq$0.03 km^2 Within 10 km from glacier	4602 4981 5701	553.9 581.2 682.4	1990* 2000** 2010***	379/27.1 (1990–2000) 720/101.2 (2000–2010)
Wang et al. (2020)	HMA	Landsat (TM/ETM+/OLI)	Manual mapping	$\geq$0.0081 km^2 Within 10 km from glacier	27,205 30,121	1806.47 2080.12	1990# 2018##	2916/273.65 (1990–2018)
Zheng et al. (2021a)	HMA	Landsat (TM/ETM/OLI) and SRTM DEM	Semi – automated with manual mapping	$\geq$0.0036 km^2 Within 10 km from glacier	25,152 26,633	1843 1968.80	1990($\pm$4) 2015($\pm$1)	1481/125.8 (1990–2015)
Ives et al. (2010)	HKH	Topographic Maps, Landsat (TM/ETM), IRS (LISS 3), SPOT (XR) and SRTM DEM	Semi – automated with manual mapping	NA	8790	801.83	1999–2004	NA
Li et al. (2022)	HKH	Landsat (TM/ETM/OLI) and SRTM DEM	Semi - automated	$\geq$0.0036 km^2, Within 10 km from glacier	5835 11,809	664.84 1073.77	1990($\pm$2) 2020($\pm$2)	5974/408.93 (1990–2020)
Present Study	IGB	Landsat (TM/OLI)	Semi – automated with manual mapping	$\geq$0.0036 km^2 $\geq$ 2900 m $\leq$20° slope	17,641 18,206 18,399 19,284	1082.56 1120.94 1147.12 1191.81	1990 ($\pm$3) 2000 ($\pm$3) 2010 ($\pm$3) 2020 ($\pm$3)	565/38.38 (1990–2000) 193/26.17 (2000–2010) 885/44.69 (2010–2020)
Li et al. (2022)	IGB	Landsat (TM/ETM/OLI) and SRTM DEM	Semi - automated	Within 10 km from glacier	9662	896.5	2020 ($\pm$2)	
Zhang et al. (2023)	IGB	Sentinel 2 A/B	Semi – automated	$\geq$0.02 km^2	3353	474.8	2020	
Wang et al. (2020)	IGB	Landsat (TM/ETM+/OLI)	Manual mapping	$\geq$0.0081 km^2 Within 10 km from glacier	14,079	1018.24	2018($\pm$2)	
Present study (down-scaled to Wang et al., 2020; Li et al., 2022; Zhang et al., 2023)	IGB	Landsat (TM/OLI)	Semi-automated (NDWI binary thresholding along with visual interpretation)	$\geq$0.0081 $\geq$0.0081 km^2 Within 10 km from glacier $\geq$0.0036 km^2 Within 10 km from glacier	16,209 13,726 16,269	1173.85 1026.08 1041.21	2020($\pm$3) 2020($\pm$3) 2020($\pm$3)	

*(1987–1996), **(1999–2002), ***($\pm$1), #1984–1995, ##2016–2020.

glacial melting at their margins (Krause et al., 2019; King et al., 2019; Mohanty and Maiti, 2021; Zhang et al., 2023a, 2023b). The expansion of glacial lakes has also led to increased water volume and hence reinforced flood and hazard potentials in recent decades (Allen et al., 2019; Zheng et al., 2021a). Besides, due to ongoing climate change, moraine dams are undergoing rapid thermal degradation, which, coupled with increased water volume, might result in a dam failure, causing severe loss and damage to the downstream infrastructure and human population (Allen et al., 2016; Emmer, 2018; Ahmed et al., 2021).

Furthermore, in the case of non-glacier-fed glacial lakes, an increase in temperature can lead to a decrease in their area in some cases due to excessive potential evaporation (Lei et al., 2014; Woolway et al., 2020). Understanding the relationship between warming, glacier recession and glacial lakes at sub-basin level in IGB basins is complex, since the macro-regional warming input is modified at local scales by precipitation patterns, topographic heterogeneity, aspect differences, etc. (Shugar et al., 2020; Li et al., 2022; Zhang et al., 2022).

5.3. *Implications of uncertainty*

Uncertainty in mapping of glacial lakes using satellite imagery has significant implications for hydrological assessment and flood management (Nie et al., 2017). Inaccurate delineation of lake boundaries can lead to errors in calculating lake area, which subsequently can affect total volume estimation of glacial lakes, change detection, monitoring, identifying potentially hazardous glacial lakes, policy development, and deployment of early warning systems (Wang et al., 2020). Smaller glacial lakes, which are harder to detect, and have higher ratio of mixed pixels are more prone to the higher level of uncertainties (Wang et al., 2020) (Fig. 10). Therefore, accurate area measurement of glacial lakes is of immense importance for GLOF risk assessment, since minor discrepancies can alter predictions of flood extent and related impacts (Zhang et al., 2015). Therefore, reducing the uncertainty in satellite-based lake mapping is essential to improve predictive models and support more effective risk mitigation for downstream communities and ecosystems.

Overall, the uncertainty of the glacial lake area is inversely proportional to the lake size (Fig. 10d). Smaller glacial lakes (<0.02 km^2) have higher median relative uncertainty (%) ranging between 34 % to 38 % at the major basin level (Fig. 10 a-c). Among the major basins, glacial lakes in the Ganga basin had the highest median relative uncertainty of 38.17 %, followed by the Brahmaputra basin 36.15 %, while the Indus basin had the lowest median relative uncertainty of 34.35 %, suggesting the Ganga and Brahmaputra basins have higher concentration of smaller lakes as compared to the Indus basin. This uncertainty in smaller lakes is mainly associated with a higher ratio of contacted mixed pixel with pure water pixel (Wang et al., 2020). By contrast, larger glacial lakes with a size of more than 1 km^2, had relative uncertainty ranging between 5 % and 6 % only (Fig. 10a-c). These results point to the need to improve mapping techniques for smaller glacial lakes in order to reduce the concerned uncertainty.

6. Conclusion

Continuous monitoring and analysis of glacial lake evolution is of immense importance in the HKH region, given the rapid growth of glacial lakes, the increased GLOF potential and the GLOF event-related damage in the study domain in recent decades. Especially for the potential transboundary GLOFs, their timely assessment is essentially

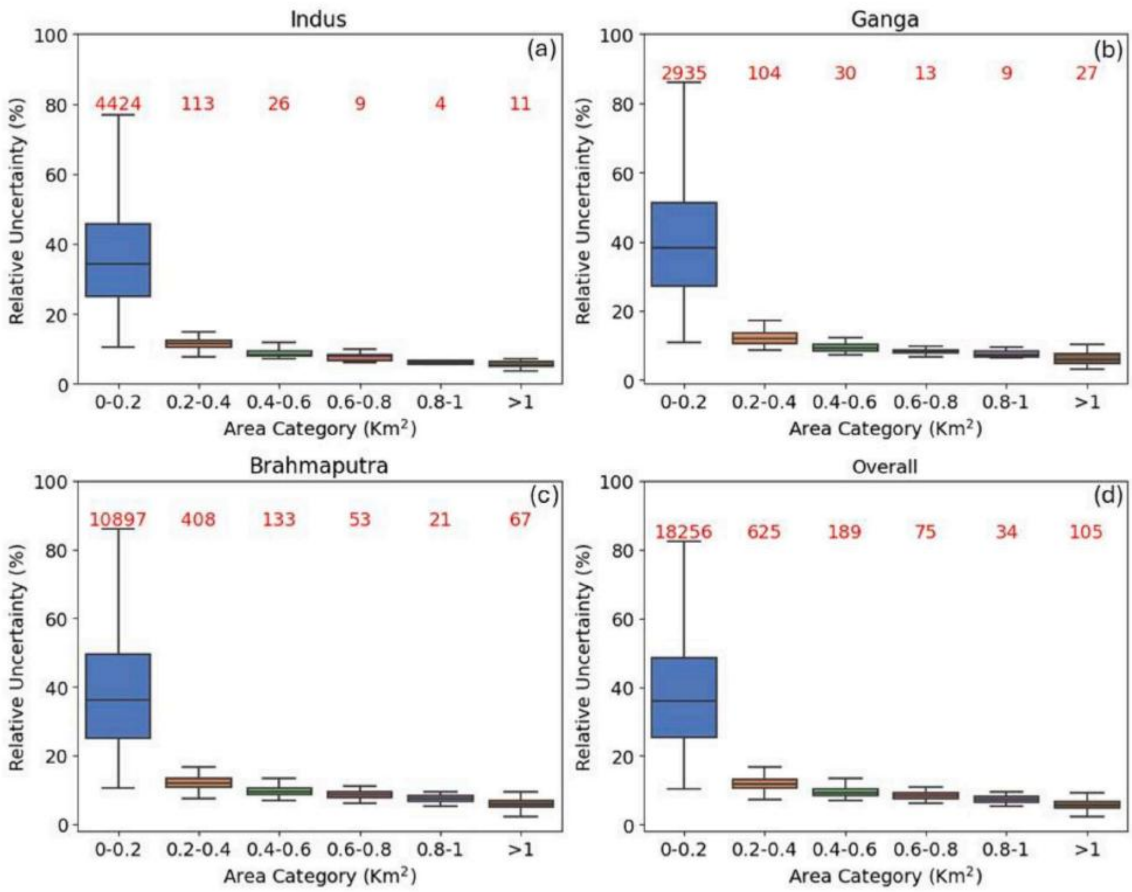

Fig. 10. Box plot representing the relationship between relative uncertainty (%) and area of glacial lakes, where a, b, c, and d show the relationship in the Indus basin, Ganga basin, Brahmaputra basin, and over the entire study domain, respectively.

required. It helps in appropriate GLOF risk assessments and mitigation measures of potential GLOF events. The present study generated four glacial lake inventories (1990, 2000, 2010 and 2020) and observed rapidly expanding glacial lakes, caused due to ongoing above-average warming rates in the study domain. The growth of glacial lakes is observed to be higher in the Ganga basin as compared with others. The increase in the mean elevation (~17 m asl) of glacial lakes and the declining mean distance between glacial lakes and glaciers suggests glacial lakes expansion and warming at higher elevations, especially in the Ganga basin, which also has the highest population density among the HKH regions. Critical infrastructure, particularly at higher elevations in the vicinity of these lakes, is at higher risk.

The present study can be used as an important input for the first order current and future assessments of potential GLOFs at sub-basin level. In addition, GLOF hazards and risks assessment can be aided with the help of the present study, contributing to early warning systems to mitigate their impacts in the likely affected regions. It can further assist in the planning of future critical infrastructure in relatively safer and unaffected locations. Disaster management agencies and local governments can further benefit from it to minimize losses and damages caused by GLOF events.

CRediT authorship contribution statement

Atul Kumar: Writing – review & editing, Writing – original draft, Visualization, Validation, Methodology, Funding acquisition, Formal analysis, Data curation, Conceptualization. **Suraj Mal:** Writing – review & editing, Visualization, Validation, Supervision, Resources, Project administration, Methodology, Conceptualization. **Udo Schickhoff:** Writing – review & editing, Supervision, Resources, Project administration, Methodology, Investigation, Funding acquisition, Conceptualization. **A.P. Dimri:** Writing – review & editing, Methodology.

Declaration of competing interest

The authors declare the following financial interests/personal relationships which may be considered as potential competing interests.

Atul Kumar reports financial support was provided by German Academic Exchange Service. If there are other authors, they declare that they have no known competing financial interests or personal relationships that could have appeared to influence the work reported in this paper.

Acknowledgements

This work is supported by doctoral research grant provided by German Academic Exchange Service (DAAD) (funding ID: 57507871). The authors are thankful towards United States Geological Survey (USGS) for providing free access to the Landsat satellite imagery. The authors also acknowledge CHELSA (https://chelsa-climate.org/) for providing high resolution climate data.

Appendix A. Supplementary data

Supplementary data to this article can be found online at https://doi.org/10.1016/j.gloplacha.2024.104656.

Data availability

The complete lake database is available at doi: https://doi.org/10.5281/zenodo.14192205.

References

Ahmed, R., Wani, G.F., Ahmad, S.T., Sahana, M., Singh, H., Ahmed, P., 2021. A review of glacial lake expansion and associated glacial lake outburst floods in the Himalayan region. Earth Syst. Environ. 5 (3), 695–708.

Ahmed, R., Wani, G.F., Ahmad, S.T., Mir, R.A., Faisal, A.A., Rather, A.F., Saeed, S., 2023. Expansion of Moraine-Dammed Glacial Lakes and Historical GLOF events in Cordillera Blanca Region of Peruvian Andes. Earth Syst. Environ. 7 (1), 131–150. https://doi.org/10.1007/s41748-022-00330-0.

Allen, S.K., Linsbauer, A., Randhawa, S.S., Huggel, C., Rana, P., Kumari, A., 2016. Glacial lake outburst flood risk in Himachal Pradesh, India: an integrative and anticipatory approach considering current and future threats. Nat. Hazards 84, 1741–1763. https://doi.org/10.1007/s11069-016-2511-x.

Allen, S.K., Zhang, G., Wang, W., Yao, T., Bolch, T., 2019. Potentially dangerous glacial lakes across the Tibetan Plateau revealed using a large-scale automated assessment approach. Sci. Bull. 64 (7), 435–445. https://doi.org/10.1016/j.scib.2019.03.011.

Ashraf, A., Naz, R., Iqbal, M.B., 2017. Altitudinal dynamics of glacial lakes under changing climate in the Hindu Kush, Karakoram, and Himalaya ranges. Geomorphology 283, 72–79. https://doi.org/10.1016/j.geomorph.2017.01.033.

Bajracharya, S.R., Mool, P., 2009. Glaciers, glacial lakes and glacial lake outburst floods in the Mount Everest region, Nepal. Ann. Glaciol. 50 (53), 81–86. https://doi.org/10.3189/172756410790595895.

Bhambri, R., Mehta, M., Dobhal, D.P., Gupta, A.K., 2015. Glacier Lake Inventory of Uttarakhand. Wadia Institute of Himalayan Geology.

Bhambri, R., Misra, A., Kumar, A., Gupta, A.K., Verma, A., Tiwari, S.K., 2018. Glacier lake inventory of Himachal Pradesh. Himal. Geol. 39 (1), 1–32.

Bhattacharya, A., Bolch, T., Mukherjee, K., King, O., Menounos, B., Kapitsa, V., Yao, T., 2021. High Mountain Asian glacier response to climate revealed by multi-temporal satellite observations since the 1960s. Nat. Commun. 12 (1), 4133. https://doi.org/10.1038/s41467-021-24180-y.

Bhutiyani, M.R., Kale, V.S., Pawar, N.J., 2010. Climate change and the precipitation variations in the northwestern Himalaya: 1866-2006. Int. J. Climatol. 30 (4), 535. https://doi.org/10.1002/joc.1920.

Bolch, T., Kulkarni, A., Kääb, A., Huggel, C., Paul, F., Cogley, J.G., Stoffel, M., 2012. The state and fate of Himalayan glaciers. Science 336 (6079), 310–314. https://doi.org/10.1126/science.1215828.

Bolch, T., Shea, J.M., Liu, S., Azam, F.M., Gao, Y., Gruber, S., Zhang, Y., 2019. Status and Change of the Cryosphere in the Extended Hindu Kush Himalaya Region. The Hindu Kush Himalaya Assessment: Mountains, Climate Change, Sustainability and People, pp. 209–255.

Campbell, J.G., Pradesh, H., 2005. Inventory of Glaciers, Glacial Lakes and the Identification of Potential Glacial Lake Outburst Floods (GLOFs) Affected by Global Warming in the Mountains of India, Pakistan and China/Tibet Autonomous Region. International Centre for Integrated Mountain Development, GP O, Box, p. 3226.

Chen, F., Zhang, M., Guo, H., Allen, S., Kargel, J.S., Haritashya, U.K., Watson, C.S., 2021. Annual 30 m dataset for glacial lakes in High Mountain Asia from 2008 to 2017. Earth Syst. Sci. Data 13 (2), 741–766. https://doi.org/10.5194/essd-13-741-2021.

Dimri, A.P., Chevuturi, A., Dimri, A.P., Chevuturi, A., 2016. Western Disturbances–Indian Winter Monsoon. In: Western Disturbances-An Indian Meteorological Perspective, pp. 83–111.

Dimri, A.P., Allen, S., Huggel, C., Mal, S., Ballesteros-Canovas, J.A., Rohrer, M., Pandey, A., 2021. Climate change, cryosphere and impacts in the Indian Himalayan Region. Curr. Sci. https://doi.org/10.18520/cs/v120/i5/774-790.

Emmer, A., 2018. GLOFs in the WOS: Bibliometrics, geographies and global trends of research on glacial lake outburst floods (Web of Science, 1979–2016). Nat. Hazards Earth Syst. Sci. 18 (3), 813–827.

Emmer, A., Allen, S.K., Carey, M., Frey, H., Huggel, C., Korup, O., Yde, J.C., 2022. Progress and challenges in glacial lake outburst flood research (2017–2021): a research community perspective. Nat. Hazards Earth Syst. Sci. 22 (9), 3041–3061. https://doi.org/10.5194/nhess-22-3041-2022.

Gao, B.C., 1996. NDWI—A normalized difference water index for remote sensing of vegetation liquid water from space. Remote Sens. Environ. 58 (3), 257–266. https://doi.org/10.1016/S0034-4257(96)00067-3.

Gardelle, J., Arnaud, Y., Berthier, E., 2011. Contrasted evolution of glacial lakes along the Hindu Kush Himalaya mountain range between 1990 and 2009. Glob. Planet. Chang. 75 (1–2), 47–55. https://doi.org/10.1016/j.gloplacha.2010.10.003.

Gupta, A., Maheshwari, R., Sweta, Guru, N., Rao, B. S., Raju, P. V., & Rao, V. V., 2022. Updated Glacial Lake inventory of Indus River Basin based on high-resolution Indian remote sensing satellite data. J. Indian Soc. Remote Sens. 1-26.

Hanshaw, M.N., Bookhagen, B., 2014. Glacial areas, lake areas, and snow lines from 1975 to 2012: status of the Cordillera Vilcanota, including the Quelccaya Ice Cap, northern central Andes, Peru. The Cryosphere 8 (2), 359–376.

Harrison, S., Kargel, J.S., Huggel, C., Reynolds, J., Shugar, D.H., Betts, R.A., Vilímek, V., 2018. Climate change and the global pattern of moraine-dammed glacial lake outburst floods. Cryosphere 12 (4), 1195–1209.

Hock, R., Rasul, G., Adler, C., Cáceres, B., Gruber, S., et al., 2019. High mountain areas. In: IPCC (Ed) Special Report on the Ocean and Cryopshere in a Changing Climate. IPCC, Geneva, pp. 131–202.

Hu, J., Yao, X., Duan, H., Zhang, Y., Wang, Y., Wu, T., 2022. Temporal and Spatial changes and GLOF Susceptibility Assessment of Glacial Lakes in Nepal from 2000 to 2020. Remote Sens. 14 (19), 5034. https://doi.org/10.3390/rs14195034.

ICIMOD, 2011. Glacial Lakes and Glacial Lakes Outburst Floods in Nepal. ICIMOD, Kathmandu.

ICIMOD, 2021. Sub-sub-basins of Hindu Kush Himalaya (HKH) Region [Data set]. ICIMOD. https://doi.org/10.26066/RDS.7952.

Immerzeel, W.W., Lutz, A.F., Andrade, M., Bahl, A., Biemans, H., Bolch, T., Baillie, J.E. M., 2020. Importance and vulnerability of the world's water towers. Nature 577 (7790), 364–369.
Ives, J.D., Shrestha, R.B., Mool, P.K., 2010. Formation of Glacial Lakes in the Hindu Kush-Himalayas and GLOF Risk Assessment. ICIMOD, Kathmandu, pp. 10–11.
Ji, L., Zhang, L., Wylie, B., 2009. Analysis of dynamic thresholds for the normalized difference water index. Photogramm. Eng. Remote. Sens. 75 (11), 1307–1317. https://doi.org/10.14358/PERS.75.11.1307.
Khadka, N., Zhang, G., Thakuri, S., 2018. Glacial lakes in the Nepal Himalaya: Inventory and decadal dynamics (1977–2017). Remote Sens. 10 (12), 1913. https://doi.org/10.3390/rs10121913.
King, O., Dehecq, A., Quincey, D., Carrivick, J., 2018. Contrasting geometric and dynamic evolution of lake and land-terminating glaciers in the central Himalaya. Glob. Planet. Chang. 167, 46–60. https://doi.org/10.1016/j.gloplacha.2018.05.006.
King, O., Bhattacharya, A., Bhambri, R., Bolch, T., 2019. Glacial lakes exacerbate Himalayan glacier mass loss. Sci. Rep. 9 (1), 18145. https://doi.org/10.1038/s41598-019-53733-x.
Krause, L., Mal, S., Karki, R., Schickhoff, U., 2019. Recession of Trakarding glacier and expansion of Tsho Rolpa lake in Nepal Himalaya based on satellite data. Himal. Geol. 40 (2), 103–114.
Krishnan, R., Shrestha, A.B., Ren, G., Rajbhandari, R., Saeed, S., Sanjay, J., Ren, Y., 2019. Unravelling Climate Change in the Hindu Kush Himalaya: Rapid Warming in the Mountains and Increasing Extremes. The Hindu Kush Himalaya Assessment: Mountains, Climate Change, Sustainability and People, pp. 57–97.
Lei, Y., Yang, K., Wang, B., Sheng, Y., Bird, B.W., Zhang, G., Tian, L., 2014. Response of inland lake dynamics over the Tibetan Plateau to climate change. Climatic Change 125, 281–290.
Lesi, M., Nie, Y., Shugar, D.H., Wang, J., Deng, Q., Chen, H., 2022. Landsat and Sentinel-derived glacial lake dataset in the China-Pakistan Economic Corridor from 1990 to 2020. Earth Syst. Sci. Data Discuss. 2022, 1–33. https://doi.org/10.5194/essd-14-5489-2022, 2022.
Li, W., Wang, W., Gao, X., Wang, X., Wang, R., 2022. Inventory and Spatiotemporal patterns of Glacial Lakes in the HKH-TMHA Region from 1990 to 2020. Remote Sens. 14 (6), 1351.
Lützow, N., Veh, G., Korup, O., 2023. A global database of historic glacier lake outburst floods. Earth Syst. Sci. Data Discuss. 2023, 1–27. https://doi.org/10.5194/essd-15-2983-2023.
Maharana, P., Kumar, D., Das, S., Tiwar, P.R., 2021. Present and future changes in precipitation characteristics during Indian summer monsoon in CORDEX-CORE simulations. Int. J. Climatol. 41 (3), 2137–2153. https://doi.org/10.1002/joc.6951.
Maharjan, S.B., Mool, P.K., Lizong, W., Xiao, G., Shrestha, F., Shrestha, R.B., Baral, P., 2018. The Status of Glacial Lakes in the Hindu Kush Himalaya-ICIMOD Research Report 2018/1. International Centre for Integrated Mountain Development (ICIMOD).
Mal, S., Kumar, A., Bhambri, R., Schickhoff, U., Singh, R.B., 2020. Inventory and spatial distribution of glacial lakes in Arunachal Pradesh, Eastern Himalaya, India. J. Geol. Soc. India 96, 609–615. https://doi.org/10.1007/s12594-020-1610-1.
Mal, S., Allen, S.K., Frey, H., Huggel, C., Dimri, A.P., 2021. Sectorwise Assessment of Glacial lake outburst flood danger in the Indian Himalayan Region. Mt. Res. Dev. 41 (1), R1–R12.
Mohanty, L.K., Maiti, S., 2021. Regional morphodynamics of supraglacial lakes in the Everest Himalaya. Sci. Total Environ. 751, 141586. https://doi.org/10.1016/j.scitotenv.2020.141586.
Mool, P.K., Bajracharya, S.R., Joshi, S.P., 2001a. Inventory of Glaciers, Glacial Lakes and Glacial Lake Outburst Floods. Monitoring and Early Warning Systems in the Hindu Kush-Himalayan Region: Bhutan, p. 365.
Mool, P.K., Bajracharya, S.R., Joshi, S.P., 2001b. Inventory of Glaciers, Glacial Lakes and Glacial Lake Outburst Floods. Monitoring and Early Warning Systems in the Hindu Kush-Himalayan Region: Nepal, p. 365.
Nie, Y., Liu, Q., Liu, S., 2013. Glacial lake expansion in the Central Himalayas by Landsat images, 1990–2010. PLoS One 8 (12), e83973. https://doi.org/10.1371/journal.pone.0083973.
Nie, Y., Sheng, Y., Liu, Q., Liu, L., Liu, S., Zhang, Y., Song, C., 2017. A regional-scale assessment of Himalayan glacial lake changes using satellite observations from 1990 to 2015. Remote Sens. Environ. 189, 1–13. https://doi.org/10.1016/j.rse.2016.11.008.
Pant, G.B., Kolli, Rupakumar, 1997. Climates of South Asia. Wiley.
Pepin, N., Bradley, R., Diaz, H., Baraer, M., Caceres, E.B., Forsythe, N., Yang, D.Q., 2015. Elevation-dependent warming in mountain regions of the world. Nat. Clim. Chang. 5, 424–430. https://doi.org/10.1038/nclimate2563.
Rao, B.S., Gupta, A., Sweta Waheswari, R., Raju, P.V., Rao, V.V., 2021. Glacial Lake Atlas of Ganga River Basin. National Remote Sensing Centre, ISRO, Hydrabad, India, pp. 1–194.
RGI Consortium, 2017. Randolph Glacier Inventory - A Dataset of Global Glacier Outlines, Version 6 [Indicate subset used].. National Snow and Ice Data Center, Boulder, Colorado USA. NSIDC. https://doi.org/10.7265/4m1f-gd79.
Rinzin, S., Zhang, G., Wangchuk, S., 2021. Glacial lake area change and potential outburst flood hazard assessment in the Bhutan Himalaya. Front. Earth Sci. 9, 775195. https://doi.org/10.3389/feart.2021.775195.
Rounce, D.R., Hock, R., Maussion, F., Hugonnet, R., Kochtitzky, W., Huss, M., McNabb, R.W., 2023. Global glacier change in the 21st century: every increase in temperature matters. Science 379 (6627), 78–83. https://doi.org/10.1126/science.abo1324.
Salerno, F., Thakuri, S., D'Agata, C., Smiraglia, C., Manfredi, E.C., Viviano, G., Tartari, G., 2012. Glacial lake distribution in the Mount Everest region: Uncertainty of measurement and conditions of formation. Glob. Planet. Chang. 92, 30–39. https://doi.org/10.1016/j.gloplacha.2012.04.001.
Schickhoff, U., Mal, S., 2020. Current changes in Alpine Ecosystems of Asia. In: Goldstein, M.I., DellaSala, D.A. (Eds.), Encyclopedia of the world's Biomes, vol. 1. Elsevier, Amsterdam, pp. 589–598. https://doi.org/10.1016/B978-0-12-409548-9.12399-1.
Schickhoff, U., Singh, R.B., Mal, S., 2016. Climate change and dynamics of glaciers and vegetation in the Himalaya: An overview. In: Singh, R.B., Schickhoff, U., Mal, S. (Eds.), Climate Change, Glacier Response, and Vegetation Dynamics in the Himalaya. Contributions toward Future Earth Initiatives. Springer, Switzerland, pp. 1–26.
Schickhoff, U., Bobrowski, M., Mal, S., Schwab, N., Singh, R., 2022. The World's Mountains in the Anthropocene. In: Schickhoff, U., Singh, R., Mal, S. (Eds.), Mountain Landscapes in Transition. Sustainable Development Goals Series. Springer, Cham, pp. 1–144. https://doi.org/10.1007/978-3-030-70238-0_1.
Shrestha, F., Steiner, J.F., Shrestha, R., Dhungel, Y., Joshi, S.P., Inglis, S., Zhang, T., 2023. A comprehensive and version-controlled database of glacial lake outburst floods in High Mountain Asia. Earth Syst. Sci. Data 15 (9), 3941–3961. https://doi.org/10.5194/essd-15-3941-2023.
Shugar, D.H., Burr, A., Haritashya, U.K., Kargel, J.S., Watson, C.S., Kennedy, M.C., Strattman, K., 2020. Rapid worldwide growth of glacial lakes since 1990. Nat. Clim. Chang. 10 (10), 939–945. https://doi.org/10.1038/s41558-020-0855-4.
Shugar, D.H., Jacquemart, M., Shean, D., Bhushan, S., Upadhyay, K., Sattar, A., Westoby, M.J., 2021. A massive rock and ice avalanche caused the 2021 disaster at Chamoli, Indian Himalaya. Science 373 (6552), 300–306. https://doi.org/10.1126/science.abh4455.
Taylor, C., Robinson, T.R., Dunning, S., Rachel Carr, J., Westoby, M., 2023. Glacial lake outburst floods threaten millions globally. Nat. Commun. 14 (1), 487. https://doi.org/10.1038/s41467-023-36033-x.
Veh, G., Korup, O., von Specht, S., Roessner, S., Walz, A., 2019. Unchanged frequency of moraine-dammed glacial lake outburst floods in the Himalaya. Nat. Clim. Chang. 9 (5), 379–383. https://doi.org/10.1038/s41558-019-0437-5.
Veh, G., Lützow, N., Kharlamova, V., Petrakov, D., Hugonnet, R., Korup, O., 2022. Trends, breaks, and biases in the frequency of reported glacier lake outburst floods. Earth's Future 10 (3), e2021EF002426. https://doi.org/10.1029/2021EF002426.
Wang, X., Guo, X., Yang, C., Liu, Q., Wei, J., Zhang, Y., Tang, Z., 2020. Glacial lake inventory of high-mountain Asia in 1990 and 2018 derived from Landsat images. Earth Syst. Sci. Data 12 (3), 2169–2182.
Woolway, R.I., Kraemer, B.M., Lenters, J.D., Merchant, C.J., O'Reilly, C.M., Sharma, S., 2020. Global lake responses to climate change. Nat. Rev. Earth & Environ. 1 (8), 388–403. https://doi.org/10.1038/s43017-020-0067-5.
Worni, R., Huggel, C., Stoffel, M., 2013. Glacial lakes in the Indian Himalayas—from an area-wide glacial lake inventory to on-site and modeling based risk assessment of critical glacial lakes. Sci. Total Environ. 468, S71–S84. https://doi.org/10.1016/j.scitotenv.2012.11.043.
Xin, W., Shiyin, L., Wanqin, G., Xiaojun, Y., Zongli, J., Yongshun, H., 2012. Using remote sensing data to quantify changes in glacial lakes in the Chinese Himalaya. Mt. Res. Dev. 32 (2), 203–212. https://doi.org/10.1659/MRD-JOURNAL-D-11-00044.1.
Yang, X., Lu, X., Park, E., Tarolli, P., 2019. Impacts of climate change on lake fluctuations in the Hindu Kush-Himalaya-Tibetan Plateau. Remote Sens. 11 (9), 1082. https://doi.org/10.3390/rs11091082.
Yao, X., Liu, S., Han, L., Sun, M., Zhao, L., 2018. Definition and classification system of glacial lake for inventory and hazards study. J. Geogr. Sci. 28, 193–205. https://doi.org/10.1007/s11442-018-1467-z.
Zhang, G., Yao, T., Xie, H., Wang, W., Yang, W., 2015. An inventory of glacial lakes in the Third Pole region and their changes in response to global warming. Glob. Planet. Chang. 131, 148–157. https://doi.org/10.1016/j.gloplacha.2015.05.013.
Zhang, M., Chen, F., Zhao, H., Wang, J., Wang, N., 2021. Recent changes of glacial lakes in the high mountain asia and its potential controlling factors analysis. Remote Sens. 13 (18), 3757. https://doi.org/10.3390/rs13183757.
Zhang, M., Chen, F., Guo, H., Yi, L., Zeng, J., Li, B., 2022. Glacial Lake area changes in high mountain asia during 1990–2020 using satellite remote sensing. Research. https://doi.org/10.34133/2022/9821275.
Zhang, G., Bolch, T., Yao, T., Rounce, D.R., Chen, W., Veh, G., Wang, W., 2023a. Underestimated mass loss from lake-terminating glaciers in the greater Himalaya. Nat. Geosci. 16 (4), 333–338. https://doi.org/10.1038/s41561-023-01150-1.
Zhang, T., Wang, W., An, B., Wei, L., 2023b. Enhanced glacial lake activity threatens numerous communities and infrastructure in the Third Pole. Nat. Commun. 14 (1), 8250. https://doi.org/10.1038/s41467-023-44123-z.
Zheng, G., Allen, S.K., Bao, A., Ballesteros-Cánovas, J.A., Huss, M., Zhang, G., Stoffel, M., 2021a. Increasing risk of glacial lake outburst floods from future Third Pole deglaciation. Nat. Clim. Chang. 11 (5), 411–417.
Zheng, G., Bao, A., Allen, S., Ballesteros-Cánovas, J.A., Yuan, Y., Jiapaer, G., Stoffel, M., 2021b. Numerous unreported glacial lake outburst floods in the Third Pole revealed by high-resolution satellite data and geomorphological evidence. Sci. Bull. 66, 1270–1273.

Article II

Kumar, A., Mal, S., Schickhoff, U., Allen, S., & Dimri, A. P. (**Accepted)**. Assessing the role of regional characteristics in estimating the volume of glacial lakes in the upper Indus-Ganga-Brahmaputra basins, Hindu Kush Himalaya (Manuscript No: HYDROL60046R1)

Assessing the role of regional characteristics in estimating the volume of glacial lakes in the upper Indus-Ganga-Brahmaputra basins, Hindu Kush Himalaya

Atul Kumar[1*], Suraj Mal[2], Udo Schickhoff[1], Simon Allen[3], A.P. Dimri[4]

[1]CEN Center for Earth System Research and Sustainability, Institute of Geography, University of Hamburg, Germany.

[2]Centre for the Study of Regional Development, Jawaharlal Nehru University, New Delhi, India.

[3]Department of Geography, University of Zurich, Zurich, Switzerland.

[4]School of Environmental Sciences, Jawaharlal Nehru University, New Delhi, India.

*Corresponding author

E-mail address: atul.sbsc@gmail.com (Atul Kumar)

Assessing the role of regional characteristics in estimating the volume of glacial lakes in the upper Indus-Ganga-Brahmaputra basins, Hindu Kush Himalaya

Abstract

Glacial lakes have exponentially increased in the recent decades across the world's mountains, particularly in the Hindu Kush Himalaya (HKH), caused by rapid rates of climate change. Consequently, their water volume and hence the hazard potential has also increased in recent decades. Robust water volumes of hazardous glacial lakes located in remote locations are rarely available, limiting the accuracy of current glacial lake outburst flood(GLOF) models that heavily rely on empirical water volume estimation equations. Currently used equations are based on data collected in the European Alps and have limited applicability in the HKH region. Thus, accurately predicting GLOF extents and likely damages in the downstream regions remains a critical challenge in the HKH region. In this study, we developed eight empirical equations to estimate mean depth (4) and volume (4) of glacial lakes in the upper Indus-Ganga-Brahmaputra (IGB) river basins. The study is based on a field-based bathymetric dataset of 25 glacial lakes from different parts of the upper IGB river basins. Separate equations were formulated for the major basins to understand the influence of regional lake characteristics on depth and volume estimations of glacial lakes. Our analysis revealed a non-linear negative relationship between the circularity ratio of glacial lakes and their mean depth, indicating that elongated lakes tend to be deeper than the circular ones. The average circularity ratio of glacial lakes in the upper IGB basins was 0.51 (as of 2020).

We estimated the mean depth and total volume for a dataset comprising 19,284 glacial lakes in the upper IGB basins. The estimated mean depth and total estimated volume of these lakes in 2020 was 7.20 m and 28.88 km^3, respectively. The empirical equations generated in the study based on the field-based bathymetry will be helpful in assessing the GLOF threats from continuously expanding glacial lakes in the upper IGB basins.

Keywords: Area-scaling method, Glacial lakes, Glacial Lake Outburst Floods (GLOFs), Hindu Kush Himalaya

Abbreviations:

Glacial Lake Outburst Floods : (GLOFs)

Hindu Kush Himalaya: (HKH)

High Mountain Asia: (HMA)

Indus-Ganga-Brahmaputra: (IGB)

1. Introduction

Glacial lakes are an essential component of the mountain cryosphere, which is one of the largest freshwater reservoirs in the world **(Barry, 2011; Huggel et al., 2015)**. These lakes play a crucial role in regional hydrology, water resources, and pose potential hazards to downstream infrastructure and human population in case of their breach/failure **(Yao et al., 2018)**. Due to recent accelerated climate change and associated glacier recession in the high mountain environments **(Hock et al., 2019; Schickhoff et al., 2022)**, glacial lakes are evolving at a never-seen rate (~52 %) across the glaciated regions of the world **(Shugar et al., 2020)**. However, the rate of glacial lake expansion is uneven across the different mountain ranges. **Wilson et al. (2018)** observed an increase in the total number (43 %) and area (7 %) of glacial lakes in the central and Patagonian Andes between 1986 and 2016. **Ma et al. (2021)** estimated that the total number of glacial lakes (area = ≥0.01) increased at a rate of 2.68 % in the European Alps between 2000 and 2019. Similarly, glacial lakes in High Mountain Asia **(HMA)** showed extraordinary growth rates in the recent decades **(Zhang et al., 2015; Bolch et al., 2019; Wang et al., 2020)**. **Zhang et al. (2015)** conducted one of the first spatio-temporal analyses of glacial lakes (>0.003 km^2) in HMA and observed an increase of 23.88 % and 23.19 % in their number and area, respectively, between 1990 and 2010. **Wang et al. (2020),** reported a 10.71 % (15.14 %) increase in the total number and area of glacial lakes between 1990 and 2020. Furthermore, there are sub-regional patterns of glacial lakes growth in the HKH region, with southern slopes of central Himalaya observing very high growth rates (23 %), as compared to western Himalaya (5 %) and eastern Himalaya (11.1 %) between 1990 and 2015 (**Nie et al. 2017**). Estimates of glacial lakes volumes, which is an important input for GLOF modelling assessment, at the global level, are rather poor due to limited accessibility and resources **(Shugar et al., 2020; Taylor et al., 2023)**. **Shugar et al. (2020)** observed that the total volume of glacial lakes increased by ~48 % at the global scale between 1990 and 2018 and from 3.17 km^3 (1990) to 4.58 km^3 (2015) (44.47 %) in HMA.

The main cause of the rapid expansion of glacial lakes in HMA is accelerated melting of glaciers caused by enhanced climate change rates (Zhang et al., 2015; Bolch et al., 2019; Zhang et al., 2021). The annual mean temperature increased by 0.1°C/10yr in HMA between 1901 and 2014 **(Krishnan et al., 2019)**. Furthermore, the region has observed an increase in the occurrence of extreme warm days and nights by 0.85 days/10yr and 2.40 days/10yr, respectively **(Krishnan et al., 2019)**, leading to accelerated expansion of glacial lakes in the region **(Bolch et al., 2019; Hock et al., 2019)**. Climate change, glacier recession and glacial lakes expansion follow a similar pattern in the HKH mountain region.

However, there are regional variations in the glacial response to the ongoing increase in the annual mean temperature, such as the "Karakoram anomaly" with most glaciers exhibiting a positive mass balance in recent decades **(Gardelle et al., 2012, 2013; Shean et al., 2020)**. In recent years, however, the rate of glacier mass losses has increased in the Karakoram as well **(Xu et al., 2023)**. Glaciers across the upper IGB basins have been predominantly retreating since the mid-18th century, although with regional variations **(Bolch et al., 2019)**. According to **Bhambri et al. (2011)**, glaciers area in the western Himalaya (Himachal Pradesh, upper Indus) decreased by 6.8 % between 1962 and 2001. In the upper Ganga basin (Central Himalaya), glaciers of the Khumbu region shrank by ~13 % between 1962 and 2011 **(Bolch et al., 2011a)**. Furthermore, the glaciers in the eastern Himalaya (Sikkim region), upper Brahmaputra basin shrunk by approximately 13 % between 1989 and 2010, while the glaciers in Bhutan decreased by approximately 22 % between 1980 and 2010 **(Basnett et al., 2013; Bajracharya et al., 2014)**.

Some of these rapidly expanding glacial lakes have caused devastating Glacial Lake Outburst Floods (GLOFs) in the upper IGB region, leading to significant losses in human population, infrastructure, and the natural environment **(Veh et al., 2019; Taylor et al., 2023)**. In the upper IGB basin, moraine-dammed lakes are particularly vulnerable to GLOFs, primarily because of their unstable dams made of dead ice and unconsolidated moraine deposition **(Veh et al., 2020; Ahmed et al., 2021)**. Glacial lakes near avalanche and rockfall zones, highly active tectonic zones, and areas with heavy rainfall can also cause GLOF events, like the Chorabari event in Uttarakhand in 2013 **(Emmer et al., 2013; Mal et al., 2014; Allen et al., 2015; Mehta et al., 2017; Dahal et al., 2024)**. Finding potentially dangerous glacial lakes and monitoring them all the time is very important for lowering the risk of GLOFs and making policies to deal with it **(Bolch et al., 2011b; Allen et al., 2019; Zhang et al., 2022)**.

Researchers have widely used lake characteristics such as surface area, depth, volume, shape, distance from the glacier, dam material, and dam slope to identify potentially hazardous glacial lakes and model GLOF events **(Fujita et al., 2013; Cook and Quincey, 2015)**. Information about lake mean depth and volume is of extreme importance for GLOF modelling, as it helps in calculating potential flood volume, peak discharge, potential flood route, hydraulic head, hydrostatic pressure, generating flood hydrographs, and mapping inundation extents **(Ng and Liu, 2009; Evans et al., 2009; Carrivick, 2010; Westoby et al., 2014)**. However, there is limited information available about the mean depth and volume of more than 19,000 glacial lakes in the upper IGB region **(Wang et al., 2012; Yao et al., 2012; Sakai, 2012; Fujita et al., 2013; Patel et al., 2017; Sharma et al., 2018; Qi et al., 2022; Zhang et al., 2023)**. The main reasons for the limited availability of information are the rugged terrain and inaccessibility of Himalayan glacial lakes and the massive cost of conducting field-based bathymetric surveys in the region **(Sakai, 2012; Qi et al., 2022)**.

Empirical equations based on relationships between lake characteristics, satellite-derived bathymetry (SDB), and computer-aided simulation are some of the most common ways to estimate the mean depth and volume of glacial lakes **(Huggel et al., 2002; Cook and Quincey, 2015; Qi et al., 2022)**. SDB requires satellite images with low glacial lake water turbidity for better prediction of glacial lake depth; however, finding glacial lakes with low water turbidity levels is difficult, especially in the HKH region (**Cook and Quincey, 2015; Armon et al., 2020**). Furthermore, due to low or no penetration of electromagnetic waves in deep glacial lakes, the depth prediction becomes extremely difficult (**Saylam et al., 2017; Liu et al., 2024**). The empirical approach is the most common among researchers for the estimation of the mean depth and volume of glacial lakes in highly inaccessible terrain and in cases of limited logistics **(Huggel et al., 2002; Sakai, 2012; Wang et al., 2012; Fujita et al., 2013; Kapitsa et al., 2017; Patel et al., 2017; Muñoz et al., 2020; Qi et al., 2022)**. The majority of these equations are based on relationships between area, depth, and volume of glacial lakes **(Cook and Quincey, 2015; Muñoz et al., 2020)**. The area, depth, and volume of glacial lakes have a non-linear relationship with each other; therefore, these should be evaluated carefully before directly being applied to the glacial lakes **(Cook and Quincey, 2015; Muñoz et al., 2020; Qi et al., 2022; Kapitsa et al., 2023).** Glacier movement, bedrock, sedimentation rate, local topography, dam material, and shape of the lake are significant factors affecting the non-linear relationship between the area, depth, and volume of glacial lakes **(Cook and Quincey, 2015; Muñoz et al., 2020; Qi et al., 2022).** Furthermore, the on-going climate change poses significant changes to the performance of these empirical equations. The rapid melting of glaciers, aided by a steady increase in the annual mean temperature, is expected to cause alteration in the area, sedimentation rate, depth, and volume of glacial lakes **(Bolch et al., 2019; Shugar et al., 2020; Zhang et al., 2024)**. This dynamic nature of glacial lakes under the influence of on-going climate change makes it more difficult to predict the mean depth and volume of these lakes and encourages periodic validation with updated field-based data. Therefore, to ensure the reliability of these empirical equations, validation with field-based data (wherever possible) and the execution of uncertainty assessment are of immense importance **(Cook and Quincey, 2015)**. Addressing these uncertainties strengthens the estimation power of area-based empirical models and helps increase the accuracy of lake mean depth and volume estimations. Several methods have been adopted over the period of time to validate or calculate the uncertainty between observed and estimated values. One of the most commonly used statistical methods to validate the positively strong relationship between glacial lake area, volume, and depth is the coefficient of determination (R^2) **(Huggel et al., 2002; Cook and Quincey, 2015; Muñoz et al., 2020; Qi et al., 2022; Kapitsa et al., 2023)**. A higher R^2 might indicate a good fit; however, it does not confirm the causal relationship between glacial lake area, volume, and depth, especially in the case of glacial lake area and depth **(Cook and Quincey, 2015; Muñoz et al., 2020)**. Typically, researchers utilize Root Mean Square Error (RMSE) to evaluate the precision of empirical models by measuring the differences between observed and estimated values **(Huggel et al., 2002; Cook and Quincey, 2015; Qi et al., 2022)**. Researchers particularly favour

RMSE because it assigns a higher weight to larger errors, thereby making it suitable for identifying extreme discrepancies. Furthermore, another powerful method for estimating the uncertainty between observed and estimated volume and depth is the use of the Bayesian inference method **(Gantayat et al., 2024)**. Unlike traditional uncertainty methods, Bayesian methods allow for the integration of prior knowledge with observed data to generate a probability distribution of the estimated parameters.

Several empirical equations were developed to estimate the mean depth and volume of glacial lakes using field-based data from different parts of the upper IGB basins **(Sakai, 2012; Fujita et al., 2013; Patel et al., 2017; Sharma et al., 2018; Qi et al., 2022)**. For example, **Sakai et al. (2012)** developed an equation to estimate the volume based on the volume data collected from the central Himalaya. Similarly, **Wang et al. (2012)** and **Yao et al. (2012)** developed equations to estimate the mean depth and volume of glacial lakes primarily in the central and eastern Himalaya. **Wang et al. (2012)** used 20 glacial lakes as the sample size for their equation development, while **Yao et al. (2012)** based their equation on a single glacial lake. Furthermore, **Patel et al. (2017)** developed an equation to estimate the depth of glacial lakes using two glacial lakes from the western Himalaya.

Therefore, the present study aims 1) to develop reliable empirical equations to estimate the mean depth and volume of glacial lakes incorporating all possible samples (our samples and those available from the literature) from the upper IGB basins, 2) to understand the relationship between different lake characteristics, and 3) to estimate the mean depth and volume of all the mapped glacial lakes in the upper IGB basins.

2. Study Area

The upper Indus-Ganga-Brahmaputra (IGB) basins in HKH extend from 26°21'10"N to 36°29'38"N latitudes and 68°58'25"E to 97°44'43"E (**Fig. 1**). The total geographical area of the study domain is ~$1.2*10^6$ km^2 (upper Indus: ~$5.19*10^5$ km^2, upper Ganga: ~$1.79*10^5$ km^2, upper Brahmaputra: ~$5.23*10^5$ km^2). The study domain exhibits a vast range of physiographic, climatic, and ecological variations.

The physiography of the HKH is remarkably heterogeneous, being home to all 14 eight-thousanders and hundreds of peaks over 6,000 m **(Sharma et al., 2019)**. Based on the elevation, the study domain is divided into four zones (foothills, lower Himalaya, greater Himalaya, and Trans-Himalaya) (**Singh et al., 1997**). The elevation ranges between 300 m asl near the foothills in the south to 8,848 m asl (Mount Everest) in the north, exhibiting a south-north elevational gradient.

The topography of the study region plays a crucial role in the distribution and characterization of glacial lakes. The annual mean temperature of the region varies between 35°C (summer) and -35°C (winter), showing considerable spatio-seasonal variations (**Krishnan et al., 2019**). The Indian Summer Monsoon (ISM) significantly dominates the region’s annual precipitation totals and spatio-seasonal distribution, accounting for about 80 %, while western disturbances contribute about 10 % (**Dimri et al., 2015; Ghimire et al., 2018; Krishnan et al., 2019**).

The study domain is commonly referred to as the "Third Pole", as it contains the largest reserves of glaciers outside of the Artic and Antarctica **(Sharma et al., 2019)**. According to **Bolch et al. (2012)**, the total glaciated area in the upper IGB basins is ~40,775 km^2. The glaciated area is continuously decreasing in the study domain **(Bolch et al., 2019)**. However, the rate of reduction is varies within the study domain. Furthermore, **Nie et al. (2017)**, found that the total area of glacial lakes increased by 14.1 % from 146.72 km^2 to 167.41 km^2 between 1990 and 2015.

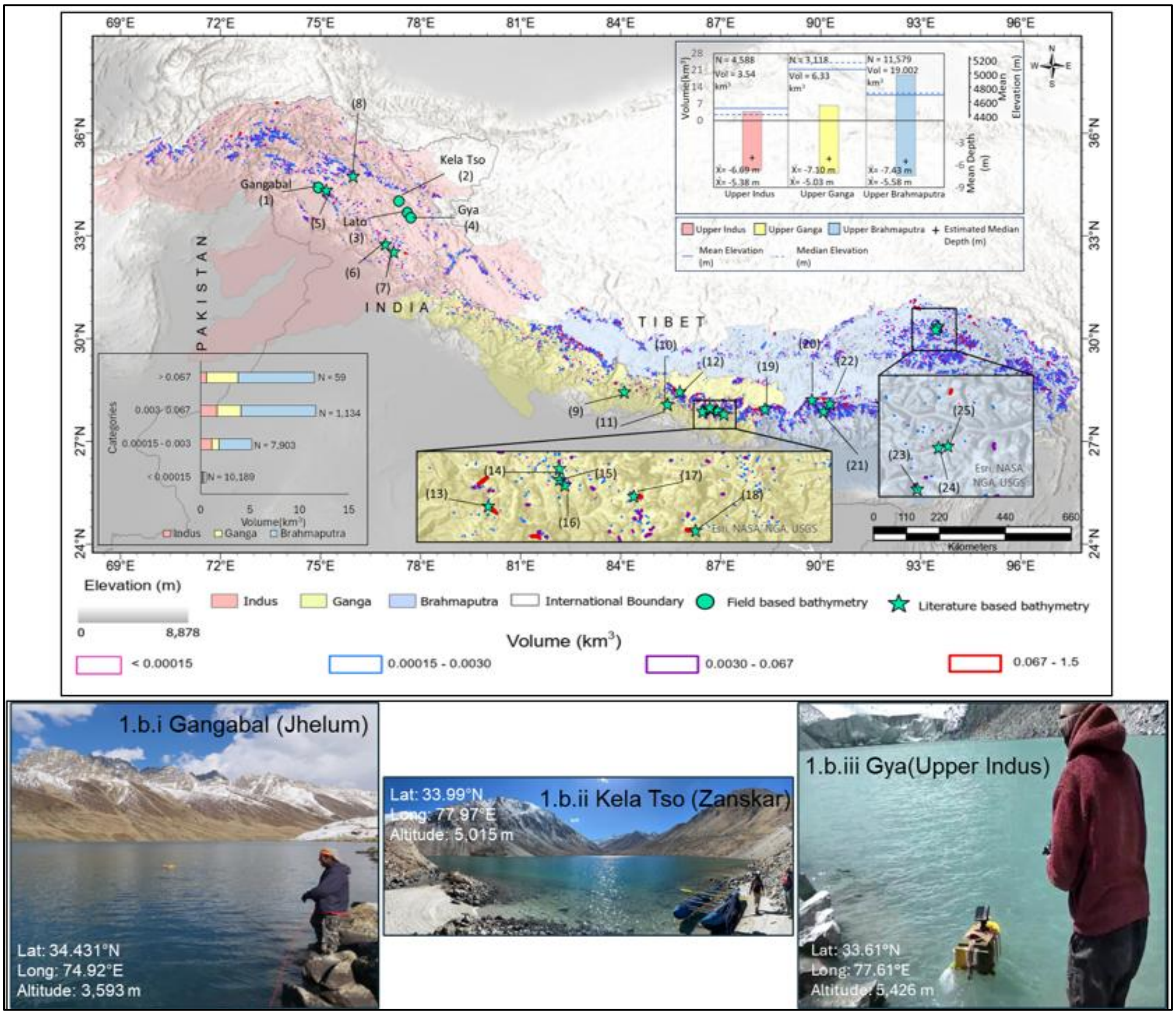

Fig. 1. Spatial distribution of glacial lakes in the upper IGB basins. The different colors of glacial lakes on the map show the volume (km^3). The inset figure shows the total volume (km^3) (primary axis), average estimated mean depth (m) (secondary axis), and mean elevation (m). The + symbol shows the estimated median depth at the major basin level. Solid circles and star symbols for glacial lakes on the map show field-based and literature-based bathymetry, respectively **(Supplementary Table 1)**. **Fig. 1b** shows the bathymetric surveys of the glacial lakes, surveyed between September 2021 and September

2023, where (a) Gangabal Lake was surveyed using remote-controlled vehicle and ropes. Ropes were used to complete the inaccessible sections for remote-controlled vehicles and safety against the strong waves and wind in and around the lake; (b) a survey of Kela Tso Lake was completed in September 2022 using a Catamaran raft; and (c) a survey of Gya Lake using the remote-controlled vehicle in September 2023.

3. Material and Methods

3.1. Material

3.1.1. Glacial lake bathymetry

The bathymetric surveys of glacial lakes (n=8) were conducted between September 2021 and September 2023 in the western part (upper Indus) of the study domain **(Fig. 1 & 1b)**. The month of September was primarily selected for the bathymetric field-survey, as it marks the end of the ablation season, which is characterized by the minimum snow extent, cloud cover, calm weather and full extents of the glacial lakes and is ideal for cryosphere studies in the study domain. The primary motive of the bathymetry surveys in the region was the complete absence of such information/studies due to its harsh climates, geomorphology, remoteness, health challenges and heavy demands for logistics and other resources. Of the 8 glacial lakes attempted for bathymetric survey, only 4 could not be successfully surveyed due to poor weather conditions and partial freezing of lakes, which limited the full coverage and accuracy of the measurements **(Fig. 1 & 1b)**. The weather conditions, including heavy cloud cover, precipitation, partial freezing of lakes and wind speed can significantly influence the accuracy and feasibility of bathymetric surveys in the study domain. Dense cloud cover limits the visibility and interferes with the GPS signals, crucial for precise depth measurements **(Hordyniec et al., 2018)**. High temperatures and heavy precipitations can intensify the turbidity of glacial lakes destabilizing the bathymetry instrument, which diminishes the penetration of sonar signals and results in poor depth measurements **(Fisher et al., 2013)**. Henceforth, four glacial lakes with successful bathymetric surveys (a) Gangabal, (b) Gya, (c) Kela Tso, and (d) Lato were selected for the present study **(Figs. 1 and 3)**. The primary criteria for selecting these glacial lakes were, (a) the glacial origin; and (b) the distance from the parent glaciers (<10 km). A remote-controlled vehicle with Garmin's echoMAP 52dv and GT20-TM transducer was used to conduct the bathymetric surveys. The GT20-TM transducer, operates in two versions: (1) traditional view, and (2) ClearVü. The present study used the traditional view, which can reach a depth of approximately 580 m at an operating frequency of 77/200 kHz, while ClearVü can reach a depth of approximately 228 m at an operating frequency of 455/800 kHz. The traditional view is mainly used in the present study because it allows for depth measurements up to ~580 m, which is essential given the variability in the lake depths across the study area. There are several glacial lakes in the upper IGB basins, which exceed the maximum depth of ~228 m range of the ClearVü.

In addition, bathymetry of 21 additional glacial lakes from previous studies (**Fig. 1 and Supplementary Table 1**), of which 8 are in the upper Indus basin, 10 in the upper Ganga basin, and 7 in the upper Brahmaputra basin, provides data for a total of 25 glacial lakes.

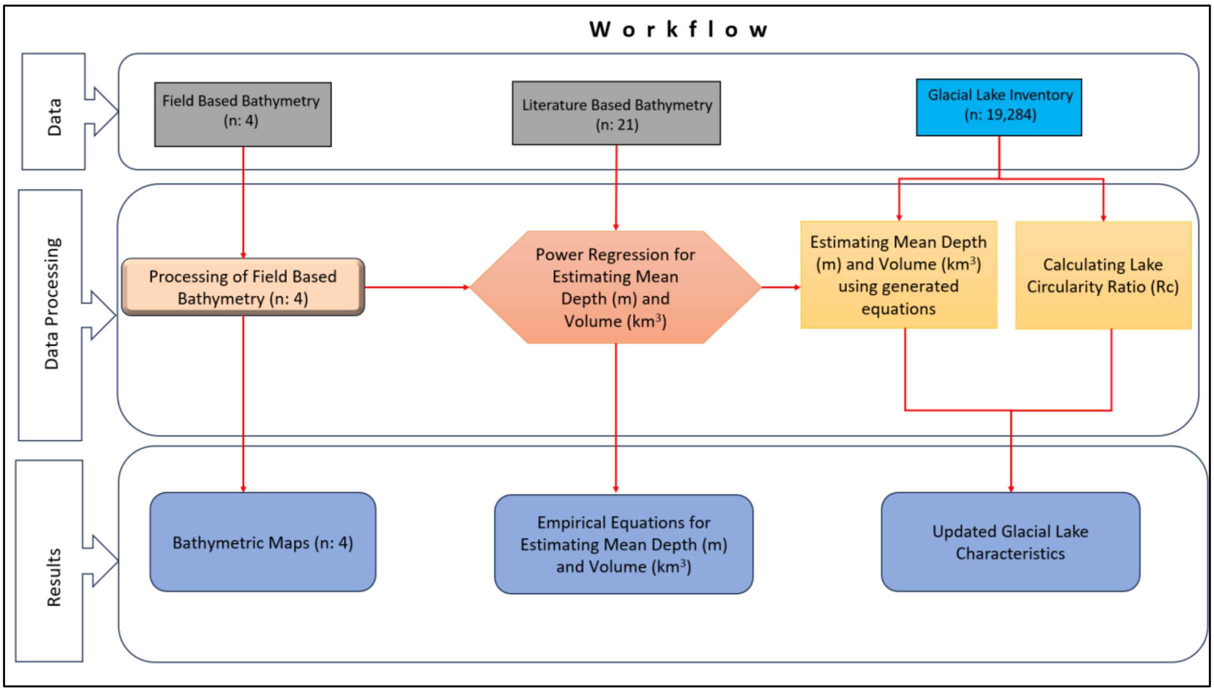

Fig. 2 Flowchart depicting the methodology of the study.

3.1.2. Glacial lake inventory

The glacial lake inventory (n = 19,284; and area = 1,191.81±209.21 km^2), used in the present study for the estimation of mean depth and volume of glacial lakes in the upper IGB basins, was developed by **Kumar et al. (2024).** The glacial lake inventory is based on 109 Landsat 8 Operational Land Imager (OLI) (spatial resolution: 30 m) satellite images, obtained from the United States Geological Survey (https://earthexplorer.usgs.gov). The minimum mapping unit (MMU) of the glacial lakes was taken as 4 pixels (0.0036 km^2) **(Zheng et al., 2021; Li et al., 2022)**. However, it is important to mention that this MMU excludes smaller glacial lakes (< 0.0036 km^2), especially the ice-dammed supraglacial lakes. MMU threshold, as affected by the pixel size of the satellite data, has a significant influence on the total number of glacial lakes. This not only reduces the total number of mapped glacial lakes, total area, and total estimated volume of glacial lakes, but also has implications on overall GLOFs threat assessments **(Mal et al., 2021)**, especially in the case of ice-dammed lakes. It is, however, pertinent to note that these very smaller glacial lakes (< 0.0036 km^2) can feed larger downstream lakes in the cases of dam breaching or overtopping, which may further accelerate the expansion of downstream glacier-fed lakes and increases the GLOF threat **(King et al., 2018; Zhang et al., 2024)**.

The inventory was developed using a semi-automated method (**Kumar et al., 2024**). The first step to generate the glacial lake inventory was to develop a Normalized Difference Water Index (NDWI: Green - NIR) / (Green + NIR) composite layer for the upper IGB basin. A NDWI threshold of 0.3 was applied to the water mask to identify the potential glacial lakes. Furthermore, a slope threshold of 20° and elevation threshold of 2.900 m were employed using Shuttle Radar Topographic Mission v4 (SRTM) (spatial resolution: 30 m) **(https://earthexplorer.usgs.gov/)** to remove the potential misclassification of glacial lakes. These thresholds were applied to reduce the misclassification from potential sources such as extended snow cover, areas with shadow, mixed land use, and dense vegetation, which greatly improved the accuracy of lake mapping. The hillshade extracted from the SRTM DEM further helped in minimizing the misclassification of glacial lakes due to the shadow effect from the mountain ridges. Furthermore, the elevation threshold helped us identifying non-glacial lakes. Eventually, manual inspection helped in removing misclassification due to the mixed land use, and the lake classification was done with the help of google earth, where each lake was carefully inspected and assigned to a particular class **(Kumar et al., 2024)**. It is important to highlight here that the method used to generate the glacial lake inventory is specifically built for extracting glacial lakes in the HKH region after carefully reviewing the literature **(Zhang et al., 2015; Nie et al., 2017; Maharjan et al., 2018; Shugar et al., 2020)**. Applying the same method to other glaciated regions might yield erroneous results because of the different geomorphological settings. For example, applying the elevation threshold of 2,900 m in the Alps will lead to under-representation of glacial lakes in the Alps, as the lowest ELA in the Alps is at ~2,300 m **(Kerschner et al., 2008)**.

3.2. Methods

3.2.1. Processing of field-based bathymetry data (n = 4)

The in-situ bathymetry data was processed using Garmin's Homeport software and ArcGIS Pro (Version 3.2). The first step was to import the depth waypoints to Garmin's Homeport software from Garmin's echoMAP 52dv sonar. The second step was to export depth waypoints for a lake to a CSV and clean the lake's depth data for any anomalies. The bathymetry data points were then interpolated using the spline technique, with lake outlines as a barrier, which produced raster surface of lake depth. This mean depth raster surface was multiplied by lake area to estimate the volume of the glacial lakes.

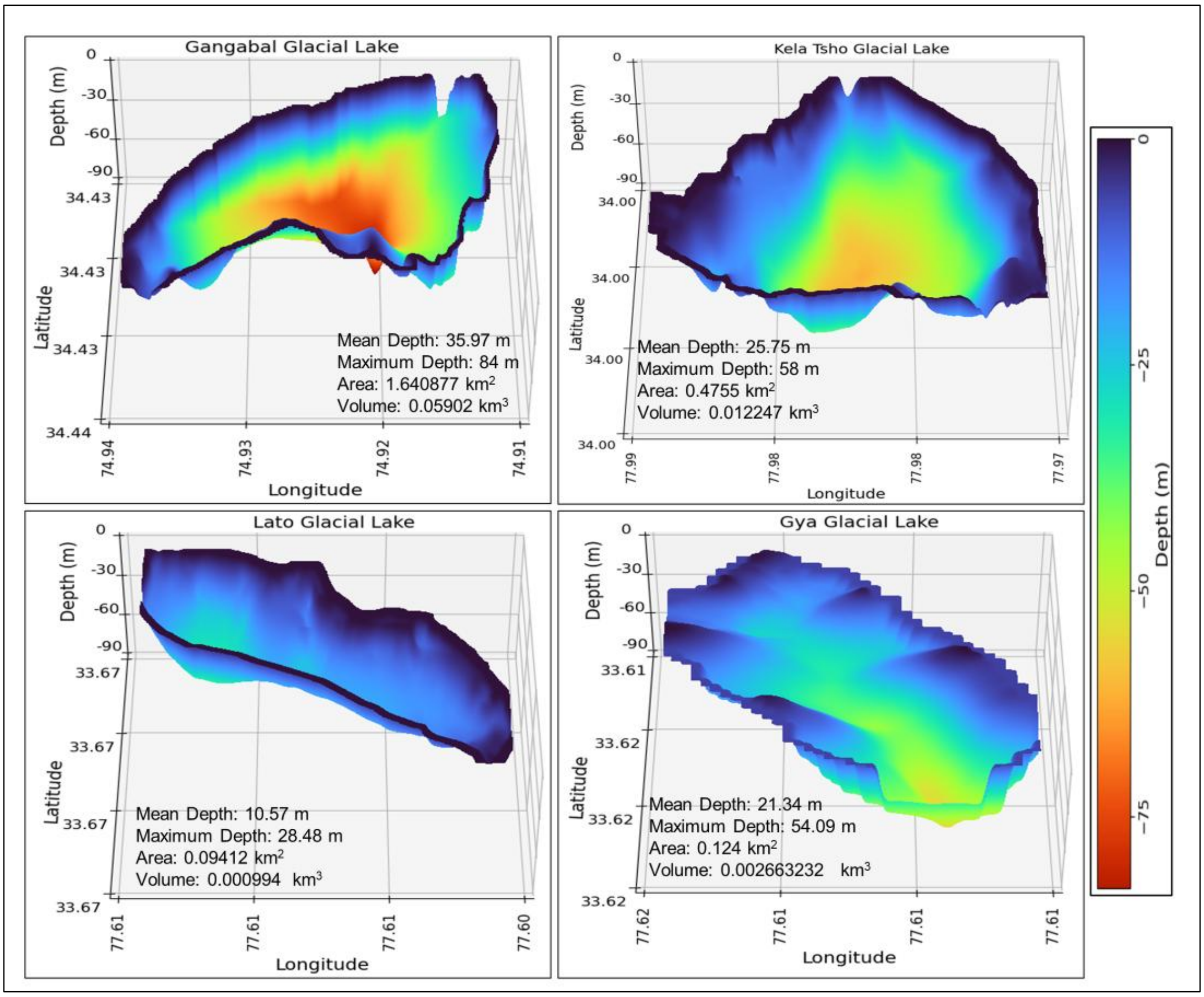

Fig. 3. Bathymetric maps of surveyed glacial lakes in the upper Indus basin between September 2021 and September 2023.

3.2.2. Empirical equations for estimation of mean depth and volume based on our and literature based bathymetry (n = 25)

Estimating the mean depth and volume of glacial lakes is crucial for estimating potential flood volumes, run-off distance, and modelling GLOF scenarios (**Huggel et al., 2002; Fujita et al., 2013**). The area-scaling function has been widely used to develop empirical equations for estimating the depth and volume of glacial lakes (**Qi et al., 2022**), which enables the modelling of the relationship between dependent (depth) and independent variable, i.e., area, due to their significant correlation (**Huggel et al., 2002**). However, in most cases the relationship between area and depth, and between area and volume of glacial lakes is non-linear (**Cook and Quincey, 2015**).

In the present study, we developed 8 empirical equations using power regression between lake depth/volume and lake area for the upper Indus, upper Ganga, upper Brahmaputra, and entire HKH for a better understanding of regional characteristics of the relationship between lake depth/volume and lake area (**Fig. 4**). Equations (a to d) and (e to h) were developed to estimate the mean depth and volume (m^3) of glacial lakes as a function of lake area, respectively. The study is based on the following assumptions: (i) There is a consistent and predictable relationship between surface area, depth, and volume of glacial lakes; (ii) Geometric similarities exist between different sizes of glacial lakes; and (iii) scaling laws accurately describe how mean depth and volume change with surface area. **Fig. 4** (a and e) represents the relationship of area with depth and volume of glacial lakes (n = 8) for the upper Indus basin. **Fig. 4** (b and f), (c and g), and (d and h) represent the relationship of area with depth and volume of glacial lakes for upper Ganga (n = 10), upper Brahmaputra (n = 7), and for the entire IGB (n = 25), respectively. All previously surveyed glacial lakes used in the present study were based on primary bathymetric sonar surveys, providing a higher level of consistency in data collection methods. Although minor variations in resolution or equipment settings may exist, the standardized use of sonar minimizes significant discrepancies, supporting reliable integration of data from multiple sources. Furthermore, average residual and Residual Mean Square Error (RMSE) were calculated after applying the equations to all the selected glacial lakes for the validation of the empirical equations.

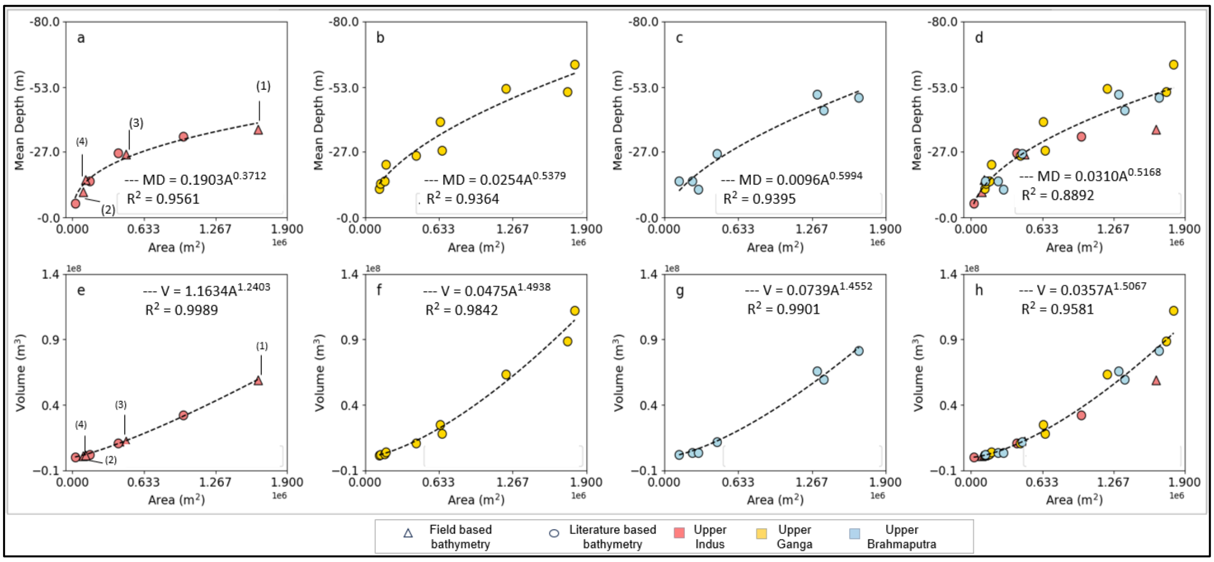

Fig. 4. Empirical equations for estimating the mean depth and volume of glacial lakes, where sample lakes (a) to (d) were used to develop the equation to estimate the mean depth using glacial lakes (a) in the upper Indus, (b) in upper Ganga, (c) in upper Brahmaputra, and (d) in upper IGB. Similarly, equations (e) to (h) were developed to estimate the volume (m^3) using glacial lakes (e) in upper Indus, (f) in upper Ganga, (g) in upper Brahmaputra, and (h) in upper IGB. Field and literature-based bathymetry, as mentioned in supplementary Table 1.

3.2.3. Uncertainty Assessment of Mean Depth and Volume Estimation

The uncertainty assessment of estimated mean depth and volume of glacial lakes is of immense importance, as it provides valuable insights into the reliability of the volume and depth measurements. To improve the precision of our estimated mean depth and volume across the 19,284 glacial lakes, we employed a Bayesian updating approach that integrates both observed data and model estimates **(Gantayat et al., 2024)**. For each matric, we first calculated the Root Mean Square Error (**RMSE)** between observed and model-estimated values. The RMSE, representing the typical model error, served as the standard deviation for the prior distribution. The Bayesian update formula we used to obtain the posterior mean ($\boldsymbol{\mu}_{post}$) and posterior standard deviation (σ_{post}) combines the prior information with observed data as follows:

$$\mu_{post} = \frac{\left(\frac{\mu_{prior}}{\sigma^2_{prior}}\right)+\left(\frac{\mu_{obs}}{\sigma^2_{obs}}\right)}{\left(\frac{1}{\sigma^2_{prior}}\right)+\left(\frac{1}{\sigma^2_{obs}}\right)} \qquad \text{(ix)}$$

$$\sigma_{post} = \sqrt{\frac{1}{\left(\frac{1}{\sigma^2_{prior}}\right)+\left(\frac{1}{\sigma^2_{obs}}\right)}} \qquad \text{(x)}$$

Where $\boldsymbol{\mu}_{prior}$ and σ_{prior} represent the prior mean and standard deviation from the model estimates, while $\boldsymbol{\mu}_{obs}$ and σ_{obs} are the mean and standard deviation of the observed data **(Gelman et al., 2013)**. For total estimated volume, we scaled the posterior mean to align with the known total estimated volume of 28.8 km^3, yielding a refined 95 % confidence interval that captures the full dataset's uncertainty. The uncertainty of the estimated volume using the Bayesian approach was between 28.79 km^3 and 28.99 km^3.

Similarly, for estimated mean depth, we adjusted the posterior mean to reflect the estimated mean depth of 7.20 m across all lakes. This scaling produces a final estimate of mean depth with a 95 % confidence interval that represents the range within which the true mean likely falls. The uncertainty of the estimated mean depth using the Bayesian approach was between 4.70 m and 9.70 m. The Bayesian updating approach uses both observed data and model estimates to find the best balance between empirical accuracy and practical constraints. This lets us get strong uncertainty intervals for both the estimated mean depth and volume. The method is particularly valuable for large-scale assessments in remote, data-limited regions where field measurements are challenging, thereby providing a statistically grounded basis for future glacial lake risk assessment **(Carlin and Louis, 2009)**.

3.2.4. Circularity ratio

The circularity ratio measures the compactness or roundness of a geomorphic feature (**Küçük et al., 2021**). The value of the circularity ratio ranges between 0 and 1, where values close to 0 and 1 suggest elongated and circular shapes, respectively (**Küçük et al., 2021**). The circularity ratio of each glacial lake is calculated as follows:

$$CR = 4\pi(\text{Area})/(\text{Perimeter})^2 \qquad \text{(i)}$$

The circularity ratio equates the area to the square of the perimeter of a feature, normalized by a factor derived from the properties of a circle. The circularity ratio helps better understand the role of shape in establishing the relationship between the area and depth of glacial lakes. The circular shape of glacial lakes suggests a linear relationship between the area and depth, suggesting relatively higher predictability to estimate the depth and volume of glacial lakes using the area-scaling method (**Supplementary Fig. 2**). In contrast, the elongated shape of glacial lakes suggests a non-linear relationship between the area and depth, suggesting a relatively lower predictability to estimate the depth and volume of glacial lakes using area-scaling methods **(Cook and Quincey, 2015)**.

4. Results

4.1. Bathymetry of surveyed (n: 4) and literature based glacial lakes (n: 21)

The area of selected glacial lakes varies between 0.022 km^2 (Neelkanth Lake) and 1.8 km^2 (Lower Barun Lake). The mean depth varies between 5.78 m (Neelkanth Lake) and 62.39 m (Lower Barun Lake), the volume varies between 0.00013 km^3 (Neelkanth Lake) and 0.11 km^3 (Lower Barun Lake), and the circularity ratio varies between 0.17 (Tsho Rolpa Glacier Lake) and 0.74 (Tsomgo Lake). Furthermore, out of 25 glacial lakes, 16 were end moraine-dammed lakes, 6 were lateral moraine-dammed lakes, 2 were cirque lakes, and 1 was other bedrock-dammed lake **(Supplementary Table 1)**.

Among the 21 literature-based bathymetry dataset, Lower Barun Lake has the maximum mean depth of 62.38 m (upper Ganga basin), whereas Neelkanth had the lowest mean depth of 5.78 m (upper Indus basin). In terms of total water volume, Lower Barun has the maximum water volume of 0.112 km^3, whereas Neelkanth has the lowest water volume of 0.0001 km^3 (**Supplementary Table 1**).

4.2 Relationship of area with mean depth of glacial lakes (n: 25)

There is a strong positive correlation (0.92) between the area and the mean depth of glacial lakes (n = 25) in the study region (**Table 1**). The relationship is, however non-linear, which is caused by the shape of the glacial lakes (**Supplementary Fig. 2**).

Table 1: Correlation matrix (r-values) between glacial lake characteristics for the selected glacial lakes (n = 25) in the upper IGB basin using Pearson correlation coefficient

	Area (km^2)	**Mean Depth (m)**	**Volume (km^3)**	**Circularity ratio**	**Elevation (m asl)**
Area (km^2)	1	0.92	0.97	-0.66	-0.04
Mean Depth (m)		1	0.94	-0.66	0.08
Volume (km^3)			1	-0.66	0.007

Circularity ratio				1	-0.27
Elevation (m asl)				-0.27	1

Therefore, we employed the power regression function to generate the empirical equation that estimates the mean depth of glacial lakes as a function of its area. We developed four empirical equations to estimate the mean depth, utilizing area of glacial lakes as independent variable (Equation a to d) (**Fig. 4 & Table 2**). Equation (a) was developed using glacial lakes (n = 8) in the upper Indus basin, (b) was developed using glacial lakes (n = 10) in the upper Ganga basin, (c) was developed using glacial lakes (n = 7) in the upper Brahmaputra basin, and (d) was developed using glacial lakes (n = 25) in the upper IGB basin (**Fig. 4**). Furthermore, the coefficient of determination (**R^2**), average residual (***e***), and Root Mean Square Error (RMSE) were calculated for each empirical equation to assess the respective performance (**Table 2**). Equation (a) has the highest R^2 (0.956) among the four equations (**Fig. 5 & Table 2**). However, equation (d) performed best with the lowest average residual (0.029 m) and RMSE (5.21 m) (**Table 2**).

We observed that glacial lakes with a lower circularity ratio have a higher mean depth than those with a higher circularity ratio (**Supplementary Table 1**). The average circularity ratio of the selected lakes was 0.405. The mean depth of glacial lakes with a circularity ratio less than 0.405 was 37.20 m, whereas the mean depth of glacial lakes with a circularity ratio of more than 0.405 was 17.95 m.

4.3 Relationship of area with volume of glacial lakes (n: 25)

Similarly, area and volume of selected glacial lakes show a strong positive correlation (0.97) (**Table 1**); however, the relationship is non-linear (**Supplementary Fig. 3**). Four empirical equations (e to h) were developed, using the same sample size used for area and mean depth (eq. a to d), to estimate the volume of glacial lakes in the upper IGB basins, with area being an independent variable (**Fig. 4**). Among the four equations, equation (e) has the highest **R^2** (0.99). However, equation (h) had the lowest average residual ($3.2*10^4$ m^3) and RMSE ($0.67*10^7$ m^3) **(Fig. 5 & Table 2**).

Table 2. Empirical equations developed for different regions

	Region	No. of glacial lakes	Equation	Empirical equation	Coefficient of determination (R^2)	Average Residual (*e*)	RMSE
Estimated Mean Depth (m)	Upper Indus	8	a	$MD = 0.1903*A^{0.3712}$	$R^2 = 0.9561$	-3.44334 m	8.14 m
	Upper Ganga	10	b	$MD = 0.0254*A^{0.5379}$	$R^2 = 0.9364$	2.5016 m	6.09 m
	Upper Brahmaputra	7	c	$MD = 0.0096*A^{0.5994}$	$R^2 = 0.9395$	-1.56719 m	5.57 m
	Upper IGB	25	d	$MD = 0.0310*A^{0.5168}$	$R^2 = 0.8892$	0.0298 m	5.21 m
Estimated	Upper Indus	8	e	$V = 1.1634*A^{1.2403}$	$R^2 = 0.9989$	$-5.68*10^6$ m^3	$1.31*10^7$ m^3

	Upper Ganga	10	f	$V = 0.0475*A^{1.4938}$	$R^2 = 0.9842$	$3.02*10^6$ m^3	$0.80*10^7$ m^3
	Upper Brahmaputra	7	g	$V = 0.0739*A^{1.4552}$	$R^2 = 0.9901$	$2.02*10^5$ m^3	$0.674*10^7$ m^3
	Upper IGB	25	h	$V = 0.0357*A^{1.5067}$	$R^2 = 0.9581$	$3.2*10^4$ m^3	$0.671*10^7$ m^3

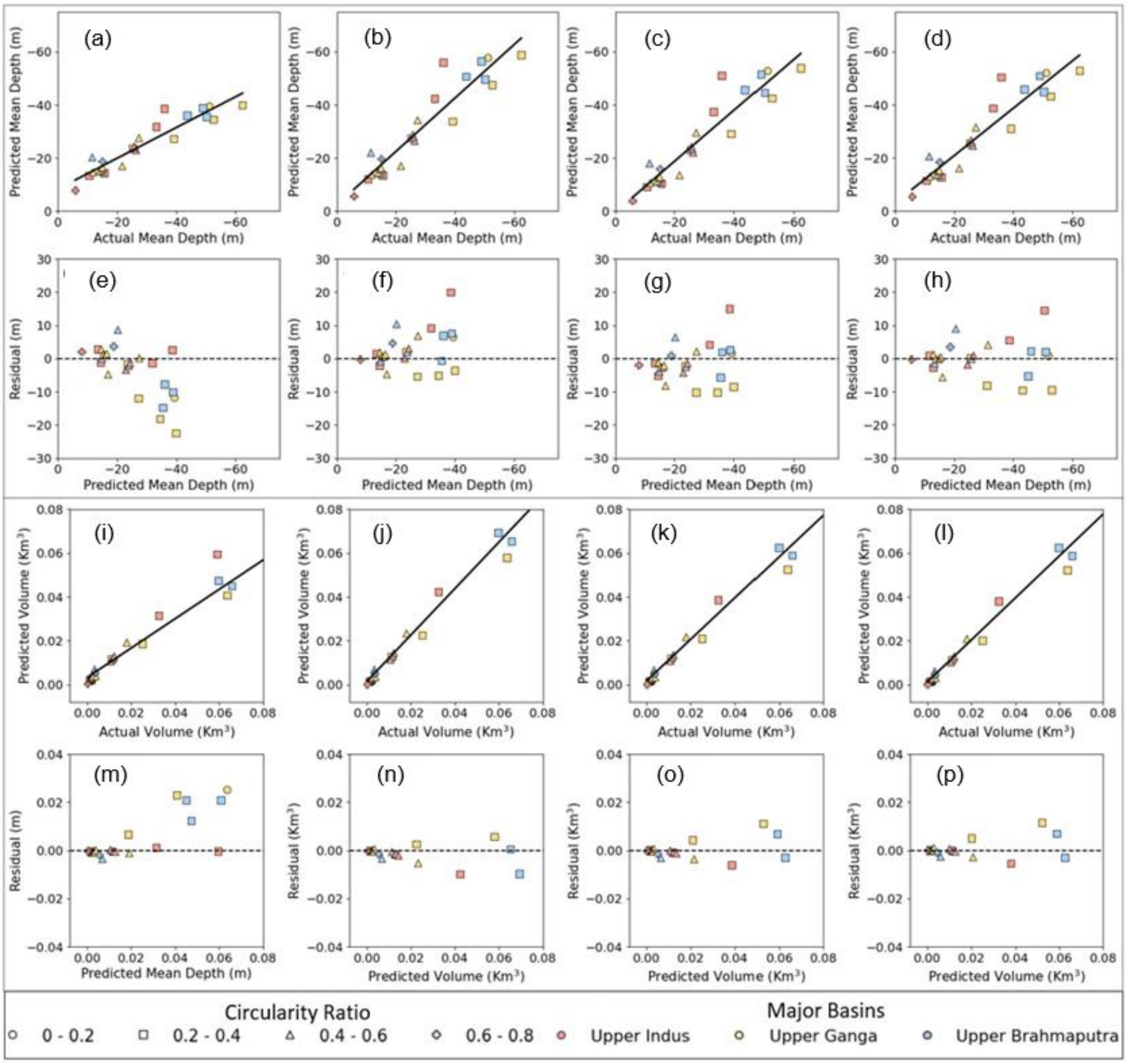

Fig. 5. Linear relationships between actual and predicted values for mean depth and volume of glacial lakes using different empirical equations. Subplots (a) to (d) show the linear relationship between actual and predicted mean depth, where (a) uses the equation developed for upper Indus, (b) uses the equation developed for upper Ganga, (c) uses the equation developed for upper Brahmaputra, and (d) uses the equation developed for upper IGB basins in figure 3. Subplots (e) to (h) show the residual between actual and predicted mean depth, where (e) uses the equation developed for upper Indus, (f) uses the equation developed for upper Ganga, (g) uses the equation developed for upper Brahmaputra, and (h) uses the equation developed for upper IGB basins. Subplots (i) to (l) are the same as for (a) to (d), but

for the linear relationship between actual and predicted volume. Subplots (m) to (p) are the same as for (e) to (h), but for the relationships between residuals between actual and predicted mean depth.

4.4 Mean depth and volume of glacial lakes in the upper IGB basin (n: 19,284)

In the present study, we used the glacial lake inventory (n = 19,284 and area = 1191.81±209.21 km^2) developed by **Kumar et al. (2024)** to estimate the mean depth and volume of glacial lakes. Among the major basins, the upper Brahmaputra basin had the highest number of glacial lakes (n = 11,579; a = 763.59±132.14 km^2), followed by the upper Indus (n = 4,587; a = 217.47±43.39 km^2) and the upper Ganga (n = 3,118; a = 210.74±33.66 km^2).

The average estimated mean depth and volume of glacial lakes in the upper IGB is 7.20 m and 28.8 km^3, respectively. The uncertainty of the estimated mean depth using the Bayesian approach was between 4.70 m and 9.70 m. And, the uncertainty of the estimated volume using the Bayesian approach was between 28.79 km^3 and 28.99 km^3. Among the major river basins, the upper Brahmaputra basin has the highest average estimated mean depth (7.43 m) and total estimated volume (19.002 km^3), followed by the upper Ganga basin (depth: 7.10 m and total volume: 6.33 km^3), and the upper Indus basin (depth: 6.69 m and total volume: 3.55 km^3). In general, the mean depth and total volume of the glacial lakes decrease from the eastern Himalaya (Brahmaputra basin) to the central Himalaya (Ganga basin) and further towards the western Himalayan region (Indus basin); thus, the mean depth and the estimated volume are strongly correlated (**Table 1 and Fig. 6**). It is essential to highlight that the upper Ganga basin (n = 3,118; a = 210.74±33.66 km^2) had a higher estimated volume per glacial lake (0.002 km^3) than the upper Brahmaputra (n = 11,579; a = 763.59±132.14 km^2, volume/lake: 0.0016 km^3) and the upper Indus basin (n = 4,587; a = 217.47±43.39 km^2, volume/lake: 0.0008 km^3) (**Fig. 1**).

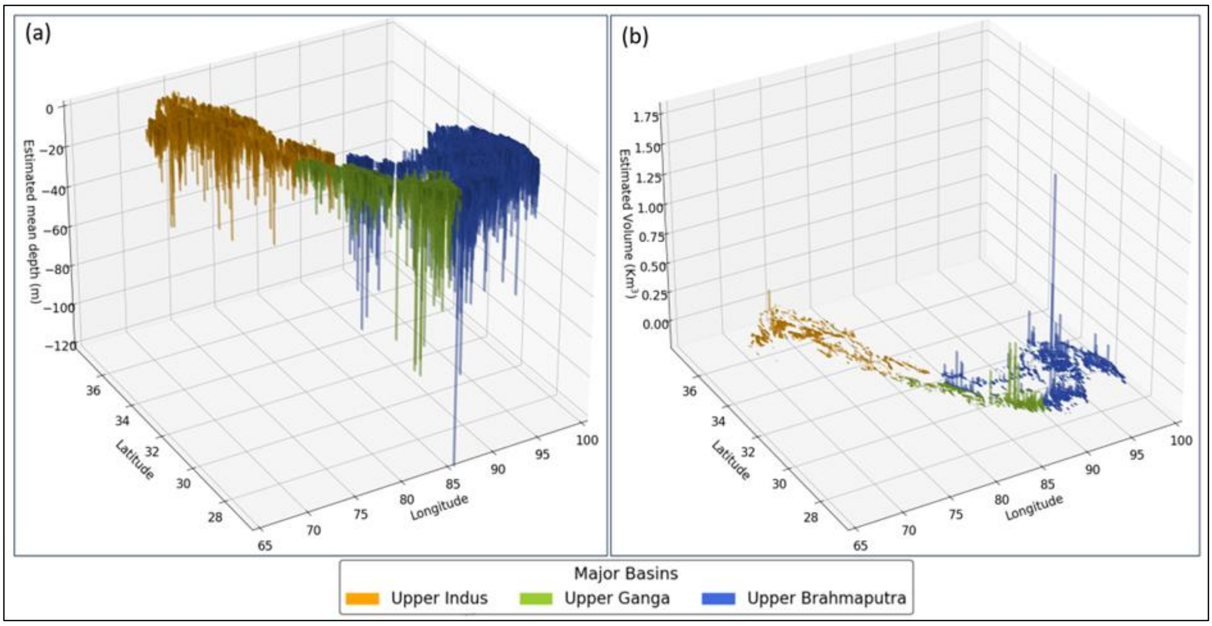

Fig. 6. 3D bar plot showing the spatial distribution of estimated (a) mean depth and (b) volume of glacial lakes in the upper IGB basin.

4.5 Influence of circularity ratio on depth and volume estimation

To understand the relationship between circularity ratio and mean depth/volume of selected glacial lakes (n = 25), we divided the circularity ratio into three categories and piecewise regression was conducted (**Table 3**). In terms of the mean depth of selected glacial lakes, Category II (n = 13) had the steepest slope of -186.17, followed by Category I (n = 6) with a slope of -67.04, and least steep slope (-50.36) in Category III (n = 6). This shows glacial lakes with lower circularity ratio have higher range of depth, and non-linearity between circularity ratio and mean depth (**Supplementary Fig. 2**). Category I has the maximum mean depth of 40.91 m, followed by, Category II (depth = 26.44 m), and Category III (depth: -18.31 m) (**Table 3**). Furthermore, all categories have negative correlation with mean depth, however, Category II has the strongest negative correlation (-0.81), followed by Category III (-0.65), and Category I (-0.12) (**Table 3**).

Table 3: Relationship between circularity ratio and mean depth/volume for the selected glacial lakes (n: 25) using piecewise regression

	Number of Glacial Lakes	**Correlation (r) between circularity ratio and mean depth (m)**	**Slope (β) between circularity ratio and mean depth (m)**	**Mean depth (m)**	**Correlation (r) between circularity ratio and volume (km^3)**	**Slope (β) between circularity ratio and volume (km^3)**	**Mean Volume (km^3)**
Category I (0 – 0.3)	6	-0.12	-67.04	-40.91	-0.23	-0.307	0.057
Category II (0.3 – 0.5)	13	-0.81	-186.17	-26.44	-0.82	-0.354	0.023
Category III (0.5 – 0.8)	6	-0.65	-50.36	-18.31	-0.49	-0.023	0.005
Overall (0.8 – 1)	25	-0.668	-75.75	-27.96	-0.662	-0.157	0.027

Similarly, piecewise regression was used to understand the relationship between circularity ratio and volume (km^3) of selected glacial lakes. Category II (n: 13) had the steepest slope of -0.354, followed by Category I (n: 6) with a slope of -0.307, and Category 3 (n: 6) with a slope of -0.023 (**Table 3**). The data reveals a non-linear relationship between the circularity ratio and the volume of glacial lakes. Specifically, glacial lakes with a lower circularity ratio tend to have a more dynamic water volume profile compared to those with a higher circularity ratio (**Supplementary Fig. 3**). The highest mean volume of glacial lakes was found in Category I (0.057 km^3), followed by Category II (Mean Vol = 0.023 km^3), and Category III (Mean Vol = 0.0005 km^3) (**Table 3**).

Furthermore, we observed that the relationship between circularity ratio and mean depth/volume also holds true for the estimated mean depth and volume using equation d and h, respectively, for 19,284 glacial lakes in the upper IGB basin (**Fig. 7**). The non-linearity between the circularity ratio and the estimated mean depth/volume of glacial lakes also exists for the glacial lake inventory (n = 19,284). The correlation between circularity ratio and estimated mean depth/volume continues to exhibit a negative relationship (**Fig. 7**). However, the relationship weakens a bit the correlation between circularity ratio and estimated mean depth was negative and moderately strong (-0.47), and the correlation between circularity ratio and estimated volume was weakly negative (-0.12) (**Supplementary Table 2**). This can be due to underperformance of the equation when estimating the mean depth and volume of glacial lakes in the upper IGB basin. Therefore, it is suggested that the role of circularity ratio should be further explored in estimating the mean depth and volume of glacial lakes.

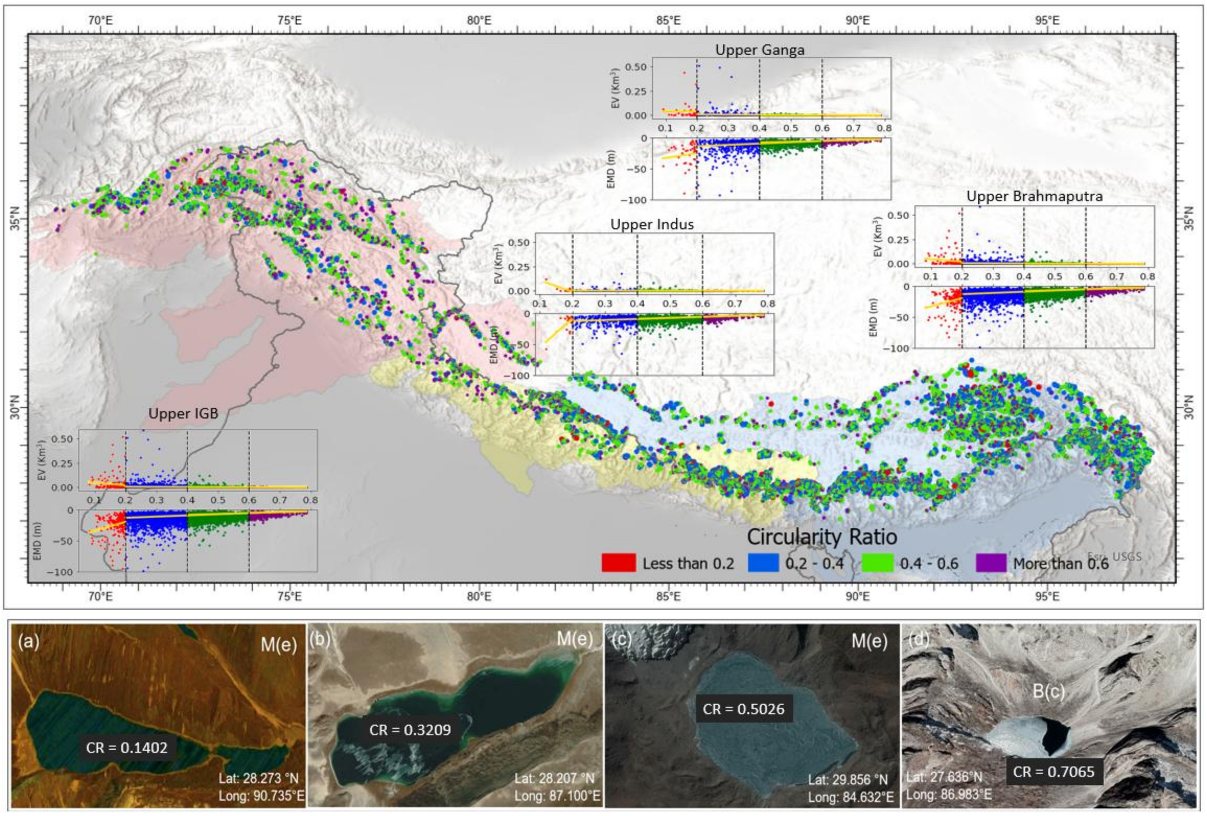

Fig. 7. Spatial distribution of the circularity ratio of glacial lakes in the upper IGB basin. The subplots within the map show the piecewise regression: 1) between the circularity ratio and the estimated mean depth of glacial lakes and 2) between the circularity ratio and the estimated volume of glacial lakes at major basin level. The lakes in the bottom panel are from Google Earth, showing glacial lakes with different circularity ratios.

4.6 Altitudinal distribution of mean depth and volume of glacial lakes

Glacial lakes were mapped between the elevation zones of 3,000 m asl and 6,216 m asl. Based on the elevation, we divided glacial lakes into 16 zones (at an interval of 200 m asl). The result shows that each elevation zone has a distinct distribution pattern of lake characteristics (**Fig. 8**).

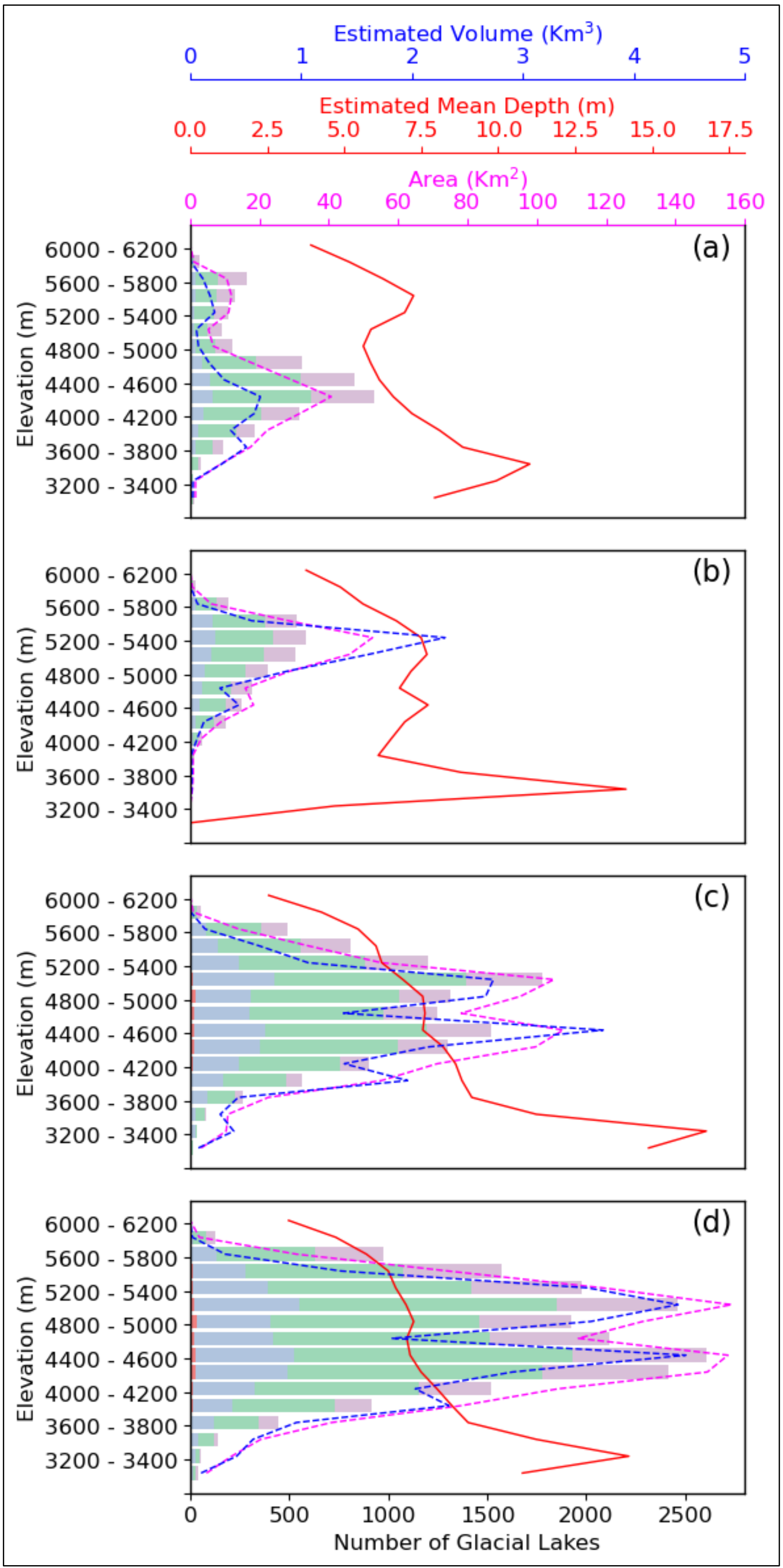

Fig. 8. Altitudinal distribution of glacial lakes according to number of glacial lakes (segmented bars showing number of lakes in different categories of circularity ratio), area (km^2) (dashed violet line), estimated mean depth (m) (red line), and estimated volume (km^3) (dashed blue line) of glacial lakes,

with (a) representing the upper Indus basin, (b) the upper Ganga basin, (c) the upper Brahmaputra basin, and (d) the entire upper IGB basin.

In the upper Indus, the majority of the glacial lakes are distributed between the altitudes of 4,200 m asl and 4,800 m asl (n = 50.61 %). However, total estimated volume (31.31 %) and total area (40.37 %) were relatively low between 4,200 m asl and 4,800 m asl in the upper Indus basin (**Fig. 8a**).

In the upper Ganga basin, the majority of glacial lakes were distributed between the altitudes of 5,000 m asl and 5,600 m asl (52.95 %). In these altitudinal zones, the total estimated volume of glacial lakes was (70.42 %) and the total area of glacial lakes was (60.12 %) (**Fig. 8b**). And in the upper Brahmaputra basin, the altitudinal zones between 4,200 m asl and 5,400 m asl has the maximum concentration of glacial lakes (n = 72.15 %, a = 70.86 %, and estimated volume = 72.18 %) (**Fig. 8c**). At the upper IGB level, elevation between 4,200 m asl and 5,400 m asl has the maximum concentration of glacial lakes (n = 69.99 %, a = 71.96 %, and estimated volume = 68.98 %). (**Fig. 8d**). Furthermore, we found that the rise in estimated volume is closely related to the rise in the average mean depth. Altitudinal zones with a higher estimated mean depth have a higher estimated volume of glacial lakes (**Fig. 8**). However, lower elevation zones (less than 4,000 m asl) have the deepest average mean depth of glacial lakes across the upper IGB (**Fig. 8**). This is mainly due to the smaller number of glacial lakes (n = 8.23 %) in the lower elevation zones (less than 4,000 m asl).

5. Discussion

5.1 Factors affecting the estimation of depth and volume of glacial lakes

Estimating the mean depth and volume of glacial lakes is a complex process. Key factors that influence the estimation of the depth and volume of glacial lakes are the availability of in-situ data, lake geometry (area, width, shape), dam material, melting rate of glaciers, distance from the glacier, sub-glacial topography and rock structure, precipitation pattern, and sedimentation rate (**Cook & Quincey, 2015; Muñoz et al., 2020; Qi et al., 2022**). The area of glacial lakes, which is positively strongly related to both depth and volume of glacial lakes, is widely used to estimate the depth/volume (**Huggel et al., 2002; Qi et al., 2022**). However, there is no universal equation to accurately estimate the mean depth/volume of glacial lakes using the area-scaling method. This is mainly due to other local lake characteristics such as shape, sedimentation rate, parent glacier activity, dam material, and precipitation patterns, continuously influencing the relationship between lake area and depth/volume (**Cook and Quincey, 2015**). Few studies attempted to understand the role of local lake characteristics in influencing the relationship between area and mean depth/volume of glacial lakes (**Huggel et al., 2002; Cook and Quincey, 2015; Muñoz et al., 2020; Qi et al., 2022; Zhang et al., 2023**). **Cook and Quincey (2015)** suggested that the shape of the glacial lake influences the relationship between area and mean depth/volume. However, they did not quantify it. In our study, we have used the circularity ratio to quantify the shape of glacial lakes. Our study shows that there is a negative correlation between circularity ratio and mean depth/volume of glacial lakes. Furthermore, we found the low circularity ratio of glacial lakes is the key reason for the non-linearity between the area and mean depth/volume of glacial lakes.

We also attempted to evaluate the relationship between dam type and other lake characteristics (area, mean depth, volume, and circularity ratio) **(Fig. 9)**. We found that the region is dominated by end moraine-dammed lakes (M(e)), followed by other bedrock-dammed lakes (B(o)), supraglacial lakes (S), lateral moraine-dammed lakes (M(l)), other-type of glacial lakes (O), cirque lakes (B(c)) and other moraine-dammed lakes (M(o)) **(Fig. 9)**. B(o) lakes tend to have a broader range of characteristics, with notable variability in area and estimated volume, potentially indicating greater morphometric diversity **(Fig. 9)**. The supraglacial lakes had the lowest average estimated mean depth (4.13 m), whereas B(o) lakes had the highest average estimated mean depth (7.44 m), highlighting the different geomorphic settings where such lakes form and differences in dam geometries. Therefore, it is of immense importance to acknowledge the differences in the dam-type before developing future empirical equations.

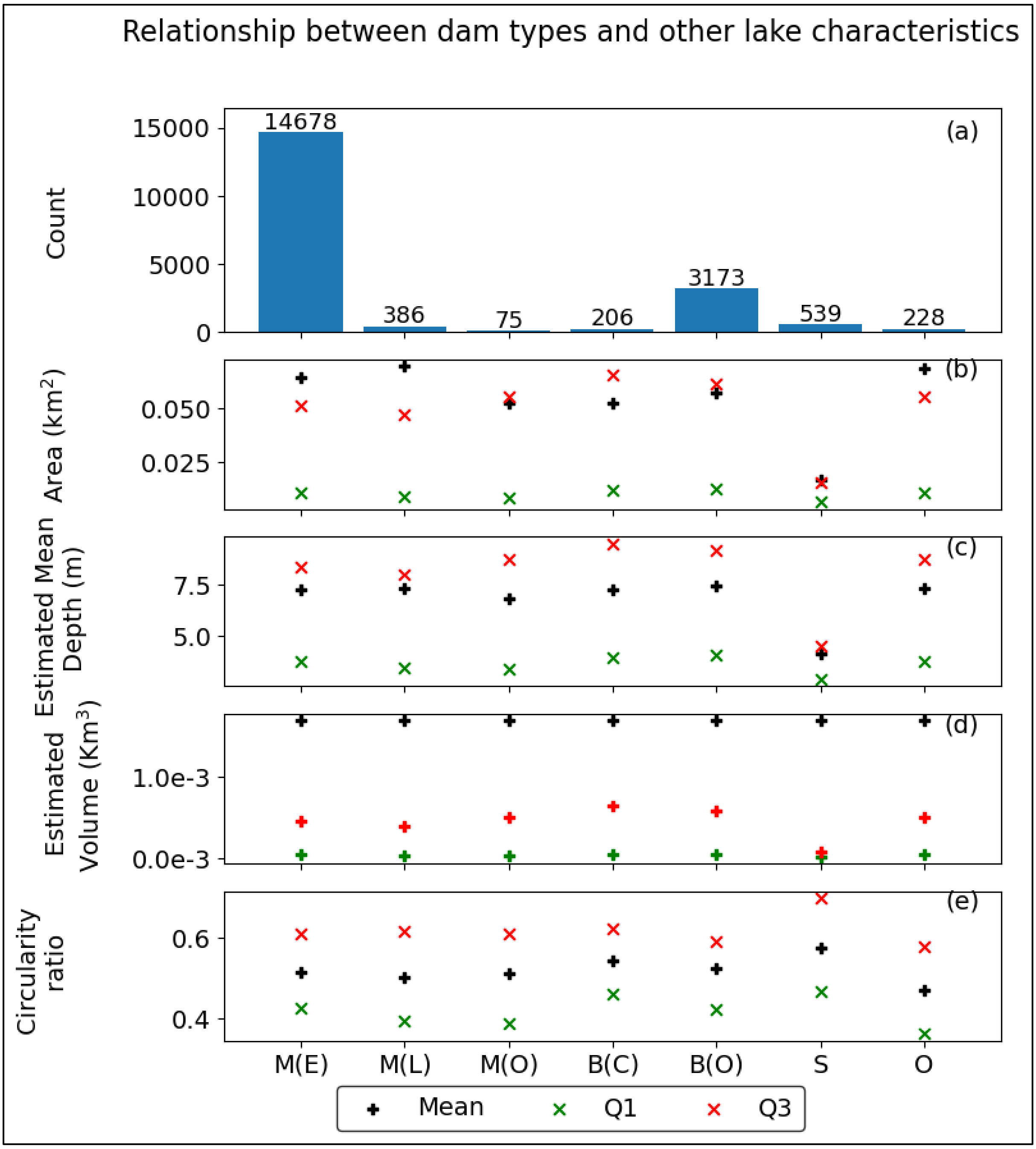

Fig 9. Relationship between dam type and different glacial lake characteristics, where (a) shows the relationship between different dam types and count, (b) dam type and area (km^2), (c) dam type and estimated mean depth (m), (d) dam type and estimated volume (km^3), and (e) dam type and circularity ratio. Where (+) shows the mean, (x) in green color shows the first quartile, and (x) in red color shows the third quartile.

5.2 Comparison with previous studies related to glacial lake mean depth/volume estimation

Globally, several empirical equations were developed to estimate the mean depth and volume of glacial lakes (**Evans 1986; O'Connor 2001; Huggel et al. 2002; Sakai 2012; Fujita et al., 2013; Muñoz et al., 2020; Qi et al., 2022**). However, no specific empirical equation is based on samples from across the HKH (Zhang et al., 2023). Local topography, glacio-fluvial processes, and parent material play a crucial role in determining glacial lake properties, especially the depth (**Cook and Quincey, 2015; Muñoz et al., 2020; Qi et al., 2022**). Therefore, all the global and regional equations developed previously underperform in the study domain (**Table 4**). Several parameters were used to estimate the mean depth and volume of glacial lakes. However, glacial lake area is the most commonly used variable to estimate the mean depth and volume of glacial lakes (**Muñoz et al., 2020; Qi et al., 2022**). We calculated average residual (***e***), coefficient of determination (**R^2**) and **RMSE** for the selected previous empirical equations developed to estimate the mean depth and volume of glacial lakes (**Table 4**). All the previous equations underperformed to estimate the mean depth and volume (**Table 4**). The main reason is the influence of local lake characteristics. Furthermore, none of the previous equations was developed using samples from across the longitudinal profile of HKH.

Among the previously developed equations to estimate the mean depth, the equation developed by Wang et al. (2012) had the lowest RMSE (-6.41 m) for the selected lakes, while those by Fujita et al. (2013) had the highest RMSE (-18.31 m) (**Table 4**). For volume estimation, the equation developed by Zhang et al. (2023) had the lowest RMSE ($7.16*10^6$ m^3), and the equation developed by Fujita et al. (2013) had the highest RMSE ($40.86*10^6$ m^3) (**Table 4**). Furthermore, because of the self-correlation between area, estimated mean depth, and estimated volume, it is advisable that R^2 is not the best indicator for assessing the performance of an equation.

Table 4: Comparison of different empirical equations based on selected glacial lakes in present study

	Studies	**Study area and sample lakes**	**Empirical Equation**	**R^2 (actual and predicted values)**	**Average Residual (e)**	**RMSE**
Estimating Mean Depth	Present Study	UI (n: 8)	$MD = 0.1903A^{0.3712}$	0.72	-3.44 m	-8.14 m
		UG (n: 10)	$MD = 0.0254A^{0.5379}$	0.84	2.50 m	-6.09 m
		UB (n: 7)	$MD = 0.0096A^{0.5994}$	0.87	-1.56 m	-5.57 m
		UIGB (n: 25)	$MD = 0.0310*A^{0.5168}$	0.88	0.029 m	-5.21 m
	Huggel et al. (2002)	Swiss Alps (n: 15)	$D = 0.104A^{0.42}$	0.81	-2.28 m	-6.71 m
	Wang et al. (2012)	CH (n: 20)	$D = 0.087A^{0.434}$	0.83	-2.06 m	-6.41 m
	Fujita et al. (2013)	CH (n: -)	$D = 0.055A^{0.25}$	-0.36	-13.71 m	-18.31 m

	Patel et al. (2017)	WH (n: 2)	$D = 4 \times 10^{-5} \times A + 5.0564$	0.46	3.351 m	-11.42 m
	Muñoz et al. (2020)	Peruvian Andes (n: 121)	$Md\_Wi = 0.041 \times Width + 2$	0.64	-1.68 m	-9.29 m
Estimating Volume	Present Study	UI (n: 8)	$V = 1.1634*A^{1.2403}$	0.83	$-5.68*10^{6}$ m^{3}	$13.15*10^{6}$ m^{3}
		UG (n: 10)	$V = 0.0475*A^{1.4938}$	0.93	$3.02*10^{6}$ m^{3}	$8.09*10^{6}$ m^{3}
		UB (n: 7)	$V = 0.0739*A^{1.4552}$	0.95	$0.202*10^{6}$ m^{3}	$6.74*10^{6}$ m^{3}
		UIGB (n: 25)	$V = 0.0357*A^{1.5067}$	0.95	$0.03*10^{6}$ m^{3}	$6.71*10^{6}$ m^{3}
	Evans (1986)	Canada (n: 1)	$V = 0.035A^{1.5}$	0.93	$-2.87*10^{6}$ m^{3}	$8.12*10^{6}$ m^{3}
	Huggel et al. (2002)	Swiss Alps (n: 15)	$V = 0.104A^{1.42}$	0.91	$-3.61*10^{6}$ m^{3}	$9.29*10^{6}$ m^{3}
	Wang et al. (2012)	CH (n: 20)	$V = 0.0354A^{1.3724}$	-0.23	$-22.93*10^{6}$ m^{3}	$36.45*10^{6}$ m^{3}
	Sakai (2012)	CH & EH (n: 15)	$V = 43.244x(Area\ (km^{2}))^{1.5307}$	0.93	$2.99*10^{6}$ m^{3}	$8.29*10^{6}$ m^{3}
	Fujita et al. (2013)	CH & EH (n: -)	$V = 0.055A^{1.25}$	-0.55	$-25.88*10^{6}$ m^{3}	$40.86*10^{6}$ m^{3}
	Loriaux and Casassa (2013)	Northern Patagonia (n: 31)	$V = 0.2933A^{1.3324}$	0.79	$-7.6*10^{6}$ m^{3}	$14.78*10^{6}$ m^{3}
	Kapitsa et al. (2017)	Tien Shan (n: 32)	$V = 0.036A^{1.49}$	0.88	$-5.43*10^{6}$ m^{3}	$10.91*10^{6}$ m^{3}
	Muñoz et al. (2020)	Peruvian Andes (n: 121)	$V = A*Md\_Wi$	0.83	$-4.08*10^{6}$ m^{3}	$13.42*10^{6}$ m^{3}
	Zhang et al. (2023)	HKH	$V = 42.95A^{1.4082}$	0.96	$0.71*10^{6}$ m^{3}	$7.16*10^{6}$ m^{3}

* where, UI stand for upper Indus, UG for upper Ganga, UB for upper Brahmaputra, UIGB for upper Indus-Ganga-Brahmaputra, CH for central Himalaya, and EH for eastern Himalaya

Furthermore, it is important to mention here that equations developed in the present study specifically focus on upper IGB basins (HKH). While effective within this geographic context, applying these equations in other areas, particularly those with different geological structures or lake morphologies, may yield to less accurate results. For example, development of glacial lakes in upper IGB is significantly influenced by steep side slopes, and monsoon-driven hydrology, whereas, glacial lakes in the arid or polar climates may exhibit different morphological and hydrological behaviour **(Yao et al., 2018)**. Therefore, to adapt these equations to new settings, it would be essential to recalibrate parameters using localized data or conduct validation studies that consider specific geological and hydrological factors of the target region. Such recalibration could involve adjusting for factors like lake shape, turbidity levels, or parent glacier characteristics, ensuring greater accuracy in assessing glacial lake volume.

5.3 Impact of ongoing climate change

The swift melting of glaciers as a result of ongoing global warming stands out as the primary factor driving the expansion of glacial lakes in the HKH region **(Shugar et al., 2020; Zhang et al., 2024)**. **Krishnan et al. (2019)** indicate that the annual mean temperature in the HKH region increased by 0.1°C per decade from 1901 to 2014, with projections suggesting an accelerated increase in the future. The glaciers, particularly in the central and eastern Himalaya, are receding at a concerning pace as a result of a consistent rise in regional temperatures **(Wester et al., 2019)**. In contrast, most glaciers of the Karakoram region exhibited stable mass balance **(Azam et al., 2018)**. The differing responses of glaciers are influencing significant alterations in the creation, growth, and deepening of glacial lakes **(Nie et al., 2017; Bolch et al., 2019)**. Considering these changes, empirical equations obtained from area scaling methods—developed through both literature-based approaches and primary bathymetric surveys—provide useful tools for estimating lake depth and volume **(Shugar et al., 2020; Qi et al., 2022)**. Nonetheless, the current variability in climate change prompts enquiries regarding the enduring relevance of these equations, especially as glacial lakes transform due to increased glacier melting, sediment dynamics, and the instability of moraine dams.

The area-scaling method typically employed to formulate these empirical equations relies on the premise that a consistent positive relationship exists among area, depth, and volume **(Huggel et al., 2002; Cook and Quincey, 2015)**. Nonetheless, these relationships may experience considerable variability, primarily influenced by the connection with parent glaciers **(Cook and Quincey, 2015)**. The ongoing climate change can lead to an increase in the number of glacial lakes, which exhibit a highly unpredictable relationship between area and depth/volume **(Zhang et al., 2023)**. Consequently, we recommend ongoing monitoring of glacial lakes and the execution of additional bathymetric surveys for specific lakes at regular intervals to enhance our understanding of the evolving relationships between area, depth, and volume. This will aid in the formulation of a revised empirical equation that considers these on-going variabilities in the relationship between area and depth/volume.

6. Conclusion

The present study developed empirical equations to estimate the mean depth (m) and volume (km^3) of glacial lakes in the upper IGB basins. Equation 4 (mean depth) and equation 8 (volume) proved to be the most accurate, reflecting strong correlations with observed data. These equations provide an effective tool for assessing glacial lake characteristics, particularly for the moraine-dammed lakes, which form the majority of the lakes used for developing the equations. The study's findings hold significant value for the scientific community and stakeholders engaged in glacial lake hazards assessments, particularly in regions vulnerable to GLOFs. The developed empirical equations can be instrumental for rapid and reliable estimation of lake depth and volume, offering practical applications for climate change adaptation and risk mitigation strategies in the upper IGB region. By facilitating early assessments, these methods can support disaster preparedness and policy-making efforts in managing potential hazards from glacial lakes.

However, the study also has certain limitations. The empirical equations were developed solely on glacial lakes in the upper IGB region, and their applicability to other mountainous regions remains untested. Lack of field-based data for ice-dammed lakes and supraglacial lakes may introduce uncertainties, especially in the estimation of mean depth and volume. Finally, future research should (i) aim to validate these empirical equations in other mountain ranges (such as the Alps, Andes, or Rocky Mountains); (ii) apply the equations in generating GLOF scenarios; and (iii) assist in the development of early warning systems (EWS) for GLOFs.

Acknowledgement:

This work is supported by doctoral research grant provided by German Academic Exchange Service (DAAD) (funding ID: 57507871). The authors are thankful towards United States Geological Survey (USGS) for providing free access to the Landsat satellite imagery. The authors also acknowledge the vital contribution of porters and guides for their assistance during the collection of in-situ based bathymetry.

Data Availability

The complete glacial lake inventory is available at https://doi.org/10.5281/zenodo.14192205.

References

Ahmed, R., Wani, G. F., Ahmad, S. T., Sahana, M., Singh, H., & Ahmed, P. (2021). A review of glacial lake expansion and associated glacial lake outburst floods in the Himalayan region. *Earth Systems and Environment*, *5*(3), 695-708. https://doi.org/10.1007/s41748-021-00230-9

Allen, S. K., Zhang, G., Wang, W., Yao, T., & Bolch, T. (2019). Potentially dangerous glacial lakes across the Tibetan Plateau revealed using a large-scale automated assessment approach. *Science Bulletin*, *64*(7), 435-445. https://doi.org/10.1016/j.scib.2019.03.011

Allen, S. K., Rastner, P., Arora, M., Huggel, C., & Stoffel, M. (2016). Lake outburst and debris flow disaster at Kedarnath, June 2013: hydrometeorological triggering and topographic predisposition. *Landslides*, *13*, 1479-1491. https://doi.org/10.1007/s10346-015-0584-3

Armon, M., Dente, E., Shmilovitz, Y., Mushkin, A., Cohen, T. J., Morin, E., & Enzel, Y. (2020). Determining bathymetry of shallow and ephemeral desert lakes using satellite imagery and altimetry. *Geophysical Research Letters*, *47*(7). https://doi.org/10.1029/2020GL087367

Azam, M. F., Wagnon, P., Berthier, E., Vincent, C., Fujita, K., & Kargel, J. S. (2018). Review of the status and mass changes of Himalayan-Karakoram glaciers. *Journal of Glaciology*, *64*(243), 61-74. https://doi.org/10.1017/jog.2017.86

Bajracharya, S. R., Maharjan, S. B., & Shrestha, F. (2014). The status and decadal change of glaciers in Bhutan from the 1980s to 2010 based on satellite data. *Annals of Glaciology*, 55(66), 159–166. https://doi.org/10.3189/2014AoG66A125

Barry, R. G. (2011). The cryosphere–past, present, and future: a review of the frozen water resources of the world. *Polar Geography*, *34*(4), 219-227.

Basnett, S., Kulkarni, A. V., & Bolch, T. (2013). The influence of debris cover and glacial lakes on the recession of glaciers in Sikkim Himalaya, India. *Journal of Glaciology*, 59(218), 1035–1046. https://doi.org/10.3189/2013JoG12J184

Bhambri, R., Bolch, T., Chaujar, R. K., & Kulshreshtha, S. C. (2011). Glacier changes in the Garhwal Himalayas, India, from 1968 to 2006 based on remote sensing. *Journal of Glaciology*, 57(203), 543–556. https://doi.org/10.3189/002214311796905604

Bolch, T., Pieczonka, T., & Benn, D. I. (2011a). Multi-decadal mass loss of glaciers in the Everest area (Nepal Himalaya) derived from stereo imagery. *The Cryosphere*, 5(2), 349–358. https://doi.org/10.5194/tc-5-349-2011

Bolch, T., Peters, J., Yegorov, A., Pradhan, B., Buchroithner, M., & Blagoveshchensky, V. (2011b). Identification of potentially dangerous glacial lakes in the northern Tien Shan. *Natural Hazards*, *59*, 1691-1714. https://doi.org/10.1007/s11069-011-9860-2

Carlin, B. P., & Louis, T. A. (2008). *Bayesian methods for data analysis*. CRC press.

Carrivick, J. L. (2010). Modelling glacier lake outburst floods from moraine-dammed glacial lakes. *Geomorphology*, 120(3–4), 267–287. DOI: 10.1016/j.geomorph.2010.03.002

Cook, S. J., & Quincey, D. J. (2015). Estimating the volume of Alpine glacial lakes. *Earth Surface Dynamics*, *3*(4), 559-575. https://doi.org/10.5194/esurf-3-559-2015

Cook, K. L., Andermann, C., Gimbert, F., Adhikari, B. R., & Hovius, N. (2018). Glacial lake outburst floods as drivers of fluvial erosion in the Himalaya. *Science*, *362*(6410), 53-57. https://doi.org/10.1126/science.aat4981

Dahal, D.R., Mehta, M., Bhatt, C.M., Luirei, K. (2024) Flash floods and its cascading tumult: An example from Teesta River valley, Eastern Himalaya, Sikkim. Current Science 126 (10), 1280-1284.

Deswal, S., Sharma, M. C., Saini, R., Dalal, P., & Kumar, P. (2020). Preliminary results of hybrid bathymetry and GLOF risk assessment for Neelkanth lake, Lahaul Himalaya, India. *CURRENT SCIENCE*, *119*(9), 1555.

Dimri, A. P., Niyogi, D., Barros, A. P., Ridley, J., Mohanty, U. C., Yasunari, T., & Sikka, D. R. (2015). Western disturbances: a review. Reviews of Geophysics, 53(2), 225-246. https://doi.org/10.1002/2014RG000460

Dubey, S., & Goyal, M. K. (2020). Glacial lake outburst flood hazard, downstream impact, and risk over the Indian Himalayas. *Water Resources Research*, *56*(4). https://doi.org/10.1029/2019WR026533

Emmer, A., & Cochachin, A. (2013). The causes and mechanisms of moraine-dammed lake failures in the Cordillera Blanca, North American Cordillera, and Himalayas. *AUC GEOGRAPHICA*, *48*(2), 5-15. https://doi.org/10.14712/23361980.2014.23

Evans, S. G. (1986). The maximum discharge of outburst floods caused by the breaching of man-made and natural dams. *Canadian Geotechnical Journal*, *23*(3), 385-387.

Evans, S. G., Delaney, K. B., Hermanns, R. L., & Strom, A. (2009). The formation and failure of natural dams. In *Natural and Artificial Rockslide Dams* (pp. 7–34). Springer. DOI: 10.1007/978-3-642-04764-0_2

Fujita, K., & Nuimura, T. (2011**).** Spatially heterogeneous wastage of Himalayan glaciers. *Proceedings of the National Academy of Sciences*, 108(34), 14011–14014. https://doi.org/10.1073/pnas.1106242108Fisher, M., Chowdhury, M. N., Khan, A. A., & Atamturktur, S. (2013). An evaluation of scour measurement devices. *Flow Measurement and Instrumentation*, *33*, 55-67. https://doi.org/10.1016/j.flowmeasinst.2013.05.001

Fujita, K., Sakai, A., Takenaka, S., Nuimura, T., Surazakov, A. B., Sawagaki, T., & Yamanokuchi, T. (2013). Potential flood volume of Himalayan glacial lakes. *Natural Hazards and Earth System Sciences*, *13*(7), 1827-1839. https://doi.org/10.5194/nhess-13-1827-2013

Gantayat, P., Sattar, A., Haritashya, U. K., Watson, C. S., & Kargel, J. S. (2024). Bayesian Approach to Estimate Proglacial Lake Volume (BE-GLAV). *Earth and Space Science*, *11*(6), e2024EA003542.

Gardelle, J., Berthier, E., & Arnaud, Y. (2012). Slight mass gain of Karakoram glaciers in the early twenty-first century. *Nature Geoscience*, 5(5), 322–325. https://doi.org/10.1038/ngeo1450

Gardelle, J., Berthier, E., Arnaud, Y., & Kääb, A. (2013). Region-wide glacier mass balances over the Pamir-Karakoram-Himalaya during 1999–2011. *The Cryosphere*, *7*(4), 1263-1286.

Gelman, A., & Shalizi, C. R. (2013). Philosophy and the practice of Bayesian statistics. *British Journal of Mathematical and Statistical Psychology*, *66*(1), 8-38. https://doi.org/10.1111/j.2044-8317.2011.02037.x

Ghimire, S., Choudhary, A., & Dimri, A. P. (2018). Assessment of the performance of CORDEX-South Asia experiments for monsoonal precipitation over the Himalayan region during present climate: part I. Climate dynamics, 50, 2311-2334. https://doi.org/10.1007/s00382-015-2747-2

Harrison, S., Kargel, J. S., Huggel, C., Reynolds, J., Shugar, D. H., Betts, R. A., ... & Vilímek, V. (2018). Climate change and the global pattern of moraine-dammed glacial lake outburst floods. *The Cryosphere*, *12*(4), 1195-1209. https://doi.org/10.5194/tc-12-1195-2018

Hock, R., G. Rasul, C. Adler, B. Cáceres, S. Gruber, Y. Hirabayashi, M. Jackson, A. Kääb, S. Kang, S. Kutuzov, Al. Milner, U. Molau, S. Morin, B. Orlove, and H. Steltzer, 2019: High Mountain Areas. In: IPCC Special Report on the Ocean and Cryosphere in a Changing Climate [H.-O. Pörtner, D.C. Roberts, V. Masson-Delmotte, P. Zhai, M. Tignor, E. Poloczanska, K. Mintenbeck, A. Alegría, M. Nicolai, A. Okem, J. Petzold, B. Rama, N.M. Weyer (eds.)]. Cambridge University Press, Cambridge, UK and New York, NY, USA, pp. 131–202. https://doi.org/10.1017/9781009157964.004

Hordyniec, P., Kapłon, J., Rohm, W., & Kryza, M. (2018). Residuals of tropospheric delays from GNSS data and ray-tracing as a potential indicator of rain and clouds. *Remote Sensing*, *10*(12), 1917. https://doi.org/10.3390/rs10121917

Huettmann, F., Regmi, G.R. (2020). Mountain Landscapes and Watersheds of the Hindu Kush-Himalaya (HKH) and Their Biogeography: A Descriptive Overview and Introduction for 18 Nations in the Anthropocene. In: Regmi, G., Huettmann, F. (eds) Hindu Kush-Himalaya Watersheds Downhill: Landscape Ecology and Conservation Perspectives. Springer, Cham. https://doi.org/10.1007/978-3-030-36275-1_1

Huggel, C., Kääb, A., Haeberli, W., Teysseire, P., & Paul, F. (2002). Remote sensing based assessment of hazards from glacier lake outbursts: a case study in the Swiss Alps. *Canadian Geotechnical Journal*, *39*(2), 316-330.

Huggel, C. et al. (Ed.). (2015). *The high-mountain cryosphere*. Cambridge University Press.

Islam, S. T., Dar, S. A., Sofi, M. S., Bhat, S. U., Sabha, I., Hamid, A., ... & Bhat, A. A. (2021). Limnochemistry and Plankton diversity in some high altitude lakes of Kashmir Himalaya. *Frontiers in Environmental Science*, 387.

Kapitsa, V., Shahgedanova, M., Machguth, H., Severskiy, I., & Medeu, A. (2017). Assessment of evolution and risks of glacier lake outbursts in the Djungarskiy Alatau, Central Asia, using Landsat imagery and glacier bed topography modelling. *Natural Hazards and Earth System Sciences*, *17*(10), 1837-1856. https://doi.org/10.5194/nhess-17-1837-2017

Kapitsa, V., Shahgedanova, M., Kasatkin, N., Severskiy, I., Kasenov, M., Yegorov, A., & Tatkova, M. (2023). Bathymetries of proglacial lakes: a new data set from the northern Tien Shan, Kazakhstan. *Frontiers in Earth Science*, *11*. https://doi.org/10.3389/feart.2023.1192719

Kandel, S., Khadka, N., Tiwari, D., Shrestha, D., & Rijal, K. (2023). Evolution and bathymetry of glacial lake at the lowest elevation in Nepal Himalaya. *Journal of Mountain Science*, *20*(1), 141-144. https://doi.org/10.1007/s11629-022-7615-z

Kerschner, H., & Ivy-Ochs, S. (2008). Palaeoclimate from glaciers: Examples from the Eastern Alps during the Alpine Lateglacial and early Holocene. *Global and Planetary Change*, *60*(1-2), 58-71.

Krishnan, R., Shrestha, A. B., Ren, G., Rajbhandari, R., Saeed, S., Sanjay, J., ... & Ren, Y. (2019). Unravelling climate change in the Hindu Kush Himalaya: rapid warming in the mountains and increasing extremes. *The Hindu Kush Himalaya assessment: Mountains, climate change, sustainability and people*, 57-97.

Kumar, V, Mehta, M and Shukla, T (2021) Spatially resolved estimates of glacial retreat and lake changes from Gepang Gath Glacier, Chandra Basin, Western Himalaya, India. Journal of Geological Society of India, 97, 520-526.

Kumar, A., Mal, S., Schickhoff, U., and Dimri, A., P. (2024) Basin-scale spatio-temporal development of glacial lakes in the Hindukush-Karakoram-Himalayas, *Global and Planetary Change*, 245, 104656. https://doi.org/10.1016/j.gloplacha.2024.104656.

Küçük, C., & Sarp, G. (2021). Evaluation of formation mechanism of lakes in terms of morphometric aspect; lakes region and their vicinity, SW of Turkey. *Episodes Journal of International Geoscience*, *44*(3), 285-297.

Li, W., Wang, W., Gao, X., Wang, X., & Wang, R. (2022). Inventory and Spatiotemporal Patterns of Glacial Lakes in the HKH-TMHA Region from 1990 to 2020. Remote Sensing, 14(6), 1351.

Liu, K., & Song, C. (2022). Modeling lake bathymetry and water storage from DEM data constrained by limited underwater surveys. Journal of Hydrology, 604, 127260. https://doi.org/10.1016/j.jhydrol.2021.127260

Liu, K., Song, C., Zhao, S., Wang, J., Chen, T., Zhan, P., ... & Zhu, J. (2024). Mapping inundated bathymetry for estimating lake water storage changes from SRTM DEM: A global investigation. *Remote Sensing of Environment*, *301*, 113960. https://doi.org/10.1016/j.rse.2023.113960

Luo, W., Zhang, G., Chen, W., & Xu, F. (2020). Response of glacial lakes to glacier and climate changes in the western Nyainqentanglha range. *Science of The Total Environment*, *735*, 139607. https://doi.org/10.1016/j.scitotenv.2020.139607

Ma, J., Song, C., & Wang, Y. (2021). Spatially and Temporally Resolved Monitoring of Glacial Lake Changes in Alps During the Recent Two Decades. *Frontiers in Earth Science*, *9*, 723386.

Maharjan, S. B., Mool, P. K., Lizong, W., Xiao, G., Shrestha, F., Shrestha, R. B., ... & Baral, P. (2018). The Status of Glacial Lakes in the Hindu Kush Himalaya-ICIMOD Research Report 2018/1. International Centre for Integrated Mountain Development (ICIMOD).

Mal, S., & Singh, R. B. (2014). Changing glacial lakes and associated outburst floods risks in Nanda Devi Biosphere Reserve, Indian Himalaya. *Proceedings of the International Association of Hydrological Sciences*, *364*, 255-260. https://doi.org/10.5194/piahs-364-255-2014

Mal, S., Allen, S. K., Frey, H., Huggel, C., & Dimri, A. P. (2021). Sectorwise assessment of glacial lake outburst flood danger in the Indian Himalayan region. Mountain Research and Development, 41(1), R1. https://doi.org/10.1659/MRD-JOURNAL-D-20-00043.1

McElreath, R. (2018). *Statistical rethinking: A Bayesian course with examples in R and Stan*. Chapman and Hall/CRC.

Mehta, M., Shukla, T., Bhambri, R., Gupta, A. K., Dobhal, D. P. (2017). Terrain changes, caused by the 15-17 June 2013 heavy rainfall in the Garhwal Himalaya, India: A case study of Alaknanda and Mandakini basins, Geomorphology, 284, 53-71.

Muñoz, R., Huggel, C., Frey, H., Cochachin, A., & Haeberli, W. (2020). Glacial lake depth and volume estimation based on a large bathymetric dataset from the Cordillera Blanca, Peru. *Earth surface processes and landforms*, *45*(7), 1510-1527. https://doi.org/10.1002/esp.4826

Nie, Y., Sheng, Y., Liu, Q., Liu, L., Liu, S., Zhang, Y., & Song, C. (2017). A regional-scale assessment of Himalayan glacial lake changes using satellite observations from 1990 to 2015. *Remote Sensing of Environment*, *189*, 1-13. https://doi.org/10.1016/j.rse.2016.11.008

Ng, F., & Liu, S. (2009). Temporal dynamics of a jökulhlaup system. *Journal of Glaciology*, 55(191), 651–663. DOI: 10.3189/002214309789470897

O'Connor, J. E., Hardison, J. H., & Costa, J. E. (2001). *Debris flows from failures of Neoglacial-age moraine dams in the Three Sisters and Mount Jefferson Wilderness areas, Oregon* (No. 1606). US Geological Survey.

Pandey, P., Ali, S. N., & Champati Ray, P. K. (2021). Glacier-glacial lake interactions and glacial lake development in the central Himalaya, India (1994–2017). *Journal of Earth Science*, 1-12. https://doi.org/10.1007/s12583-020-1056-9

Panigrahy, S., Patel, J. G., & Parihar, J. S. (2012). National Wetland Atlas: high altitude lakes of India. *Space Applications Centre, ISRO, Ahmedabad, India*.

Patel, L. K., Sharma, P., Laluraj, C. M., Thamban, M., Singh, A., & Ravindra, R. (2017). A geospatial analysis of Samudra Tapu and Gepang Gath glacial lakes in the Chandra Basin, Western Himalaya. *Natural Hazards*, *86*, 1275-1290. https://doi.org/10.1007/s11069-017-2743-4

Qi, M., Liu, S., Wu, K., Zhu, Y., Xie, F., Jin, H., ... & Yao, X. (2022). Improving the accuracy of glacial lake volume estimation: A case study in the Poiqu basin, central Himalayas. *Journal of Hydrology*, *610*, 127973. https://doi.org/10.1016/j.jhydrol.2022.127973

Randhawa, S. S., Thakur, N., Sharma, P., & Rana, K. (2020). Glacial lake outburst floods (GLOFs): A case Study of Geepang Gath Glacial Lake, Lahul & Spiti and Chamba Districts, Himachal Pradesh.

Rounce, D. R., Watson, C. S., & McKinney, D. C. (2017). Identification of hazard and risk for glacial lakes in the Nepal Himalaya using satellite imagery from 2000–2015. *Remote Sensing*, *9*(7), 654. https://doi.org/10.3390/rs9070654

Sakai, A. (2012). Glacial lakes in the Himalayas: a review on formation and expansion processes. *Global Environmental Research*, *16*(2011), 23-30.

Schickhoff, U., Bobrowski, M., Mal, S., Schwab, N., & Singh, R.B. (2022). The world's mountains in the Anthropocene. In: Schickhoff, U., Singh, R.B., & Mal, S, (eds,): Mountain landscapes in transition: effects of land use and climate change. Springer, Cham, pp 1-144.

Sharma, C. M., Sharma, S., Bajracharya, R. M., Gurung, S., Jüttner, I., Kang, S., ... & Li, Q. (2012). First results on bathymetry and limnology of high-altitude lakes in the Gokyo Valley, Sagarmatha (Everest) National Park, Nepal. *Limnology*, *13*, 181-192.

Sharma, E., Molden, D., Rahman, A., Khatiwada, Y. R., Zhang, L., Singh, S. P., ... & Wester, P. (2019). Introduction to the hindu kush himalaya assessment. *The Hindu Kush Himalaya Assessment: mountains, climate change, sustainability and people*, 1-16.

Sharma, R. K., Pradhan, P., Sharma, N. P., & Shrestha, D. G. (2018). Remote sensing and in situ-based assessment of rapidly growing South Lhonak glacial lake in eastern Himalaya, India. *Natural Hazards*, *93*, 393-409. https://doi.org/10.1007/s11069-018-3305-0

Shean, D. E., Bhushan, S., Montesano, P., Rounce, D. R., Arendt, A., & Osmanoglu, B. (2020). A systematic, regional assessment of high mountain Asia glacier mass balance. *Frontiers in Earth Science*, *7*, 363.

Singh, P., & Kumar, N. (1997). Effect of orography on precipitation in the western Himalayan region. Journal of Hydrology, 199(1-2), 183-206. https://doi.org/10.1016/S0022-1694(96)03222-2

Somos-Valenzuela, M. A., McKinney, D. C., Byers, A. C., Rounce, D. R., & Portocarrero, C. (2013). *Modeling Mitigation Strategies for Risk Reduction at Imja Lake, Nepal*. Center for Research in Water Resources, University of Texas at Austin.

Shugar, D. H., Burr, A., Haritashya, U. K., Kargel, J. S., Watson, C. S., Kennedy, M. C., ... & Strattman, K. (2020). Rapid worldwide growth of glacial lakes since 1990. *Nature Climate Change*, *10*(10), 939-945. https://doi.org/10.1038/s41558-020-0855-4

Steffen, T., Huss, M., Estermann, R., Hodel, E., & Farinotti, D. (2022). Volume, evolution, and sedimentation of future glacier lakes in Switzerland over the 21st century. *Earth Surface Dynamics*, *10*(4), 723-741. https://doi.org/10.5194/esurf-10-723-2022

Saylam, K., Brown, R. A., & Hupp, J. R. (2017). Assessment of depth and turbidity with airborne Lidar bathymetry and multiband satellite imagery in shallow water bodies of the Alaskan North Slope. *International journal of applied earth observation and geoinformation*, *58*, 191-200. https://doi.org/10.1016/j.jag.2017.02.012

Singh, N., Solanki, R., Ojha, N., Naja, M., Dumka, U. C., Phanikumar, D. V., ... & Dhaka, S. K. (2016). Variations in the cloud-base height over the central Himalayas during GVAX: association with the monsoon rainfall. *Current Science*, 109-116.

Taylor, C., Robinson, T. R., Dunning, S., Rachel Carr, J., & Westoby, M. (2023). Glacial lake outburst floods threaten millions globally. *Nature Communications*, *14*(1), 487. https://doi.org/10.1038/s41467-023-36033-x

Veh, G., Korup, O., von Specht, S., Roessner, S., & Walz, A. (2019). Unchanged frequency of moraine-dammed glacial lake outburst floods in the Himalaya. *Nature Climate Change*, *9*(5), 379-383. https://doi.org/10.1038/s41558-019-0437-5

Veh, G., Korup, O., & Walz, A. (2020). Hazard from Himalayan glacier lake outburst floods. *Proceedings of the National Academy of Sciences*, *117*(2), 907-912. https://doi.org/10.1073/pnas.1914898117

Wackerly, D. D., Mendenhall, W., & Scheaffer, R. L. (2008). *Mathematical statistics with applications* (Vol. 7). Belmont, CA: Thomson Brooks/Cole.

Wang, W., Xiang, Y., Gao, Y., Lu, A., & Yao, T. (2015). Rapid expansion of glacial lakes caused by climate and glacier retreat in the Central Himalayas. *Hydrological Processes*, *29*(6), 859-874. https://doi.org/10.1002/hyp.10199

Wang, X., Guo, X., Yang, C., Liu, Q., Wei, J., Zhang, Y., ... & Tang, Z. (2020). Glacial lake inventory of high-mountain Asia in 1990 and 2018 derived from Landsat images. *Earth System Science Data*, *12*(3), 2169-2182. https://doi.org/10.5194/essd-12-2169-2020, 2020

Wester, P., Mishra, A., Mukherji, A., & Shrestha, A. B. (2019). *The Hindu Kush Himalaya assessment: mountains, climate change, sustainability and people* (p. 627). Springer Nature.

Worni, R., Huggel, C., & Stoffel, M. (2013). Glacial lakes in the Indian Himalayas—From an area-wide glacial lake inventory to on-site and modeling based risk assessment of critical glacial lakes. *Science of the Total Environment*, *468*, S71-S84. https://doi.org/10.1016/j.scitotenv.2012.11.043

Xu, X., Wang, W., Huang, D., Hu, X., & Fu, W. (2023). Assessment of interannual and seasonal glacier mass changes in the Karakoram during 2018–2022 using ICESat-2 data. *Journal of Hydrology*, *626*, 130223.

Yao, X., Liu, S., Sun, M., Wei, J., & Guo, W. (2012). Volume calculation and analysis of the changes in moraine-dammed lakes in the north Himalaya: a case study of Longbasaba lake. *Journal of Glaciology*, *58*(210), 753-760.

Yao, X., Liu, S., Han, L., Sun, M., & Zhao, L. (2018). Definition and classification system of glacial lake for inventory and hazards study. *Journal of Geographical Sciences*, *28*, 193-205. https://doi.org/10.1007/s11442-018-1467-z

Zhang, G., Yao, T., Xie, H., Wang, W., & Yang, W. (2015). An inventory of glacial lakes in the Third Pole region and their changes in response to global warming. *Global and Planetary Change*, *131*, 148-157. https://doi.org/10.1016/j.gloplacha.2015.05.013Zhang, G., Bolch, T., Chen, W., & Crétaux, J. F. (2021). Comprehensive estimation of lake volume changes on the Tibetan Plateau during 1976–2019 and basin-wide glacier contribution. *Science of the Total Environment*, *772*, 145463. https://doi.org/10.1016/j.scitotenv.2021.145463

Zhang, G., Bolch, T., Yao, T., Rounce, D. R., Chen, W., Veh, G., ... & Wang, W. (2023). Underestimated mass loss from lake-terminating glaciers in the greater Himalaya. *Nature Geoscience*, *16*(4), 333-338. https://doi.org/10.1038/s41561-023-01150-1

Zhang, M., Chen, F., Zhao, H., Wang, J., & Wang, N. (2021). Recent changes of glacial lakes in the high mountain asia and its potential controlling factors analysis. *Remote Sensing*, *13*(18), 3757. https://doi.org/10.3390/rs13183757

Zhang, T., Wang, W., Gao, T., An, B., & Yao, T. (2022). An integrative method for identifying potentially dangerous glacial lakes in the Himalayas. *Science of the total Environment*, *806*, 150442. https://doi.org/10.1016/j.scitotenv.2021.150442

Zhang, T., Wang, W., & An, B. (2023). A conceptual model for glacial lake bathymetric distribution. *The Cryosphere Discussions*, *2023*, 1-35. https://doi.org/10.5194/tc-17-5137-2023

Zheng, G., Allen, S. K., Bao, A., Ballesteros-Cánovas, J. A., Huss, M., Zhang, G., ... & Stoffel, M. (2021). Increasing risk of glacial lake outburst floods from future Third Pole deglaciation. Nature Climate Change, 11(5), 411-417.

Article III

Kumar, A., Mal, S., Schickhoff, U., & Sreekesh, S. (2024). Glacial Lake Dynamics in Dibang Valley District, Arunachal Pradesh, Eastern Himalaya. *Journal Of The Geological Society Of India*, *100*(11), 1521-1530.4.4. doi: https://doi.org/10.17491/jgsi/2024/174012

Jour. Geol. Soc. India (2024) 100 (11) : 1521-1530
https://doi.org/10.17491/jgsi/2024/174012

RESEARCH ARTICLE

Glacial Lake Dynamics in Dibang Valley District, Arunachal Pradesh, Eastern Himalaya

Atul Kumar[1*], Suraj Mal[2], Udo Schickhoff[1] and S. Sreekesh[2]
[1]CEN Center for Earth System Research and Sustainability, Institute of Geography, University of Hamburg, Germany
[2]Center for Study of Regional Development, Jawaharlal Nehru University, Delhi, India
***E-mail:** *atul.sbsc@gmail.com*

Received: 19 October 2023 / Revised form Accepted: 6 December 2023

ABSTRACT

Glacial lakes (GLs) are integral components of the cryospheric environment. Due to the persistent melting of glaciers and steady rise in the annual mean temperatures, GLs are expanding across the Himalayan mountains. Since the 1980s, the eastern Himalaya have observed a steady increase (0.031°C/year) in annual mean temperature, causing rapid glacial melting, formation of new GLs and expansion of existing ones. Therefore, to assess the role of the increasing annual mean temperature on the expansion of GLs in the eastern Himalaya, we generated GL inventories for 1987, 2005 and 2018 for Dibang Valley district, Arunachal Pradesh, in the eastern Himalaya. We used Landsat multi-temporal satellite images along with the ASTER Digital Elevation Model V2 (DEM). Using the Segment Mean Shift (SMS) method, the GL inventories were generated. Our results show that there were 509 GLs in 2018, whereas only 484 in 2005 and 469 in 1987. GLs observed a growth rate of 8.52% in number and 11.13% in area between 1987 and 2018. Most of the GLs in the study area were of Moraine-dammed lakes (MDL) (~56%), whereas Ice-dammed lakes (IDL) showed the highest expansion rate between 1987 to 2018. GL hotspots show a concentration of GLs in the eastern and southern sections of Dibang Valley but new GLs are forming in the north-western and eastern sections of the study area. An increase in annual mean temperature enhanced the glacial melt water, leading to the growth of GLs connected with the glaciers.

Keywords: Glacial lakes, Dibang Valley, Climate Change, Himalaya

INTRODUCTION

Glacial lakes (GLs) are a critical element of the mountain hydrosphere and play a crucial role as a storehouse of freshwater (Wilson et al., 2018, Kaushik et al., 2020). These GLs generally develop on/below and in the forefields of glaciers, mainly because of glacial dynamics and meltwater accumulation in depressions created by glaciers (Yao et al., 2018). The ongoing increase in mean air temperature (0.2°C/decade) between 1951 and 2014 (Kulkarni et al., 2020; Dimri et al., 2021) caused the emergence of new GLs and enlargement of existing ones (Bolch et al., 2012; Nie et al., 2017; Shugar et al., 2020). Consequently, the number, area and volume of GLs therein have increased substantially in the last decades (Ives et al., 2010; Zhang et al., 2015; Nie et al., 2017). Their results, however, are significantly different due to the differences in methodologies and databases employed (Mal et al., 2020). For instance, Zhang et al. (2015) mapped 2,247 (≥0.003 km^2) GLs in Brahmaputra basin, Nie et al. (2017) 1,552 (≥0.0081 km^2) in eastern Himalaya, Maharjan et al. (2018) 13,642 (≥0.003 km^2) in Brahmaputra basin, Li et al. (2022) 3,115 (≥0.0036 km^2) GLs. Mal et al. (2020) mapped 1,532 GLs in Arunachal Pradesh using Landsat 8 satellite images (2018), which is the second-highest number of GLs among the Indian Himalayan states. Furthermore, the density of GLs is relatively higher in the eastern part of the Himalaya as compared to the western and central Himalayan regions (Gardelle et al., 2011; Nie et al., 2017). Nie et al. (2017) inferred glacial lakes expanded at the rate of ~11% between 1990 to 2010, while Li et al. (2022) estimated that the expansion rate was ~31% between 1990 and 2020 in the eastern Himalayan region.

A large number of these GLs are dammed by unconsolidated and fragile moraines, making these lakes ephemeral and susceptible to breaching (Richardson and Reymolds, 2000; Worni et al., 2013, Maharjan et al., 2018, Kaushik et al., 2020). Dam failure due to triggering events such as moraine degradation, ice/rock avalanches, rock fall, heavy precipitation, earthquakes, etc., causes abrupt release of water from these GLs and entrained debris material, can lead to Glacial Lake Outburst Flood (GLOF) in the lower reaches, where populations and infrastructure are unprepared to cope up (Bajracharya and Mool, 2009; Ives et al., 2010; Aggarwal et al., 2017). GLOF events are regarded as one of the most prominent cryospheric natural hazards in the Himalayan region (Nie et al., 2018, Veh et al., 2019), and have immense potential to cause damage to the environment and social and economic infrastructure in the GLOF's paths (Worni et al., 2014; Allen et al., 2016). Nie et al. (2018) identified 62 GLOF events in the Himalaya between 1935 and 2016, out of which 13 GLOFs occurred in the eastern Himalayan region. However, amid different methodologies and datasets used in the study, various studies have come up with different results related to potential GLOFs (Allen et al., 2019; Veh et al., 2020; Dimri et al., 2021; Mal et al., 2021; Zheng et al., 2021).

Continuous monitoring of GLs is, therefore, immensely important in the Himalaya, not only for a comprehensive view of regional GLOF mechanisms but also for disaster mitigation. It can further help in developing early warning systems for GLOF-prone regions in the Himalaya e.g., Nepal (Zheng et al., 2021). Remotely sensed satellite data play a pivotal role in monitoring and improving the understanding of GLs in the eastern Himalaya, as field-based surveys are difficult to conduct due to rugged topography and their remote locations (Raj and Kumar 2016; Aggarwal et al., 2017; Bhambri et al., 2018, 2019).

In the recent past, there have been several attempts to map and monitor the development of GLs for different parts of the Himalayan region (Worni et al., 2013, Zhang et al., 2015, Nie et al., 2017). There are few studies, which mapped GLs at the district level (Panigrahy et al., 2012, Mal et al., 2020). Panigrahy et al. (2012) mapped 1,672 (118.64 km^2) high-altitude lakes, which also included non-glacial lakes and the eastern Himalaya have the second highest distribution of GLs in the Indian Himalayan states. Mal et al. (2020) made the first attempt to prepare the first GL inventory for Arunachal Pradesh at the district level. However, the evolution of glacial lakes and changes in their densities are still missing in the study region in particular and in the eastern Himalaya in general.

Therefore, the objectives of the present study are (1) to develop a GL inventory using Landsat satellite images for Dibang Valley (DV) District; (2) to analyse GL dynamics and regional heterogeneity for three periods (i.e., 1987, 2005, and 2018; (3) to understand the clustering and concentration of GLs using point density function; and (4) to analyse the patterns of climate variables (i.e. precipitation and temperature) for better understanding of GL dynamics in DV District, Arunachal Pradesh, India, eastern Himalaya.

STUDY AREA

Dibang Valley lies between 28°35'36"N to 29°27'48"N latitude and 95°14'33"E to 96°36'56"E longitude (Fig. 1). DV is bounded by the Tibet Autonomous Region in the North and northeast, East Siang district in the west and Lower Dibang Valley in the South. DV is the largest district in the state of Arunachal Pradesh, with an area of 9,129 km^2 and has mountainous topography. The district's elevation varies from 629 m asl in the southern part to 5340 m asl in the northern and northeastern reaches. DV District is named after the river Dibang, a tributary of the Brahmaputra River, which is the main river in the region. It lies in the zone of heavy precipitation with an annual precipitation of about ~ 328 cm (CGWB, 2013). According to the census of India (2011), DV district is the least populated district of India with a total of 7,948 people.

MATERIAL AND METHODS

Satellite Data

To generate the GL inventory, we employed Landsat's Thematic Mapper (TM) and Operational Land Imager (OLI) along with ASTER DEM V2 (https://earthexplorer.usgs.gov/). Landsat satellite images were deliberately chosen because they are readily obtainable. Satellite images mainly from November and December with minimal cloud cover (Table 1) Bhambri et al., 2018; Mal et al., 2020) were used in the study.

Climate Data

The Asian Precipitation Highly Resolved Observation Data Integration Towards Evaluation (APHRODITE) (https://www.chikyu.ac.jp) mean annual temperature (1981 to 2015, version APHRO_TAVE_MA_V1801) and precipitation data were used to analyse the role of recent climate change on GL dynamics. We used the time frame of 1981 to 2015 to collect temperature and precipitation data because our GL inventory was temporally distributed between 1987 and 2018. APHRODITE's gridded precipitation and temperature products available at a spatial resolution of 0.25° were used. In the case of precipitation, two versions of data (for the period 1981 to 2006 version APHRO_MA_025deg_V1101 and for the period 2007 to 2015 version APHRO_MA_025deg_V1101_EXR1) were acquired from https://www.chikyu.ac.jp and used in the present study as it is based on high frequency of gauge data collected directly from the Indian Meteorological Department (IMD).

Glacial Lake Inventory

There have been several attempts to prepare GL inventories from

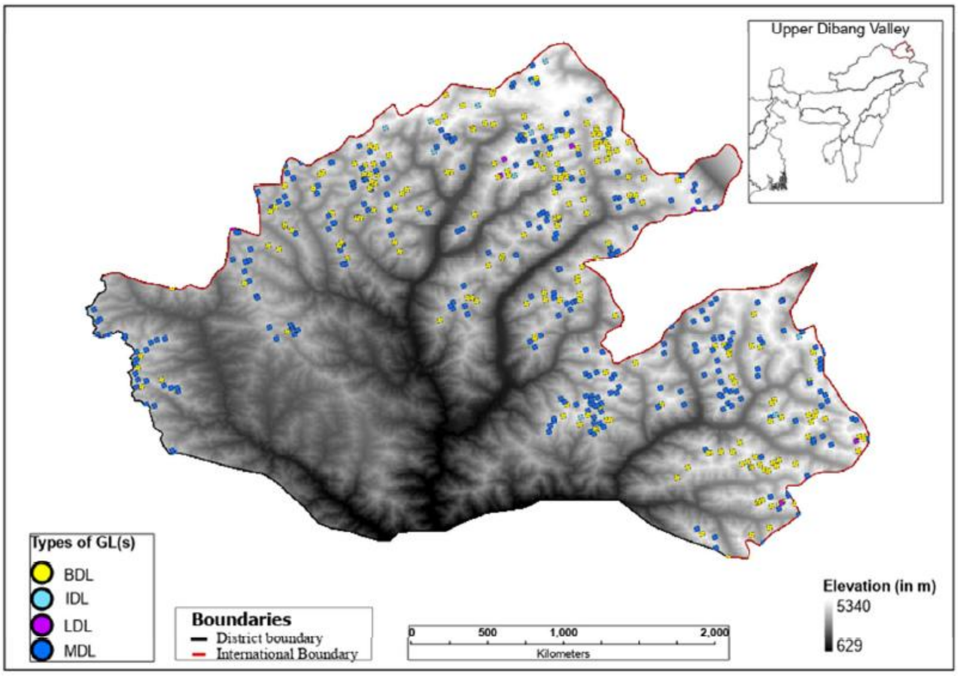

Fig. 1. Distribution of GLs in DV district, Arunachal Pradesh (2018), showing MDL (Moraine-dammed lakes), BDL (Bedrock-dammed lakes), IDL (Ice-dammed lakes) and LDL (Landslide-dammed lakes).

Table 1. List of Landsat satellite images used to prepare GL inventories.

Path and Row	Date	Cloud Cover (%)	Image ID
134/40	02-11-2019	<10	LC08_L1TP_134040_20191102_20191115_01_T1
135/40	22-11-2018	<10	LC08_L1TP_135040_20181122_20181129_01_T1
134/40	11-11-2005	<10	LT05_L1TP_134040_20051111_20161124_01_T1
135/40	17-12-2004	<10	LT05_L1TP_135040_20041217_20161129_01_T1
134/40	10-11-1987	<10	LT05_L1TP_134040_19871110_20170418_01_T1
135/40	03-12-1987	<10	LT05_L1TP_135040_19871203_20170210_01_T1

the micro scale to the macro scale using different data sources and methods (Bajracharya and Mool, 2009; Ukita et al., 2011; Worni et al., 2013; Aggarwal et al., 2017; Nie et al., 2017). Satellite datasets such as Landsat (Zhang et al., 2015; Nie et al., 2017; Maharjan et al., 2018), Indian Remote Sensing (IRS) (Prakash and Nagarajan, 2017), SPOT (Quincey et al., 2007; Nagai et al., 2017), Advanced Spaceborne Thermal Emission and Reflection Radiometer (ASTER) (Ukita et al., 2011; Tadono et al., 2012), and Sentinel 1 (Wangchuk et al., 2019; Zhang et al., 2019) have been widely used to develop GL inventories in the Himalaya. The methods used to map and generate inventories of GL based on satellite images can be generally classified into three categories:(a) Manual (Mal et al., 2020, Wang et al., 2020), (b) Semi-automated (Govindha Raj et al., 2013, Song et al., 2016); and (c) Automated (Li and Sheng et al., 2012; Wangchuk et al., 2019).

Manual mapping of GLs is a highly labour-intensive and time-consuming technique but with greater accuracy depending on the mapping skills (Aggarwal et al., 2017). To overcome these demerits researchers have developed semi-automated and automated methods for regional and global level studies. However, their results suffer from large uncertainties, hence requiring manual corrections. Semi-automated methods, in particular, are often preferred over both manual and automated methods given the time efficiency and hence the relatively better accuracy can be achieved. This study used a semi-automated method followed by manual corrections to map GLs (Fig. 2).

After calibrating the Landsat satellite images according to Top of Atmosphere (TOA) reflectance, the next step was to develop the semi-automated method to generate GL inventories for the years 1987, 2005 and 2018. In this process, the Segment Mean Shift (SMS) algorithm was applied using the image classification function in ArcGIS. SMS was initially developed for raster feature analysis (Fukunaga and Hosteler, 1975) and then further developed to identify image modes corresponding to similar raster features (Comaniciu and Meer, 2002). Consequently, different groups of pixels in the raster scene were generated to represent different surface features based on distinguishing spatial-spectral characteristics. The range of SMS function varies from 1 to 20, where values close to 1 indicate smoothened results, while close to 20 relate to sharpened results. Here, the threshold value of 15.5 was selected for better edge detection and mapping of every GL.

SMS can work on one raster characteristic at a time. In this case, we have used spectral characteristics of Landsat 8 images, which leads to false identification of glaciated and shadow regions as potential GLs. To overcome this problem, terrain analysis was employed using ASTER DEM V2. Based on DEM-derived gradient analysis, it has been found that generally, GLs have a surface gradient of less than 10°, while shadowed features in raster scenes are generally located in the darker part of the scene, where the reach of sunlight is least, making a surface gradient of shadowed region high (Li and Sheng; 2012). To solve this problem, slope and hill shade maps of the study area were produced. The slope map with a threshold of 10° was overlaid on the GLs to identify misclassified GLs. Finally, each lake was manually inspected with the help of Google Earth Pro for the final inventory of GLs for respective years.

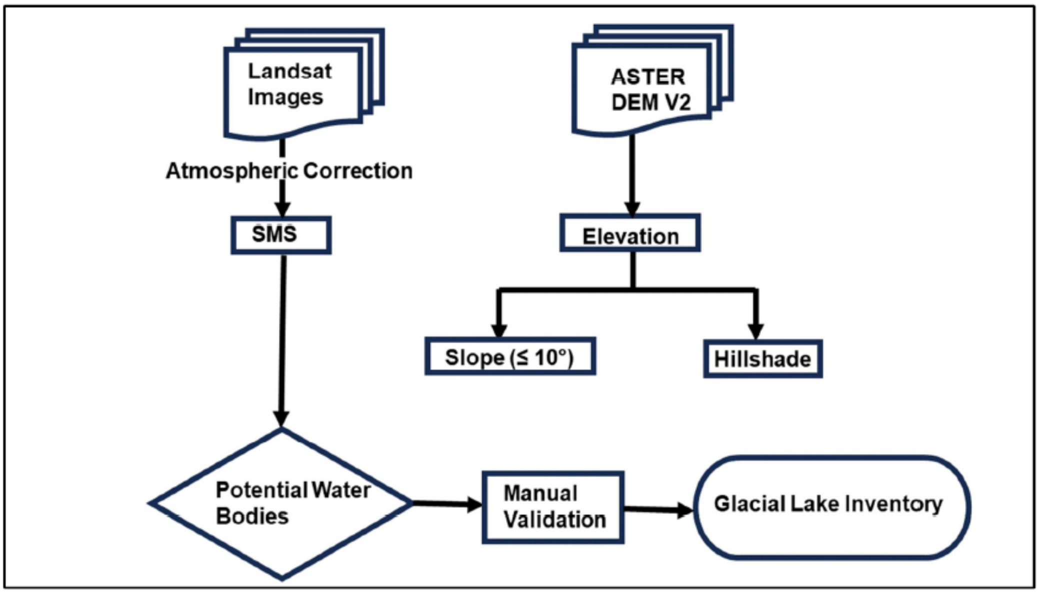

Fig.2. Workflow to develop GL inventory from Landsat satellite images using the semi-automated mapping method.

Several authors (Clague and Evans, 2000; ICIMOD 2011; Emmer et al., 2016; Mal et al., 2020) have attempted to classify GLs based on the process of formation and dam types for their better understanding (Zheng et al., 2021). In this study, each GL was classified into one of four types based on dam characteristics following (Emmer et al., 2016): (1) Bedrock-dammed lakes (BDL), (2) Ice-dammed lakes (IDL), (3) Landslide-dammed lakes (LDL), and (4) Moraine-dammed lakes (MDL).

Hotspot Analysis

To understand the concentration of GLs and the formation of new clusters, we conducted a hotspot analysis of GLs using the point density tool under the spatial analyst toolbox in ArcGIS Pro for all the GL inventories (1987, 2005 and 2018). The point density function is a powerful tool to understand the clustering of GLs. It quantitates intensity per unit of area of point features within the neighbourhood of each raster cell. To calculate the point density, the first step is to convert polygon features into point features. The point density tool only considers those points which fall within the neighbourhood output cell (Silverman, 1986).

Statistical Analysis of Climate Data

To explore the relationship between climate dynamics and the formation of GLs in DV, trend analysis was performed on temperature and precipitation datasets. Mann-Kendall (Mann, 1945; Kendall, 1975) test was employed to test the direction of the trend in temperature and precipitation, while Sen's slope (Sen, 1968) estimator was used to determine the magnitude of the trend. Mann-Kendall test is a non-parametric test used to identify linear monotonic trends in time-series data (Singh et al., 2014; Mal et al., 2022a). The Mann-Kendall test starts with Null Hypothesis (H_0) assuming that the given data have no significant trend. This test does not require data to be normally distributed and the results are not affected by missing values (Mal et al., 2022b).

RESULTS

Glacial Lake Distribution

In DV district, a total of 469 (44.55 km^2) GLs in 1987, 484 (45.48 km^2) in 2005 and 509 (49.51 km^2) in 2018 were detected. GLs have increased in both numbers (40) and area (4.96 km^2) from 1987 to 2018. In 2018, out of 509 GLs 369 had an area of less than 0.1 km^2, whereas 140 had an area of more than 0.1 km^2. However, the aggregate area of GLs (<0.1 km^2) was 13.54 km^2, and the aggregate area of GLs (>0.1 km^2) was 35.42 km^2. Regarding the orientation of the GLs (2018), it was found that out of 509 GLs, 107 are oriented towards north, followed by 75 towards northeast, 72 towards south, 65 towards southest, 59 towards northwest, 51 towards southwest, 47 towards west, and 33 towards east (Fig. 3). Orientation of GLs is important in assessing the GLOF hazard/risk, as it controls the lake expansion and the path of inundation in the regions downstream. In our study, we found GLs are located between the elevation of 3,509 m asl and 4,609 m asl. The mean elevation of GLs was 4,104.72 m in 2018.

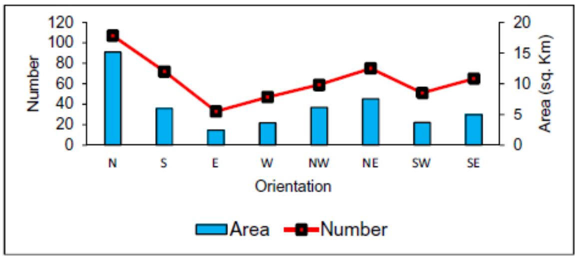

Fig. 3. Distribution of GLs in DV District based on the orientation (2018).

Out of 509 GLs in 2018, 289 (24.27 km^2) were MDL, 199 (23.83 km^2) were BDL, 12 (1.06 km^2) were IDL and 7 (0.29 km^2) were LDL. Furthermore, in terms of mean elevation of GLs, IDL had the highest mean elevation of 4,321.98 m, followed by LDL (4,121.85 m), BDL (4,040.79 m) and MDL had the lowest mean elevation of 3,932.51 m. In terms of orientation, out of 107 north-facing GLs, 61 were MDL, followed by BDL (41) and IDL (5). Of the 75 northeast-facing GLs, 49, 22, 3 and 1 were of MDL, BDL, IDL, and LDL types, respectively. On the contrary, of the 72 south-facing GLs, 36 each belong to MDL and BDL. 65 south-east facing GLs consists of 44 (MDL), 19 (BDL), 1 (LDL) and 1 (IDL), whereas 59 north-west facing consists of 33 (MDL), 22 (BDL), 3 (LDL) and 1 (IDL). Of the total 51 GLs orienting southwest, 27 and 24 belong to MDL and BDL, respectively, whereas west-facing GLs have a nearly similar distribution as of southwest. The GLs orienting east (33) include 18 (MDL), 13 (BDL), 1 (LDL) and 1 (IDL).

Glacial Lake Dynamics

Between 1987 to 2018, the DV district observed an increase of 40 (4.96 km^2) GLs. However, changes were not uniform across the time frame. We observed an increase of 15 (0.81 km^2) GLs from 1987 to 2005 and an increase of 25 (4.11 km^2) GLs from 2005 to 2018. Out of 469 GLs (1987), 93 GLs observed negative change in the area, whereas 371 GLs observed an expansion. Between 1987 to 2018, of the newly emerged GLs, smaller lakes (26, <0.1 km^2) increased with an area of 0.92 km^2, whereas relatively larger lakes (14, >0.1 km^2) increased by 4.04 km^2.

Type-wise Changes in Glacial Lakes

All types of GLs observed a surge in the number and area of GLs from 1987 to 2018, MDL (23) observed the highest increase in terms of number, followed by BDL (8), IDL (8), and least in LDL (1). Furthermore, in terms of changes in the area, MDL observed an increase of 2.81 km^2, followed by BDL (1.43 km^2), IDL (0.69 km^2) and LDL (0.03 km^2) from 1987 to 2018 (Supplementary Table S1). The majority of the GLs have been highly dynamic from 1987 to 2018, e.g., 40 (BDL), 1 (IDL), 3 (LDL) and 53(MDL) show the $R \leq 0$, while 153 (BDL), 3 (IDL), 3 (LDL) and 213 (MDL) show an increasing trend with $R > 0$ (Fig.4 and Supplementary Table S3). Changes among GLs have also been observed altitudinally as well. BDL (9.43%) and MDL (45.45%) show maximum R at the elevation range of 4200-4300m, while IDL (108.1%) and LDL (23.07%) at the elevation ranges of 4300-4400m and 4100-4200m, respectively (Supplementary Table S2). On the other hand, a minor decline in the trend of area change rate is observed for BDL (-8.33%) and an increase in MDL (2.95%) at the elevation range of 4400-4500m and 3800-3900m, respectively. While analysing the changes in the mean area of GLs according to their types for 2018, it was found that BDLs have a maximum mean area of 0.12 km^2, followed by 0.09 km^2 for IDL, 0.08 km^2 for MDL and 0.04 km^2 for LDL (Table 2).

MDL accounts for the maximum number of small GLs (< 0.1 km^2)

Table 2. Changes in the mean area (km^2) of different types of GLs in the study area between 1987 to 2018. Red/green colours show a decrease/increase in the GL area.

Type of Glacial Lakes	1987	2005	2018
BDL	0.1188	0.1158	0.1188
IDL	0.0906	0.1244	0.0906
LDL	0.0438	0.0495	0.0438
MDL	0.0838	0.0786	0.0838

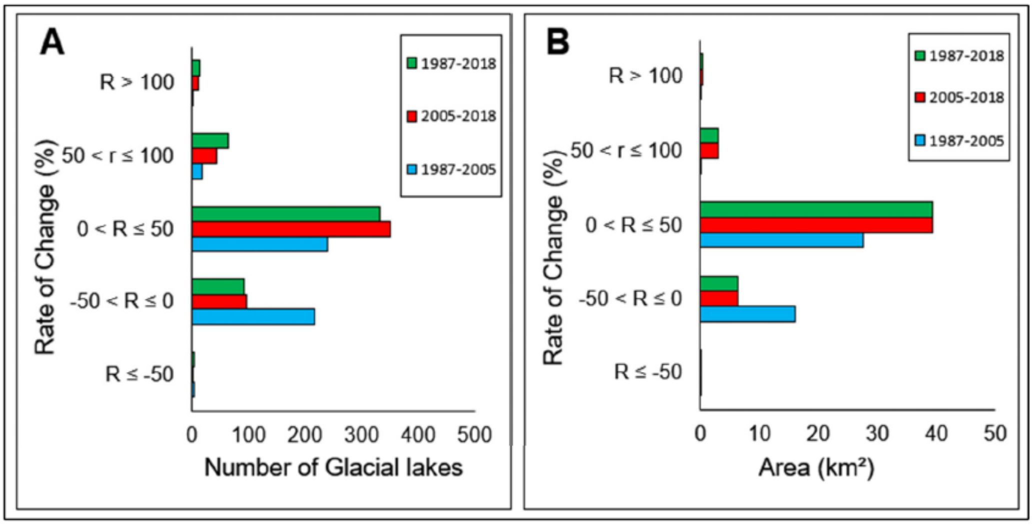

Fig 4. **(A)** number and **(B)** Total area of GLs with respect to the area change rate (%) (R).

between 1987 to 2018, where they increased from 209 (1987), to 217 (2005) and further to 227 (2018). The BDL increased from 124 (1987), to 127 (2005) and further to 128 (2018). The IDLs, though account for a small number, increased from 2 (1987) to 8 (2018). The LDLs have remained unchanged over the study period. On the other hand, BDL accounts for the majority of the large GLs ($\geq$ 0.1 km^2), and increased from 67 (1987), to 69 (2005) and further to 71 (2018), followed by MDL from 57 (1987) to 65 (2018), IDL from 2 (1987) to 4 (2018) and LDL did not observe any change (Fig. 5).

Newly Emerged Glacial Lakes

From 1987 to 2018, we found that 40 new GLs emerged in the DV district (Fig. 6). The new GLs are developing at an altitude higher than the mean altitude of GLs in 1987. The mean elevation of newly formed GLs is 4185.49 m asl, whereas the average elevation of all GLs in 1987 was 4,078.91 m asl. The total area of emerged GLs is 2.30 km^2 (1987-2018). Out of 40 newly developed GLs, the maximum share was of MDL (23), followed by IDL (8), BDL (8), and LDL (1). In terms of orientation of emerged GLs, 15 GLs developed on the northern slopes, 13 developed on the southern

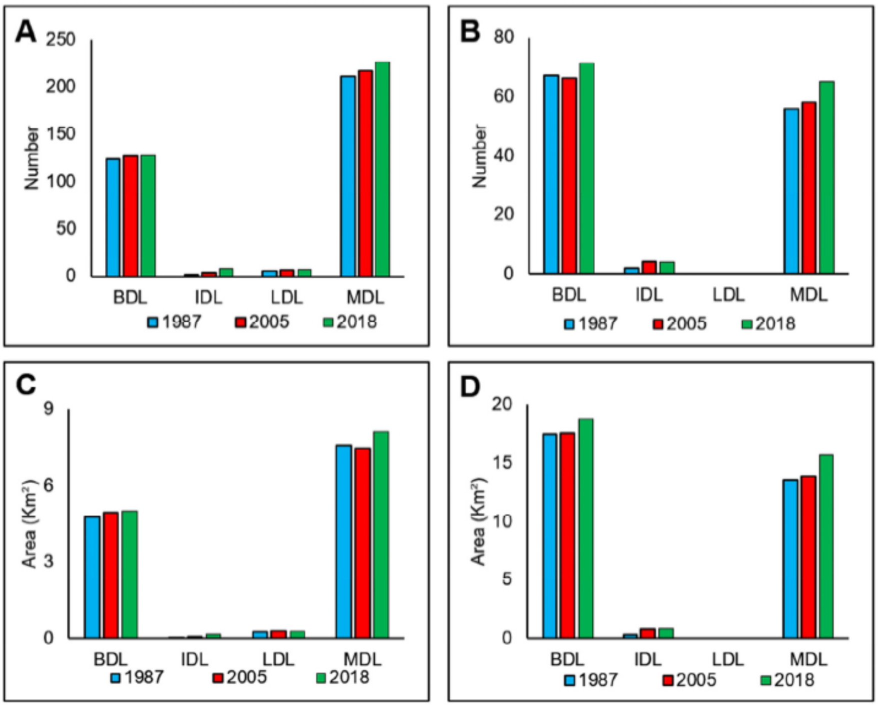

Fig. 5. Distribution of GLs (number and area) according to different types. **(A)** Number of GLs with area <0.1 km^2; **(B)** Number of GLs with area $\geq$ 0.1 km^2; **(C)** Area of GLs with area <0.1 km^2; and **(D)** Area of GLs with area $\geq$ 0.1 km^2.

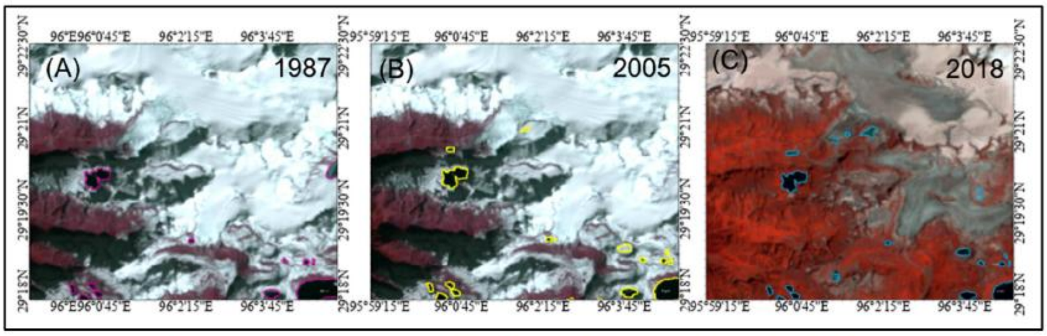

Fig.6 Emergence of new GLs between 1987 and 2018 in Dibang Valley district, Arunachal Pradesh, Eastern Himalaya, where (a) shows the formation of GLs in 1987, (b) in 2005, and (c) in 2018.

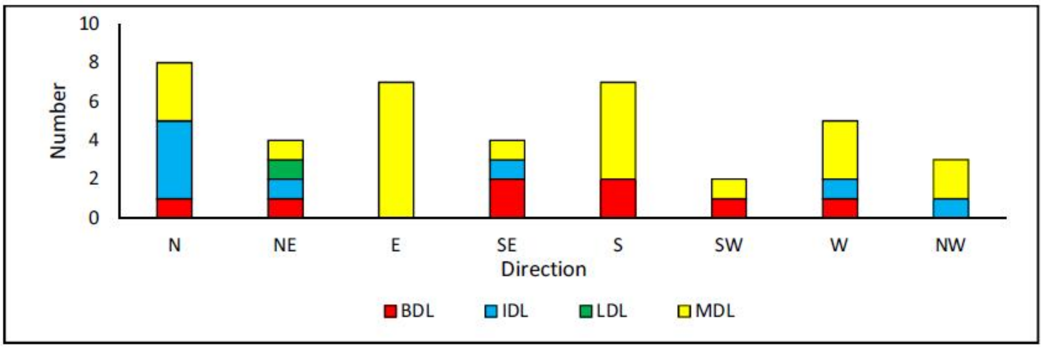

Fig. 7. Distribution of new GLs based on orientation (1987-2018).

slopes, 7 on the eastern slopes and 5 on the western slopes (Fig. 7).

Hotspot Analysis

To understand the concentration and clustering of GLs in DV district, we employed hotspot analysis using the point density function. We found the maximum density of GLs increased from 16 per sq. km (1987) to 21 per sq. km (2018) keeping the output cell setting at 3.84 and neighbourhood settings at a rectangle with height and width of cells at 2 km. The hotspot analysis helped us find clusters of GLs in the north and northeast parts of the DV district. Furthermore, we observed the formation of new clusters of GLs in the northern part of the DV district (Fig. 8).

Climate Change and Glacial Lake Dynamics

Trend analysis of APHRODITE climate data (precipitation and temperature) was conducted for Dibang Valley from 1981 to 2015, to examine the impact of climate change on the evolution of GLs in Eastern Himalaya. Annual and seasonal trends were calculated using the Mann-Kendall trend test and Sen's slope estimator.

Annual temperature shows a statistically significant increasing trend of 0.031°C/year using Sen's slope estimator between 1981 to 2015. The pre-monsoon and post-monsoon did not show any significant trend at the seasonal scale. However, monsoon and winter seasons showed statistically significant increasing temperatures (Table 3). Rising temperatures cause rapid melting of glaciers, leading to new GLs. In general, precipitation did not show any trend at the annual scale. Pre-monsoon, post-monsoon and winter seasons showed no significant trend; however, monsoon season showed a decreasing trend of -0.17mm/year (Table 4).

Glacial Lake Mapping and Dynamics

GLs mapping using remotely sensed data, e.g., Landsat and ASTER are a dynamic and continuous process. In high-altitude areas, large shadows caused by large mountains can cause overestimation of the GLs. Besides, seasonal snow cover, cloud cover and turbidity levels owing to moraine deposition also affected the estimation of GLs in the study area. These difficulties are tied over by the conjunctive use of DEM from ASTER satellite and Landsat satellite images together to extract GLs. Furthermore, each lake was manually inspected to remove the discrepancies in the delineation of GLs.

There are no universally accepted classification methods for GLs;

Table 3. Mann-Kendall test statistics (Z) of Temperature (°C) from 1981 to 2015

	Temperature (°C/year)			
	Z-score (α=0.05)	Sen's Slope	P-value (α=0.05)	Trend
Pre-Monsoon (MAM)	1.88	0.013	0.058	Increasing
Monsoon (JJAS)	2.88	0.005	0.0039	Increasing
Post-Monsoon (OND)	1.16	0.007	0.24	No Trend
Winter (JF)	2.82	0.024	0.004	Increasing
Annual	4.57	0.031	0.0000048	Increasing

Table 4. Mann-Kendall test statistics (Z) of Precipitation (mm/year) from 1981 to 2015

	Precipitation (mm/year)			
	Z-score (α=0.05)	Sen's Slope	P-value (α=0.05)	Trend
Pre-Monsoon (MAM)	1.16	0.13	0.24	No Trend
Monsoon (JJAS)	-1.99	-0.17	0.04	Decreasing
Post-Monsoon (OND)	-1.56	-0.05	0.11	No Trend
Winter (JF)	-0.22	-0.01	0.82	No Trend
Annual	-1.07	-1.8	0.28	No Trend

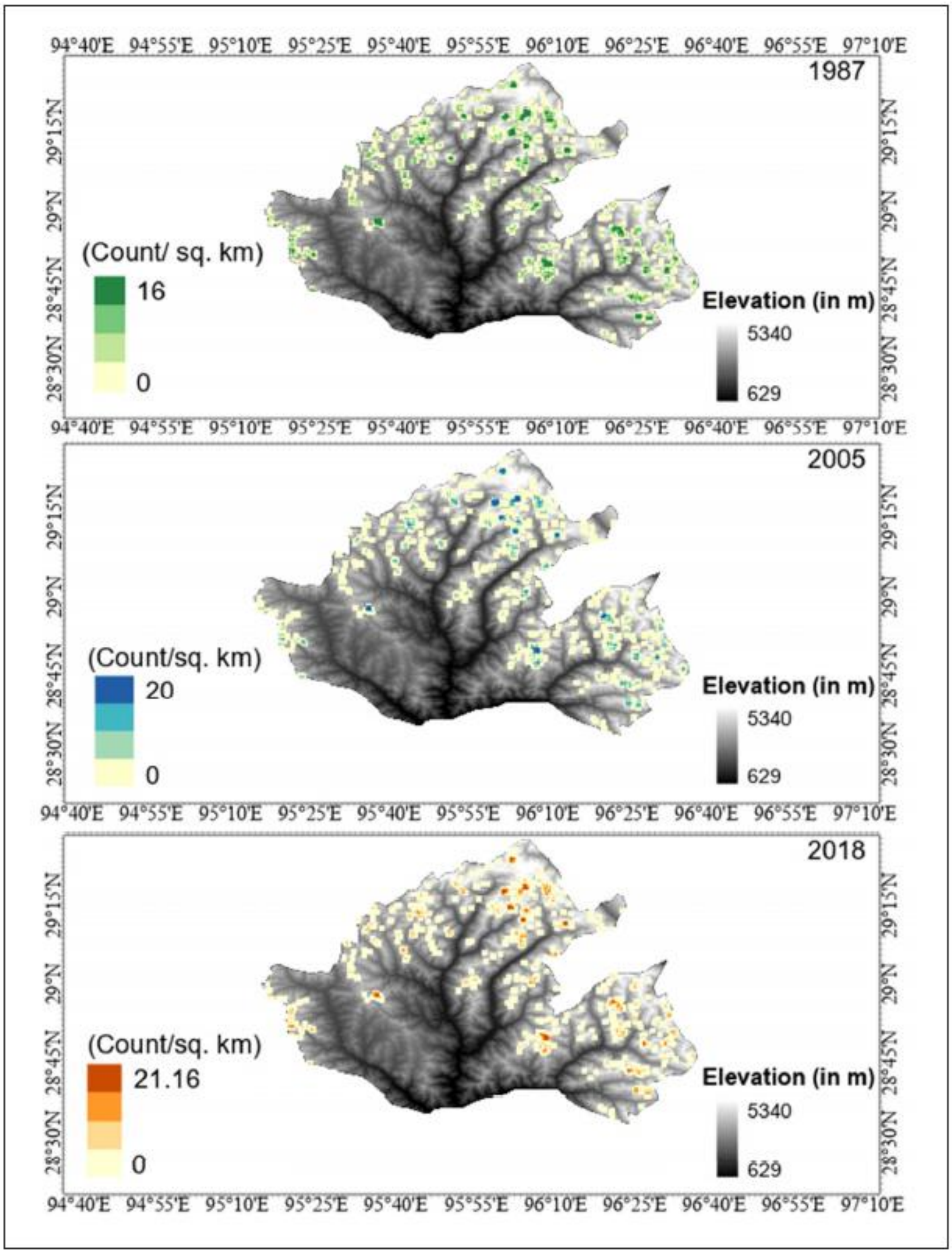

Fig. 8. GL hotspot plot using point density function (output cell size = 3.84, rectangular shape, cell size = 2 km), shown for 1987, 2005 and 2018 in DV, district.

they can be classified into several categories based on the process of formation, location, dam types etc., (Xiaojun et al., 2018). In this study, GLs were classified into 4 broad categories BDL, IDL, LDL and MDL based on the types of dams formed following Emmer et al. (2016). Here, dam type is chosen as a criterion to classify GLs, which is important given their potential for failure leading to GLOFs (Zheng et al., 2021). The results show that GLs increased from 469 [BDL (193), IDL (3), LDL (6) and MDL (266)] in 1987 to 484 [BDL (195), IDL (8), LDL (7) and MDL (274)] in 2005 and 509 [BDL (201), IDL (12), LDL (7) and MDL (289)] in 2018. MDLs have a maximum number of GLs and the highest GL area (24.23 km^2) between 1987 to 2018, which corroborates well with the previous studies (Mal et al., 2020; Zheng et al., 2021). According to Zheng et al., 2021, the eastern Himalaya have the greatest number of MDLs across the third pole region, making the eastern Himalaya one of the GLOF hotshots. Panigrahy et al. (2012), Maharjan et al. (2018) and Mal et al. (2020) attempted to map GLs of high mountainous parts of HKH, which included DV district. Panigrahy et al. (2012) mapped 619 (54.67 km^2) GLs using IRS 3 satellite images and semi-automated mapping technique; Maharjan et al. (2018) mapped 608 (55.6 km^2) GLs using 2005 Landsat satellite

Table 5. Comparison of GL studies in Dibang Valley

Study Area	Panigrahy et al. (2012)			Maharjan et al. (2018) >0.003 km^2			Mal et al. (2020) >0.001 km^2			Present study ≥0.0036		
	Number	Area (km^2)	Time period of data used	Number	Area (km^2)	Time period of data used	Number	Area (km^2)	Time period of data used	Number	Area (km^2)	Time period of data used
Dibang valley	619	54.67	2006-07	608	55.6	2005±3	479	47.08	2016-18	509	49.51	2018-19

data and semi-automated mapping technique, mapping all GLs greater than 0.003 km^2 in area; and Mal et al. (2020) mapped 479 (47.08 km^2) using 2016-2018 Landsat 8 satellite images, mapping all GLs with area more than 0.001 km^2 (Table 5). The inconsistency in the number of GLs and area mapped between the studies is due to differences in the data used, and mapping techniques, e.g., the difference in selecting a threshold of the smallest GLs to be mapped and the study period.

GLs with area ≤0.1 km^2 dominates the frequency of GLs in all three time periods 1987 (343), 2005 (355) and 2018 (369), accounting about 73.12%, 73.34% and 72.49% of GLs in 1987, 2005 and 2018, respectively, while the area of these GLs does not contribute significantly to the total GL area [28.46% (1987), 28.27% (2005) and 27.65% (2018)]. On the other hand, GLs with an area ≥ 0.1 km^2 are less in numbers 126 (1987), 131 (2005) and 140 (2018), but their contribution to the total GL area is higher at 71.53% (1987), 71.72% (2005) and 72.34% (2018).The clusters of GLs can be seen dominating in the northern and north-eastern parts of the Dibang valley continuously from 1987 to 2018, but new GLs were observed in the north-western and eastern parts of the district in 2005 and 2018 (Fig. 8). The new GLs are forming at the higher elevations, mainly due to melting of glaciers at the higher elevations. The mean elevation has also increased by 133.71 m from 1987 to 2018. Mohanty et al. (2021) in central Himalaya and Nie et al. (2018) in Indian Himalaya observed a similar trend of increase in the mean altitude of GLs. The possible reason for this phenomenon in the region is rapid glacier melting due to increased annual mean temperature (Maharjan et al., 2018).

Climate Change Implication on Glacial Lakes

Across the Himalayan region, precipitation and temperature patterns are changing (Sreekesh and Debnath, 2016; Kulkarni et al., 2020; Dimri et al., 2021), which also act as drivers of GL dynamics. An analysis of rainfall and temperature trends reveals that there is insignificant change in annual and seasonal precipitation, but the annual mean temperature has increased significantly from 1981 to 2015 (Tables 3 and 4).

Previous studies (Wang et al., 2013, Prakash and Nagarajan, 2017; Harrison et al., 2018; Kaushik et al., 2020) further proved the sensitivity of GLs to a rise in mean annual temperature in the Himalaya. Sharma et al. (2009) reported an overall rise in mean annual temperature between 0.01-0.04°C/year over Himalaya, which also substantiate our results (0.031°C/year). The increasing mean annual temperature trend can help in explaining the growth of IDL (8) and their increasing mean altitude in Dibang Valley. Further, other environmental conditions such as black carbon present in glaciers can also lead to rapid glacial melting leading to the growth of GL in the Himalayan region (Kang et al., 2020).

Table 6. Comparison of previous studies

Author(s)	Study Area	Expansion rate of GLs (%)	Temperature trend
Present Study	Dibang Valley	8.52%	0.031°C/a
Zhang et al. (2015)	Brahmaputra basin	20.61%	N/A
Nie et al. (2017)	Eastern Himalaya	11.1%	0.37°C/10a - 0.52°C/10a
Li et al. (2022)	Eastern Himalaya	30%	2°C/30a - 2.5°C/30a

CONCLUSION

GLs in the Himalayan region are experiencing growth due to unprecedented climate change. However, only a few studies have tried to understand the relationship between GLs dynamics and climate change in the eastern Himalaya. The present study attempted to map the GL of DV district, India to understand GL dynamics and their relation to climate change using multi-temporal Landsat data collected between 1987 and 2018. GL increased by 8.53% from 469 to 509 with a growth in total area of 10.92% from 44.49 km^2 to 49.35 km^2, with a shift in mean altitude from 4077.9 m asl to 4104.72 m asl. This indicates that glaciers are retreating to higher elevations and more GL are being formed or existing ones are expanding. It was found that most of the GL are of smaller size than (0.1 km^2), but they account for only ~27% of the total GL area. MDL occupies the majority in terms of the number and area of GL throughout the period with ~56% of GLs and ~48% of the total area between 1987 to 2018 making DV a hotspot for future GLOF events (Zheng et al., 2021). These changes further reiterate that glacial melting is accelerated due to temperature rise. The accelerated melting is causing more morainal deposits, especially supra-glacial morainal deposits leading to the formation of more MDL. Therefore, to enhance comprehension of GLs dynamics and develop early warning systems for GLOF in the region, continuous monitoring of GLs is urgently required. Our study can be helpful to researchers working in the field for an updated inventory and policymakers as well for better future planning of infrastructure and management.

Acknowledgement: AK is thankful to the CEN Center for Earth System Research and Sustainability, Institute of Geography, Hamburg University, Germany, for providing the facilities for the present study. Further, the funding support from DAAD is acknowledged.

References

Aggarwal, S., Rai, S.C., Thakur, P.K. and Emmer, A. (2017) Inventory and recently increasing GLOF susceptibility of glacial lakes in Sikkim, Eastern Himalaya. Geomorphology. v.295, pp.39-54, https://doi.org/10.1016/j.geomorph.2017.06.014

Allen, S.K., Linsbauer, A., Randhawa, S.S., Huggel, C., Rana, P., and Kumari, A. (2016) Glacial lake outburst flood risk in Himachal Pradesh, India: an integrative and anticipatory approach considering current and future threats. Natural Hazards, v.84(3), pp.1741–1763. https://doi.org/10.1007/s11069-016-2511-x

Bajracharya, S.R. and Mool, P. (2009) Glaciers, glacial lakes and glacial lake outburst floods in the Mount Everest region, Nepal. Annals of Glaciology, v.50(53), pp.81–86.

Bolch, T., Kulkarni, A., Kääb, A., Huggel, C., Paul, F., Cogley, J. G., Frey, H., Kargel, J.S., Fujita, K., Scheel, M., Bajracharya, S. and Stoffel, M. (2012) The state and fate of Himalayan glaciers. Science v.336(6079), https://doi.org/10.1126/science.1215828

Bobrowski, M., Weidinger, J. and Schickhoff, U. (2021). Is New Always Better? Frontiers in Global Climate Datasets for Modeling Treeline Species in the Himalayas. Atmosphere, v.12(5), 543.

Dimri, A.P., Allen, S., Huggel, C., Mal, S., Ballesteros-Cánovas, J.A., Rohrer, M., ... and Pandey, A. (2021) Climate change, cryosphere and impacts in the Indian Himalayan Region. Curr. Sci., v.120(5), pp.774-790.

Emmer, A., Klimes, J., Mergili, M., Vilímek, V. and Cochachin, A. (2016) 882 lakes of the Cordillera Blanca: An inventory, classification, evolution and assessment of susceptibility to outburst floods. Catena, v.147, https://doi.org/10.1016/j.catena.2016.07.032

Fujita, K., Suzuki, R., Nuimura, T. and Sakai, A. (2008). Performance of ASTER and SRTM DEMs, and their potential for assessing glacial lakes in the Lunana region, Bhutan Himalaya. Jour. Glaciol., v.54(185) https://doi.org/10.3189/002214308784886162

Fukunaga K. and Hostetler L. (1975) The estimation of the gradient of a density function with applications in pattern recognition. IEEE Trans. Inform. Theory, v.21(1), pp.32-40.

Gardelle, J., Arnaud, Y. and Berthier, E. (2011) Contrasted evolution of glacial lakes along the Hindu Kush Himalaya Mountain range between 1990 and 2009. Global and Planetary Change, v.75(1-2). pp.47-55 https://doi.org/10.1016/j.gloplacha.2010.10.003

Govindha Raj, B.K., Kumar, V.K. and Remya, S.N. (2013) Remote sensing-based inventory of glacial lakes in Sikkim Himalaya: Semi-automated approach using satellite data. Geomatics, Natural Hazards and Risk. v.4(3), pp.241-253 https://doi.org/10.1080/19475705.2012.707153

Harrison, S., Kargel, J. S., Huggel, C., Reynolds, J., Shugar, D. H., Betts, R. Emmer, A., Glasser, N., Haritashya, U.K., Klimes, J., Reinhardt, L., Schaub, Y., Wiltshire, A., Regmi, D. and Vilímek, V. (2018) Climate change and the global pattern of moraine-dammed glacial lake outburst floods. Cryosphere, v.12(4), pp.1195-1209.

Ives, J.D., Shrestha, R.B. and Mool, P.K. (2010) Formation of Glacial Lakes in the Hindu Kush-Himalayas and GLOF Risk Assessment. *In:* ICIMOD (Inernational Centre for Integrated Mountain Development).

Karger, D.N., Conrad, O., Böhner, J., Kawohl, T., Kreft, H., Soria-Auza, R.W., ... and Kessler, M. (2017) Climatologies at high resolution for the earth's land surface areas. Scientific data, v.4(1), pp.1-20.

Kang, S., Zhang, Y., Qian, Y. and Wang, H. (2020) A review of black carbon in snow and ice and its impact on the cryosphere. Earth-Sci. Rev., v.210, 103346.

Kendall, M.G. (1975). Rank Correlation methods, Griffin, London. UK.

Kaushik, S., Rafiq, M., Joshi, P.K. and Singh, T. (2020) Examining the glacial lake dynamics in a warming climate and GLOF modelling in parts of Chandra basin, Himachal Pradesh, India. Sci. Total Environ.. v.714. https://doi.org/10.1016/j.scitotenv.2019.136455

Li, J. and Sheng, Y. (2012) An automated scheme for glacial lake dynamics mapping using Landsat imagery and digital elevation models: A case study in the Himalayas. Internat. Jour. Rem. Sens.. v.33(16). pp.5194-5213. https://doi.org/10.1080/01431161.2012.657370

Li, W., Wang, W., Gao, X., Wang, X. and Wang, R. (2022). Inventory and Spatiotemporal Patterns of Glacial Lakes in the HKH-TMHA Region from 1990 to 2020. Rem. Sens., v.14(6), 1351. https://doi.org/10.3390/rs14061351

Maharjan, S.B., Mool, P.K., Lizong, W., Xiao, G., Shrestha, F., Shrestha, R.B., Khanal, N. R., Bajracharya, S. R., Joshi, S., Shai, S., and Baral, P. (2018) The Status of Glacial Lakes in the Hindu Kush Himalaya. ICIMOD Res., (2018/1), 70.

Mal, S., Kumar, A., Bhambri, R., Schickhoff, U. and Singh, R.B. (2020) Inventory and Spatial Distribution of Glacial Lakes in Arunachal Pradesh, Eastern Himalaya, India. Jour. Geol. Soc. India, v.96(6), pp 609-615 https://doi.org/10.1007/s12594-020-1610-1

Mal, S., Allen, S.K., Frey, H., Huggel, C. and Dimri, A.P. (2021) Sectorwise assessment of glacial lake outburst flood danger in the Indian Himalayan region. Mountain Res. Develop., v.41(1), R1.

Mal, S., Rani, S. and Maharana P. (2022) Estimation of spatio-temporal variability in land surface temperature over the Ganga River Basin using MODIS data. Geocarto Internat., v.37(13), pp.3817-3839, https://doi.org/10.1080/10106049.2020.1869331

Mal, S., Arora, M., Banerjee , A., Singh, R.B., Scott C.A., Allen S.A. and Karki R. (2022) Spatial Variations and Long-Term Trends (1901-2013) of Rainfall Across Uttarakhand Himalaya, India. *In:* Schickhoff, U., Singh R., Mal, S. (Eds.), Mountain Landscape in Transition. Sustainable Development Goals Series, Cham.

Mann, H. (1945) Nonparametric tests against trend. Econometrica, v.13, pp.344-355.

Mohanty, L.K. and Maiti, S. (2021) Regional morphodynamics of supraglacial lakes in the Everest Himalaya. Sci. Total Environ., v.751, 141586.

Nagai, H., Ukita, J., Narama, C., Fujita, K., Sakai, A., Tadono, T., Yamanokuchi, T. and Tomiyama, N. (2017) Evaluating the scale and potential of GLOF in the bhutan himalayas using a satellite-based integral glacier-glacial lake inventory. Geosciences (Switzerland), v.7(3), pp.77. https://doi.org/10.3390/geosciences7030077

Nie, Y., Liu, Q., Wang, J., Zhang, Y., Sheng, Y. and Liu, S. (2018) An inventory of historical glacial lake outburst floods in the Himalayas based on remote sensing observations and geomorphological analysis. Geomorphology, v.308, pp.91-106. https://doi.org/10.1016/j.geomorph.2018.02.002

Nie, Y., Sheng, Y., Liu, Q., Liu, L., Liu, S., Zhang, Y. and Song, C. (2017) A regional-scale assessment of Himalayan glacial lake changes using satellite observations from 1990 to 2015. Rem. Sens. Environ., v.189, pp.1-13. https://doi.org/10.1016/j.rse.2016.11.008

Panigrahy, S., Patel, J. and Pariha, J. (2012) National Wetland Atlas. High Altitude Lakes on India. Space Applications Centre, ISRO, Ahmedabad, India.

Prakash, C. and Nagarajan, R. (2017) Glacial lake inventory and evolution in northwestern indian himalaya. IEEE Jour. Selected Topics in Applied Earth Observations and Remote Sensing, v.10(12). pp.5285-5294. https://doi.org/10.1109/JSTARS.2017.2767098

Quincey, D.J., Richardson, S.D., Luckman, A., Lucas, R.M., Reynolds, J.M., Hambrey, M.J. and Glasser, N.F. (2007) Early recognition of glacial lake hazards in the Himalaya using remote sensing datasets. Global and Planetary Change. https://doi.org/10.1016/j.gloplacha.2006.07.013

Richardson, S.D. and Reynolds, J.M. (2000) An overview of glacial hazards in the Himalayas. Quaternary Internat., https://doi.org/10.1016/S1040-6182(99)00035-X

Sen, P.K. (1968). Estimates of the regression coefficient based on Kendall's tau. Jour. Amer. Statist. Assoc., v.63, pp.1379-1389.

Sharma, E. and Tsering, K. (2009) Climate change in the Himalayas: the vulnerability of biodiversity. Sustainable Mountain Development, v.55, pp.10-12.

Silverman, B.W (1986) Density Estimation for Statistics and Data Analysis. New York: Chapman and Hall.

Shugar, D.H., Burr, A., Haritashya, U.K., Kargel, J.S., Watson, C.S., Kennedy, M.C., Bevington, A.R., Betts, R.A., Harrison, S. and Strattman, K. (2020) Rapid worldwide growth of glacial lakes since 1990. Nature Climate Change, v.10(10), pp.939-945. https://doi.org/10.1038/s41558-020-0855-4

Singh, R.B. and Mal S. (2014) Trends and variability of monsoon and other rainfall seasons in Western Himalaya, India. Atmos. Sci. Lett., v.15, pp.218-226.

Song, C., Sheng, Y., Ke, L., Nie, Y. and Wang, J. (2016) Glacial lake evolution in the southeastern Tibetan Plateau and the cause of rapid expansion of proglacial lakes linked to glacial-hydrogeomorphic processes. Jour. Hydrol., v.540, pp.504–514. https://doi.org/10.1016/j.jhydrol.2016.06.054

Sreekesh, S. and Debnath M. (2016) Spatio-Temporal Variability of Rainfall and Temperature in Northeast India. *In:* N. J. Raju, (Edited) Geostatistical and Geospatial Approaches for the Characterization of Natural Resources in the Environment: Challenges, Processes and Strategies. pp-873-879. Springer, Switzerland. https://doi.org/10.1007/978-3-319-18663-4

Su, T. et al. (2015) Image segmentation using mean shift for extracting croplands from high-resolution remote sensing imagery, *Rem. Sens. Lett.,* v.6(12), pp.952-961, https://doi.org/10.1080/2150704X.2015.1093188

Tadono, T., Kawamoto, S., Narama, C., Yamanokuchi, T., Ukita, J., Tomiyama, N. and Tabuki, H. (2012). Development and Validation of New Glacial Lake Inventory in the Bhutan Himalayas Using ALOS 'DAICHI.' Global Environ. Res., v.16(1). pp.31-40.

Ukita, J., Narama, C., Tadono, T., Yamanokuchi, T., Tomiyama, N., Kawamoto, S., Abe, C., Uda, T., Yabuki, H., Fujita, K. and Nishimura, K. (2011). Glacial lake inventory of Bhutan using ALOS data: Methods and preliminary results. Annals Glaciol., v.52(58). pp.65-71. https://doi.org/10.3189/172756411797252293

Veh, G., Korup, O., von Specht, S., Roessner, S. and Walz, A. (2019) Unchanged frequency of moraine-dammed glacial lake outburst floods in the

Himalaya. *In:* Nature Climate Change, v.9(5). pp. 379-383. https://doi.org/10.1038/s41558-019-0437-5

Wang, W., Yang, X. and Yao, T. (2012). Evaluation of ASTER GDEM and SRTM and their suitability in hydraulic modelling of a glacial lake outburst flood in southeast Tibet. Hydrol. Process., v.26(2). https://doi.org/10.1002/hyp.8127

Wang, X., Siegert, F., Zhou, A.G. and Franke, J. (2013) Glacier and glacial lake changes and their relationship in the context of climate change, Central Tibetan Plateau 1972–2010. Global and Planetary Change, v.111, pp.246-257.

Wang, X., Guo, X., Yang, C., Liu, Q., Wei, J., Zhang, Y., Liu, S., Zhang, Y., Jiang, Z. and Tang, Z. (2020) Glacial lake inventory of High Mountain Asia (1990–2018) derived from Landsat images. Earth System Science Data Discussions, v.12(3), https://doi.org/10.5194/essd-2019-212

Wangchuk, S., Bolch, T. and Zawadzki, J. (2019). Towards automated mapping and monitoring of potentially dangerous glacial lakes in Bhutan Himalaya using Sentinel-1 Synthetic Aperture Radar data. Internat. Jour. Rem. Sens., v.40(12), pp.4642-4667. https://doi.org/10.1080/01431161.2019.1569789

Wilson, R., Glasser, N. F., Reynolds, J. M., Harrison, S., Anacona, P. I., Schaefer, M. and Shannon, S. (2018). Glacial lakes of the Central and Patagonian Andes. Global and Planetary Change, v.162, pp. 275-291. https://doi.org/10.1016/j.gloplacha.2018.01.004

Worni, R., Huggel, C., Clague, J.J., Schaub, Y. and Stoffel, M. (2014) Coupling glacial lake impact, dam breach, and flood processes: A modeling perspective. Geomorphology, v.224, pp.161-176. https://doi.org/10.1016/j.geomorph.2014.06.031

Worni, R., Huggel, C. and Stoffel, M. (2013) Glacial lakes in the Indian Himalayas - From an area-wide glacial lake inventory to on-site and modeling-based risk assessment of critical glacial lakes. Sci. Total Environ., v.468, pp.S71–S78. https://doi.org/10.1016/j.scitotenv.2012.11.043

Yao, X., Liu, S., Han, L., Sun, M. and Zhao, L. (2018). Definition and classification system of glacial lake for inventory and hazards study. Jour. Geograph. Sci., v.28(2), pp.193-205 https://doi.org/10.1007/s11442-018-1467-z

Zhang, G., Bolch, T., Allen, S., Linsbauer, A., Chen, W. and Wang, W. (2019) Glacial lake evolution and glacier – lake interactions in the Poiqu River basin, central Himalaya, 1964 – 2017. v.65, pp.347–365. https://doi.org/10.1017/jog.2019.13

Zhang, G., Yao, T., Xie, H., Wang, W. and Yang, W. (2015) An inventory of glacial lakes in the Third Pole region and their changes in response to global warming. Global and Planetary Change, v.131, pp.148–157. https://doi.org/10.1016/j.gloplacha.2015.05.013

Zhang, M., Chen, F., Tian, B., Liang, D. and Yang, A. (2020) High-frequency glacial lake mapping using time series of sentinel-1A/1B sar imagery: An assessment for the southeastern tibetan plateau. Internat. Jour. Environ. Res. Public Health, v.17(3), 1072. https://doi.org/10.3390/ijerph17031072

Zheng, G., Allen, S.K., Bao, A., Ballesteros-Cánovas, J.A., Huss, M., Zhang, G., ... and Stoffel, M. (2021) Increasing risk of glacial lake outburst floods from future Third Pole deglaciation. Nature Climate Change, pp.1-7.

Atul Kumar is a doctoral candidate at the CEN, Center for Earth System Research and Sustainability, Department of Geography, University of Hamburg, Hamburg, Germany. His research interests include climate change, glacial lakes dynamics and associated hazards in the Himalaya.

Udo Schickhoff is a Professor at CEN, Center for Earth System Research and Sustainability, Department of Geography, University of Hamburg, Hamburg, Germany. His research interests include bio-geography, climate change, glaciers, glacial lake dynamics and tree line changes in the Himalaya.

Suraj Mal is an Associate Professor at the Center for the Study of Regional Development, Jawaharlal Nehru University, New Delhi, India. His research interests include climate change, glacier changes, Glacial lake dynamics, and associated hazards in the Himalaya.

S. Sreekesh is a Professor at the Centre for the Study of Regional Development, Jawaharlal Nehru University, New Delhi. His research interests include climate change, and hydrology with experiences in diverse ecosystems such as mountain, coastal, wetland, urban, mining, micro watersheds, etc.

Article IV

Kumar, A., Mal, S., & Schickhoff, U. (**accepted**). Spatio-temporal evolution of glacial lakes in the Upper Ganga Basin, Central Himalayas. Himalaya: Mountains of Destiny, Springer book series.

Spatio-temporal evolution of glacial lakes in the Upper Ganga Basin, Central Himalayas

Atul kumar[1], Suraj Mal[2*], and Udo Schickhoff

[1]Atul Kumar
CEN Center for Earth System Research and Sustainability, Institute of Geography, University of Hamburg, Germany.
Email: atul.sbsc@gmail.com

[2]Suraj Mal
Jawaharlal Nehru University, Delhi, India,
Email: surajmal@jnu.ac.in

[1]Udo Schickhoff
CEN Center for Earth System Research and Sustainability, Institute of Geography, University of Hamburg, Germany.
Email: udo.schickhoff@uni-hamburg.de

[*]Corresponding Author

Abstract:

Glacial lakes in the central Himalayas are expanding at an unprecedented rate due to the rapid melting and thinning of glaciers. Continuous growth of glacial lakes increases the availability of freshwater for the downstream communities, and escalates the risk of future Glacial Lake Outburst Floods (GLOFs) in the upper Ganga basin. In the present study, glacial lake inventories for the years 1990, 2000, 2010 and 2020 were prepared at the sub-basin level to understand the evolution of glacial lakes in the upper Ganga basin at the micro-regional scale. We found that, between 1990 and 2020, the total number of glacial lakes increases by 564 (22.08%) and the total area increased by 40.71 km^2 (23.93%). We found that glacial lakes were present in the 28 sub-basins of the upper Ganga basin. Among different types of glacial lakes, end moraine-dammed (M(e)) (n: 2,413 & a: 178.89 km^2) had the highest proportion both in terms of number and area of different types of glacial lakes.

We, furthermore, estimated the volume and mean depth of glacial lakes using Huggel et al. (2002) empirical equations. The total estimated volume of glacial lakes was 5.548 km^3 (2020) and the average

estimated mean depth was 8.26 m (2020). Between 1990 and 2020, the estimated volume of glacial lakes increased by 1.46 km^3 and the average estimated mean depth decreased by -0.20 m.

Keywords: Central Himalayas, Glacial Lakes, Ganga basin, Inventory

Introduction:

Glacial lakes are water bodies mainly of melted glaciated water deposited in the depressions created by glacial processes. They are a vital component of watersheds in the cryospheric environment of the Indian subcontinent. Several of the glacial lakes in the Himalayan region are a source of the largest rivers in the Indian sub-continent. Ganga and its tributaries receive large amounts of freshwater from these glacial lakes and fed the downstream region before discharging the water into the Bay of Bengal. In the recent past, several studies have highlighted expansion of glacial lakes in the Hindukush-Karakoram-Himalayas (HKH) **(Zhang et al., 2015; Nie et al., 2017; Maharjan et al., 2018; Shugar et al., 2020). Zhang et al. (2015)** showed that the number of glacial lakes increased by 23.88% and the area increased of those glacial lakes by 23.19% between 1990 and 2010 in the High Mountain Asia (HMA). Similarly, **Nie et al. (2017)** found that the number of glacial lakes increased by 8.81% and area increased by 14.16% between 1990 and 2015 in the Himalayan region. **Nie et al. 2013** in another study found that the number of glacial lakes increased by 10.32% and the area increased by 17.10% in the central Himalayan region. The increase in the number and area of glacial lakes not only increases the availability of freshwater resources but also causes potential Glacial Lake Outburst Floods (GLOFs) risk (**Veh et al., 2019**). The upper Ganga river basin, which covers the central Himalayan region, observed highest expansion of glacial among major river basins in the Indian subcontinent (**Zhang et al., 2015; Nie et al., 2017; Li et al., 2022). Zhang et al. (2015)** found that the number of glacial lakes increased by 23.8% and the area of glacial lakes increased by 51.1% between 1990 and 2010 in the Ganga basin. **Nie et al. (2017)** found that glacial lakes are expanding at a rate of 23% in the central Himalayan region. **Khadka et al. (2018)** found 511 newly emerged glacial lakes between 1987 and 2017 in the Nepal Himalayas. Therefore, it is vital to monitor the evolution of glacial lakes in the upper Ganga basin continuously.

Several studies have been conducted to map the glacial lakes in the upper Ganga basin or parts of it (**Nie et al., 2013; Zhang et al., 2015; Khadka et al., 2018; Maharjan et al., 2018; Pandey et al., 2021; Rao et al., 2021; Li et al., 2022**). Zhang et al. (2015) mapped 4,082 (>0.003 km^2) glacial lakes with a total area of 208.59 km^2 in the Ganga basin using the Landsat (TM & ETM+) missions. **Rao et al. (2021)** mapped 4,707 (>0.0025 km^2) with a total area of 206.85 km^2 in the Ganga basin using the Resourcesat-2 satellite mission. **Pandey et al., 2021** mapped 1,353 (0.0005 km^2) glacial lakes with an area of 7.96 km^2 in the Uttarakhand state of India (northern part of the Ganga basin). **Khadka et al. (2018)** mapped 1541 (≥0.0036 km^2) glacial lakes with a total area of 80.95±15.25 km^2 using the Landsat (MSS, TM & OLI) mission. In previous studies, it has been found that the majority of the glacial lakes are end-moraine type (**Nie et al., 2013; Maharjan et al., 2018).**

Furthermore, end moraine-dammed lakes experienced the highest growth rates among different types of glacial lakes in the upper Ganga basin **(Nie et al., 2017; Pandey et al., 2021; Li et al., 2022).** These lakes are generally connected to the glaciers. The rapid melting of glaciers in the upper Ganga basin is the prime reason for the exponential growth of these glacial lakes **(Zhang et al., 2023**). End-moraine lakes are dammed by terminal moraine, which are highly unstable in nature. In scenarios of dam failure, end-moraine lakes can cause huge GLOF events in the downstream region **(Aggarwal et al., 2017; Mal et al., 2021)**. Therefore, it becomes more important to continuously monitor the growth of these glacial lakes.

Glacial lake volume is an important lake characteristic which helps in identifying potential hazardous glacial lakes (**Fujita et al., 2013; Mal et al., 2021**). However, it is extremely difficult to calculate the volume of each glacial lake because of limited availability of bathymetric surveys in the upper Ganga basin **(Zhang et al., 2023)**. This is one of the major reasons why none of the existing inventories attempted to calculate or estimate the volume of glacial lakes in the upper Ganga basin. However, there are several existing empirical equations developed by researchers which can estimate volume and mean depth of glacial lakes (**Huggel et al., 2002; Cook & Quincey, 2015).** These equations can help researchers to estimate the volume and mean depth of glacial lakes, which plays a crucial role in identifying potentially hazardous glacial lakes.

Discrepancies in the results of different glacial lake inventories mainly because of different data sources employed and methods used makes it extremely complicated to understand the evolution and expansion of glacial lakes between past and present. Furthermore, to our knowledge, none of the existing studies attempted to examine the evolution of glacial lakes in the upper Ganga basin in terms of numbers, area, estimated volume and estimated mean depth at the sub-basin level. Therefore, the main objectives of the present study are 1) to generate an updated glacial lake inventory for the upper Ganga basin; 2) to understand the evolution of glacial lakes between 1990 and 2020 at the sub-basin level; and 3) to generate information about the estimated volume and mean depth of glacial lakes.

Study area:

The upper Ganga river system is the largest river system in the central Himalayas. The river system is spread across three countries (China, India, and Nepal), forming a transboundary river system. Geographically, the study domain lies between 28°29’36’’N and 31°28’12’’N (latitudes); and 77°35’27’’E and 88°56’36’’E (longitudes). The total area of the study domain is 162792.81 Km^2, out of which, 59.14% lies in Nepal, followed by China (20.63%), and India (20.22%). The study domain has 32 sub-basins, out of which the Arun sub-basin (30144.81 km^2) is the largest sub-basin.

The physiography of the study domain is mainly dominated by Mountains and valleys. The elevation ranges between 0 – 8,848 m asl, including the highest peak of the world (Mt. Everest). The climate of the study domain is dominated by the Indian summer Monsoon, maximum temperature reaches ~40°C (June), whereas in winter temperature drops as lower than ~-10°C. The study domain receives ~80% of its precipitation in the months of July, August and September (liquid precipitation), whereas ~20% is in solid form (winter months) **(Krishnan & Indu, 2023).**

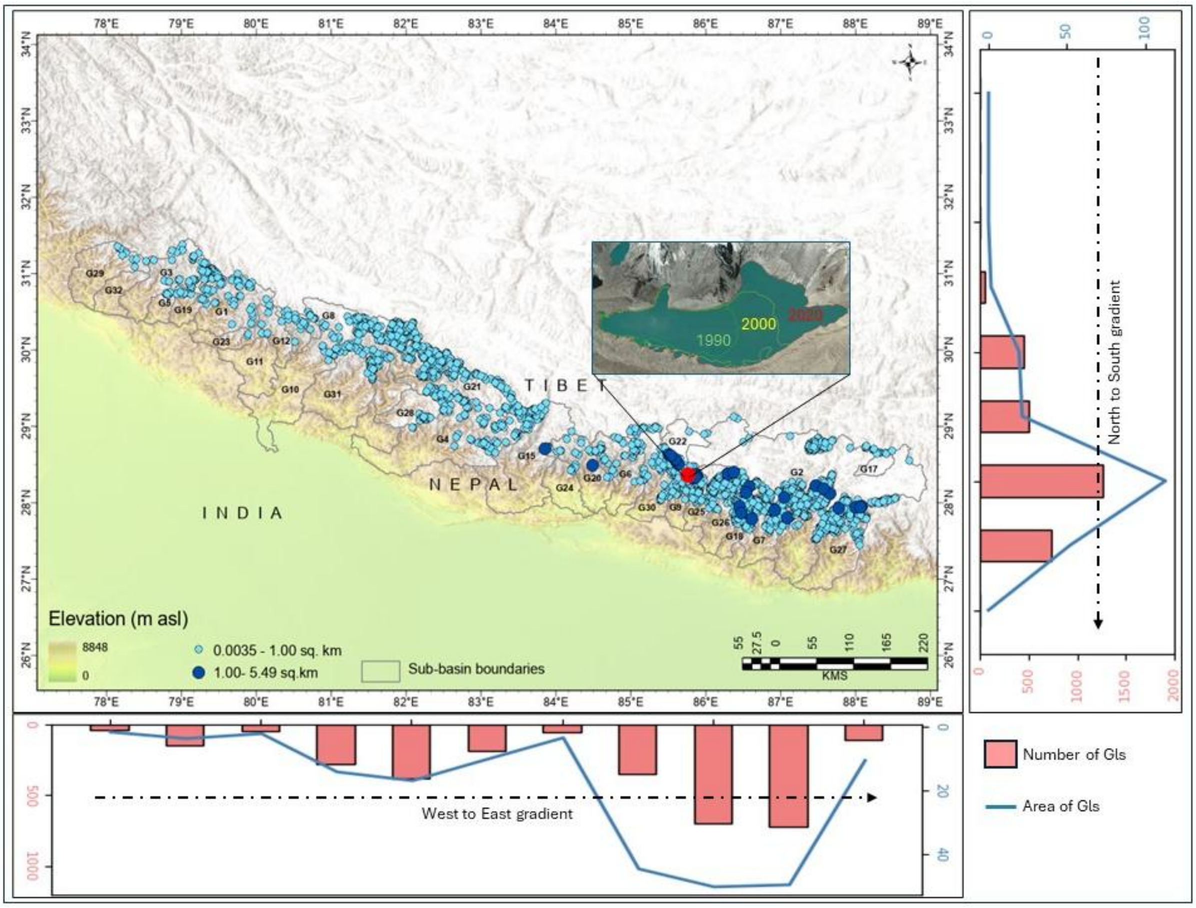

Fig.1 Map of study domain showing distribution of glacial lakes at the sub basin level. The left sub-plot is showing latitudinal distribution of glacial lakes and lower sub-plot is showing the longitudinal distribution of glacial lakes. The insert map is showing the evolution of largest glacial lake in the study domain.

Data and Methods:

Data

Glacial lakes can be mapped using in-situ surveys, toposheets and remotely sensed aerial/satellite images (**Dou et al., 2023**). In-situ surveys are cost-intensive, time-consuming and difficult to conduct in unreachable mountainous terrain. In the past decades, due to the recent advancements in the satellite-based remote sensing, satellite images is regarded as the most reliable source to map glacial lakes. Satellite images from several missions (Landsat, IRS, SPOT, Sentinel-1&2) are regularly used to map glacial lakes (**Nie et al., 2013; Aggarwal et al., 2017; Mal et al., 2020**). In the present study, we used satellite images from the Landsat mission (Landsat 5 & 8) to map the glacial lakes for 1990, 2000, 2010 and 2020 (https://earthexplorer.usgs.gov/). Mainly because it allows us to monitor the continuous growth of glacial lakes since the early 1990s, and they are easy to acquire. The majority of the images were collected between September and December, because of the minimum presence of snow and cloud cover in the study domain (**Table 1**). In addition, we also used the Shuttle Radar Topography Mission (SRTM) V4 (30 m) Digital Elevation Model (DEM) (https://earthexplorer.usgs.gov/) for better identification of glacial lakes, using hillshade, slope and elevation information.

Table 1: Details of the satellite images used in the study

Year	Satellite Mission	Sensor	Spatial Resolution	Number of Satellite images used for individual inventory
1990	Landsat 5	Thematic Mapper (TM)	30 m	148
2000	Landsat 5	Thematic Mapper (TM)	30 m	138
2010	Landsat 5 & 8	Thematic Mapper (TM) & Operational Land Imager (OLI)	30 m	88
2020	Landsat 8	Operational Land Imager (OLI)	30 m	109

Methods

Glacial lake mapping

The methods used to map the glacial lakes using remotely sensed satellite images can be divided into three categories: (i) manual (Rao et al., 2021), (ii) semi-automated **(Mal et al., 2020, Zheng et al., 2021)**, and (iii) automated **(Dou et al., 2023)**. Manual method yields high accuracy, however, it is time-consuming, cost & labor intensive, and requires high level of expertise in identification of glacial lakes. Automated mapping on the other hand is a cost effective and time saving technique, however, if left unsupervised, it can lead to misidentification of glacial lakes **(Nie et al., 2017; Mal et al., 2020**). Semi-automated method is the middle path between the two (manual and automated). It have the cost and time efficiency of automated mapping and high accuracy of the manual mapping (**Mal et al., 2020**). Therefore, in the present study we used semi-automated mapping technique to generate the glacial lake inventories (**Fig. 2**). We used binary thresholding method to generate the water mask using the Normalized Difference Water Index (NDWI). NDWI is a band ratio between Green and Near Infrared (NIR) bands **(Huggel et al., 2002)** (**Equation 1**). The values ranges between -1 to 1. An optimal threshold of NDWI (≥0.2) was selected by hit and trial method to extract the water bodies.

$$NDWI = \frac{(Band_{GREEN} - Band_{NIR})}{(Band_{GREEN} + Band_{NIR})} \qquad (1)$$

The next step, was to use the elevation threshold of 3000 m asl and slope of less than 15° to identify the potential glacial lakes in the study domain. The elevation threshold of ≥2,400 m asl was chosen to identify the glacial lakes because based on the previous studies the minimum elevation of glacial lakes in the upper Ganga basin was 2,462 m asl (**Maharjan et al., 2018**). Furthermore, the slope threshold of ≤20° was selected for the identification of potential glacial lakes, because glacial lakes requires stable slopes for accumulation of melted water from glaciers (**Khadka et al., 2018**).

The next step was to select the minimum mapping area of glacial lakes. We selected the minimum mapping area of 0.0036 km^2. Previous studies showed that, for effective identification of any feature, in our case glacial lakes, at least 4 pixels of Landsat satellite images (0.0036 km^2) are required for effective identification of glacial lakes (Maharjan et al., 2018; Mal et al., 2020). The last step was to inspect the each glacial lake manually using Google Earth Pro for misidentification and final corrections in the glacial lake inventories of 1990, 2000, 2010 and 2020.

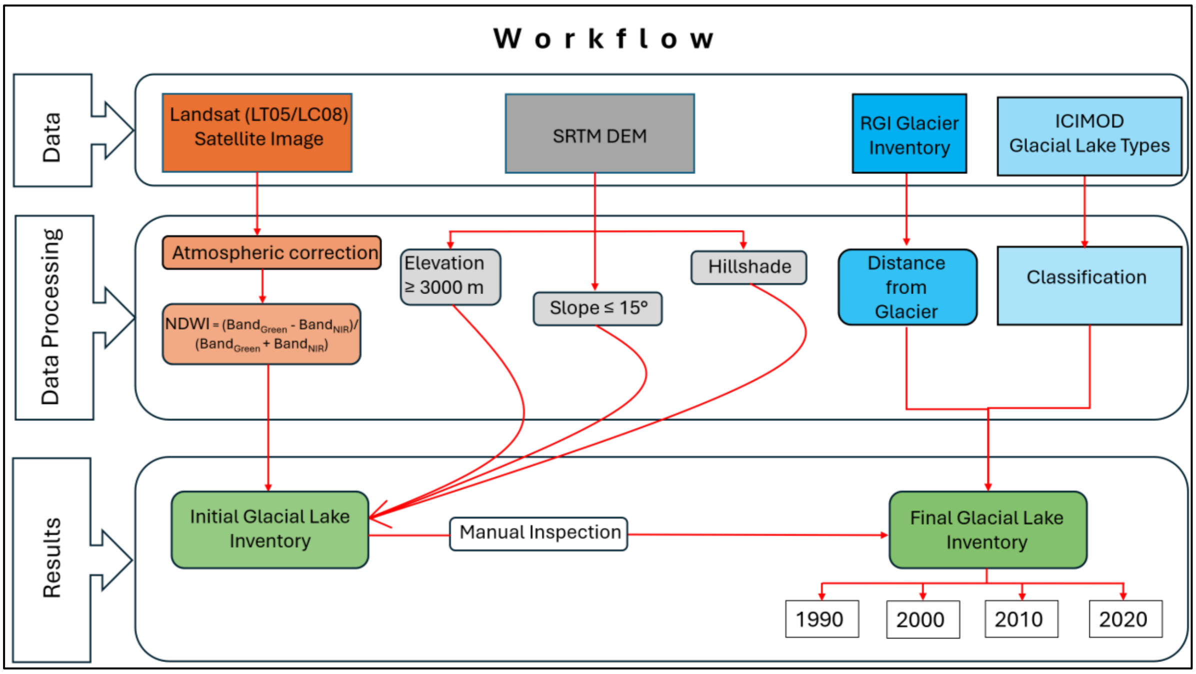

Fig. 2 Workflow diagram showing the data sources and methodology used to map the glacial lakes.

Glacial lake classification

There is no internationally recognized classification available for glacial lakes. However, several studies, came up with their own classification schemes for glacial lakes (**Bhambri et al. 2018; Maharjan et al. 2018**). In the present study, we followed the glacial lake classification provided by ICIMOD, because we aims to classify the glacial lakes in the upper Ganga basin based on the dam types. ICIMOD classified glacial lakes based dam types. Their classification is divided into four major types and eight sub-types (**Maharjan et al. 2018**).

Estimation of volume and mean depth of glacial lakes

Information about the volume and mean depth of glacial lakes is of vital importance. The information helps in estimating total water volume, calculating run-off distance, and GLOF modelling **(Fujita et al., 2013)**. However, there is a lack of information about the volume and mean depth of glacial lakes, mainly due to limited bathymetric surveys of glacial lakes in the study domain. Therefore, in the present study, we attempted to estimate the volume and mean depth of glacial lakes based on the empirical equations developed by Huggel et al. (2002) (**Equation 2 & 3**). The equation was developed by Huggel et al. (2002) using bathymetric survey of glacial lakes in the Swiss Alps. The equation includes both moraine-dammed and ice-dammed glacial lakes. This is the main reason for selecting the following equations:

$$D = 0.104A^{0.42} \qquad (2)$$

$$V = 0.104A^{1.42} \qquad (3)$$

Results

Spatio-temporal distribution and growth of glacial lakes at sub-basin level

The total number of glacial lakes in the upper Ganga basin increased was 2,554 (a: 170.16 km^2) in 1990, which increased to 2,783 (a: 191.04 km^2) in 2000, 2,834 (a: 201.14 km^2) in 2010, and 3,118 (a: 210.88 km^2) in 2020 (**Fig. 3**). Between 1990 and 2020, total number of glacial lakes increased by 564 (22.08%) and total area increased by 40.72 km^2 (23.93%). In terms of decadal change, 2010-2020 observed the highest increase in total number of glacial lakes of 284 (10.02%), followed by 1990-2000 with an increase of 229 (8.97%), and 2000-2010 observed the lowest increase in the total number of glacial lakes 51 (1.83%). In terms of decadal change in total area of glacial lakes, 1990-2000 observed the maximum expansion of 20.88 km^2 (12.27%), followed by 2000-2010 with an increase of 10.41 km^2 (5.45%), and 2010-2020 observed the minimum expansion of 9.43 km^2 (4.68%) (**Table 3)**.

Table 3. Decadal change in the number and area of glacial lakes

	Number	**Area**
1990 – 2000	229 (8.97%)	20.87 (12.27%)
2000 – 2010	51 (1.83%)	10.41 (10.41%)
2010 – 2020	284 (10.02%)	9.42 (4.68%)
1990 – 2020	564 (22.08%)	40.71 (23.93%)

Out of 32 sub-basins, glacial lakes were found in 28 sub-basin in the study domain. In the updated glacial lake inventory of 2020, out of 28 sub-basins with glacial lakes, Arun have the highest number of glacial lakes 740 (23.73%), followed by Humla with 303 (11.45%), Dudh Koshi with 279 (8.95%), Tama Koshi with 251 (8.05%), Mugu with 236 (7.57%), Tamor with 234 (7.50%), Trishuli with175 (5.61%), Sun Koshi with 149 (4.78%), Bheri with 141 (4.52%), Alaknanda with 104 (3.34%), Kali Gandaki with 55 (1.76%), Tila with 51 (1.64%), Bhagirathi with 50 (1.60%), Budi Gandaki with 46 (1.48), Kali with 34 (1.09%), Marshyangdi with 33 (1.06%), Kawari and Pelkhu with 31 (0.99%) each, West Seti with 30 (0.96%), Likhu with 21 (0.67%), Bhilanga with 16 (0.51%), Tons with 15 (0.48%), Indrawati and Mandakini with 12 (0.38%) each, Koshi1 with 5 (0.16%), Trunk Karnali 4 (0.13%), and finally Pindar and Seti have 3 (0.10%) each. However, between 1990 and 2020, Alaknanda sub-basin (76.27) had the highest growth rate of numbers, and lowest was in Tons sub-basin (-6.25). Out of 28 sub-basins with glacial lakes, 22 sub-basins observed positive growth rate, 5 observed no changes in the number, and 1 sub-basin observed negative growth rate (**Fig. 3**).

In 2020, Arun have the maximum area of glacial lakes 60.38 km^2 (30%), followed by Sun Koshi with 21.70 km^2 (10.29%), Dudh Koshi with 19.49 km^2 (9.24%), Pelkhu with 17.94 km^2 (8.51%), Humla with 17.60 km^2 (8.35%), Tama Koshi with 15.52 km^2 (7.36%), Tamor with 9.22 km^2 (4.37%), Mugu with 8.20 Km^2 (3.89%), Trishuli with 7.53 km^2 (3.57%), Marshyangdi with 6.28 km^2 (2.98%), Bheri with 5.53 km^2 (2.62%), Tila with 3.33 km^2 (1.58%), Alaknanda with 2.81 km^2 (1.33%), Kali Gandaki with 2.45 km^2 (1.16%), Budi Gandaki with 1.76 km^2 (0.83%), Kali with 1.45 km^2 (0.69%), Kawari with 1.29 km^2 (0.69%), West Seti with 1.27 (0.60%), Bhagirathi with 0.99 (0.47%), Tons with 0.75 (0.35%), Mandakini with 0.73 (0.35%), Likhu with (0.29%), Bhilanga with 0.39 (0.19%), Trunk Karnali with 0.36 (0.17%), Indrawati with 0.22 (0.11%), Pindar with 0.08 (0.04%), Koshi1 with 0.06 (0.03%) and Seti with 0.05 (0.03%). Between 1990 and 2020, Mandakini sub-basin (73.28%) had the highest growth rate of area, and lowest was in Tons sub-basins (-1.19). Out of 28 sub-basins, 23 sub-basins observed positive growth rate in the area of glacial lakes, 4 sub-basins observed no change and 1 sub-basin observed negative change in the area of glacial lakes **(Fig. 3**).

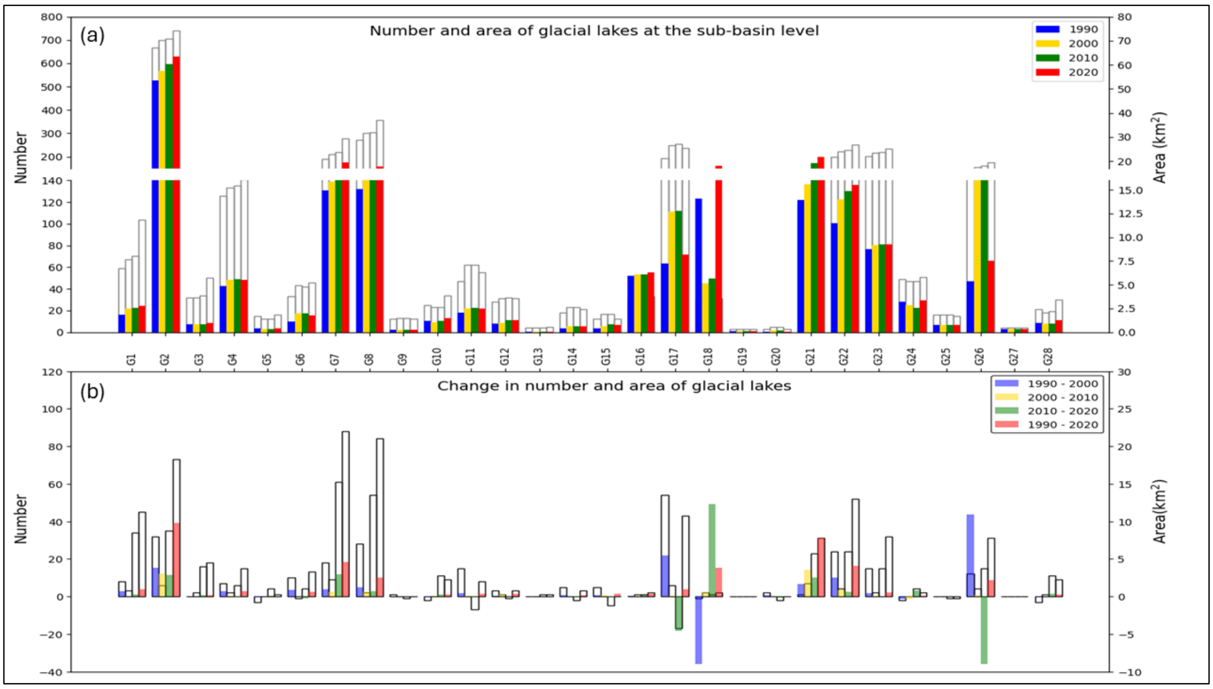

Fig. 3 (a) is showing total number and area of glacial lakes in individual sub-basin between 1990 and 2020; and (b) is showing change in the number and area of glacial lakes in individual sub-basins at the decadal level.

Estimated mean depth and volume of glacial lakes

For better understanding of glacial lake dynamics, we estimated mean depth and volume of glacial lakes using Huggel et al. (2002) empirical equations. The equations are based on the area of glacial lakes. We estimated the average mean depth of glacial lakes was 8.45 m (1990), 8.47 m (2000), 8.49 m (2010), and 8.26 m (2020). Between 1990 and 2020, the average estimated mean depth of glacial lakes decreased by -0.19 m. At the decadal level estimated mean depth of glacial lakes increased between 1990 and 2000 by 0.02 m. Similarly, 2000 and 2010 show an increase in the average estimated mean depth by 0.02 m. However, the average estimated mean depth reduced by -0.23 between 2010 and 2020 (**Fig. 4**). At the sub-basin level, for the updated glacial lake inventory of 2020, Pelkhu had the highest average estimated mean depth of glacial lakes (18.51 m), and Koshi1 had the lowest of 5.18 m. Between 1990 and 2020, 13 sub-basins shown an increase in the estimated average mean depth and 15 sub-basins shown decrease in the estimated average mean depth (**Fig. 4**).

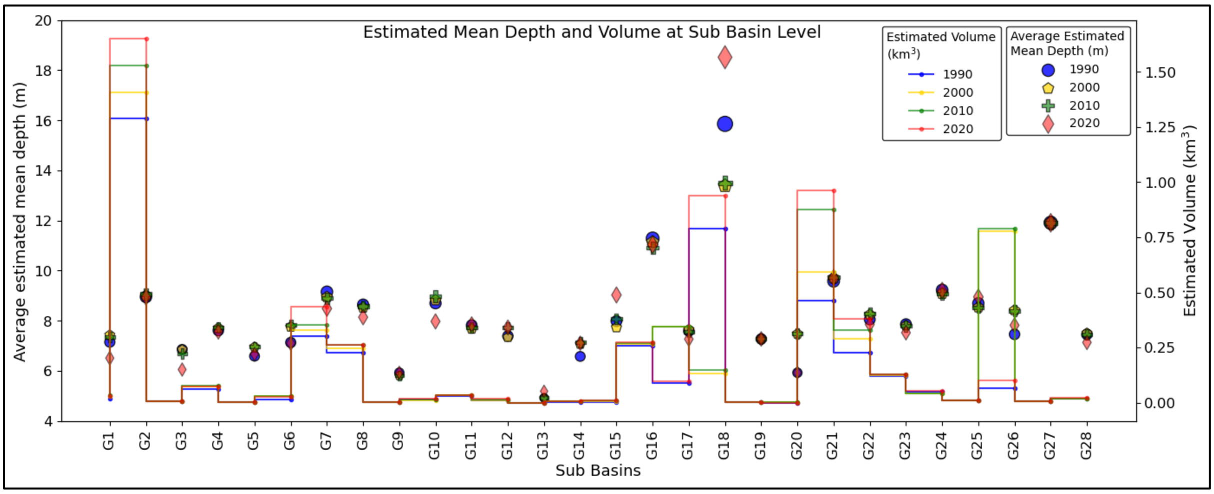

Fig. 4 Sub-basin wise distribution of estimated volume (km^3) and average estimated mean depth of glacial lakes.

Th total estimated volume of glacial lakes was 4.07 km^3 (1990), followed by 4.8 km^3 (2000), 5.33 km^3 (2010), and 5.54 km^3 (2020). Between 1990 and 2020, total estimated volume of glacial lakes increased by 1.47 km^3. At the decadal level estimated volume of glacial lakes increased by 0.73 km^3 (1990-2000), 0.53 km^3 (2000-2010), and 0.21 km^3 (2010-2020). At the sub-basin level, in 2020, Arun sub-basin (1.65 km^3) had the maximum estimated volume and Koshi1 (0.00035 km^3) had the minimum estimate volume of glacial lakes among the sub-basins **(Fig. 4)**.

Type wise changes in the glacial lakes

Based on the ICIMOD's glacial lake classification, in 2020, we were able to found M(e), M(l), M(o), B(c), B(o), supraglacial lakes and other glacial lakes in the upper Ganga basin. Out of 3118 glacial lakes, 2413 (77.39%) were M(e), followed by supraglacial lakes with 268 (8.6%), B(o) lakes with 227 (7.28%), M(l) with 158 (5.07%), other glacial lakes with 21 (0.67%), M(o) lakes with 19 (0.57%), and B(C) lakes only had 12 (0.35%). In terms of the area, out of 210.88 km^2, M(e) lakes had the highest proportion of 178 km^2 (84.83%), followed by M(l) lakes with 13.42 km^2 (6.36%), B(o) lakes with 11.22 km^2 (5.32%), supraglacial lakes with 4.88 km^2 (2.31%), other glacial lakes with 1.55 km^2 (0.73%), M(o) lakes with 0.57 km^2 (0.27%) and B(c) lakes only had glacial lake area of 0.35 km^2 (0.16%). In terms of the total estimated volume, out of 5.548 km^3, M(e) had the maximum total estimated volume of 4.986 km^3 (89.86%), followed by M(l) lakes with 0.325 km^3 (5.86%), B(o) lakes with 0.155 km^3 (2.79%), supraglacial lakes with 0.048 km^3 (0.86%), other glacial lakes with 0.024 km^3 (0.43%), M(o) with 0.006 km^3 (0.10%), and B(c) had the lowest estimated volume of glacial lakes with only 0.003 km^3 (0.05%). In terms of the estimated mean depth, other glacial lakes (9.74 m) had the highest average estimated mean depth among different types of glacial lakes, followed by M(l) lakes with 9 m, M(e) lakes with 8.50 m, B(o) lakes with 8.41 m, B(c) lakes with 7.18 m, M(o) lakes with 6.96 m, and supraglacial lakes had the lowest average estimated mean depth (5.59 m).

In terms of absolute change in the number of glacial lakes, between 1990 and 2020, M(e) shown highest increase in number of glacial lakes with 332, followed by supraglacial lakes with 208, M(l) and B(o) shown an increase of 11 glacial lake each, B(c) and other glacial lakes shown an increase of 1 glacial lake each, and M(o) observed no change in the number of glacial lakes between 1990 and 2020 **(Fig. 5**). In terms of absolute change in the area of glacial lakes between 1990 and 2020, M(e) shown maximum increase with an area of 35.80 km^2, followed by supraglacial lakes with 3.97 km^2, M(l) lakes with 0.72 km^2, B(o) lakes with 0.28 km^2, and B© with 0.03 km^2. Whereas, M(o) lakes shown a decrease of -0.05 km^2 and other glacial lakes shown a decrease of -0.03 km^2 area of the glacial lakes (**Fig. 5)**. In terms of absolute change in the volume of glacial lakes between 1990 and 2020, M(e) lakes shown an increase of 1.407 km^3, followed by supraglacial lakes with 0.038 km^3, M(l) lakes with 0.0203 km^3, B(o) lakes with 0.0025 km^3, and B(c) lakes with 0.00019 km^3. Whereas, M(o) and other glacial lakes observed an decrease 0f -0.0013 km^3 and -0.0004 km^3, respectively (**Fig. 5**). In terms of changes in the average estimated mean depth between 1990 and 2020, supraglacial lakes shown highest increase of 0.51 m, followed by M(o) with 0.04 m, and B(c) with 0.01 m. Whereas, four sub-basins shown decrease in the average estimated mean depth. Other glacial lakes shown a decline of -0.45 m, followed by M(l) with -0.05 m, B(o) with -0.08 m, and M(e) with -0.02 m (**Fig. 5**).

To further understand the type wise changes in the distribution of glacial lakes, we analyzed each sub-type at the sub-basin level.

End moraine-dammed lakes (M(e)):

M(e) had the largest share among distinct types of glacial lakes. In 1990 there were 2081 M(e) lakes, which increased to 2263 (2000), 2293 (2010), and 2413 (2020). At the sub-basin level in the out of 28 sub-basins, M(e) lakes were present in 27 sub-basins between 1990 and 2020. Arun sub-basin had the highest number of M(e) lakes across the decades. There were 594 M(e) lakes in 1990, which increased to 624 (2000), 632 (2010), and 635 (2020). Seti sub-basin had the lowest number of M(e) lakes across the decades. There were only 2 M(e) lakes in 1990, 3 (2000), 3 (2000), and 2 (2020). Between 1990 and 2020, 22 sub-basins shown increase in the number of M(e) lakes, 4 sub-basins shown no change and 1 sub-basin shown decrease in the number of M(e) lakes (**Fig. 5**).

The total area of M(e) lakes increased from 143.09 km^2 (1990), 162.55 km^2 (2000), 172.38 km^2 (2010), and 178.89 km^2 (2020). Arun sub-basin had the maximum area of M(e) lakes across the decades. The total area of M(e) lakes was 49.92 km^2 (1990), followed by 53.63 km^2 (2000), 56.53 km^2 (2010), and 58.52 km^2 (2020). Seti had the lowest total area of among the M(e) lakes across the decades. In 1990 the total area of M(e) lakes in Seti sub-basin was 0.016 km^2 (1990), followed by 0.028 km^2 (2000). Between 1990 and 2020, 25 sub-basins shown an increase in the area of M(e) lakes, 1 sub-basin shown no change, and 1 sub-basin shown decrease in the area of M(e) lakes (**Fig. 5**).

Supraglacial lakes:

In 2020, supraglacial lakes (268) had the second highest number of glacial lakes. In 1990, there were 60 supraglacial lakes, followed by 91 (2000), 111 (2010), and 268 (2020). Out of 28 sub-basins with glacial lakes, supraglacial lakes were present in only 8 (1990) sub-basins, which increased to 11 (2000), 13 (2010), and 15 (2020). Among the sub-basins, Dudh Koshi had the highest number of supraglacial lakes across the decades. There were 21 supraglacial lakes in Dudh Koshi sub-basin in 1990, which increased to 35 (2000), 43 (2010), and 86 (2020). Between 1990 and 2020, 15 sub-basin shown positive change in the number of glacial lakes, whereas no sub-basin shown negative change in the number of supraglacial lakes (**Fig. 5)**.

In terms of the share in the total area of glacial lakes, supraglacial lakes had 4th largest share. The total area of supraglacial lakes was only 0.91 km^2 in 1990, which increased to 1.81 km^2 (2000), 2.17 km^2

(2010), and 4.88 km^2 (2020). In terms of the sub-basins Dudh Koshi had the largest share of total area of supraglacial lakes. In 1990 the area of supraglacial lakes in Dudh Koshi was 0.32 km^2, which increased to 0.62 km^2 (2000), 0.75 km^2 (2010), and 1.63 Km^2 (2020). Dudh koshi sub-basins shown an increase of 1.30 km^2 between 1990 and 2020. Similar to the changes in the number of glacial lakes, all 15 sub-basin shown an increase in the area of supraglacial lakes (**Fig. 5**).

Other bedrock dammed lakes (B(o)):

In 2020, there were 227 B(o) lakes, which is third highest among different types of glacial lakes in the upper Ganga basin. In 1990, there were 216 B(o) lakes, followed by 227 (2000), 228 (2010), and 227 (2020). Between 1990 and 2020, B(o) lakes increased by 11. However, at the decadal time frame, B(o) increased by 11 (1990-2000) and 1 (2000-2010), and decreased by 1 (2010-2020). Out of 28 sub-basins, B(o) lakes were present in 19 sub-basins, across the decades. Among these 19 sub-basins, Mugu had the highest number of B(o) lakes. There were 36 B(o) lakes in Mugu in 1990, which increased to 40 in 2000 and remained the same in 2010, and in 2020 it reduced to 39 **(Fig. 5**). Between 1990 and 2020, out of 19 sub-basins with B(o) lakes, only 7 shown positive change in the number of glacial lakes, whereas 12 shown no change in the number of B(o) lakes **(Fig. 5**).

In terms of the area, B(o) lakes had the third highest share in the total glacial lake area. In 1990, the total area of B(o) lakes was 10.94 km^2, followed by 11.20 km^2 (2000), 11.22 km^2 (2010 & 2020). Between 1990 and 2020, the total area of B(o) lakes increased by 0.28 km^2. In terms of the area of B(o) lakes, Tila sub-basin had the highest area of B(o) lakes. In 1990, the total area of B(o) lakes in Tila basin was 2.105 km^2, followed by 1.832 km^2 (2000 & 2010), and 2.197 km^2 (2020). The total area of B(o) lakes increased by 0.091 km^2 between 1990 and 2020 in Tila sub-basin. However, between 1990 and 2000, the Tila sub-basin shown decrease of area by -0.27 km^2, whereas there was no change in the area of B(o) lakes in Tila sub-basin between 2000 and 2010, and the sub-basin shown maximum increase in the area of B(o) lakes between 2010 and 2020 (0.36 km^2). Between 1990 and 2020, out of 19 sub-basins with B(o) lakes, 11 shown an increase in the area of B(o) lakes, whereas 7 sub-basins shown a decrease in the area of B(o) lakes, and 1 sub-basin shown no change in the area of B(o) lakes (**Fig. 5**).

Lateral moraine dammed lakes (M(l)):

In 2020, M(l) has the fourth highest number of glacial lakes among different types of glacial lakes with 158. There were 147 M(l) lakes in 1990, which increased to 152 (2000 & 2010), and 158 (2020). Between 1990 and 2020, M(l) lakes increased by 11 glacial lakes. At the decadal level, M(l) lakes increased by 5 between 1990 and 2000, increased by 6 between 2010 and 2020. Whereas, there was no change between 2000 and 2010. At the sub-basin level, out of 28 sub-basins, M(l) lakes were present in 17 sub-basin in 1990, which increased to 19 (2000 & 2010), and 18 in 2020. Among the sub-basins, Dudh Koshi had the highest number of M(l) lakes across the decades. There 26 M(l) lakes in 1990, which increased to 28 in 2000, 2010 and 2020, respectively. Between 1990 and 2020, out of 18 sub-basins with M(l) lakes, 8 sub-basin shown increase in the number of glacial lakes, 2 sub-basin shown decrease, and 8 sub-basin shown no change in number of glacial lakes (**Fig. 5**).

In terms of the area, M(l) lakes had 2nd largest share in the total area of glacial lakes. In 1990, the total area of M(l) lakes was 12.69 km^2, which increased to 13.01 km^2 (2000), 13.11 km^2 (2010), and 13.41 km^2 (2020). Between 1990 and 2020, total area of M(l) lakes increased by 0.72 km^2. In terms of decadal change, 1990-2000 shown the highest increase in the area of M(l) lakes (0.32 km^2), followed by 2010-2020 (0.29 km^2) and lowest increase was shown in 2000-2010 (0.09 km^2). In terms of the sub-basins, Dudh koshi sub-basin had the maximum share in the total area of M(l) lakes across the glacial lake inventories. In 1990, area of M(l) lakes in Dudh Koshi sub-basin was 3.582 km^2, which decreased to 3.542 (2000 & 2010), and again increased to 3.584 km^2 (2020). Between 1990 and 2020, at the sub-basin level, out of 18 sub-basin with M(l) lakes, 12 shown increase in the absolute area of M(l) lakes, 5 shown negative change and 1 shown no change in the area of M(l) lakes (**Fig. 5**).

Other glacial lakes:

In terms of number of glacial lakes, other glacial lake is 5th largest among the sub-types. There were 20 other glacial lakes in 1990, 2000, and 2010, respectively, which increased to 21 in 2020. Between 1990 and 2020, other glacial lakes increased by 1. At the sub-basin level, out of 28 sub-basins, other glacial lakes were present in 8 sub-basins across the glacial lake inventories of 1990, 2000, 2010, and 2020.

Out of 8 sub-basins, Mugu (4) had the highest number of other glacial lakes in 1990. For the year 2000 and 2010, Mugu (4) and Humla (4) shared the highest number of other glacial lakes. In 2020, Humla (5) had the highest number of other glacial lakes. Between 1990 and 2020, out of 8 sub-basins, only 1 sub-basin shown positive change in the number of other glacial lake, 1 sub-basin shown negative change in the number of other glacial lakes, and 6 sub-basins shown no change in the number of other glacial lakes (**Fig. 5**).

Other glacial lakes ranks 5th in the type wise distribution of glacial lake area. In 1990 the total area of other glacial lakes was 1.577 km^2, which reduced to 1.484 km^2 (2000 & 2010), and 1.546 km^2 (2020). Between 1990 and 2020, the total area of other glacial lakes reduced by -0.03 km^2. In terms of decadal change in the area of other glacial lakes, there was a negative change of -0.03 km^2 (1990-2000), no change in the area (2000-2010), and positive change of 0.06 km^2 (2010-2020). Out of the 8 sub-basins with other glacial lakes, Tamor sub-basin had the largest share in the area of other glacial lakes. In 1990, 2000 and 2010, the area of other glacial lakes in Tamor sub-basin was 0.438 km^2, which reduced to 0.369 km^2 in 2020. Between 1990 and 2020, 4 sub-basin shown increase and 3 shown decrease in the area of other glacial lakes (**Fig. 5)**.

Other moraine dammed lakes (M(o)):

According to the updated glacial lake inventory of glacial lake (2020), M(o) lakes ranks 6th in terms of the number of different types of glacial lake. In 1990, there were 19 M(o) lakes, which reduced to 18 (2000 and 2010), and again increased to 19 (2020). Between 1990 and 2020, M(o) lakes shown no change in the number of glacial lakes. However, between 1990 and 2000, M(o) lakes shown decrease of 1 glacial lake, and between 2010 and 2020, M(o) lakes shown an increase of 1 glacial lake. Out of 28 sub-basins with glacial lakes, M(o) lakes were present in 6 sub-basins across the decades. Out of 6 sub-basins with M(o) lakes, in 1990 Pelkhu (5) and Tama Koshi (5) had the highest number of M(o) lakes. Whereas for 2000, 2010 and 2020, Tama Koshi (5) had the highest number of M(o) lakes. Between 1990 and 2020, out of 8 sub-basins, 1 sub-basin shown positive change, 1 sub-basin shown negative change and 6 sub-basin shown no change in the number of glacial lakes (**Fig. 5**).

In terms of the share in the total area of glacial lakes, M(o) lakes ranks 6th. In 1990, the total area of M(o) lakes was 0.622 km^2, which reduced to 0.623 km^2 (2000 & 2010), and 0.574 km^2 in 2020. Between 1990 and 2020, the area of M(o) lakes reduced by -0.047 km^2. At the decadal level, the area of M(o) lakes increased by 0.00089 km^2 (1990-200), shown no change in the area of M(o) lakes between 2000 and 2010, and the area of M(o) lakes reduced by -0.048 km^2 between 2010 and 2020. In terms of the area of M(o) lakes at the sub-basin level, Pelkhu had the maximum area of 0.404 km^2 (1990, 2000 and 2010), and 0.337 km^2 in 2020. Between 1990 and 2020, out of 8 sub-basins, 3 sub-basins shown increase in the area of M(o) lakes and 3 sub-basins shown decrease in the area of M(o) lakes (**Fig. 5**).

Cirque lakes (B(c)):

B(C) had the lowest number of glacial lakes among different types of glacial lakes, across the glacial lake inventories of 1990, 2000, 2010 and 2020. In 1990, there were only 11 B(c) lakes, which increased to 12 (2000, 2010 and 2020). Between 1990 and 2020, total number of B(c) lakes increased by 1. At the decadal level, B(c) lakes increased by 1 between 1990 and 2000, whereas no change was shown in the number of B(c) between (2000 and 2010) and (2010 and 2020). Out of 28 sub-basins with glacial lakes, B(c) lakes were present in 6 sub-basins (1990) and 7 sub-basins (2000, 2010 and 2020). Among the 7 sub-basins with B(c) lakes, Humla sub-basin had the highest number of B(c) lakes (5) for 1990, 2000, 2010, and 2020, respectively. Between 1990 and 2020, only 1 sub-basin (Sun Koshi) shown positive change in the number of glacial lakes, whereas other 6 sub-basins shown no change in the number of B(c) lakes.

B(c) lakes had the lowest area of glacial lakes, and ranks 7th among the area of different types of glacial lakes, across the glacial lake inventories of 1990, 2000, 2010, and 2020. In 1990, the total area of B(c) lakes was 0.31 km^2, followed by 0.341 km^2 (2000), 0.341km^2 (2010), and 0.345 km^2 (2020). Between 1990 and 2020, the total area of B(c) lakes increased by 0.025 km^2. Among the decades, the area of B(c) lakes increased by 0.021 km^2 (1990-2000), no change in the area of B(o) lakes (2000-2010), and 0.0036 km^2 (2010-2020). At the sub-basin level, out of 7 sub-basin, Humla sub-basin had the largest share in the total area of B(c) lakes with an area of 0.129 km^2 across the glacial lake inventories of 1990, 2000, 2010 and 2020. Between 1990 and 2020, out of 7 sub-basins with B(c) lakes, 2 shown increase, 2 shown decrease, and 3 sub-basins shown no change in the area of B(c) lakes in the upper Ganga basin (**Fig. 5**).

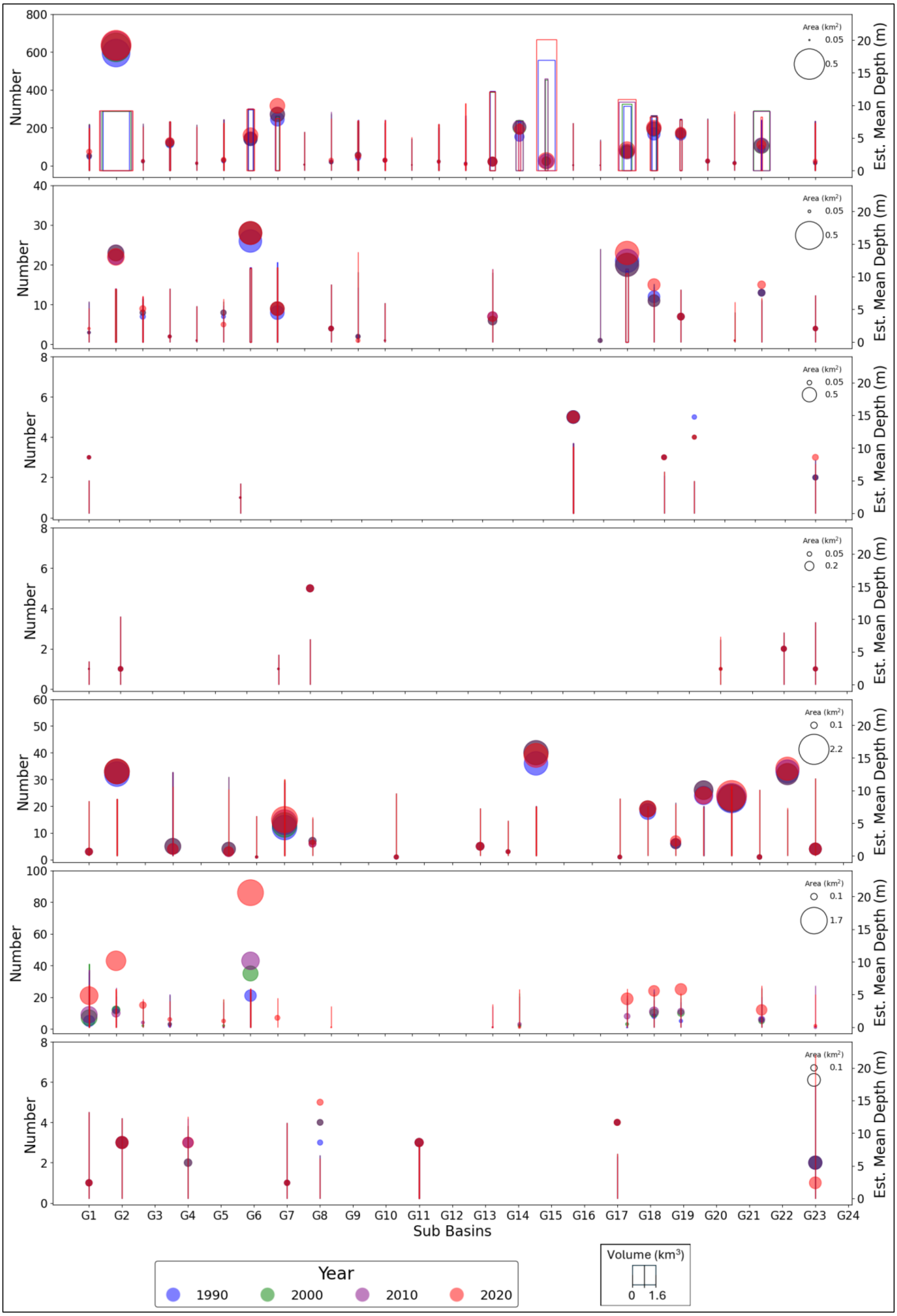
Number
Est. Mean Depth (m)
Area (km²)
Sub Basins
G1 G2 G3 G4 G5 G6 G7 G8 G9 G10 G11 G12 G13 G14 G15 G16 G17 G18 G19 G20 G21 G22 G23 G24
Year
1990 2000 2010 2020
Volume (km³)
0 1.6

Fig. 5 Type-wise changes in the glacial lakes in terms of number, area, estimated volume and average estimated mean depth.

Altitudinal distribution of glacial lakes:

Altitude plays a crucial role in identifying glacial lakes in the upper Ganga basin. The lowest altitude of glacial lakes was 3331 m asl and the highest altitude was 6216 m asl. The mean elevation of glacial lakes in the upper Ganga basin was 5045 m asl(1990), which increased to 5053.37 m asl (2000), and reduced to 5053 for 2010 and 2020, respectively. To understand the altitudinal distribution of glacial lakes, we divided glacial lakes into 16 zones based on the elevation of the glacial lakes (**Fig. 6**). The elevation zone of 5200 m – 5400 m had the largest share in the number of glacial lakes across the glacial lake inventories. In 1990 the elevation zone had 461 (18.05%) glacial lakes, which increased to 523 (18.79%) in 2000, 529 (18.66%) in 2010, and 585 (18.76%) **(Fig. 6**). However, between 1990 and 2020, the elevation zone of 5000 m – 5200 m shown highest increase in the number of glacial lakes (131). At the decadal level, between 1990 and 2000, the elevation zone 5200 m – 5400 m shown the highest increase in the number of glacial lakes (62). Between 2000 and 2010, the elevation zone of 5000 m – 5200 m shown the highest increase in the number of glacial lakes (19). And between 2010 and 2020, the elevation zone 5000 m – 5200 m shown the highest increase in glacial lakes (66).

In terms of the area of glacial lakes, the elevation zone of 5200 m – 5400 m, had the largest share of the total area of glacial lakes across the glacial lake inventories. In 1990, the total area of glacial lakes in the elevation zone of 5200 m – 5400 m was 41.72 km^2 (24.52%), which increased to 47.25 km^2 (24.73%) in 2000, 50.05 km^2 (24.89%) in 2010, and 52.60 km^2 (24.94%) in 2020. However, between 1990 and 2020, the elevational zone of 5000 m – 5200 m asl shown highest absolute change in the total area of glacial lakes with an increase of 12.58 km^2 (**Fig. 6**).

In terms of the estimated volume of glacial lakes, the elevation zone of 5200 m – 5400 m, had the largest share of the total area of glacial lakes across the glacial lake inventories. In 1990, the total area of glacial lakes in the elevation zone of 5200 m – 5400 m was 1.47 km^3 (36.26%), which increased to 1.67 km^3

(34.77%) in 2000, 1.82 km^3 (34.17%) in 2010, and 1.89 km^3 (34.11%) in 2020. Between 1990 and 2020, the altitude zone of 5000 m -5200 m shows the highest absolute change in the total estimated volume of glacial lakes with an increase of 0.576 km^3 (**Fig. 6**).

In terms of the average estimated mean depth of glacial lakes based on the elevation of the glacial lakes, the altitude zone of 3400 m – 3600 m had the highest average estimated mean depth in 1990 (12.48 m), 2010 (14.84 m) and 2020 (14.89 m). However, in the year 2000 the altitude zone of 3600 m – 3800 m had the highest estimated mean depth of 13.11 m. Between 1990 and 2020, the altitude of 3400 m – 3600 m shown the highest increase in the average estimated mean depth of 2.44 m (**Fig. 6)**.

In terms of the elevation of the glacial lakes at the sub-basin level, in 2020, KaliGandaki (5580 m) had the highest mean elevation of glacial lakes, followed by Koshi1 (5558 m), Pelkhu (5406.26 m), Tama Koshi (5219.21 m), Arun (5185.73 m), Humla (5119.94 m), Alaknanda (5105.09 m), Sun Koshi (5085.57 m), Mugu (5053.98 m), Dudh Koshi (5041.61 m), Trishuli (4984.02 m), Bhagirathi (4983.94 m), Bheri (4977.29 m), Tamor (4807.48 m), West Seti (4806.17 m), Marshyangdi (4767.85 m), Budi Gandaki (4745.07 m), Likhu (4674.81 m), Kawari (4665.9 m), Kali (4662.88 m), Indrawati (4630.08 m), Mandakini (4575.25 m), Bhilanga (4509.75 m), Trunk Karnali (4476.5 m), Tons (4452.87 m), Tila (4417.55 m), Pindar (4404.67 m), and Seti (4116.33 m). However, between 1990 and 2020, 13 sub-basin shown increase, 4 sub-basins shown no change, and 11 sub-basins shown decrease in the elevation of glacial lakes. Among the sub-basins, between 1990 and 2020, Likhu sub-basin shown highest change in the elevation of glacial lakes with 62.97 m, and Bhagirathi shown the lowest change in the elevation of glacial lakes with -220.71 m.

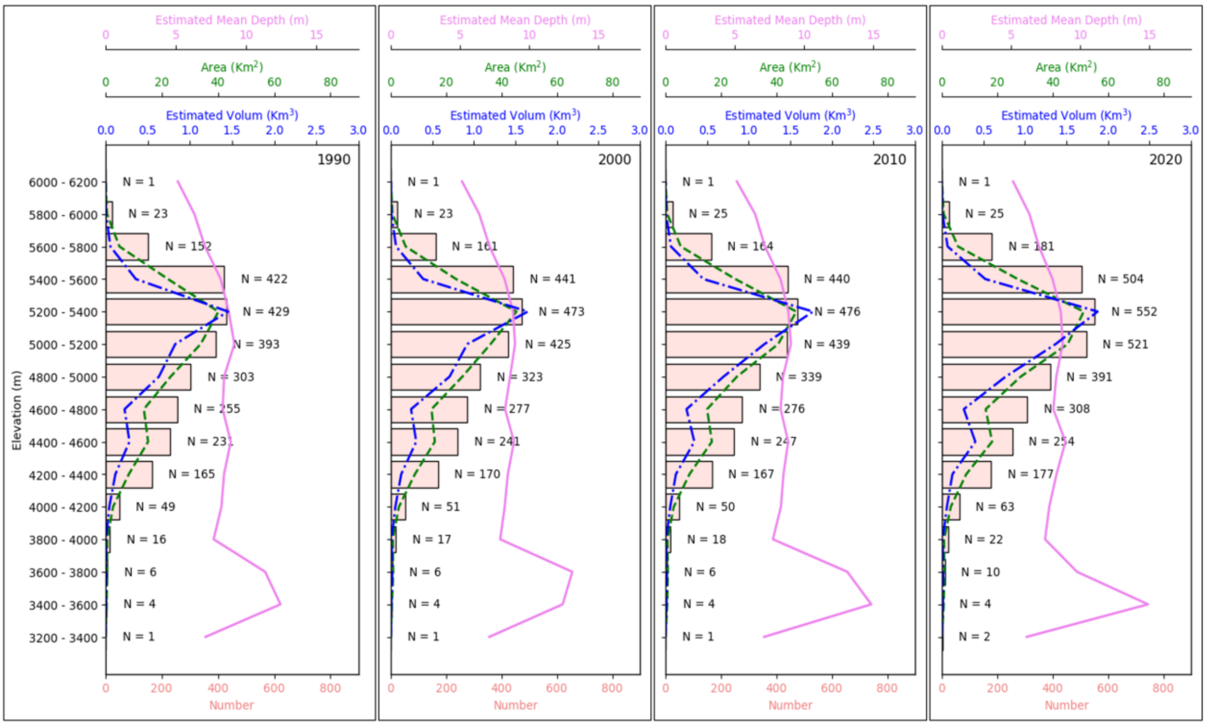

Fig. 6 Altitudinal changes in the number, area, estimated volume and average estimated mean depth of glacial lakes.

Newly emerged and disappeared:

New emerged and disappeared glacial lakes plays vital role in the growth of glacial lakes in the upper Ganga basin. Between 1990 and 2020, 651 new glacial lakes emerged, which in 2020, had total glacial lake area of 17.10 km^2, estimated volume of 0.247 km^3, average estimated mean depth of 6.15 m, and mean elevation of 5095.84 m. At the decadal level, 2010 and 2020 shown the highest increase in the number (443) of the glacial lakes, followed by 1990 – 2000 (238), and 2000 – 2010 (66) **(Fig. 7)**. In terms of the sub-basins, 22 sub-basins shown appearance of emerged glacial lakes, and 6 sub-basins reported no appearance of emerged glacial lakes between 1990 and 2020. Out of the 22 sub-basins which shown emergence of new glacial lakes, Arun sub-basin had the highest number of newly emerged glacial lakes (96) **(Fig. 7**). However, in terms of the area of newly emerged glacial lakes at the sub-basin level, Pelkhu sub-basin had the highest total area of emerged glacial lakes (2.89 km^2) **(Fig. 7**).

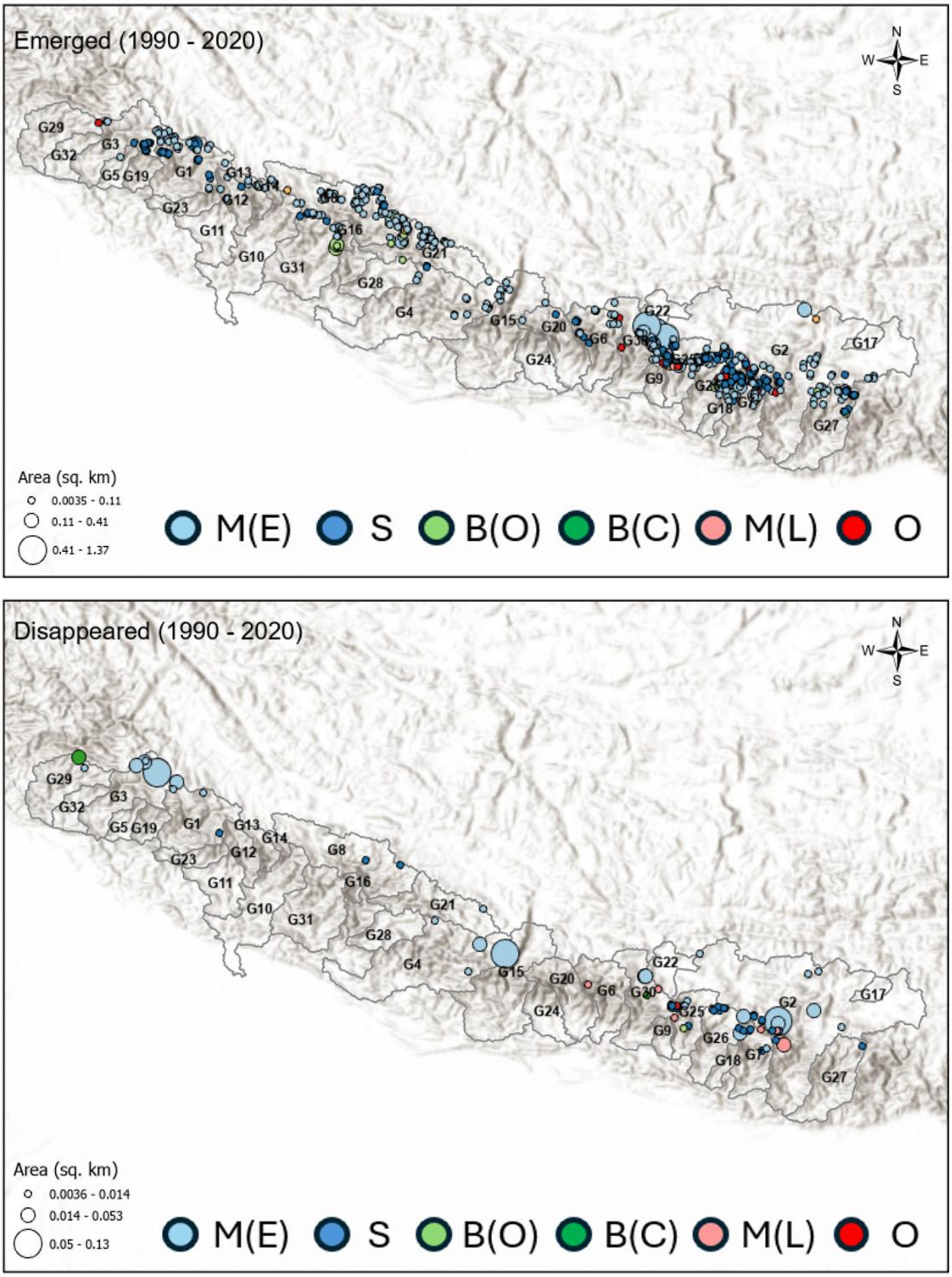

Fig. 6 Emerged and disappeared glacial lakes between 1990 and 2020. Different colors are showing different types of emerged and disappeared glacial lakes. The size of markers is indicating the area of emerged and disappeared glacial lakes.

In terms of the disappeared glacial lakes, between 1990 and 2020, 72 glacial lakes disappeared, with total area of 1.02 km^2, total estimated volume of $2.467*10^{-11}$ km^3, average estimated mean depth of 5.16 m, and mean elevation of 5128.23 m. At the decadal level, in 2010 – 2020, highest number of glacial lakes disappeared with 71 glacial lakes, followed by 1990 – 2000 (67), and 2000 – 2010 (14) **(Fig. 7**). Out of 28 sub-basins, 14 sub-basins observed disappearance and 14 sub-basins observed no disappearance of glacial lakes between 1990 and 2020. Among the 14 sub-basins, which shown disappearance of glacial lakes, Arun had the highest number of disappeared glacial lakes (17) and disappeared area of glacial lakes (0.32 km^2) **(Fig. 7**).

Finally, among different types of glacial lakes, M(e) lakes had the highest number of emerged lakes (n: 375, a: 12.38 km^2), followed by supraglacial lakes (n: 239, a: 3.79 km^2), M(l) lakes (n: 19, a: 0.44 km^2), B(o) lakes (n: 12, a: 0.38 km^2), other glacial lakes (n: 3, a: 0.03 km^2), M(o) lakes (n: 2, a: 0.032 km^2), and B(c) lakes had the lowest number of emerged lakes (n: 1, a: 0.032 km^2). In terms of the different types of disappeared glacial lakes, M(e) lakes had the highest number of disappeared lakes (n: 33, a: 0.679 km^2), followed by supraglacial lakes (n: 29, a: 0.221 km^2), M(l) lakes (n: 7, a: 0.107 km^2), M(o) lakes (n: 2, a: 0.013 km^2), other glacial lakes (n: 1, a: 0.005 km^2), and B(c) and B(o) lakes observed no disappearance between 1990 and 2020 (**Fig. 7**).

Discussion

The upper Ganga basin in the HinduKush-Karakoram-Himalayas (HKH) have been focus point of several studies related to glacial lake inventories, highlighting changing nature of glacial lakes and rising GLOF risk in the study domain (**Nie et al., 2013; Maharjan et al., 2018; Rao et al., 2021**). Previous studies successfully highlighted the expansion of glacial lakes in the study domain using remote sensing data (**Nie et al., 2013; Zhang et al., 2015; Nie et al., 2017**). However, there is no consistency in the results of already existing glacial lake inventories (**Table 4)**. Mainly because of differences in the data sources and methods used, it is difficult to compare these inventories. In the present study, we mapped each glacial lake ≥2,400 m asl in the study domain. Minimum elevation plays an important role in identifying glacial lakes. We found majority of the study mapped glacial lakes in the study domain between **2,400 m to 6,000 m asl (Ives et al. 2010; Maharjan et al. 2018**).

Table 4: Comparison of previous studies

Author(s)	Study Area	Data sources	Method	Criteria	Number and Area	Year
Nie et al. (2013)	Central Himalayas	Landsat (TM/ETM) (n: 56)	Semi – automated	Area: ≥ 0.0081 km^2	1191 (a: 168.4 km^2) 1290 (a: 185.28 km^2) 1303 (a: 190.84 km^2) 1314 (a: 197.22 km^2)	1990 2000 2005 2010
Worni et al. (2013)	Indian Himalayas	Landsat (ETM+)	Automated	Area: > 0.01 km^2	251	2000±2
Aggarwal et al. (2017)	Sikkim	Resourcesat-2 and Cartosat-2 DEM	Semi – automated		1,104 (a: 30.49 km^2)	2013
Khadka et al. (2018)	Nepal Himalaya	Landsat (MSS, TM, & OLI) (n: 45) & SRTM DEM	Semi – automated	Area: ≥ 0.0036 km^2 Slope: < 10° Shaded Relief: > 0.25 Elevation: ≥ 2450 m	1541 (80.95 ± 15.25 km^2)	2017
Zhang et al. (2015)	Ganga basin	Landsat (TM/ETM+)	Manual mapping	Area: > 0.003 km^2 Distance from glacier: 10 km	294 (30 ± 5.2 km^2) 364 (45.8 ± 7.3 km^2)	1990 2010
Maharjan et al. (2018)	Ganga basin	Landsat (TM & ETM+) (n: 151) and SRTM DEM	Semi – automated	Area: > 0.003 km^2	4,082 (a: 208.59 km^2)	2005±2
Pandey et al. (2021)	Uttarakhand	Resourcesat-2 (n: 8), Landsat (TM) (n: 9), and SRTM DEM	Automated	Area: > 0.0005 km^2, Distance from glacier: 2 km	1,353 (a: 7.96 km^2)	2015

Rao et al. (2021)	Ganga basin	Resourcesat-2 (n: 105) and Cartosat DEM	Manual mapping	Area: > 0.0025 km^2	4,707 (a: 206.85 km^2)	2016-2018
Li et al. (2022)	Central Himalayas	Landsat (TM, ETM+, & OLI) (n: 651) & ASTER DEM	Semi – automated	Distance from Glacier: < 10 km Area:	438 (53.70 ± 6.49 km^2) 677 (70.13 ± 9.12 km^2) 759 (75.88 ± 9.90 km^2) 722 (75.56 ± 9.34 km^2) 833 (80.24 ± 10.73 km^3) 845 (85.01 ± 10.88 km^2) 1149 (100.75 ± 14.33 km^2)	1990 1995 2000 2005 2010 2015 2020

Minimum mapping area and slope of bedrock are other important factors employed in identifying the glacial lakes. Previous studies used a minimum mapping area between **0.0005 km^2 and 0.05 km^2 (Table 4)** and slope of less than 20° to map the glacial lakes **(Aggarwal et al., 2017; Pandey et al., 2021; Rao et al. 2021; Li et al., 2022)**. This is another reason for the discrepancies in the number of glacial lakes in the study domain in different studies. The main reason for the discrepancies in the minimum mapping area and spatial resolution of the different data sources (**Li et al., 2022**). In the present study, a minimum mapping area of 0.0036 km^2 was selected to map the glacial lakes, because minimum of 4 pixels of Landsat images (spatial resolution: 30 m) is required to correctly identify a feature (**Mal et al., 2020**).

In our study, the number and area of glacial lakes increased by **564 (22.08%) and 40.71 km^2 (23.93%** respectively between 1990 and 2020. Previous studies confirms expansion of glacial lakes since 1990s in the upper Ganga basin **(Nie et al. 2013; Zhang et al., 2015; Nie et al. 2017; Li et al., 2022)**. Li et al. (2022) shown that number of glacial lakes increased by 711 and the area increased by 47.05 km^2 in the central Himalayan region**.** Nie et al. (2013), examined the evolution of glacial lakes for the central Himalayan region and found that the number of glacial lakes increased by 123 and area of glacial lakes increased by 28.81 km^2 **(Table 4). Pandey et al. (2021)** studied the evolution of glacial lakes in the state of Uttarakhand (western part of upper Ganga basin), and found that number of glacial lakes increased by ~9% and area of glacial lakes increased by ~57% between 1994 and 2017. And **Khadka et al. (2018),** found that number of glacial lakes increased by 404 (35.53%) and area increased by 16.39 km^2 (25%) in the Nepal Himalayas between 1987 and 2017. Present study align with the result of previous studies on the expansion of glacial lakes in the central Himalayan region. However, the rate of expansion was different in different studies, mainly because of different methods used to map the glacial lakes.

Furthermore, we estimated the volume and mean depth of glacial lakes in the study domain. In our knowledge, there is no present study which attempted to estimate the volume and mean depth for the central Himalayan region at the sub-basin scale. We used area-based empirical equation developed by **Huggel et al. (2002).** There are several other equations developed to estimate the volume and mean depth of glacial lakes **(Sakai 2012; Fujita et al., 2013; Cook & Quincey, 2015; Qi et al. 2022).** However, we used Huggel et al. (2002) equations because they developed two separate equations for estimating volume and mean depth using the same dataset.

Conclusion:

Our results agrees with the previous studies and shown expansion of glacial lakes in the upper Ganga basin at a rapid rate. Between 1990 and 2020, number of glacial lakes increased by 22.08% and the area of glacial lakes increased by 23.93%. We recommend further continues monitoring of glacial lakes at the sub-basin level for developing early warning systems for GLOF predictions and mitigation. We further found that number of glacial lakes increased at a much faster rate in the western part of the upper

Ganga basin as compared to the east part. The reason for east to west gradient should further investigated in the future studies. Furthermore, the volume and mean depth estimates can help researchers and government agencies in estimating total water volume of glacial lakes and identification of potentially hazardous glacial lakes in the upper Ganga basin.

Acknowledgement:

This work is supported by doctoral research grant provided by German Academic Exchange Service (DAAD) (funding ID: 57507871). The authors are thankful towards United States Geological Survey (USGS) for providing free access to the Landsat satellite imagery.

References:

Aggarwal, S., Rai, S. C., Thakur, P. K., & Emmer, A. (2017). Inventory and recently increasing GLOF susceptibility of glacial lakes in Sikkim, Eastern Himalaya. Geomorphology, 295, 39-54. https://doi.org/10.1016/j.geomorph.2017.06.014

Ahmed, R., Wani, G. F., Ahmad, S. T., Sahana, M., Singh, H., & Ahmed, P. (2021). A review of glacial lake expansion and associated glacial lake outburst floods in the Himalayan region. *Earth Systems and Environment*, *5*(3), 695-708. https://doi.org/10.1007/s41748-021-00230-9

Bhambri, R., Misra, A., Kumar, A., Gupta, A. K., Verma, A., & Tiwari, S. K. (2018). Glacier lake inventory of Himachal Pradesh. Himalayan Geol, 39(1), 1-32.

B. Simhadri Rao, Ankit Gupta, Sweta, Ruhi Maheshwari, P. Venkat Raju, V. Venkateshwar Rao (2021). "Glacial Lake Atlas of Ganga River Basin". National Remote Sensing Centre, ISRO, Hyderabad, India, pp. 1-194.

Cook, S. J., & Quincey, D. J. (2015). Estimating the volume of Alpine glacial lakes. *Earth Surface Dynamics*, *3*(4), 559-575. https://doi.org/10.5194/esurf-3-559-2015

Dou, X., Fan, X., Wang, X., Yunus, A. P., Xiong, J., Tang, R., ... & Xu, Q. (2023). Spatio-temporal evolution of glacial lakes in the Tibetan Plateau over the past 30 years. Remote Sensing, 15(2), 416.

Fujita, K., Sakai, A., Takenaka, S., Nuimura, T., Surazakov, A. B., Sawagaki, T., & Yamanokuchi, T. (2013). Potential flood volume of Himalayan glacial lakes. *Natural Hazards and Earth System Sciences*, *13*(7), 1827-1839. https://doi.org/10.5194/nhess-13-1827-2013

Huggel et al. (2002). Remote sensing based assessment of hazards from glacier lake outbursts: a case study in the Swiss Alps. Can. Geotech. J., 39 (2002), pp. 316-330. https://doi.org/10.1139/t01-099

Ives, J. D., Shrestha, R. B., & Mool, P. K. (2010). Formation of glacial lakes in the Hindu Kush-Himalayas and GLOF risk assessment (pp. vi+-56).

Krishnan, S., & Indu, J. (2023). Assessing the potential of temperature/vegetation index space to infer soil moisture over Ganga Basin. Journal of Hydrology, 621, 129611. https://doi.org/10.1016/j.jhydrol.2023.129611

Khadka, N., Zhang, G., & Thakuri, S. (2018). Glacial lakes in the Nepal Himalaya: Inventory and decadal dynamics (1977–2017). Remote Sensing, 10(12), 1913. https://doi.org/10.3390/rs10121913

Li, W., Wang, W., Gao, X., Wang, X., & Wang, R. (2022). Inventory and Spatiotemporal Patterns of Glacial Lakes in the HKH-TMHA Region from 1990 to 2020. Remote Sensing, 14(6), 1351. https://doi.org/10.3390/rs14061351

Nie, Y., Liu, Q., & Liu, S. (2013). Glacial lake expansion in the Central Himalayas by Landsat images, 1990–2010. PloS one, 8(12), e83973. https://doi.org/10.1371/journal.pone.0092654

Nie, Y., Sheng, Y., Liu, Q., Liu, L., Liu, S., Zhang, Y., & Song, C. (2017). A regional-scale assessment of Himalayan glacial lake changes using satellite observations from 1990 to 2015. Remote Sensing of Environment, 189, 1-13. https://doi.org/10.1016/j.rse.2016.11.008

Maharjan, S. B., Mool, P. K., Lizong, W., Xiao, G., Shrestha, F., Shrestha, R. B., ... & Baral, P. (2018). The Status of Glacial Lakes in the Hindu Kush Himalaya-ICIMOD Research Report 2018/1. International Centre for Integrated Mountain Development (ICIMOD).

Mal, S., Kumar, A., Bhambri, R., Schickhoff, U., & Singh, R. B. (2020). Inventory and spatial distribution of glacial lakes in Arunachal Pradesh, Eastern Himalaya, India. Journal of the Geological Society of India, 96, 609-615. Doi: https://doi.org/10.1007/s12594-020-1610-1

Mal, S., Allen, S. K., Frey, H., Huggel, C., & Dimri, A., P. (2021). Sectorwise Assessment of Glacial lake outburst flood danger in the Indian Himlaayan Region, Mountain Research and Development 41(1), R1-R12 (2021).

Pandey, P., Ali, S. N., & Champati Ray, P. K. (2021). Glacier-glacial lake interactions and glacial lake development in the central Himalaya, India (1994–2017). Journal of Earth Science, 1-12. https://doi.org/10.1007/s12583-020-1056-9

Shugar, D. H., Burr, A., Haritashya, U. K., Kargel, J. S., Watson, C. S., Kennedy, M. C., ... & Strattman, K. (2020). Rapid worldwide growth of glacial lakes since 1990. *Nature Climate Change*, *10*(10), 939-945. https://doi.org/10.1038/s41558-020-0855-4

Qi, M., Liu, S., Wu, K., Zhu, Y., Xie, F., Jin, H., ... & Yao, X. (2022). Improving the accuracy of glacial lake volume estimation: A case study in the Poiqu basin, central Himalayas. *Journal of Hydrology*, *610*, 127973. https://doi.org/10.1016/j.jhydrol.2022.127973

Veh, G., Korup, O., von Specht, S., Roessner, S., & Walz, A. (2019). Unchanged frequency of moraine-dammed glacial lake outburst floods in the Himalaya. Nature Climate Change, 9(5), 379-383. https://doi.org/10.1038/s41558-019-0437-5

Worni, R., Huggel, C., & Stoffel, M. (2013). Glacial lakes in the Indian Himalayas—From an area-wide glacial lake inventory to on-site and modeling based risk assessment of critical glacial lakes. Science of the Total Environment, 468, S71-S84. https://doi.org/10.1016/j.scitotenv.2012.11.043

Zhang, G., Yao, T., Xie, H., Wang, W., & Yang, W. (2015). An inventory of glacial lakes in the Third Pole region and their changes in response to global warming. Global and Planetary Change, 131, 148-157. Doi: https://doi.org/10.1016/j.gloplacha.2015.05.013

Zhang, G., Bolch, T., Yao, T., Rounce, D. R., Chen, W., Veh, G., ... & Wang, W. (2023). Underestimated mass loss from lake-terminating glaciers in the greater Himalaya. Nature Geoscience, 16(4), 333-338. https://doi.org/10.1038/s41561-023-01150-1

Supplementary Material

S1 Table 1: *Name of all peaks above 8000 m located in the HKH.*

Ranking	**Name**	**Elevation (m)**	**Latitude**	**Longitude**	**River Basin**
1	Mt. Everest	8,848	27°59'16.17"N	86°55'30.08"E	Ganga
2	K2	8,611	35°52'45.64"N	76°30'53.34"E	Indus
3	Kangchenjunga	8,586	27°42'7.72"N	88° 8'52.00"E	Brahmaputra
4	Lhotse	8,516	27°57'45.11"N	86°56'0.96"E	Ganga
5	Makalu	8,485	27°53'8.17"N	87° 5'7.88"E	Ganga
6	Cho You	8,188	28° 5'45.35"N	86°39'40.91"E	Ganga
7	Dhaulagiri	8,167	28°41'56.35"N	83°29'15.53"E	Ganga
8	Manaslu	8,163	28°33'8.12"N	84°33'25.92"E	Ganga
9	Nanga Parbat	8,126	35°14'28.16"N	74°35'20.63"E	Indus
10	Annapurna	8,091	28°36'49.33"N	83°52'20.07"E	Ganga
11	Gasherbrum I	8,080	35°43'32.54"N	76°42'10.96"E	Indus
12	Gasherbrum II	8,051	35°45'30''N	76°39'12'' E	Indus
13	Gasherbrum III	8,035	35°45'34.32"N	76°38'29.97"E	Indus
14	Shishapangma	8,027	28°21'20.43"N	85°46'37.79"E	Ganga

S1 Table 2: *List of glacial lakes used in the study to develop the empirical equations.*

Serial No	Name	Lat	Long	Type	Study	Region	Area (km^2)	Mean Depth (m)	Volume (km^3)	Circularity ratio
1	Gangbal	34°25'52" N	74°55'3 "E	M(e)	Field-based	Upper Indus	1.640	35.97	0.0590	0.326988068
2	Kela Tsho	33°59'55" N	77°58'41"E	B(o)	Field-based	Upper Indus	0.47	25.75	0.0122	0.432126567
3	Lato	33°40'17" N	77°36'26"E	M(e)	Field-based	Upper Indus	0.09	10.57	0.0009	0.215155901
4	Gya	33°37'3"N	77°36'49"E	M(e)	Field-based	Upper Indus	0.11	15.57	0.0018	0.393935272
5	Gadsar	34°25'16" N	75° 3'27"E	M(e)	Literature-based	Upper Indus	0.40	26.35	0.0107	0.526045963
6	Neelkanth	32°45'28" N	76°57'8 "E	M(l)	Literature-based	Upper Indus	0.02	5.78	0.0001	0.663045466
7	Geepeang Gath	32°31'32" N	77°13'10"E	M(e)	Literature-based	Upper Indus	0.98	33.19	0.0325	0.272557007
8	Spong Togpo	34° 3'6"N	76°43'4 "E	M(e)	Literature-based	Upper Indus	0.15	15	0.0023	0.507474679
9	Kapuche	28°26'42" N	84° 6'59"E	M(e)	Literature-based	Upper Ganga	0.12	11.83	0.0014	0.486879529

10	Bhairabkunda	27°59'22"N	85°52'46"E	B(c)	Literature-based	Upper Ganga	0.16	15	0.0024	0.480782243
11	Gosaikunda	28° 4'55"N	85°24'54"E	B(c)	Literature-based	Upper Ganga	0.13	14	0.0018	0.46326
12	Shishapangma NO. 1	28°26'38"N	85°46'51"E	M(e)	Literature-based	Upper Ganga	0.64	39.16	0.025140	0.223995
13	Tsho Rolpa Glacier Lake	27°51'39"N	86°28'32"E	M(e)	Literature-based	Upper Ganga	1.73	51.21	0.0888	0.172944432
14	Gokyo Valley 4	27° 59′ N	86° 41′ E	M(l)	Literature-based	Upper Ganga	0.65	27.37	0.0179	0.46803
15	Gokyo Valley 3	27° 57′ N	86° 42′ E	M(l)	Literature-based	Upper Ganga	0.43	25.27	0.0110	0.383102
16	Gokyo Valley 2	27° 56′ N	86° 42′ E	M(l)	Literature-based	Upper Ganga	0.17	21.72	0.0038	0.51035
17	Imja Lake	27°53'52"N	86°55'16"E	M(e)	Literature-based	Upper Ganga	1.21	52.60	0.0636	0.358499228
18	Lower Barun	27°50'30"N	87° 4'49"E	M(e)	Literature-based	Upper Ganga	1.8	62.39	0.1123	0.239455263
19	South Lhonak	27°56'44"N	88°19'56"E	M(e)	Literature-based	Upper Brahmaputra	1.31	50.23	0.065	0.313153
20	Raphstreng	28° 6'27"N	90°14'48"E	M(l)	Literature-based	Upper Brahmaputra	1.36	43.72	0.059	0.336765
21	Tsomgo	27°22'28"N	88°45'48"E	M(e)	Literature-based	Upper Brahmaputra	0.23	15	0.0035	0.74104
22	Luggye	28° 5'34"N	90°17'54"E	M(l)	Literature-based	Upper Brahmaputra	1.66	48.92	0.081	0.216907
23	Rewuco	30°20'59"N	93°30'24"E	M(e)	Literature-based	Upper Brahmaputra	0.45	26.04	0.0117	0.50089

24	Ranzeriaco	30°28'11"N	93°31'59"E	M(e)	Literature-based	Upper Brahmaputra	0.28	11.58	0.0033	0.489682574
25	Bencogucо	30°21'20"N	93°31'41"E	M(e)	Literature-based	Upper Brahmaputra	0.12	14.87	0.0018	0.403878

.

Eidesstattliche Versicherung | Declaration of Oath

Hiermit erkläre ich an Eides statt, dass ich die vorliegende Dissertationsschrift selbst verfasst und keine anderen als die angegebenen Quellen und Hilfsmittel benutzt habe.

Sofern im Zuge der Erstellung der vorliegenden Dissertationsschrift generative Künstliche Intelligenz (gKI) basierte elektronische Hilfsmittel verwendet wurden, versichere ich, dass meine eigene Leistung im Vordergrund stand und dass eine vollständige Dokumentation aller verwendeten Hilfsmittel gemäß der Guten wissenschaftlichen Praxis vorliegt. Ich trage die Verantwortung für eventuell durch die gKI generierte fehlerhafte oder verzerrte Inhalte, fehlerhafte Referenzen, Verstöße gegen das Datenschutz- und Urheberrecht oder Plagiate.

"I hereby declare and affirm that this doctoral dissertation is my own work and that I have not used any aids and sources other than those indicated.

If electronic resources based on generative artificial intelligence (gAI) were used in the course of writing this dissertation, I confirm that my own work was the main and value-adding contribution and that complete documentation of all resources used is available in accordance with good scientific practice. I am responsible for any erroneous or distorted content, incorrect references, violations of data protection and copyright law or plagiarism that may have been generated by the gAI.

Hamburg | 11.03.2025

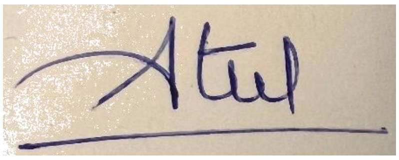

Atul Kumar